UNIVERSITE DE LIMOGES

ECOLE DOCTORALE SCIENCES TECHNOLOGIE SANTE

FACULTE DES SCIENCES ET TECHNIQUES

Année 2005 **Thèse n°73-2005**

Thèse

pour obtenir le grade de

DOCTEUR DE L'UNIVERSITE DE LIMOGES

Discipline : Electronique des Hautes Fréquences et Optoélectronique

Spécialité : "Communications Optiques et Microondes"

Alireza MAHANFAR

Le 16 Décembre 2005

Contribution au développement de méthodes d'optimisation avancées pour la conception électromagnétique de circuits et dispositifs microondes

Thèse dirigée par Michel AUBOURG et Stéphane BILA

Jury :

Mohamed MASMOUDI	Professeur à l'Université Paul Sabatier, Toulouse	Président
Raphaël GILLARD	Professeur à l'IETR, INSA Rennes	Rapporteur
Hervé AUBERT	Professeur au l'ENSEEIHT-LEN7, Toulouse	Rapporteur
Michel AUBOURG	Chargé de Recherche CNRS UMR 6615, IRCOM Limoges	Examinateur
Stéphane BILA	Chargé de Recherche CNRS UMR 6615, IRCOM Limoges	Examinateur
Alain REINEIX	Directeur de Recherche CNRS UMR 6615, IRCOM Limoges	Examinateur
Serge VERDEYME	Professeur à l'Université de Limoges, IRCOM-UMR 6615	Examinateur
Jérôme PUECH	Ingénieur au CNES, DCT/RF/HT, Toulouse	Invité
Man-Fai WONG	Ingénieur à France Télécom R&D,	Invité

To my Mother

To the Memory of my Father

Acknowledgments

I should first acknowledge Professor Serge VERDEYME, Director of the *Equipe de Circuits et Dispositifs micoondes(CDM)* for giving me the chance to work at IRCOM and funding me through the project. I also thank him for his kind and gentle attitude, brilliant management and also being an excellent listener. Without having him as the team director, I am not sure if work in IRCOM would have been such a great experience as it was.

I would like to thank my supervisors Drs Michel AUBOURG and Stéphane BILA for their supervision in my research work.

I thank Dr Stéphane Bila, CNRS research fellow *(chargé de recherche CNRS)* for his omnipresence and the invaluable help he did during my stay in Canada in the last months of my thesis work. I should also acknowledge his help in coordinating the work with the French National Center of Space Research *(Centre National D'Etudes Spatiales – CNES)* and *ANSYS-CADOE* development group. His pragmatic point of view has been an essential element of the work I did during my thesis.

I treasure Dr Michel AUBOURG for the great personality he is, both in technical and humane aspects. Working with Michel and learning from him was a pleasing and inspiring experience I will never forget. I am deeply indebted to Michel, for his constant support with his encouragement and many fruitful discussions.

I am grateful to my thesis reviewer, Dr Raphaël GILLARD, Professor of *IETR-INSA, Rennes,* for his useful comments about the work through the discussions we had before the defense. These comments helped the quality of presentation.

I wish to thank my thesis reviewer, Dr Hervé AUBERT professor of *ENSEEIHT-LEN7, Toulouse,* for his careful review of the dissertation and his positive comments during the review and defense process.

I am also grateful to the members of my defence committee, Dr Alain RENEIX, research director of *CNRS* at *IRCOM, Limoges*, Dr Mohamed MASMOUDI, professor of mathematics in *Université Paul-Sabatier, Toulouse,* Dr Man-Fai WONG from *France Télécom* and Dr Jérôme PUECH of *CNES, Toulouse*, for giving me the honor of having them as defense jury members and their helpful comments during the defense. I should more specifically acknowledge my appreciation to Jérôme PUECH for his always kind and welcoming attitude during the meetings we had.

Ms *Marrie-Laure GUILLAT*, the team secretary at *IRCOM-CDM* should definitely be acknowledged with highest regards for her kindness, help and availability.

I thank Drs *Djamchid GHAZANFARPOUR*, *Chazad MOVAHEDI* and *Vahid MEGHDADI* professors of the University of Limoges for their help, support and advices.

When I arrived at Limoges in 2001, I could only speak few words in French and thus have caused much burden for all the friends and professors to help me manage my research and everyday life. I am thus highly indebted to all my French friends for their hospitality, care and understanding.

More notably I thank *Cédrick SABOUREAU*, a great engineer and faithful friend, *Cristiano PALEGO*, an undiscovered talent in music and intellectualism, *Tony GASSELING*, with all his kindness and support, *Massimiliano SIMEONI*, whom I've learnt a lot from, *Julien GALIERE*, *Eric GABORIAUD*, *Jérôme BRAS*, *Jean-Philippe PLAZE*, and many other friends who have always been there for making all those nicely unforgettable moments of my stay in France happen.

Finally I wish to thank my previous supervisors in Tehran Polytechnic University, Dr *Rouzbeh MOINI*, Mr. *Amir KASHI*, and Dr *Amirhossein REZAIE*. I really feel indebted to them for any achievements I have had in my career.

Sommaire

CHAPTER II

OPTIMIZATION USING PARAMETERIZED EM-MODELS

CHAPTER III

EVOLUTIONARY ALGORITHMS FOR EM-BASED OPTIMIZATION

INTRODUCTION GENERALE

RÉSUMÉ

INTRODUCTION GÉNÉRALE – RÉSUMÉ

Il y a environ 4 décennies que les premières publications sur la conception assistée par ordinateur (CAO) des dispositifs micro-ondes sont apparues dans la littérature [1], [2]. Depuis, beaucoup d'améliorations ont été apportées à l'utilisation itérative de techniques numériques pour l'optimisation des circuits et dispositifs micro-ondes. Ces améliorations ont été basées principalement au départ sur le développement d'outils de CAO plus rapides et plus précis. De plus, il y a eu une tendance à développer des outils relativement généraux s'appliquant à des structures arbitraires. Naturellement, la croissance rapide des moyens informatiques et des techniques de programmation a eu un rôle majeur dans le succès des outils de CAO dans les secteurs académique puis industriel.

Une stratégie classique de CAO pour les dispositifs micro-ondes emploie une méthode numérique basée par exemple sur les lois de l'électromagnétisme pour modéliser son comportement fréquentiel ou temporel. Une fonction d'erreur par rapport à des spécifications électriques peut alors être calculée (automatiquement ou manuellement), et l'utilisateur change les paramètres de conception pour améliorer l'erreur jusqu'à ce que la valeur désirée soit atteinte. La boucle typique de conception est décrite dans la Fig. 1. Une fois la structure et les variables initiales (dimensions géométriques, propriétés des matériaux, etc.) sélectionnées, les variables sont mises à jour dans la boucle. Les mises à jour sont basées sur le calcul de la fonction d'erreur. La fonction d'erreur est généralement une fonction dépendante d'une valeur caractéristique calculée par la méthode numérique, par exemple du champ électromagnétique ou des paramètres de répartition. Bien que de nombreuses techniques différentes aient été développées jusqu'ici, toutes peuvent s'adapter à l'organigramme montré dans la Fig. 1. De plus, la plupart des développements pour l'optimisation des circuits et dispositifs micro-ondes ont été définis dans le cadre de l'optimisation classique, principalement dans deux voies, les stratégies efficaces de mise à jour des variables d'optimisation et l'analyse accélérée du champ par des techniques souvent approchées.

Les stratégies classiques de mise à jour des dimensions du dispositif ont été basées principalement sur des méthodes de gradient. Au cours des années, beaucoup de

variations des techniques de gradient ont été testées, puis durant la dernière décennie de nouvelles techniques, radicalement différentes, sont apparues et ont révolutionné la stratégie de mise à jour pour la CAO des circuits. La première tendance radicale a été le développement de techniques évolutionnaires telles que les algorithmes génétiques (AG) [3]. Une autre étape notable a été l'utilisation de concepts modernes tels que les réseaux de neurones artificiels ou le Space Mapping [4], [5]. En dépit de tous les efforts conséquents rapportés dans la littérature, très peu de travail a été vraiment effectué pour modifier la procédure classique d'optimisation impliquant une analyse électromagnétique à chaque itération.

Le chapitre I propose un examen détaillé des méthodes conventionnelles pour l'optimisation des dispositifs micro-ondes. Les différentes étapes constituant la boucle classique d'optimisation (Fig. 1) sont discutées en profondeur. Les étapes spécifiques de la procédure d'optimisation pour les dispositifs micro-ondes sont la définition de la fonction objectif et la méthode numérique donnant accès aux valeurs du champ électromagnétique.

L'analyse numérique du champ électromagnétique est un sujet de recherche très actif depuis le début des années 70, arrivant actuellement à maturité, et qui bénéficie des avancements effectués sur les calculateurs numériques. Cependant, l'analyse numérique n'étant pas le sujet prépondérant du travail effectué, les différentes méthodes ne sont abordées que succinctement dans ce premier chapitre.

La fonction objectif (également désignée sous le nom de fonction coût ou de fonction d'erreur) définie pour la CAO micro-onde doit s'adapter généralement à deux conditions distinctes, à savoir les caractéristiques désirée (idéale) et actuelle. Cette question est discutée plus en détail dans le chapitre I.

Au delà de ces deux sujets, ce chapitre adresse plusieurs techniques d'optimisation contemporaines.

Le chapitre II commence par l'introduction des techniques de paramétrisation en général. Le but de la paramétrisation est d'exprimer les caractéristiques du modèle numérique représentant le dispositif en fonction de ses différents paramètres sous une forme analytique. Normalement la réalisation d'un modèle ainsi paramétré exige

d’obtenir les caractéristiques de dispositif et ses dérivés dans une plage de variation donnée. Dans le contexte de la CAO des dispositifs micro-ondes, nous montrerons que le comportement du modèle peut être caractérisé convenablement en fonction de deux paramètres, la fréquence et la géométrie.

La paramétrisation du champ électromagnétique en fonction de la fréquence, qui permet d’accélérer l'analyse électromagnétique dans la boucle d'optimisation est rapportée dans la première partie du chapitre II.

Le corps principal du chapitre II est consacré à la paramétrisation de la géométrie et à son application à l’optimisation des dispositifs micro-ondes. Nous montrerons alors qu’en utilisant la paramétrisation géométrique, la boucle d'optimisation classique peut être fondamentalement modifiée, de sorte à limiter au strict minimum le nombre d’analyses électromagnétiques. En effet, une fois, la paramétrisation géométrique du modèle effectuée, les caractéristiques liées aux variables d’optimisation sont calculées aux itérations suivantes en utilisant le modèle paramété. Ainsi l’étape la plus coûteuse dans la boucle d'optimisation classique est court-circuitée.

Pour effectuer une analyse électromagnétique par une méthode numérique, la géométrie de la structure doit être discrétisée. Pour la plupart des méthodes numériques, comme par exemple la méthode des éléments finis qui est utilisée dans ce travail, un maillage est généré de manière quasi-aléatoire. Les gradients obtenus en appliquant une telle technique sont alors habituellement discontinus. Ainsi une étape essentielle pour constituer le modèle géométriquement paramétré, est d'employer un maillage paramétré. La méthode classique pour déformer un maillage existant est basée sur l’analogie au système masse-ressort. Cette méthode recèle cependant quelques imperfections. Dans le chapitre II de nouvelles méthodes sont étudiées. Tout d'abord, une méthode dite de coordonnées barycentriques généralisées est employée pour exprimer chaque point intérieur (noeuds du maillage) d'un polygone en fonction de ses sommets. Une seconde méthode relativement semblable est aussi étudiée dans ce chapitre et les deux techniques, déjà employées dans le contexte de l'infographie, permettent de générer un maillage paramétré remplaçant sa génération pseudo-aléatoire à chaque itération ce qui améliore d’une part les gradients donc l'exactitude et d’autre part la vitesse de parcours de la boucle. Toutes les améliorations apportées par les paramétrisations du maillage et de la géométrie sont illustrées par un exemple.

Un filtre 5 pôles à cavités cylindriques est ensuite optimisé par un modèle géométriquement paramétré avec les outils développés par la société CADOE. Le code éléments finis développé au laboratoire a été couplé à ce logiciel dans le cadre d'une action de R&T du CNES. A partir de cet exemple, une stratégie d'optimisation utilisant un modèle électromagnétique paramétré géométriquement est développée. Une initialisation performantes des variables permet d'utiliser une stratégie classique basée sur un calcul de gradient. Les résultats obtenus au bout de seulement quelques itérations sont présentés à la fin du chapitre.

Le chapitre III est consacré à l'application des algorithmes évolutionnaires dans le cadre de l'optimisation des circuits micro-ondes. Toutes les stratégies d'optimisation conventionnelles mettent à jour les paramètres du modèle (paramétré ou non) sur la base d'un calcul de gradient. Les techniques de gradient dépendant intrinsèquement du point initial choisi, si le point initial devient très éloigné du point optimal, les risques de divergence deviennent importants. Les algorithmes évolutionnaires sont l'une des solutions possibles pour résoudre les problèmes d'optimisation quand le concepteur n'a que peu voire pas d'information lui permettant d'initialiser efficacement son vecteur de paramètres.

Le chapitre débute avec une introduction générale des algorithmes évolutionnaires. Ces méthodes emploient habituellement l'analogie entre l'espace des paramètres et un système biologique. Elles consistent à sélectionner un individu parmi une population aléatoirement produite. Les individus dans cette population sont des vecteurs de paramètres et un index de forme physique (fonction objectif) est assigné à chacun des individus. La méthode évolutionnaire la plus populaire est certainement l'algorithme génétique (AG) qui est présenté avec ses dérivés dans ce chapitre.

Les algorithmes génétiques ont été employés pour l'optimisation des structures électromagnétiques depuis plus d'une décennie. L'inconvénient principal de cet algorithme est son comportement relativement lent. Afin de maintenir une certaine généralité, la population témoin doit être relativement large pour s'assurer d'avoir inclus toutes les propriétés que peut incorporer la solution optimale. Toutefois, afin de générer la population témoin, plusieurs analyses électromagnétiques sont nécessaires, ce qui peut rendre l'étape d'initialisation assez coûteuse en temps, et l'algorithme

évolutionnaire totalement incompatible avec la conception d'antennes ou de composants micro-ondes.

La technique d'optimisation par « essaims particulaires » (Particle swarm optimization - PSO) est une technique évolutionnaire plus récente qui fait son apparition dans le domaine de l'électromagnétisme et les quelques articles disponibles reflètent principalement un travail sur les antennes. La méthode permet de déterminer l'optimum global. En dépit de sa nature évolutionnaire, la méthode est considérablement plus rapide qu'un algorithme génétique et peut être vue comme un compromis approprié entre les méthodes de gradient et les algorithmes génétiques. Quelques exemples illustrent cette méthode. Les résultats montrent une rapidité d'exécution supérieure à l'algorithme génétique, tout en maintenant les performances globales.

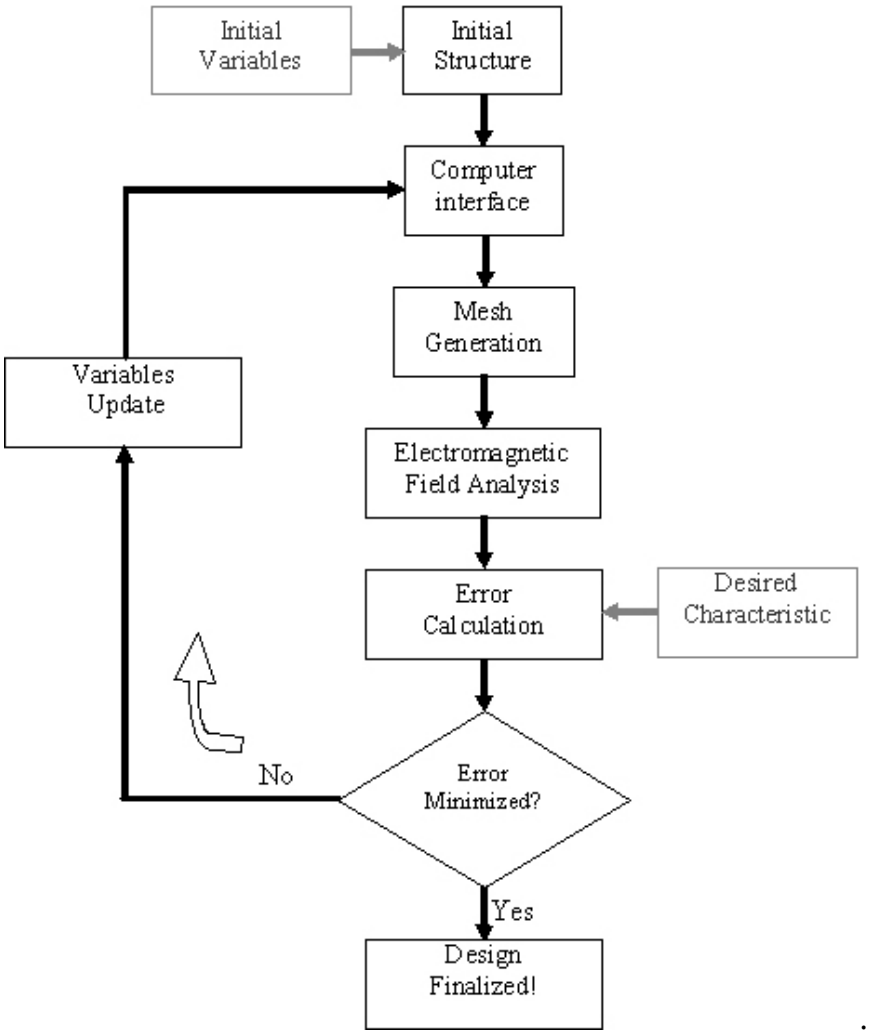

Fig. 1. Procédure d'optimisation typique pour les dispositifs micro-ondes

Références

[1] J. W. Bandler, “Optimization methods for computer aided design,” *IEEE Transaction on Microwave Theory and Techniques*, vol. MTT-17, No. 8, pp. 533-552, August 1969.

[2] G.C. Temes and D.A. Calahan (1967), “Computer-aided network optimization the state of-the-art,”. *Proc. IEEE*, vol. 55, pp. 1832-1863.

[3] J. M.Johnson and Y.Rahmat-Samii, “Genetic algorithms in electromagnetics,” *Proc. IEEE Antennas Propagat. Soc. Int. Symp.* Baltimore, MD, pp. 1480-1483, July 1996.

[4] J. W.Bandler, R. M.Biernacki, S. H.Chen, P. A.Grobelny, and R. H.Hemmers, “Space mapping technique for electromagnetic optimization,” *IEEE Trans. Microwave Theory Tech.*, vol. 42, pp. 2536-2544, Dec. 1994.

[5] J. E. Rayas-Sánchez, *Neural space mapping methods for modeling and design of microwave circuits*, Ph.D. dissertation Hamilton, ON, Canada: Dept. Elect. Comput. Eng., McMaster Univ., 2001

[6] J. Robinson and Y. Rahmat-Samii, “Particle swarm optimization in electromagnetics,” IEEE *Transactions on Antennas and Propagation*, vol. 52, No. 2, pp. 397 – 407, Feb. 2004

CHAPTER I

Generalities about EM-based Optimization of Microwave Devices

I.1 Introduction

Choosing the appropriate optimization techniques highly depends on the physics of the structure to be optimized, the required accuracy and available resources. In fact without comprehension of the nature of the problem the design process will be inefficient. Actually no algorithm for optimizing general functions exists that will always find the global optimum for a general minimization problem in a reasonable amount of time.

This chapter presents a detailed survey of the present work on computer-aided design of microwave devices and circuits.

It has been tried to provide a platforms for the suggested improvements in the following chapters (chapters 2 and 3). To completely understand the significance of the proposed techniques, certain aspects of the optimization procedure should be discussed in depth.

The chapter starts with explanation of the fundamental concepts in optimization, followed by description of each block in a classic optimization loop. Some of the components of the design optimization loop such as update strategy are common in any design practice. In contrary, some aspects of the optimization exclusively apply to the optimization in electromagnetics domain. Among all this microwave-specific components, defining the objective function is not only distinct for microwave domain (in comparison to other optimization problems) but also it varies among different microwave design problems. Thus the derivation of the objective function in microwave CAD has been covered in more detail. Numerical analysis of microwave structures is another aspect which is distinct for microwave engineering, although these methods have been deployed for different applications beforehand. Thus The numerical analysis of the microwave devices has been studied in depth, accordingly. The issues to be improved in the context of microwave CAD is addressed at the end of this chapter.

I.2 Fundamental concepts in optimization

I.2.1 Fundamental definitions

The problem is to minimize the function *T*,

$$T:\mathbb{C}^n \mapsto \mathbb{R}$$
$$T = T(\bar{p}) \qquad \textit{(I-1)}$$

and where

$$\bar{p} = \left[p_1\ p_2 \ldots p_N \right]^T \qquad \textit{(I-2)}$$

T is called the objective function or error function. The procedure to construct the objective function is discussed in detail later. $\bar{p}$ is an N-dimensional vector, called the parameter vector. The space including all the parameter vectors is called *parameter space.* The dimensionality of a parameter space is equal to the number of element of the vector $\bar{p}$.

In general the minimization is subject to constraints,

$$\bar{C}_{M\times 1}(\bar{p}) \le \bar{b}_{M\times 1} \qquad \textit{(I-3)}$$

The constraints are satisfied either during optimization or by the optimum solution. Any vector which satisfies the constraint is called *feasible*. The vector $\bar{b}_{M\times 1} = \left[b_i \right]_{M\times 1}^T, b_i \in \mathbb{R}$, defines the limits or bounds for the constraints.

Fig. I- 1 shows a 2-D contour which illustrates some features encountered in optimization problems. Hypercontours are described by the relation,

$$T(\bar{p}) = const. \qquad \textit{(I-4)}$$

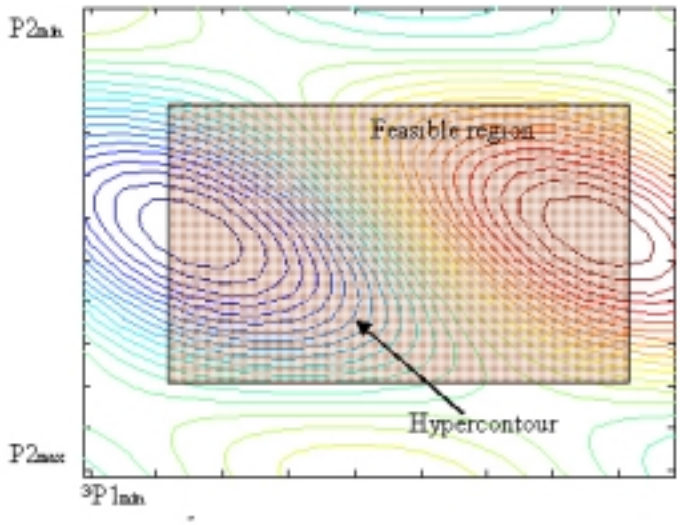

Fig. I- 1. Illustration of hyper-contours

A minimum may be located by a point $\bar{p}^{opt}$ on the response hyper-surface generated by $T(\bar{p})$ such that

$$T^{opt} = T(\bar{p}^{opt}) \le T(\bar{p}), \forall \bar{p} \qquad (I\text{-}5)$$

If we expand T we would have,

$$T(\bar{p} + \triangle \bar{p}) = T(\bar{p}) + \nabla T^T(\bar{p}).\triangle \bar{p} + \frac{1}{2} \triangle \bar{p}^T H \triangle \bar{p} + \ldots \qquad (I\text{-}6)$$

where

$$\triangle \bar{p} = \begin{bmatrix} \triangle \bar{p}_1 \\ . \\ . \\ \triangle \bar{p}_N \end{bmatrix} \qquad (I\text{-}7)$$

and,

$$\nabla T(\bar{p}) = \begin{bmatrix} \frac{\partial T(\bar{p})}{\partial p_1} \\ . \\ . \\ \frac{\partial T(\bar{p})}{\partial p_N} \end{bmatrix} \qquad (I\text{-}8)$$

is the gradient vector and

$$H(\bar{p}) = \left[h_{ij} \right]_{N \times N} \qquad \textit{(I-9)}$$

while,

$$h_{ij} = \frac{\partial^2 T(\bar{p})}{\partial p_i . \partial p_j} \qquad \textit{(I-10)}$$

Matrix $H(\bar{p})$ is called Hessian matrix. One can conclude that, $\nabla T(\bar{p}^{opt}) = 0$ and $H(\bar{p}^{opt})$ is positive definite.

We generally consider families or classes of optimization problems, characterized by particular forms of the objective and constraint functions. As an important example, the optimization problem (I-1) is called a linear problem if the objective and constraint functions are linear, i.e., satisfy

$$T(\alpha \bar{p} + \beta \bar{q}) = \alpha T(\bar{p}) + \beta T(\bar{q}) \qquad \textit{(I-11)}$$

for all $\bar{p}, \bar{q} \in \mathbb{R}^N$ and $\alpha, \beta \in \mathbb{R}$. If the optimization problem is not linear, it is called a non-linear problem.

A *convex* optimization problem is one in which the objective and constraint functions are convex, which means they satisfy the inequality

$$T(\alpha \bar{p} + \beta \bar{q}) \leq \alpha T(\bar{p}) + \beta T(\bar{q}) \qquad \textit{(I-12)}$$

with $\bar{p}, \bar{q} \in \mathbb{R}^N$, $\alpha, \beta \in \mathbb{R}$, $\alpha, \beta \geq 0$ and $\alpha + \beta = 1$. Comparing (I-12)and (I-11), we see that convexity is more general than linearity: inequality replaces the more restrictive equality, and the inequality must hold only for certain values of α and β. Since any linear problem is therefore a convex optimization problem, we can consider convex optimization to be a generalization of linear programming.

I.2.2 Solving optimization problems

A solution method for a class of optimization problems is an algorithm that computes a solution of the problem (to some given accuracy), given a particular problem from the class, i.e., an instance of the problem. Since the late 1940s, a large effort has gone into developing algorithms for solving various classes of optimization problems, analyzing their properties, and developing appropriate software implementations. The effectiveness of such an algorithm, i.e., its ability to solve the optimization problem (I-1), varies considerably, and depends on factors such as the particular forms of the

objective and constraint functions, how many variables and constraints there are, and special structure, such as sparsity, when each constraint function depends on only a small number of the variables. Even when the objective and constraint functions are smooth (for example, polynomials) the general optimization problem (I-1) is surprisingly difficult to solve.

I.2.3 Least squares problems

A least-squares problem is an optimization problem with no constraints (i.e., M =0) and an objective which is a sum of squares of terms of the form $a_i^T \bar{p} - b_i$:

$$\textit{Minimize} \qquad T(\bar{p}) = \left\| A\bar{p} - \bar{b} \right\|_2^2 = \sum_{i=1}^{N} (a_i\ \bar{p} - b_i)^2 \tag{I-13}$$

Here a_i 's are rows of A.

The solution of a least-squares problem (13) can be reduced to solving a set of linear equations,

$$(A^T A)\bar{p} = A^T \bar{b} \tag{I-14}$$

so we have the analytical solution $\bar{p}^{opt} = (A^T A)^{-1} A^T \bar{b}$. For least-squares problems there has been developed several algorithms (and software implementations) for solving the problem to high accuracy, with very high reliability. A current desktop computer can solve a least-squares problem with hundreds of variables, and thousands of terms, in a few seconds; more powerful computers, of course, can solve larger problems, or the same size problems, faster. Moreover, these solution times will decrease exponentially in the future, according to Moore's law. Algorithms and software for solving least-squares problems are reliable enough for embedded optimization. In many cases we can solve even larger least-squares problems, by exploiting some special structure in the coefficient matrix A. For extremely large problems (say, with millions of variables), or for problems with exacting real-time computing requirements, solving a least-squares problem can be a challenge. But in the vast majority of cases, one can say that existing methods are very effective, and extremely reliable. Indeed, we can say that solving least-squares problems that are not on the boundary of what is currently achievable is a mature technology that can be reliably used by many people who do not know, and do not need to know, the details.

The least-squares problem is the basis for regression analysis, optimal control, and many parameter estimation and data fitting methods. It has a number of statistical interpretations, e.g., as maximum likelihood estimation of a vector $\overline{p}$, given linear measurements corrupted by Gaussian measurement errors. Recognizing an optimization problem as a least-squares problem is straightforward; we only need to verify that the objective is a quadratic function (and then test whether the associated quadratic form is positive semi-definite). While the basic least-squares problem has a simple fixed form, several standard techniques are used to increase its flexibility in applications. In weighted least-squares, the weighted least-squares cost

$$\sum_{i=1}^{N} w_i (a_i \overline{p} - b_i)^2 \qquad \textit{(I-15)}$$

where w_i's are positive, is minimized. (This problem is readily cast and solved as a standard least-squares problem).

I.2.4 Linear problems

Another important class of optimization problems is linear programming, in which the objective and all constraint functions are linear:

$$\textit{Minimize} \qquad \overline{c}^T \overline{p} \qquad \textit{(I-16)}$$

$$\textit{Subject to} \qquad a_i^T \overline{p} \le b_i$$

$a_i, \overline{c} \in \mathbb{R}^N$ are problem parameters and b_i specify constraints.

There is no simple analytical formula for the solution of a linear problem (as there is for a least-squares problem), but there are a variety of very effective methods for solving them, and the more recent interior point methods described later in this report. While we cannot give the exact number of arithmetic operations required solving a linear problem (as we can for least-squares), we can establish rigorous bounds on the number of operations required to solve a linear problem, to a given accuracy, using an interior-point method. These algorithms are quite reliable, although perhaps not quite as reliable as methods for least-squares. We can easily solve problems with hundreds of variables and thousands of constraints on a small desktop computer, in a matter of seconds. If the problem is sparse, or has some other exploitable structure, we can often solve problems with tens or hundreds of thousands of variables and constraints.

As with least-squares problems, it is still a challenge to solve extremely large linear problem, or to solve linear problem with exacting real-time computing requirements. But, like least-squares, we can say that solving (most) linear problem is a mature technology. Linear programming solvers can be (and are) embedded in many tools and applications.

I.2.5 Convex optimization

A convex optimization problem is one of the form

$$\begin{aligned} &\textit{Minimize} && T(\overline{p}) \\ &\textit{Subject to} && \overline{c}(\overline{p}) \le \overline{b} \end{aligned} \qquad \textit{(I-17)}$$

where $\overline{p} \in \mathbb{R}^N$ the functions $T(\overline{p})$ and $\overline{c}(\overline{p})$ satisfy convexity conditions stated in (I-12). The least-squares problem (I-13) and linear problem (I-16) are both special cases of the general convex optimization problem (I-17).

There is in general no analytical formula for the solution of convex optimization problems, but (as with linear problems) there are very effective methods for solving them. Interior-point methods work very well in practice and in some cases can be proved to solve the problem to a specified accuracy with a number of operations that does not exceed a polynomial of the problem dimensions.

Like methods for solving linear problem, these interior-point methods are quite reliable. We can easily solve problems with hundreds of variables and thousands of constraints on a current desktop computer, in at most a few tens of seconds. By exploiting problem structure (such as sparsity), we can solve far larger problems, with many thousands of variables and constraints. We cannot yet claim that solving general convex optimization problems is a mature technology, like solving least-squares or linear problems. Research on interior-point methods for general non-linear convex optimization is still a very active research area, and no consensus has emerged yet as to what the best method or methods are.

I.2.6 Local optimization

In local optimization, the compromise is to give up seeking the optimal $\overline{p}$, which minimizes the objective over all feasible points. Instead we seek a point that is only locally optimal, which means that it minimizes the objective function among feasible points that are near it, but is not guaranteed to have a lower objective value than all

other feasible points. A large fraction of the research on general non-linear optimization problem has focused on methods for local optimization, which as a consequence are well developed.

Local optimization methods can be fast, can handle large-scale problems, and are widely applicable, since they only require differentiability of the objective and constraint functions. As a result, local optimization methods are widely used in applications where there is value in finding a good point, if not the very best. In an engineering design application, for example, local optimization can be used to improve the performance of a design originally obtained by manual, or other, design methods.

There are several disadvantages of local optimization methods, beyond (possibly) not finding the true, globally optimal solution. The methods require an initial guess for the optimization variable. This initial guess or starting point is critical, and can greatly affect the objective value of the local solution obtained. Little information is provided about how far from (globally) optimal the local solution is. Local optimization methods are often sensitive to algorithm parameter values, which may need to be adjusted for a particular problem, or family of problems.

Using a local optimization method is trickier than solving a least-squares problem, linear problem, or convex optimization problem. It involves experimenting with the choice of algorithm, adjusting algorithm parameters, and finding a good enough initial guess (when one instance is to be solved) or a method for producing a good enough initial guess (when a family of problems is to be solved). Roughly speaking, local optimization methods are more art than technology. Local optimization is a well developed art, and often very effective, but it is nevertheless an art. In contrast, there is little art involved in solving a least-squares problem or a linear problem (except, of course, those on the boundary of what is currently possible).

An interesting comparison can be made between local optimization methods for non-linear programming, and convex optimization. Since differentiability of the objective and constraint functions is the only requirement for most local optimization methods, formulating a practical problem as a non-linear optimization problem is relatively straightforward. The art in local optimization is in solving the problem (in the weakened sense of finding a locally optimal point), once it is formulated. In convex optimization these are reversed: The art and challenge is in problem formulation; once

a problem is formulated as a convex optimization problem, it is relatively straightforward to solve it.

I.2.7 Global optimization

In global optimization, the true global solution of the optimization problem (I-1) is found; the compromise is efficiency. The worst-case complexity of global optimization methods grows exponentially with the problem sizes n and m; the hope is that in practice, for the particular problem instances encountered, the method is far faster. While this favorable situation does occur, it is not typical. Even small problems, with a few tens of variables, can take a very long time (e.g., hours or days) to solve.

Global optimization is used for problems with a small number of variables, where computing time is not critical, and the value of finding the true global solution is very high. One example from engineering design is worst-case analysis or verification of a high value or safety-critical system. Here the variables represent uncertain parameters that can vary during manufacturing, or with the environment or operating condition. The objective function is a utility function, i.e., one for which smaller values are worse than larger values, and the constraints represent prior knowledge about the possible parameter values. The optimization problem (I-1) is the problem of finding the worst-case values of the parameters. If the worst-case value is acceptable, we can certify the system as safe or reliable (with respect to the parameter variations). A local optimization method can rapidly find a set of parameter values that is bad, but not guaranteed to be the absolute worst possible. If a local optimization method finds parameter values that yield unacceptable performance, it has succeeded in determining that the system is not reliable. But a local optimization method cannot certify the system as reliable; it can only fail to find bad parameter values. A global optimization method, in contrast, wills find the absolute worst values of the parameters, and if the associated performance is acceptable, can certify the system as safe. The cost is computation time, which can be very large, even for a relatively small number of parameters.

I.2.8 Non-convex problems

One obvious use is to convert a non-convex problem in to a convex problem by combining convex optimization with a local optimization method. Starting with a

non-convex problem, we first find an approximate, but convex, formulation of the problem. By solving this approximate problem, which can be done easily and without an initial guess, we obtain the exact solution to the approximate convex problem. This point is then used as the starting point for a local optimization method, applied to the original non-convex problem.

Convex optimization is the basis for several heuristics for solving non-convex problems. One interesting example we will see is the problem of finding a sparse vector x (i.e., one with few nonzero entries) that satisfies some constraints. While this is a difficult combinatorial problem, there are some simple heuristics, based on convex optimization, that often find fairly sparse solutions. Another broad example is given by randomized algorithms, in which an approximate solution to a non-convex problem is found by drawing some number of candidates from a probability distribution, and taking the best one found as the approximate solution. Now suppose the family of distributions from which we will draw the candidates is parameterized, we can then pose the question: which of these distributions gives us the smallest expected value of the objective? It turns out that this problem is sometimes a convex problem, and therefore efficiently solved.

I.3 Objective function for microwave device optimization

The design of microwave devices is normally accomplished through minimizing the discrepancy between the actual S-parameters and the ideal S-parameters. Thus the objective function is defined as a function of the difference of the device characteristics in terms of S- parameters with the ideal response at any stage.
The definition of objective function affects the efficiency of optimization procedure. The reasons behind this are as follows,

1- Convexity of objective function guarantees the convergence of the optimization procedure.
2- The objective function has to be calculated for several times during the optimization process, thus the design time directly depends on the computation cost of the objective function.

In this section different possible formulations of objective will be studied in detail. The emphasis is on formulations which can allow explicit and implicit constraints. This is specifically important to microwave device optimization where the range of permissible parameters is rather narrow.
Let $D_{ij}^{<k>}$ be the difference between the ideal and actual S-parameters in the frequency f at k'th iteration,

$$D_{ij}^{<k>}(f,\bar{p}) = \left|S_{ij}^{<k>}(f,\bar{p})\right| - \left|S_{ij}^{ideal}(f)\right| \qquad \textit{(I-18)}$$

where $S_{ij}^{<k>}$ is the actual, i.e. calculated S-parameter ($i,j=1,2$), $S_{ij}^{ideal}(f)$ is the ideal characteristic. The vector $\bar{p}$ is parameter vector. There might be some constraints applied on $\bar{p}$,

$$C(\bar{p}) \le \bar{b} \qquad \textit{(I-19)}$$

where $\bar{b}$ is representing constraints. C can be a linear or nonlinear function, but more commonly it is linear.

The objective function can be defined as the sum of D_{ij} 's over the all the frequencies,

$$T_{ij}^{<k>} = \sum_{s=1}^{S} D_{ij}^{<k>}(f_s, \bar{p}) \qquad \textit{(I-20)}$$

Fig. I- 2 illustrates a sample derivation of the function $T_{ij}^{<k>}$. It can be seen that $D_{ij}^{<k>}$ is negative in some frequencies and positive in some other frequencies. Thus the errors with different signs cancel out each other. The equation (I-20) is modified as,

$$D_{ij}^{<k>}(f_s, \bar{p}) = \left\| S_{ij}^{<k>}(f_s, \bar{p}) \right| - \left| S_{ij}^{ideal}(f_s) \right\| \qquad \textit{(I-21)}$$

or,

$$D_{ij}^{<k>}(f_s, \bar{p}) = \left(\left| S_{ij}^{<k>}(f_s, \bar{p}) \right| - \left| S_{ij}^{ideal}(f_s) \right| \right)^2 \qquad \textit{(I-22)}$$

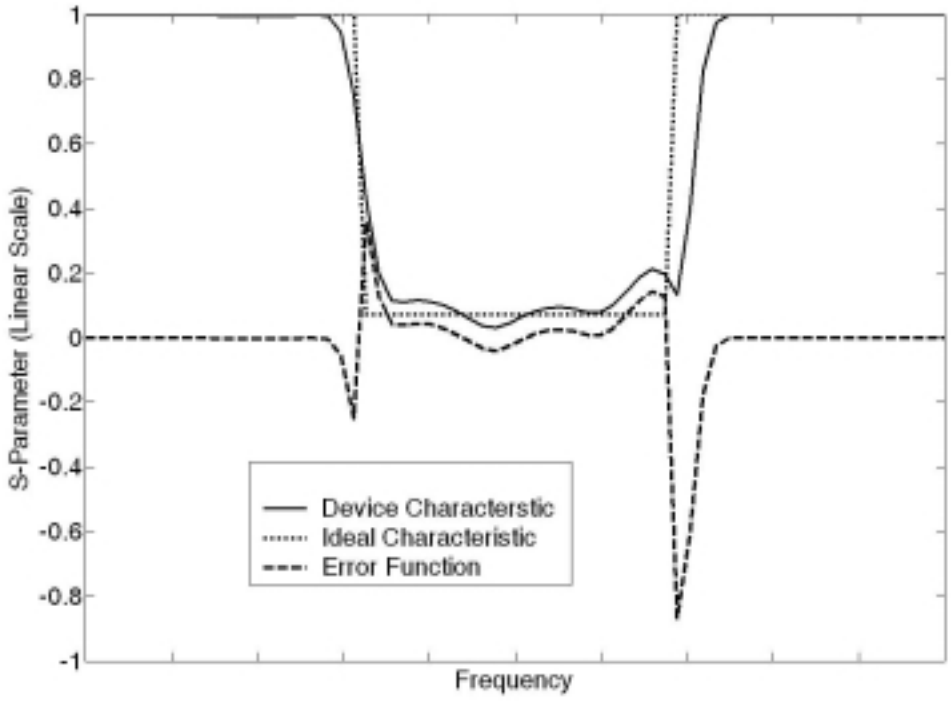

Fig. I- 2. $S_{ij}^{ideal}(f_s)$, Sij and the error function

In the last couple of equations, $D_{ij}^{<k>}$ is positive. Later we will see this property will help to construct a positive definite quadratic form. This is one of the conditions that one can assure convexity of the objective function.

I.3.1 Minimax optimization [44]- [46]

The objective function at *k*'th iteration can ideally be expressed as,

$$T^{<k>}(f,\bar{p}) = \max_{f\in[f_{\min},f_{\max}]}\left\{w_u(f).\left(\left|S_{ij}^{<k>}(f,\bar{p})\right| - \left|S_{ij}^{U-ideal}(f)\right|\right) - w_l(f).\left(\left|S_{ij}^{<k>}(f,\bar{p})\right| - \left|S_{ij}^{L-ideal}(f)\right|\right)\right\} \quad \textit{(I-23)}$$

where

$w_u(f)$ and $w_l(f)$ are upper and lower weighting factors, respectively.

$S_{ij}^{U-ideal}(f)$ is the desired upper limit of the S-parameters

$S_{ij}^{L-ideal}(f)$ is the desired lower limit of the S-parameters

The formulation is better understood by referring to Fig. I- 3.

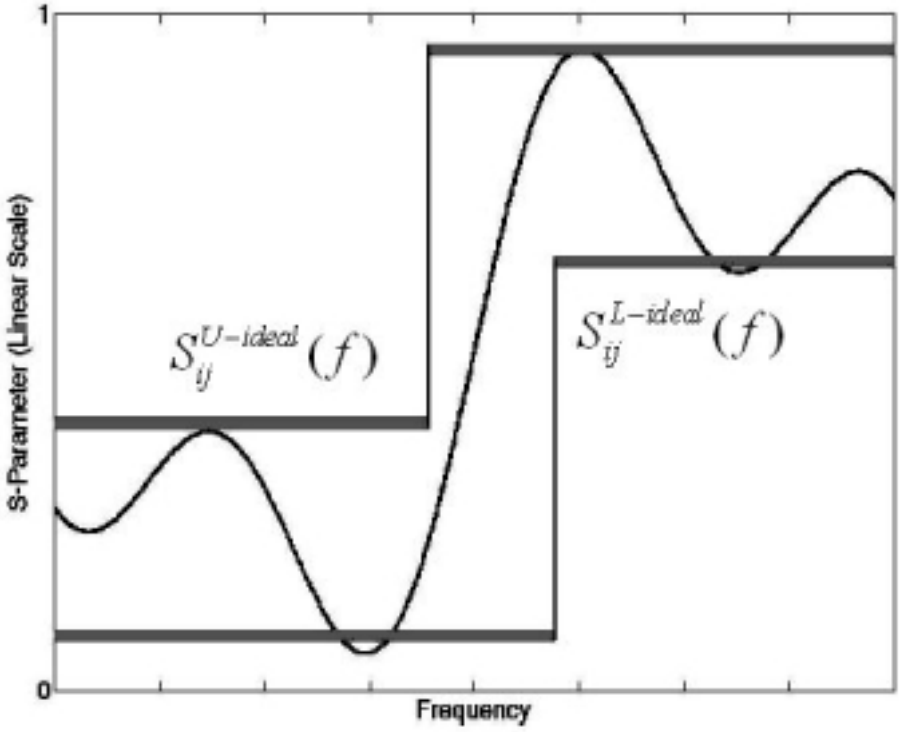

Fig. I- 3. Different sub-functions of the objective function with *minimax* formulation.

The weighting factors are supposed to be non-negative, $w_u(f) \geq 0$, $w_l(f) \geq 0$ and $\left|S_{ij}^{U-ideal}(f)\right| \geq \left|S_{ij}^{L-ideal}(f)\right|$ for $f \in [f_{\min}, f_{\max}]$. Under such circumstances both terms in equation (I-23) will be non-negative. They are equal to zero either when the weighting factor is zero or the ideal and actual responses are equal. The goal function is,

therefore, to minimize the maximum possible error that the device can produce. As a special case, when

$$S_{ij}^{U-ideal}(f) = S_{ij}^{L-ideal}(f) = S_{ij}^{ideal}(f) \tag{I-24}$$

and $w_u(f) = w_l(f) = w(f)$

$$T^{<k>}(f,\bar{p}) = \max_{f\in[f_{\min},f_{\max}]}\left\{\left|w(f).\left(\left|S_{ij}^{<k>}(f,\bar{p})\right| - \left|S_{ij}^{ideal}(f)\right|\right)\right|\right\} \tag{I-25}$$

A variation of *minimax* formulation, as addressed in [49] formulates the objective function in terms of inequality constraints as follows,

$$\textit{Minimize } T^{<k>}(f,\bar{p}) \tag{I-26}$$

Subject to,

$$\begin{cases} T^{<k>}(f,\bar{p}) \geq w(f).\left(\left|S_{ij}^{<k>}(\bar{p})\right| - \left|S_{ij}^{U-ideal}(f)\right|\right) & f \in F_u \\ T^{<k>}(f,\bar{p}) \geq -w(f).\left(\left|S_{ij}^{<k>}(\bar{p})\right| - \left|S_{ij}^{L-ideal}(f)\right|\right) & f \in F_l \end{cases}$$

where F_l and F_u are two sub-sets of the range $[f_{\min}, f_{\max}]$. The subscripts *l* and *u* are brought as a matter of convenience and do not necessarily correspond to upper and lower part of frequency span. The two sub-sets are not essentially disjoint. This way we have taken into account the requirement for relative amplitude of S-parameters are different for in- and out-bands.

I.3.2 Least squares formulation [43]

A very common class of objective function in electromagnetic domain is the least squares formulation. The last squares formulation can be symbolically shown as,

$$T^{<k>}(f,\bar{p}) = \sum_{s=1}^{S}\left|D_{ij}^{<k>}(f_s,\bar{p})\right|^2 \tag{I-27}$$

where $D_{ij}^{<k>}(f_s,\bar{p})$ is introduced in (I-18). The squared terms are always positive thus of errors with different signs will not cancel each other when being accumulated. But the main idea beyond the deployment of the Least Squares was to give a more emphasize on larger errors than smaller ones. Also within a defined proximity of the

optimum point (Here we show it as $\overline{p}^{<optim>}$) the rate of convergence is faster than the linear model.

From an algorithmic point of view, the feature that distinguishes least squares problems from the general unconstrained optimization problem is the structure of the Hessian matrix of $T^{<k>}(f,\overline{p})$. As mentioned earlier, the Least Squares method has widely been used for the optimization of microwave devices.

Examples

In [9] the generic objective form of

$$F=\frac{1}{2}[m-m^{desired}]^2 \qquad \textit{(I-28)}$$

was used as objective function. Here, *m* is an arbitrary performance measure in the circuit. The same contribution has incorporated a linear term which basically imposes dimensional constraints to the design for the problem of a waveguide with multilayer coats,

$$F=\frac{1}{2}[k_{im}^{desired}-k_{im}]^2+\sum_{i=1}^{n}\left[\frac{1}{12.7-t_i}+\frac{1}{20-\alpha_i}\right] \qquad \textit{(I-29)}$$

whereas k_{im} indicates the attenuation rate, α_i and t_i are the material property index and thickness of ***i***th coating layer. In other words the constraints are directly integrated into the cost (objective) function. This might not be an appropriate approach in general since we risk moving towards a point in parameter space which might comply perfectly with boundary conditions while getting further form the desired characteristic.

In [12] the transfer and reflection characteristics of a filter (S_{21} and S_{11}) are approximated by rational functions both for ideal case and at each iteration. Then the cost (objective) function is formed by using the location of zeros and poles of filters reflection and transfer functions,

$$C=\sum_{i=1}^{M}\left|Z_i'-Z_i\right|^2+\sum_{i=1}^{M}\left|P_i'-P_i\right|^2 \qquad \textit{(I-30)}$$

where *C* is the cost (objective) function, *N* is the number of poles, *M* is the number of (prescribed) zeros, P_i and Z_i are poles and zeros of the transfer function. Prime

superscripts indicate desired values. The authors have also claimed that with this new formation of the objective function the optimization process converges arbitrarily regardless of what the initial point has been chosen. Regardless of the validity of the claim, the fact that the choice of a proper objective function is crucial for a design has appropriately been addressed. Although the suggested scheme shows superb performance in comparison with conventional procedures the method has certain drawbacks such as,

The calculation of poles and zeros imposes an extra computation cost at each step

- One can not avoid the round off and computation errors in computing transfer and reflection characteristic poles and zeros. These errors together with computational inaccuracies and optimization procedure errors (such as gradient approximation) will considerably increase the risk of being lead to a wrong point in parameter space
- Determining the order and form of the transfer and reflection functions is not a trivial issue. It needs a minimum level of priory knowledge which is not always available.

In [20] the general problem of multiple coupled resonator filter is approached using an objective function for as follows,

$$Errf = \sum_{i=1}^{N} \left[S_{11}(f_i) \right]^2 + \sum_{j=1}^{m} \left[S_{21}(f_j) \right]^2 + \left[\varepsilon - \hat{\varepsilon} \right]^2 \qquad \textit{(I-31)}$$

where ε and $\hat{\varepsilon}$ are the actual and desired scale factors related to pass-band ripple. Including the ripple scale factor in the objective function is the unique feature introduced in [20]. Convergence of the optimization does not depend on the initial point. As the authors claim,

> *"Convergence of the minimization is very fast and all cases tested are independent of the initial coupling matrix guess. In contrast, optimization using an error function based on the difference between the mask and the response was slow, often did not converge to any acceptable solution and in all cases required an initial coupling matrix guess whose response was close to the desired response in order to converge."*

However, one can not ignore the fact that such an objective function does not introduce any criterion for stopping the optimization process. The smallest value that such an objective function can possess is unclear. When using the error function, there

is always a desired value for the error function (ideally zero) which is a function of the required accuracy. On the other hand, the orders of magnitude for ε and for S-parameters are not the same and appropriate weighting factors need to be multiplied by each of the terms of (I-31). Otherwise S-parameters will dominate the variations of the objective function.

Again, in [26] the least squares of S parameters is utilized for the optimization of a miter bend with dielectric column,

$$C(\bar{p}) = \sum_{i=1}^{N_f^p} \left[S_{11}(f_i^{\,p}) \right]^2 + \sum_{i=1}^{N_f^s} \left[S_{21}(f_i^{\,s}) \right]^2 \qquad \textit{(I-32)}$$

where all the notations of previous formula apply and superscripts *p* and *s* indicate pass-band and stop-band computed performances, respectively. N_f^p and N_f^s are the number of frequency points that in pass-band and stop-band that S-parameters are computed. The function in (15) is distinct from previous ones in that it considers different S-parameters for pass band and stop-band. In other words, while considering both absolute values of S_{11} and S_{21} rather than comparing them with a desired value, it essentially retains the policy to minimize the function for both terms in (I-32).

The same approach has been used to optimize stop-band planar filters in [36],

$$F(\vec{x}) = \sum_{pb=1}^{10} \left(\frac{S_{11}(f_{pb})}{-0.5dB} \right)^2 + \sum_{sb=1}^{5} \left(\frac{-40dB}{S_{21}(f_{sb})} \right)^2 + \sum_{sb=6}^{10} \left(\frac{-20dB}{S_{21}(f_{sb})} \right)^2 \qquad \textit{(I-33)}$$

Here, $\vec{x}$ is the parameters vector and subscripts *sb* and *pb* represent stop-band and pass-band, respectively. The optimization would stop once the criterion $F(\vec{x}) \leq 1$ is met. The insertion loss has two different values in the desired stop-band characteristics.

I.3.3 Least *p*th approximation ([7], [41], [42])

Another general category of objective is to minimize the sum of the powered magnitudes of the errors at different frequencies raised to power ρ,

$$T^{<k>}(f, \bar{p}) = \sum_{s=1}^{S} \left| D_{ij}^{<k>}(f_s, \bar{p}) \right|^{\rho} \qquad \textit{(I-34)}$$

In fact (I-34) can be considered as a generalization of the Least Squares Method. One significant feature of this approach is to emphasize or deemphasize on specific parts of frequency characteristics. While $\rho = 1$ the equation reduces to simple integration of the errors in the band. With $\rho = 2$ the method resembles to least squares. In general the higher ρ is, the more emphasize is given to larger errors (See [42], [47]). A necessary condition for having the least p approximation as efficient as possible is to having sufficient samples of the calculated objective function or in other words the number of frequencies in which the objective function is computed should be sufficiently large. Moreover the larger values of ρ will lead to more emphasize on larger errors. This statement can be proved by representing the error function as,

$$\max_{[f_{\min}, f_{\max}]} \left(\left| D_{ij}^{<k>}(f, \bar{p}^T) \right| \right) = \lim_{\rho \to \infty} \left(\frac{1}{f_{\max} - f_{\min}} \int_{f_{\min}}^{f_{\max}} \left| D_{ij}^{<k>}(f, \bar{p}^T) \right|^{\rho} .df \right)^{1/\rho} \qquad (I\text{-}35)$$

This implies that the larger ρ is, the more emphasized will be larger errors.

In .Fig. I- 4 the derivation of least *p* approximation is illustrated for different integer values of ρ. In Fig. I- 5 the least p approximation vs. different number of sample points is presented.

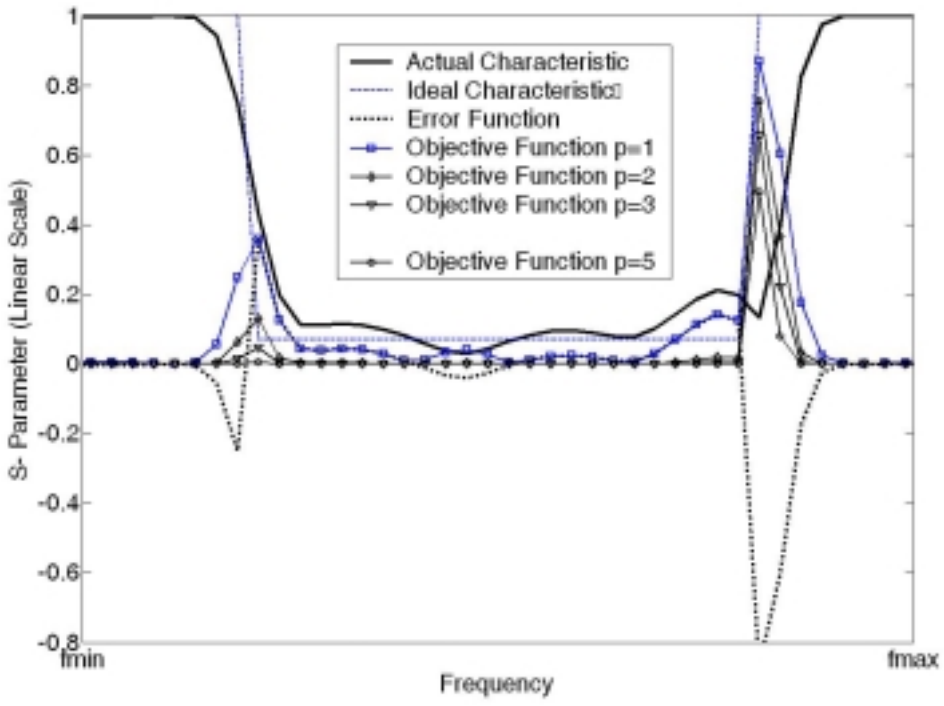

Fig. I- 4. The derivation of least *p* approximation

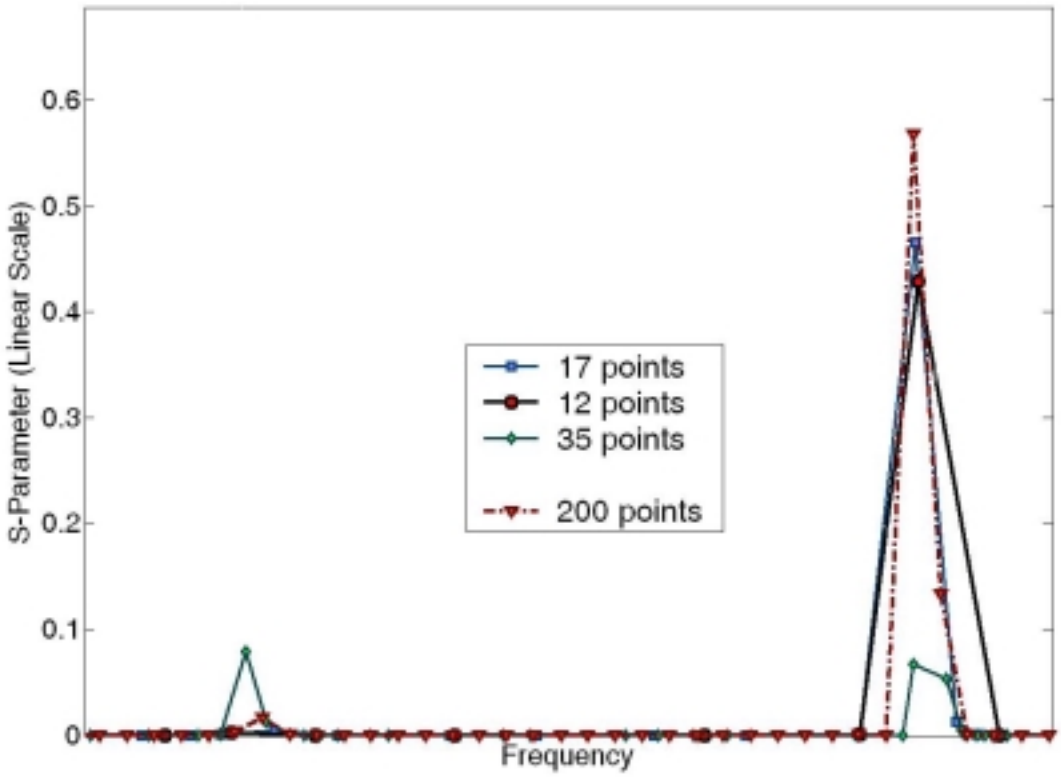

Fig. I- 5. The least p approximation vs. different number of sample points

This weighting scheme can be extended to consider the frequency aspect as well: the power can be a function of the deviation from central frequency. As the frequency gets further from a specific frequency, the errors are summed up with smaller exponent.

$$T^{<k>}(f,\bar{p}) = \sum_{s=1}^{S} \left| D_{ij}^{<k>}(f_s,\bar{p}) \right|^{p.\kappa(f,\hat{f},\hat{\tau})} \qquad \textit{(I-36)}$$

while $\kappa(f,\hat{f},\hat{\tau})$ is a function that incorporates frequency, into the power. $\hat{f} = \{ f_v \,|\, v = 1,2,...,V;\ f_v \in [\, f_{\min}, f_{\max}\,] \}$ is a vector containing all the frequencies of interest.

The size of neighborhood around each frequency $f_v \in \hat{f}$ is identified by $\tau_v \in \hat{\tau}$. Note that each $\tau_v \in \hat{\tau}$ is defined as a subset of the frequency range of interest and they have to comply with $f_1 - \tau_1 \geq f_{\min}$ and $f_V + \tau_V \leq f_{\max}$. The problem of optimizing a dual-band planar antenna seems to be an appropriate example for demonstrating the effects of vectors $\hat{f}$ and $\hat{\tau}$. The ideal return loss and the least pth approximation in an intermediate stage are shown in Fig. I- 6.

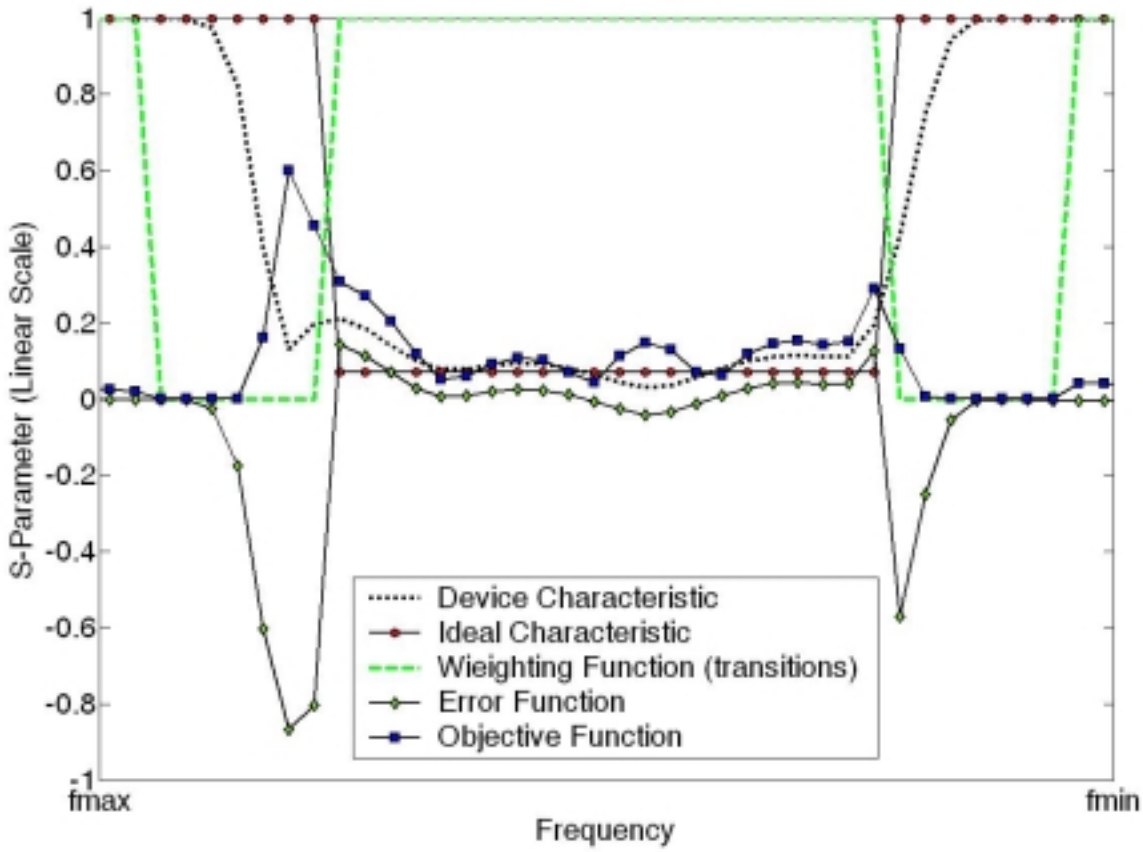

Fig. I- 6. The formation of objective function in equation (I-36) as. Here, p is equal to 3 and the function K is shown in the figure. This specific weighting function is usually used to mask the effect of transitions which diminish accuracy by producing big error terms in non-essential regions.

One potential risk of using the Least pth approximation is that the minimum of the function T in (I-34) does not necessarily correspond to the minimum point of (I-18) . The Least *p*th approximation has been used in few problems. In [16] the design of a Yagi-Yuda array and a rectangular patch antenna [16] are reported. In [38] the Least pth approximation is used for optimizing circuit performance.

I.3.4 Constrained problems

In a real world design optimization problem in microwave domain, not all possible values of the design parameters are acceptable. Almost all of the problems one has to deal with for the design of a microwave device or a network are constrained problems. Constrained optimization problems can either be solved directly with a constrained technique or converted to an equivalent unconstrained problem. The latter could either be done through,

- Defining the objective function so that all the constraints are included, or
- Transforming parameters and leaving the objective function unaltered.

The first approach is reported for example in [9] and also brought here. The latter will be explained in here, for example consider the constraint,

$$\bar{p}_{\min} \le \bar{p} \le \bar{p}_{\max} \qquad \textit{(I-37)}$$

Now we can define an unconstrained parameter vector $\bar{p}'$ in such a way that,

$$\bar{p} = \bar{p}_{\min} + (\bar{p}_{\max} - \bar{p}_{\min}) \sin^2(\bar{p}') \qquad \textit{(I-38)}$$

or

$$\bar{p} = \bar{p}_{\min} + \frac{1}{\pi}(\bar{p}_{\max} - \bar{p}_{\min}) \cot^{-1}(\bar{p}') \qquad \textit{(I-39)}$$

This is further addressed in [7] and [47].

The next step will be to solve the optimization problem for the unconstrained parameter $\bar{p}'$. Once the optimum vector for $\bar{p}'$ is determined, it will be easy to convert it to the original constrained vector $\bar{p}$. There are a handful of methods which have already been used for optimization problems with non-linear constraints. The reader is encouraged to review, for example [20] and [49]-[55].

I.3.5 Penalized objectives

Let the inequality constraints of the optimization problem be defined as a function,

$$\bar{C}(\bar{p}) = \left[C_1(\bar{p}) \quad C_2(\bar{p}) \quad . \quad . \quad . \quad C_M(\bar{p}) \right]^T \tag{I-40}$$

The vector $\bar{C}(\bar{p})$ is defined in such a way that,

$$C_m(\bar{p}) \geq 0, m = 1, ..., M. \tag{I-41}$$

For example the criterion

$$\bar{p}_{\min} \leq \bar{p} \leq \bar{p}_{\max} \tag{I-42}$$

can be reformulated as,

$$\bar{p} - \bar{p}_{\min} \geq 0 \tag{I-43}$$

$$\bar{p}_{\max} - \bar{p} \geq 0$$

Then to locate an initial point in feasible region, it is enough to deal with the following problem,

$$\textit{Minimize} \qquad -\sum_{m=1}^{M} w_m C_m(\bar{p}) \tag{I-44}$$

while the weighting factor is zero for any positive value of $C(\bar{p})$. Now the constrained domain can be transformed to an unconstrained domain with a penalized objective function,

$$T(f, \bar{p}, \upsilon) = \tilde{T}(f, \bar{p}) + \upsilon \sum_{m=1}^{M} \frac{1}{C_m(\bar{p})} \tag{I-45}$$

while $\upsilon > 0$ and $\tilde{T}(f_s, \bar{p})$ can be any of the objective functions introduced so far (see for example equations (I-23), (I-25)-(I-34)). The late equation defined the feasible region, as the interior of,

$$F = \left\{ \bar{p} \middle| \bar{C}(\bar{p}) = 0 \right\} \tag{I-46}$$

A sample of this approach is shown in equation (I-29). A critical task in here would be to choose the value of υ. At each step it is tried to reduce the coefficient υ that eventually diminishes the region *F*. In general, the requirement for convergence of

$T(f,\bar{p},\upsilon)$ in (I-45) is that $\tilde{T}(f,\bar{p})$ be convex and $C_q(\bar{p})$ be concave. In any case the problem of convergence of the original objective function $\tilde{T}(f,\bar{p})$ still lingers on. Assuming that $\tilde{T}(f,\bar{p})$ is convex and $C_m(\bar{p})$ is concave and both are differentiable, a constrained minimum at the point $\bar{p}^{opt}$ will satisfy,

$$\nabla T(\bar{p}^{opt}) = \sum_{m=1}^{M} c_m . \nabla C_m(\bar{p}^{opt})$$
$$\bar{c}.\bar{C}(\bar{p}^{opt}) = 0 \qquad \textit{(I-47)}$$

whereas $\bar{c} = \left[c_1 \ldots c_m \ldots c_M \right]$. These relations are proposed by Kuhn-Tucker [51]. They simply state that the gradient of the objective function is the linear combination of all constraint functions.

I.3.6 Exponentially penalized objective function

The goal in this section is to introduce an objective function which is as independent as possible to the initial point in parameter space. This depends on many factors including the nature of the problem and the polynomial degree of the objective function.

Moreover, the objective should have a minimum dependence on the way the ideal function is defined. In other words the tendency should be towards the goal of having minimum knowledge about the ideal design.

To define the new objective function, we restart from (I-18), and rewrite it for a single frequency f as,

$$D_{ij}^{<k>}(f,\bar{p}) = \begin{cases} \left|S_{ij}^{<k>}(f,\bar{p})\right| - \left|S_{ij}^{ideal}(f)\right| & f \in F_U \\ \left|S_{ij}^{ideal}(f)\right| - \left|S_{ij}^{<k>}(f,\bar{p})\right| & f \in F_L \end{cases} \qquad \textit{(I-48)}$$

While the same nomenclature as (I-18) is used. The frequency span is subdivided into two subsets. The subscripts *U* and *L* are chosen symbolically and do not necessarily mean *upper* and *lower* bounds. This is solely done to force the $D_{ij}^{<k>}(f,\bar{p})$ to be negative when the conditions are met. For example the insertion loss of a band pass filter is supposed to be more than a specific value in the pass band and less than a predetermined value in the stop-band. For the case of other structures such as a transition [56]or a coupler, one of the subsets F_U or F_L can be zero.

The penalized objective function has been studied in the previous chapter; the scheme proposed here is to apply the same concept for the error function. Let the objective function be defined as,

$$T(f,\bar{p}) = \begin{cases} \Phi_{NL}(D(f,\bar{p})) & D(f,\bar{p}) > 0 \\ 0 & D(f,\bar{p}) \le 0 \end{cases} \qquad \textit{(I-49)}$$

Here $\Phi_{NL}(x)$ is an arbitrary function of variable x. A discussion similar to that of the Least *p*th Approximation is valid here as well to support the idea of using nonlinear functions. The necessary condition for $\Phi_{NL}(.)$ is smoothness with respect to design variables in the feasible subset of the *N* dimensional parameter space which defines the $(f,\bar{p})$ vector. As a starting point let $\Phi_{NL}(.)$ be defined as an exponential function,

$$\Phi_{NL}(D(f,\bar{p})) = ae^{\chi.D(f,\bar{p})} \qquad \textit{(I-50)}$$

where χ and a are weighting coefficients to be determined based on the nature of problem. If we remove the point $D(f,\bar{p}) = 0$, the derivative of this function will have the form,

$$\frac{\partial \Phi_{NL}(D(f,\bar{p}))}{\partial p_i} = \frac{\partial (ae^{\chi D(f,\bar{p})})}{\partial p_i} = a\chi e^{\chi D(f,\bar{p})}.\frac{\partial (D(f,\bar{p}))}{\partial p_i} \qquad \textit{(I-51)}$$

and the second derivative will have the form of,

$$\frac{\partial^2 \Phi_{NL}(D(f,\bar{p}))}{\partial p_i^2} = a\chi e^{\chi D(f,\bar{p})}\left(\chi\left(\frac{\partial (D(f,\bar{p}))}{\partial p_i}\right)^2 + \frac{\partial^2 (D(f,\bar{p}))}{\partial p_i^2}\right) \qquad \textit{(I-52)}$$

The term $D(f,\bar{p})$ is the difference between two scattering parameters and thus the derivative can be written as,

$$\frac{\partial^n D_{ij}^{<k>}(f,\bar{p})}{\partial p_i^n} = \begin{cases} \dfrac{\partial^n \left|S_{ij}^{<k>}(f,\bar{p})\right|}{\partial p_i^n} & f \in F_U \\ -\dfrac{\partial^n \left|S_{ij}^{<k>}(f,\bar{p})\right|}{\partial p_i^n} & f \in F_L \end{cases} \qquad \textit{(I-53)}$$

Here $\left|S_{ij}^{<k>}(f,\bar{p})\right|$ is a smooth function of each parameter (p_i). Thus the function $D_{ij}^{<k>}(f,\bar{p})$ is smooth with respect to p_i as well. Thus the nonlinear function defined in (I-50) will be smooth with respect to any of design parameters.

The above discussion is not valid for smoothness of the objective function with respect to frequency but in any case the smoothness and derivability in frequency domain is out of our focus here because,

- in a gradient based optimization, the sensitivities with respect to design parameters are considered,
- the objective function for any fixed set of parameters (*i.e.* any value of parameter vector) is accumulated and these integrated variations are always smooth.

To further justify the above claim, a typical frequency-parameter space is depicted in Fig. I- 7. This figure shows typical variations of a device input characteristics versus frequency for different parameter value. In a gradient-based optimization the value of objective function is calculated as the integrated errors between the ideal and actual S-parameters in adjacent parameter planes.

The nonlinear objective described in (I-41) to (I-45) is basically designated as an unconstrained function. The approach chosen here to have this objective applicable to constrained problems is very similar to the penalized function described in (I-45).

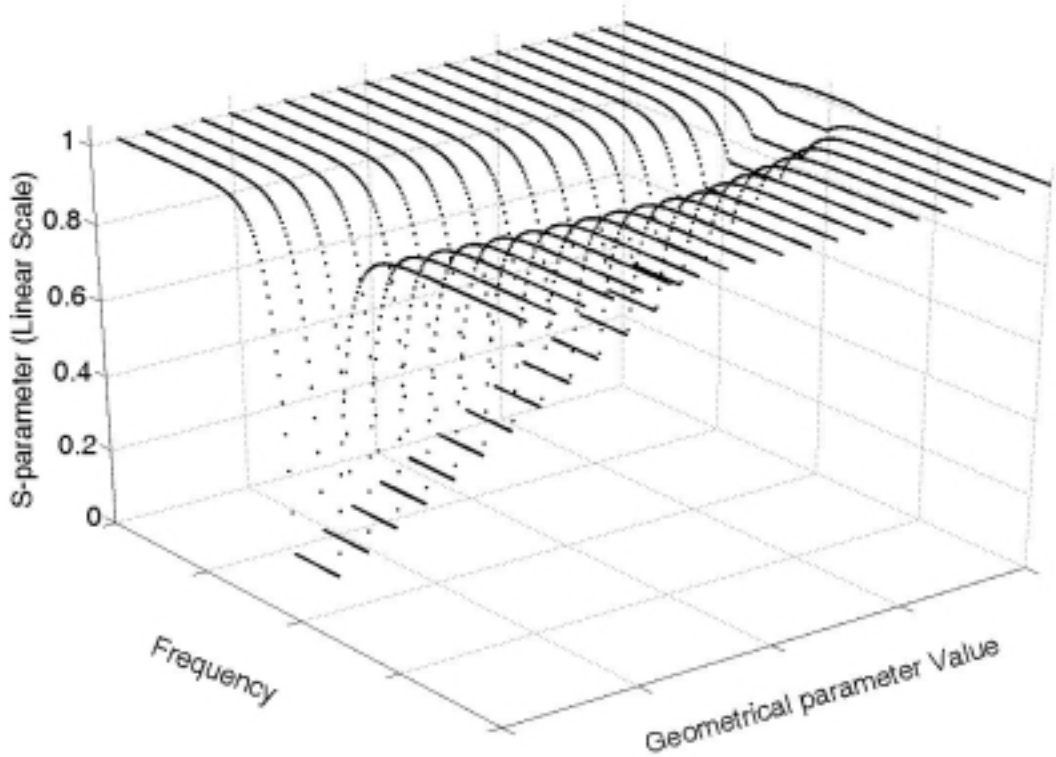

Fig. I- 7. A typical objective function with respect to frequency and geometry

Weighting factor

One major feature which improves the efficiency of the over-all optimization procedure is the ability to emphasize on specific parts of frequency characteristics. This can be done through a weighting factor. The weighting factor is a function of frequency. A very important application of the weighting factor is to mask the transient regions between pass band and stop band in filtering response for example. Normally the desired characteristic has a rectangular or trapezoid shape. The actual frequency response is an irregular curve in borders. The error produced by differentiating the calculated and desired characteristics will be dominated by the error produced in transitions. An appropriate weighting function can mask the effect of the error function. Fig. I- 8 illustrates the effect of weighting factor and the error that would appear due to the transition otherwise. For the general form of the objective function in (I-51) the weighting factor can be integrated as,

$$T(f,\bar{p}) = \begin{cases} W(f).\Phi_{NL}(D(f,\bar{p})) & D(f,\bar{p}) > 0 \\ 0 & D(f,\bar{p}) \le 0 \end{cases} \qquad \textit{(I-54)}$$

Another application of the weighting factors is when the objective function is formed of functions with different orders of magnitude. For example the objective function for the design of a resonator can be composed of its center frequency and quality factor, while these two numbers have different orders of magnitude; the center frequency (*fc*) can be of the order of GHz (10^9 Hz) when the quality factor (*Q*) is at most of the order of tens of thousands (10^4) and it's evident that an objective function in the form of,

$$T(\bar{p}) = \left| f_c^{calculated} - f_c^{ideal} \right| + \left| Q^{calculated} - Q^{ideal} \right| \qquad \textit{(I-55)}$$

is totally dominated by the frequency error. In such a case the appropriate weighting factors can be utilized in order to have both measures (frequency and Q) effective in the objective function. Thus the weighted objective function is written as,

$$T(\bar{p}) = \alpha \left| f_c^{calculated} - f_c^{ideal} \right| + \beta \left| Q^{calculated} - Q^{ideal} \right| \qquad \textit{(I-56)}$$

for a typical filter or resonator α and β would have a difference of (10^4 – 10^6) in orders of magnitude.

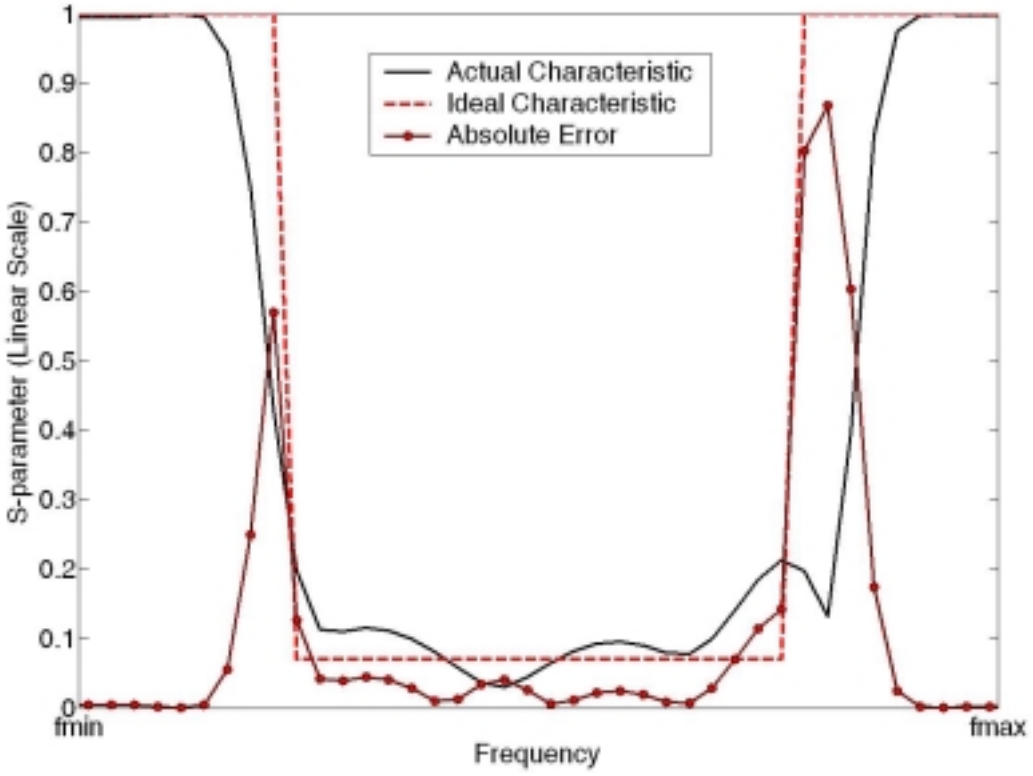

(a)

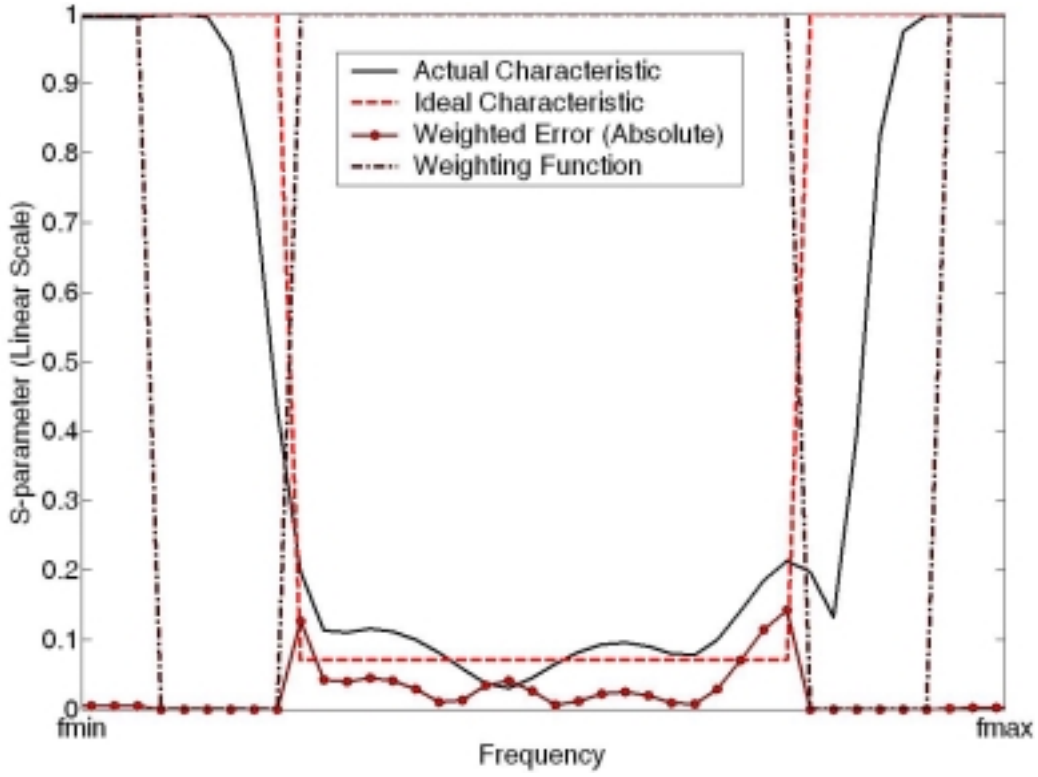

(b)

Fig. I- 8. (a) the error caused by transitions and (b) weighting factor used for masking the errors

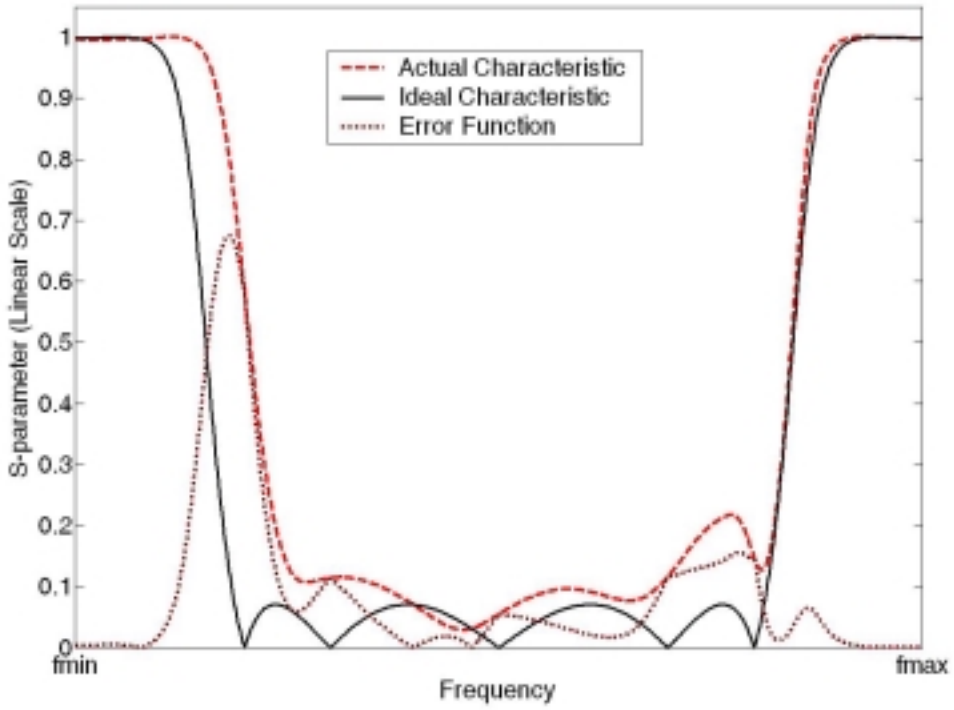

(a)

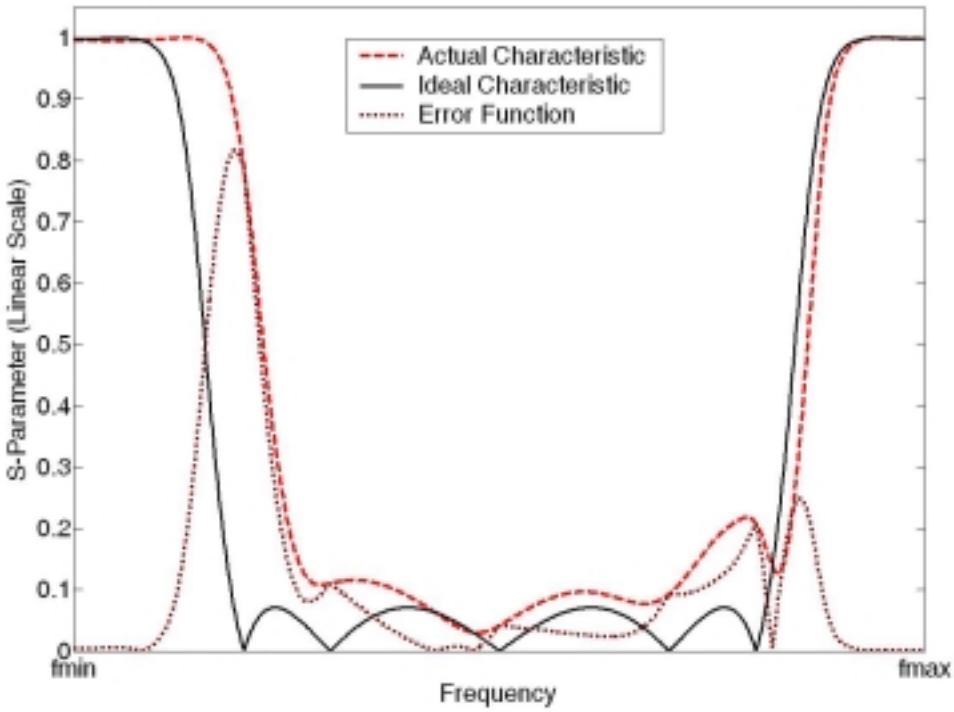

(b)

Fig. I- 9. A problem encountered when using mathematical functions for modeling the ideal (desired) characteristics. In (a) absolute error is shown. In (b) the same ideal function is applied, but due to very small change in dimensions, the filter is detuned for about 0.0001 of the central frequency. A significant change can be seen in error function, resulting the gradients being completely meaningless.

I.3.7 Ideal characteristic

The ideal characteristic of a microwave device is usually defined based on a specific mathematical function. More specifically filters have classically been designed based on known filtering functions such as Chebyshev functions, Butterworth functions, Elliptic functions, etc.[57]. For each of these functions there are very accurate equivalent circuit models which are both mathematically and physically feasible. There are established building blocks for each of these functions with given orders. With an optimization procedure that utilizes circuit analogy, defining the initial structure can be achieved through finding the appropriate microwave passive structure which corresponds to that equivalent circuit topology. An example of this procedure is explained symbolically in Fig. I- 10.

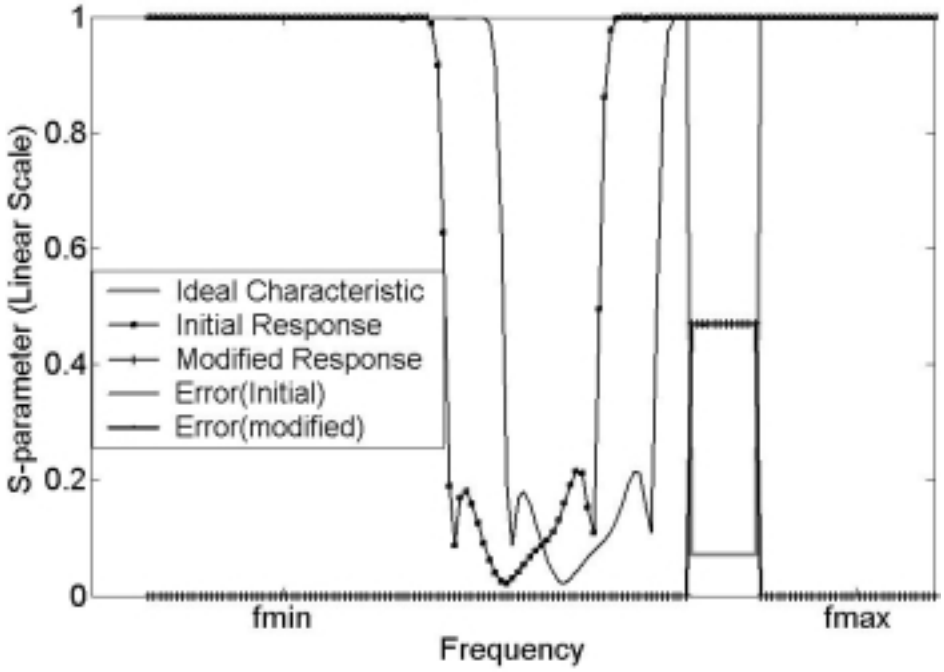

Fig. I- 10. The gradients when detuning is considerable. Note that absolute error (which could be a base for calculating the objective function) does not change and thus the gradient is zero. Although the device characteristic in (b) shows a considerable improvement, the improvement is not reflected in the error function.

Such an approach has been used in [18],[28],[45] and [56]-[58].

The above-mentioned approach has some prerequisites,

- The choice of appropriate function is very critical. Such a decision appears as an obstacle in automation of the optimization procedure. In other words, the procedure always needs an operator to choose the appropriate function which best fits the desired characteristic.
- Mathematical functions have their own limitations. Sometimes none of the conventional mathematical functions are not capable of matching the desired characteristics. For example, some non-ideal filtering factors such as ripple or bandwidth-loss trade off affect the overall convergence of optimization.
- Defining ideal characteristic in some few points in frequency domain, on the other hand, has its own drawbacks. A little discrepancy between poles and zeros may generates big error terms. Fig. I- 9 illustrates a typical problem occurred when using a pseudo-elliptic ideal characteristic. It can be viewed that initial response has to have the same central frequency in order to have the optimization converged. Thus appropriate choice of initial response is crucial when using mathematical functions.

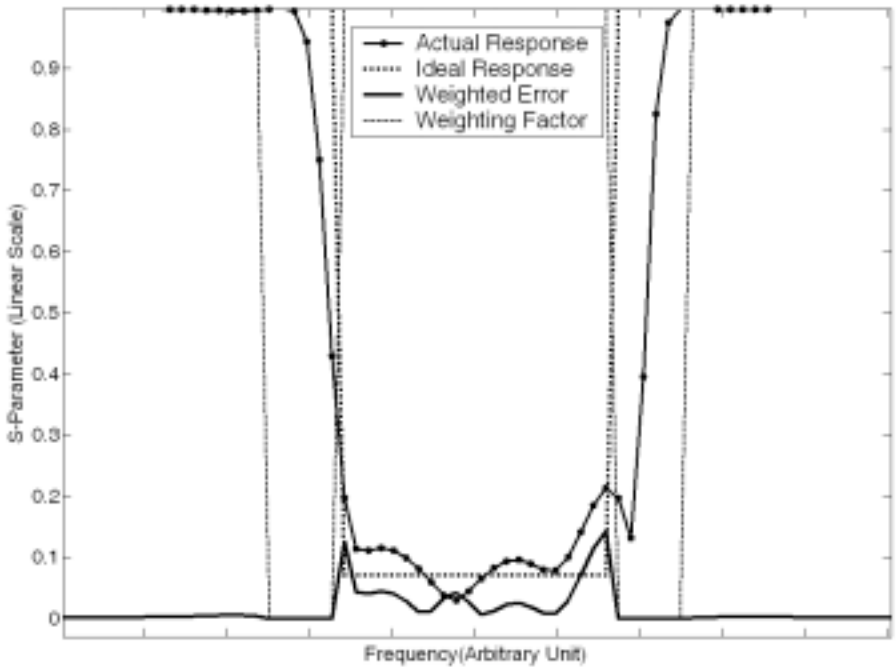

Fig. I- 11. The error produced using different scenarios

The alternative method, which is simpler, is to define the virtual barriers, so that the frequency response is upper(or Lower) than this barrier in all frequencies. In other words, the desired characteristics can be defined as a set of simple linear borders in

whole frequency range of concern. In Fig. I- 11 the ideal characteristics defined with linear borders is illustrated. Using this method, the optimization procedure is less dependent upon an operator for finding a mathematical pattern.

Two discussed methods of defining objective functions can function appropriately when the initial response is reasonably close to the ideal characteristic. Otherwise the calculated error(difference) is very small and the gradients obtained in this way are not meaningful. By meaningful we intend the gradients which really show the direction of the change in parameter vector. When the detuning is quite considerable, in such a way that the ideal and actual pass-bands have no or a very small overlap. Such an ideal response is utilizable as long as the initial response has a considerable overlap with this rectangular region. What happens in a real design practice is somehow different. Normally the detuning is quite considerable in such a way that the ideal and actual pass-bands have no or a very small overlap. This would make gradients approximated through Finite differencing meaningless. As a possible way, the proposed ideal response is slightly modified so that the gradient can be obtained when ideal and actual functions have no overlap; *e.g.* when a filter is strongly detuned. The modified ideal function can be expressed as,

$$S_{11}^{<MOD>}(f)=\begin{cases} D_{ij}^{<k>}(f_s,\bar{p}).\left(1-\exp\left(\dfrac{f-f_c-BW/2}{\zeta}\right)\right) & f \geq f_c+BW/2 \\ S_{11}^{inband} & |f-f_c| \leq BW/2 \\ D_{ij}^{<k>}(f_s,\bar{p}).\left(1-\exp\left(\dfrac{f-f_c+BW/2}{\zeta}\right)\right) & f \leq f_c-BW/2 \end{cases} \qquad \textit{(I-57)}$$

where $D_{ij}^{<k>}(f,\bar{p})$ is defined in (I-18).

The modified ideal response is shown in Fig. I- 12. Using this ideal response, the gradients are less precise or better to say less sensitive to variations of the dimensions. This is because when integrating the error between the actual and ideal S_{11} the area under the ideal response is relatively larger and the error produced in this way is less sensitive to variations of the dimensions. On the other hand, using a bigger ζ would guarantee catching a more exaggerated detuning; *i.e.* when the initial working band is very far from the desired characteristic.

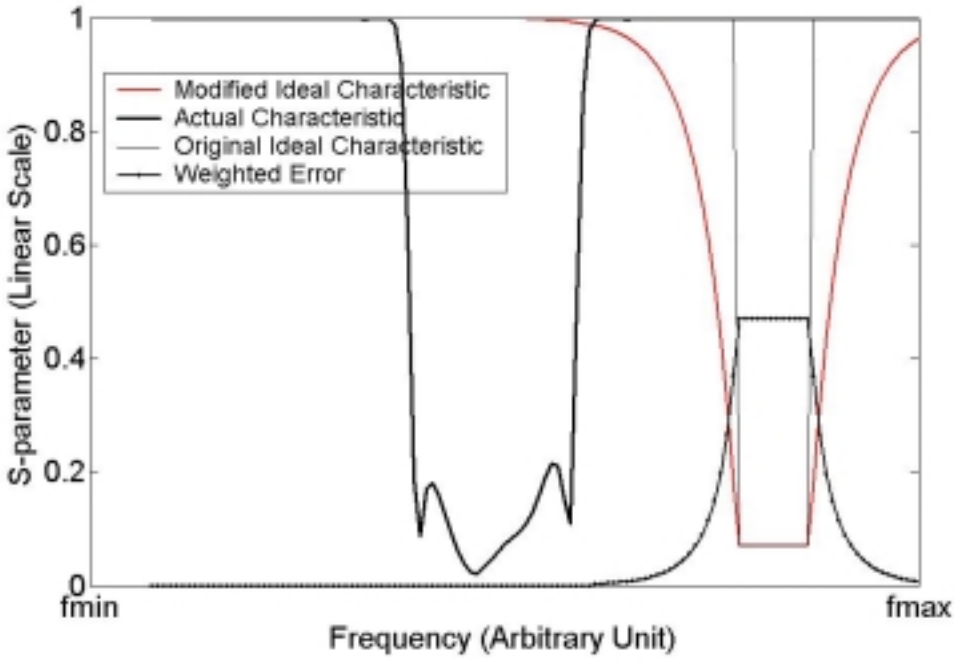

(a)

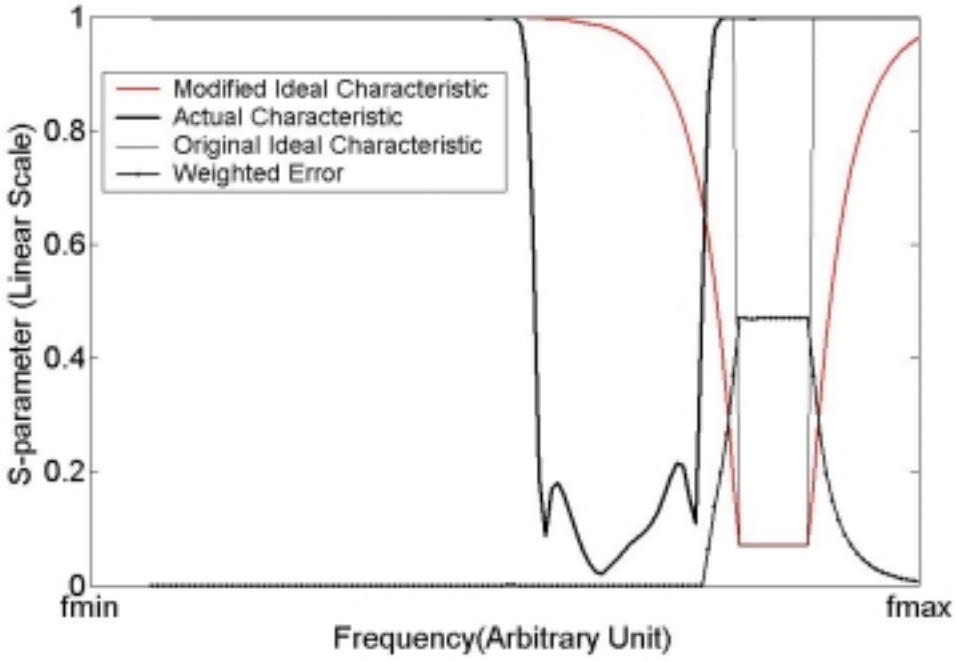

(b)

Fig. I- 12. The modified ideal response and calculated error $T_{11}(f)$. It can be noticed that moving the central frequency (beteen the positions shown in (a) and (b)) could be detected in the objective function.

So, there should be a trade-off between sensitivity and frequency span. Let the index η be defined as,

$$\eta = \eta\left(f_{\det} - f_c, \zeta\right) \qquad \textit{(I-58)}$$

which is a measure of precision. Apparently η is a function of detuning (f_{det} and f_c are frequencies of detuned and ideal responses) and ζ in (I-57). To model such a trade off a numerical experiment has been conducted using a sample detuned S_{11} and different values of ζ. Then the error function is calculated with respect to different f_{det} and ζ. In Fig. I- 13 variations of normalized η versus different parameters is demonstrated. Fig. I- 14 shows a normalized contour of the gradients of the objective function with respect to ζ and $f_{det.}$ For a given f_{det} ,the chosen value of ζ is the point where the gradient of error function has it's minimum acceptable value (this is a function of precision of numerical method chosen and the required design precision as well).

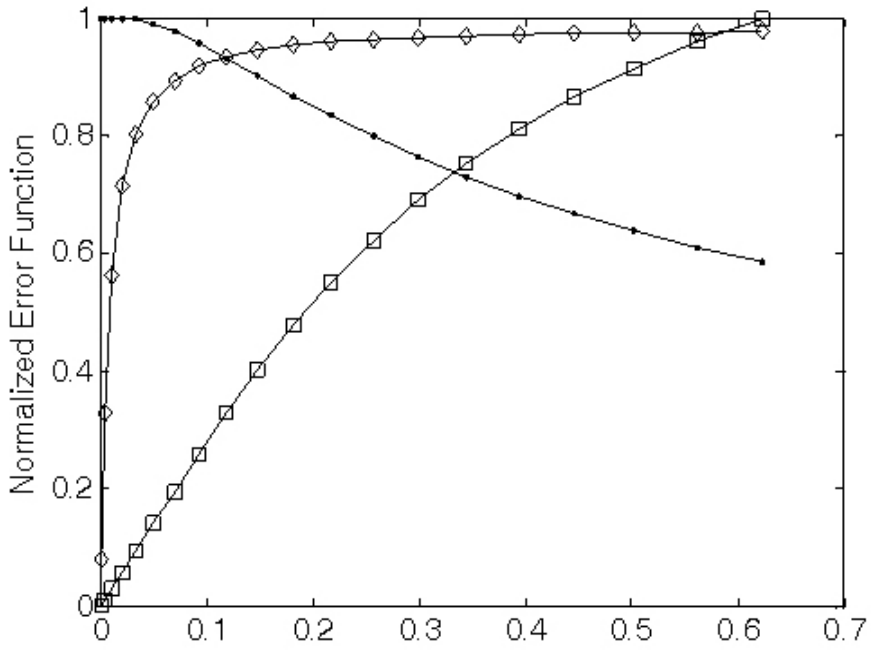

Fig. I- 13. Normalized η vs different values of ζ / f_c . –Normalized Error Function of the example shown in Fig. 3. ◊-Ratio between Modified and classical error functions -Modified Error function

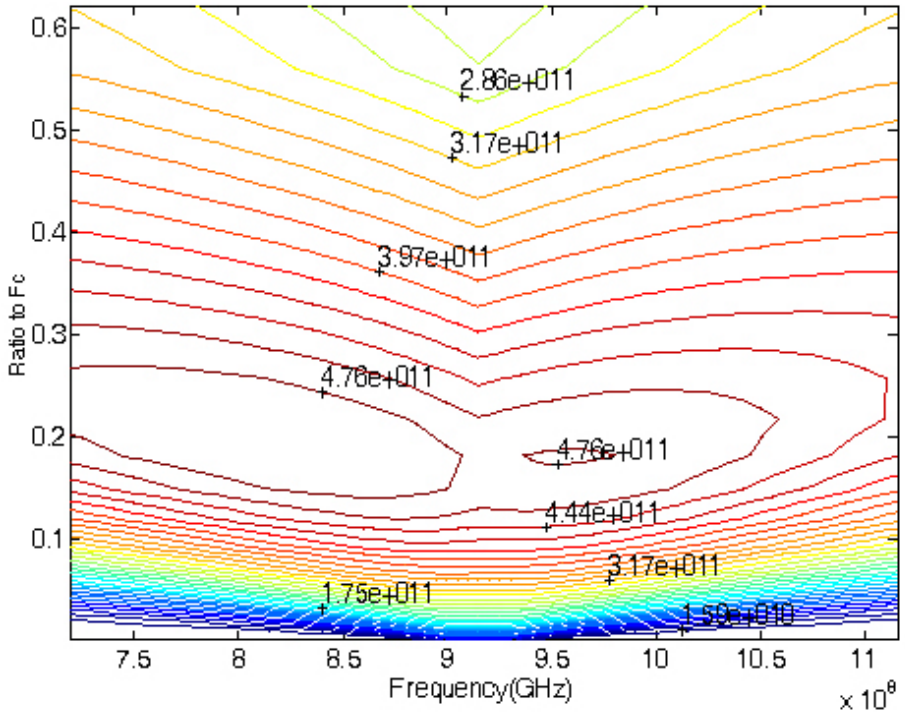

Fig. I- 14. Normalize η vs Detuning (f_{det} :Horizontal) and ζ / f_c ratio (Vertical). The feasible region is chosen on the basis of design tolerances and accuracy of the EM solver.

I.4 Search strategies

Perhaps the core step in computer-aided design (CAD) of microwave component design algorithm is the optimum search process. Once an appropriate objective function is defined, an efficient search strategy must be utilized to update the dimensions in the optimization cycle until the required criterion are met. Optimization, as an independent research area, has been established since long time ago. A wide variety of optimization algorithms have been offered by researchers of this area, from purely random procedures to very deterministic methods. Each of these methods has its own advantages and drawbacks. Obviously, judging about the viability of a technique depends on the application and also the metrics we are trying the method with. Relatively long computation time of an electromagnetic field solver is the major bottleneck that every designer has to deal with. While a typical objective function calculation in other disciplines (*e.g.* economy, management, operational research) can take less than a second, every calculation of objective function in microwave domain might take a few hours to few days. This in turn limits both parameter space dimensionality and number of iterations. In other words, a proper candidate for search algorithm in CAD of microwave components should be a method which minimizes (or maximizes) the objective function in a parameter space of small dimensionality in the least possible iterations.

The previous work on CAD of microwave devices and circuits can be categorized into three main groups, namely, stochastic methods such as Genetic Algorithms (GA) and Design of Experiments (DoE), indirect optimization methods such as Neural Networks (NN) and Gradient Optimization (GO). Among all the methods, Gradient Optimization method is the oldest and still the most practical method for optimization because of its efficiency and consistence. Comparing to two other methods, gradient methods require much fewer number of iteration until they converge to the desired solution. Moreover gradient methods are less dependent on the problem than other two categories. What made researchers to look for alternatives for GO is the fact that these methods are inherently local methods. In other words the success of optimization depends on the initial set of parameters chosen to start the optimization. All that a GO can do is to find the closest minimum (maximum) to the initial point in the parameter space. Thus there is always a risk of failure by being trapped in a local

minimum. The other shortcoming of GO's is that they need precise calculation of gradients at every step. Calculating gradients is computationally an expensive task.

Evolutionary algorithms (EA) on the other hand, are stochastic methods which reach to an optimum by evolving a randomly initiated population (a group of parameter vectors in feasible region) into minimum (maximum). Evolutionary algorithms are global methods, and as long as the initial population is large enough, the success of the optimization does not depend on the appropriate choice of initial point.

A typical microwave design problem has to deal with a multidimensional parameter. The dimensionality of space usually does not exceed 20-30, and it is often smaller, but anyways the search algorithm should be chosen considering such a dimensionality. Thus most of this chapter is devoted to the introduction of multidimensional search algorithms which fit more to microwave design applications. The rational method to pursue such a design problem is to use multidimensional search, but in some cases it is possible to use several uni-dimensional algorithms to optimize different dimensions.

I.5 Direct search methods [59]

Direct methods form a minor branch of search strategies. At each step, direct search methods decide the next trial solution based on the experience from past steps. Unlike gradient optimization techniques, these methods only rely on evaluation of value of the function for deciding the search direction. Although the direct methods have not been used as widely as gradient methods, they are addressed in detail since the understanding the methods used later in this dissertation require priori knowledge of direct methods. One major advantage of direct methods in microwave domain is when a commercial package is used as the EM solver and only absolute field values are available. Computing derivatives at each point requires an extra cost of multiple calculations which diminishes the efficiency of the algorithms. A direct algorithm then becomes very instrumental.

I.5.1 Pattern search [68],[69]

Pattern search attempts to find the direction of search along the valley. Since this method attempts to follow the pattern drawn by hyper contours, it performs very well in narrow valleys. The method is explained in Fig. I- 15. The method starts with comparing two adjacent points which are aligned with one of coordinates. After finding the right direction of declining towards the minimum, the same procedure repeats with other coordinates. Once the decline direction with a complete set of coordinates is identified, a vector addition of all the decline directions is composed and the next point is decided based on this vector.

I.5.2 Simplex optimization [18]-[21]

The simplex methods are based on an initial design of k+1 trials, where k is the number of variables. A k+1 geometric figure in a k-dimensional space is called a simplex. The corners of this figure are called vertices. Fig. I- 16 shows a simplex in two dimensional parameter space.

With two variables the first simplex design is based on three trials, for three variables it is four trials, etc. This number of trials is also the minimum for defining a direction of improvement. Therefore, it is a timesaving and economical way to start an optimization project.

After the initial trials the simplex process is sequential, with the addition and evaluation of one new trial at a time. The simplex searches systematically for the best levels of the design parameters. The optimization process ends when the optimization objective is reached or when the responses cannot be improved further.

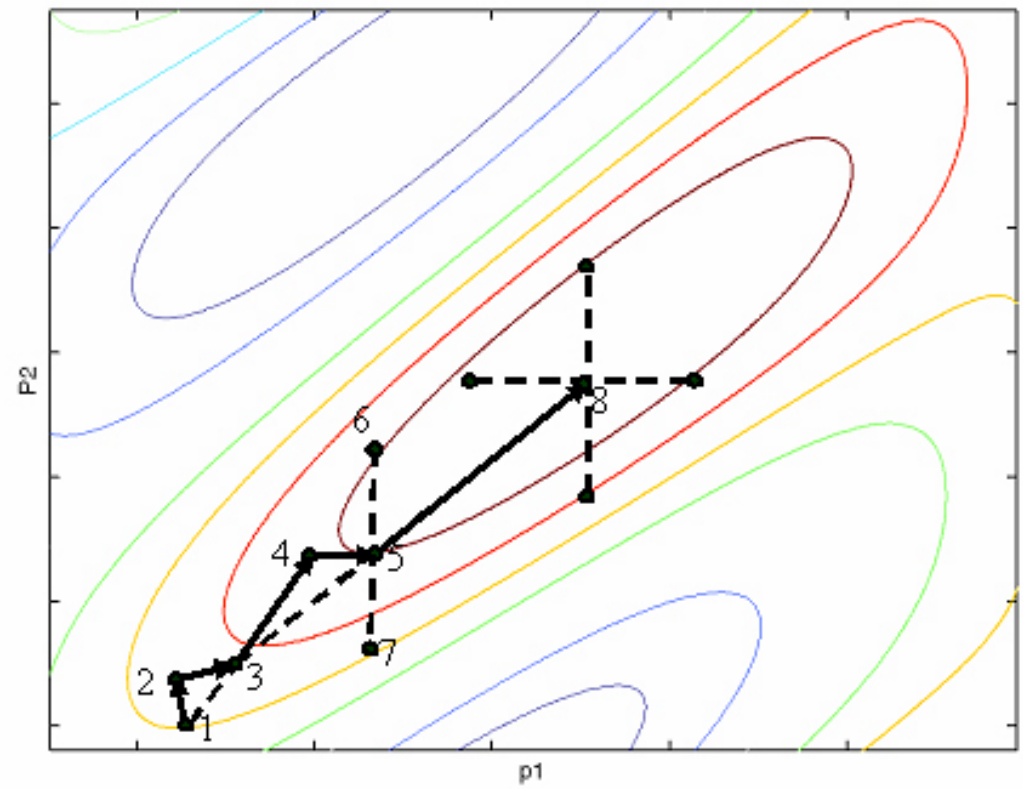

Fig. I- 15. Pattern search method

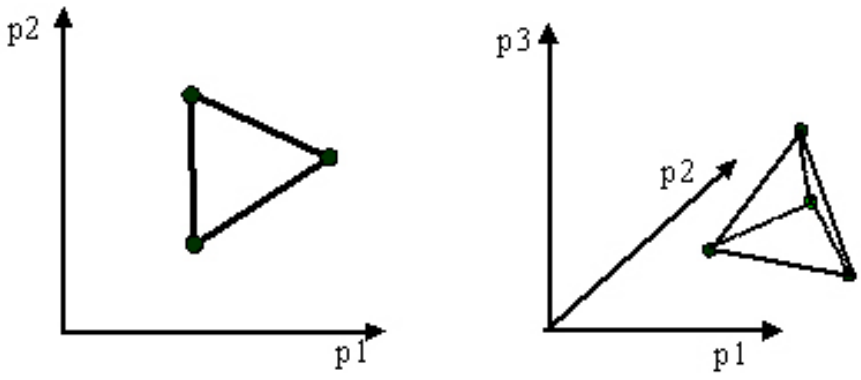

Fig. I- 16. Simplex in two and three dimensional parameter spaces

I.5.2.1 Basic simplex method

The basic simplex method is easy to understand and apply. The optimization begins with the initial trials. The trial conditions are spread out efficiently. The number of initial trials is equal to the number of design parameters plus one. These initial trials form the first simplex. The shapes of the simplex in a one, a two and a three variable search space, are a line, a triangle or a tetrahedron. A geometric interpretation is difficult with more variables, but the basic mathematical approach outlined below can handle the search for optimum conditions.

The basic simplex algorithm consists of a few rules,

The first rule is to reject the trial with the least favorable response value in the current simplex.

A new set of design parameter levels is calculated, by reflection into the design parameter space opposite the undesirable result. This new trial replaces the least favorable trial in the simplex. This leads to a new least favorable response in the simplex that, in turn, leads to another new trial, and so on. At each step you move away from the least favorable conditions. By that the simplex will move steadily towards more favorable conditions.

The second rule is never to return to design parameter levels that have just been rejected.

The calculated reflection in the design parameters can also produce a least favorable result. Without this second rule the simplex would just oscillate between the two design parameter levels. This problem is nicely avoided by choosing the second least favorable condition and moving away from it. (Fig. I- 17)

Besides the two main rules, two more rules are also used :

- Trials retained in the simplex for a specified number of steps are reevaluated. The reevaluation rule avoids the simplex to be stuck around a false favorable response.
- Calculated trials outside the effective boundaries of the design parameters are not made. Instead a very unfavorable response is applied, forcing the simplex to move away from the boundary.

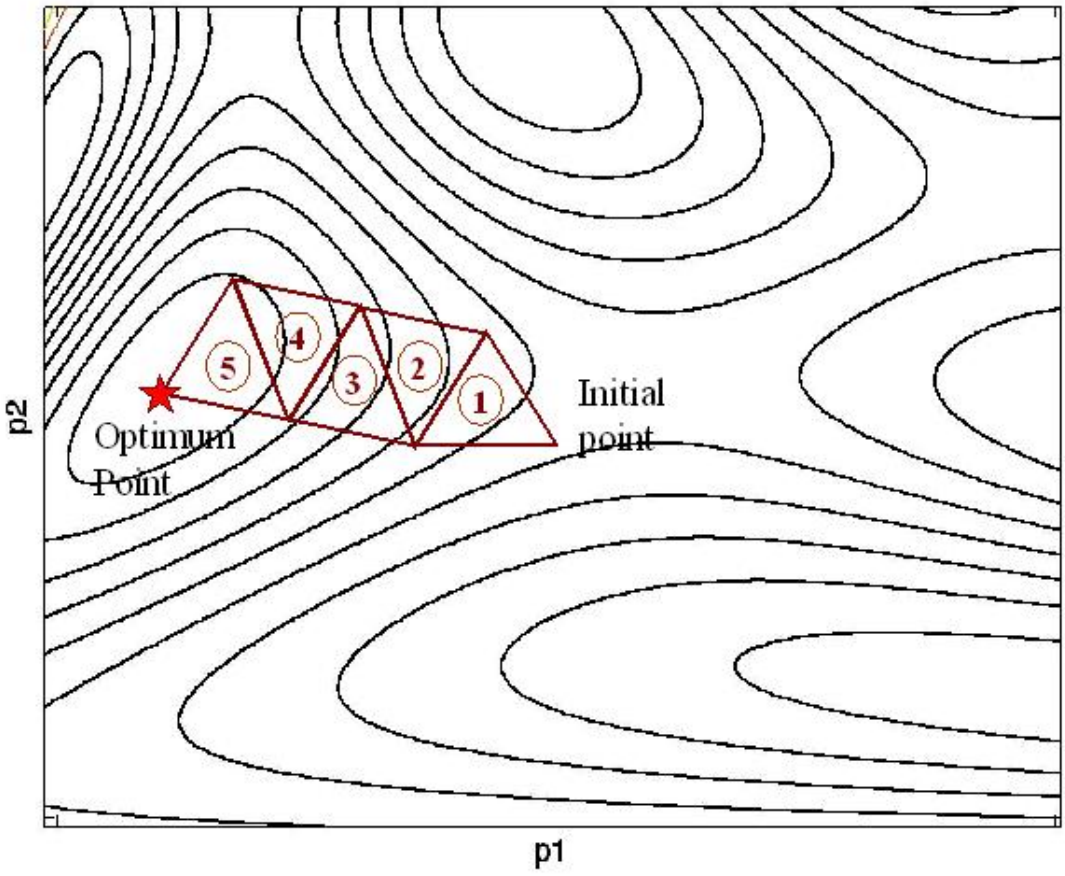

Fig. I- 17. Simplex method.

I.5.2.2 Modified simplex method

The modified simplex method has much in common with the basic method, but can adjust its shape and size depending of the response in each step. This method is also called the variable-size simplex method. Several new rules are added to the basic simplex rules. These new rules make the simplex:

- expand in a direction of more favorable conditions, or
- contract if a move was taken in a direction of less favorable conditions.

The procedures for expansion and contraction enable the modified simplex both to accelerate along a successful track of improvement and to home in on the optimum conditions. Therefore the modified simplex will usually reach the optimum region quicker than with the basic method and pinpoint the optimum levels more closely.

The degree of contraction depends on how unfavorable the new response is. Fig. I- 18 illustrates the different moves with the modified simplex method.

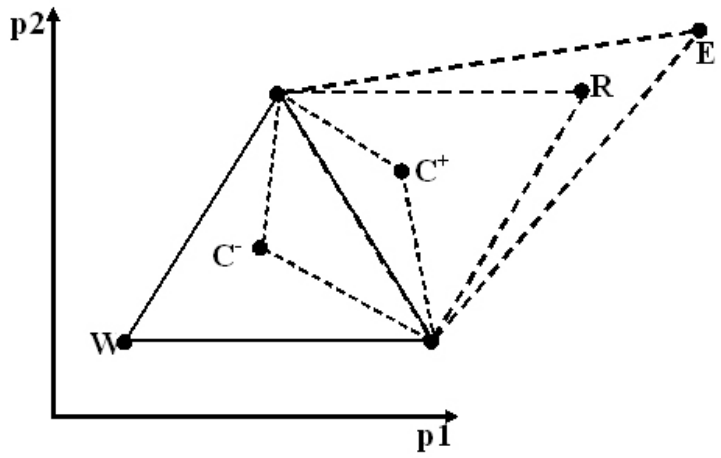

Fig. I- 18. Modified Simplex method

For each simplex the following labels are used: ***W*** for the least favorable trial or the trial being rejected, ***B*** for the most favorable trial and $\boldsymbol{N_w}$ for the second least favorable trial (i.e. next-to-the worst).

The different projections away from the rejected trial are calculated according to the following formulas:

$$R = \bar{C} + \alpha(\bar{C} - W) \qquad \textit{(I-59)}$$
$$E = \bar{C} + \gamma(\bar{C} - W)$$
$$C^{\pm} = \bar{C} + \beta^{\pm}(\bar{C} - W)$$

where

W is the rejected trial,

$\bar{C}$ is the centroid of the remaining face/hyperface, i.e. the average levels for the remaining trials,

α is the reflection coefficient,

γ is the expansion coefficient,

$\beta^{\pm}$ is the positive or negative contraction coefficient.

Simplex method has rarely been used to optimize microwave devices and networks. In fact the method does not offer any specific advantages over other contemporary methods. Example applications of simplex method can be found in [74]and [75].

I.6 Gradient search methods

Gradient methods include all the methods that utilize partial derivatives of objective function at each step to find the next step. Despite shortcomings of these methods reported, gradient methods are still found to be the most viable techniques in microwave domain. The fact that these methods are very efficient has encouraged research to overcome their drawbacks. Here the major gradient methods are described. In practice, more sophisticated methods are used to meet requirements of complex problems. These sophisticated methods are combination of basic methods described in here.

In the following chapters, it has been tried to follow a simple to complicated trend in explaining the gradient methods.

I.6.1 Notations

A microwave optimization problem can be defined as,

$$\textit{Find} \quad \bar{p}^{<optimum>}, \qquad \textit{So that} \quad T(\bar{p}^{<optimum>}) = \min\{T(\bar{p})\} \tag{I-60}$$

where T is the error function.

The procedure to construct the objective function was discussed in detail before. $\bar{p} = [p_1\ p_2 \ldots p_N]^T$ is an N-dimensional vector, called the parameter vector. The space including all the parameter vectors is called *parameter space.* The dimensionality of a parameter space is equal to the number of element of the vector $\bar{p}$.

In general the minimization is subject to constraints,

$$\bar{C}_{M\times 1}(\bar{p}) \le \bar{b}_{M\times 1} \tag{I-61}$$

The objective function can be expanded with Taylor series as,

$$T(\bar{p}+\Delta\bar{p}) = T(\bar{p}) + [\nabla T(\bar{p})]^T .\Delta\bar{p} + \frac{1}{2}.\Delta\bar{p}^T .H\left(T(\bar{p})\right).\Delta\bar{p} + \ldots \tag{I-62}$$

The vector

$$\nabla T(\bar{p}) = \left[\frac{\partial T(\bar{p})}{\partial p_1}\ \frac{\partial T(\bar{p})}{\partial p_2} \ldots \frac{\partial T(\bar{p})}{\partial p_N}\right]^T \tag{I-63}$$

is called the gradient vector. The vector containing the second order derivatives is called Hessian Matrix,

$$H\left(T(\bar{p})\right)=\begin{bmatrix} \frac{\partial^2 T(\bar{p})}{\partial p_1^2} & \frac{\partial^2 T(\bar{p})}{\partial p_1 \partial p_2} & \cdot & \cdot & \frac{\partial^2 T(\bar{p})}{\partial p_1 \partial p_N} \\ \frac{\partial^2 T(\bar{p})}{\partial p_2 \partial p_1} & \cdot & & & \cdot \\ \cdot & & \cdot & & \cdot \\ \cdot & & & \cdot & \cdot \\ \frac{\partial^2 T(\bar{p})}{\partial p_N \partial p_1} & \cdot & \cdot & \cdot & \frac{\partial^2 T(\bar{p})}{\partial p_N^2} \end{bmatrix} \qquad \textit{(I-64)}$$

or it can be represented as,

$$H_{ij}\left(T(\bar{p})\right)=\frac{\partial^2 T(\bar{p})}{\partial p_i \partial p_j} \qquad \textit{(I-65)}$$

In the following chapter, the classical gradient-based methods are discussed. In practice, very often different variations of these methods or combination of different methods are used to fit the specific applications of interest.

I.6.2 Steepest descent method [76]-[77]

The core idea of the steepest descent method is to use the derivatives of the objective function to find the stationary point. More physically speaking, if one tries to follow a path towards the lowest point of the valley, the simplest possible path will be to find the steepest path at each point.

The left hand side of (I-62) can be re-written as,

$$T(\bar{p}+\Delta\bar{p})=T(\bar{p})+\Delta T(\bar{p}) \qquad \textit{(I-66)}$$

Considering only first two terms of right hand side of (3) would yield a linear approximation,

$$\Delta T(\bar{p})=\left[\nabla T(\bar{p})\right]^T.\Delta\bar{p} \qquad \textit{(I-67)}$$

which means that the gradient vector coincides with the direction of fastest move towards minimum or maximum change. The steepest descent strategy is based on moving backwards this gradient vector at each step, to find out the normalized vector

which shows the direction of steepest descent, the normalized gradient vector is written as,

$$\vec{s} = \frac{\nabla T(\bar{p})}{\left\|\nabla T(\bar{p})\right\|} \qquad \textit{(I-68)}$$

Thus at each iteration, the steepest descent update strategy will be,

$$\bar{p}^{<k+1>} = \bar{p}^{<k>} - w^{<k>}\vec{s}^{<k>} \qquad \textit{(I-69)}$$

Whereas superscripts *k* shows the iteration number, and $w^{<k>}$ is a positive scalar called weighting factor which can be chosen adaptively. When the initial point is very far from the local maximum, taking long steps (bigger values of $w^{<k>}$) accelerated the convergence. On the other hand at vicinity of the optimum point, smaller steps should be taken to avoid skipping the local minimum. Fig. I- 19 shows the concept of the steepest descent in a two-dimensional parameter space.

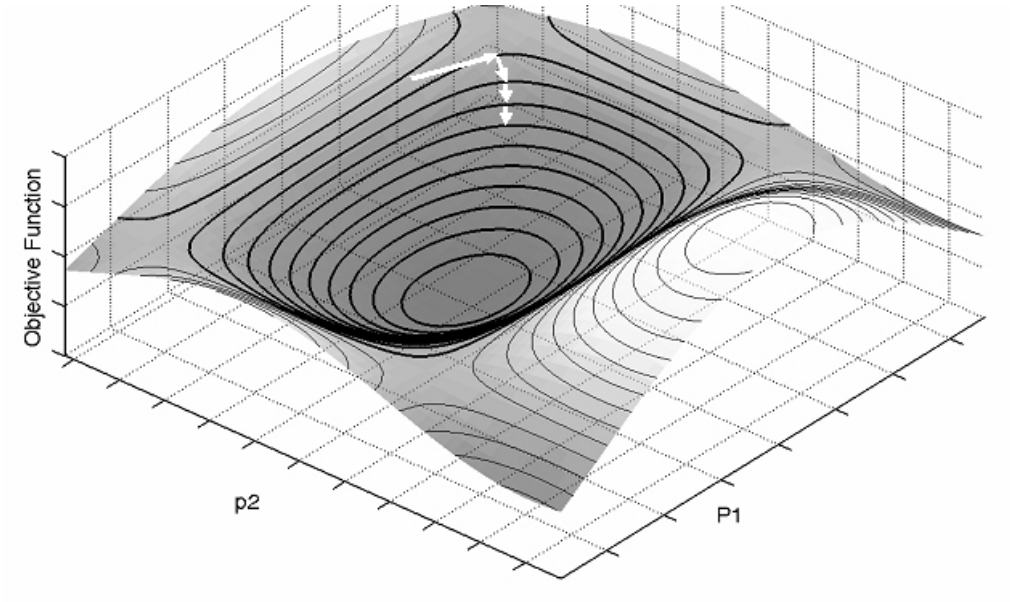

Fig. I- 19. Steepest descent method

The steepest descent method and its variation is one the most frequently used techniques in optimization. The method is very easy to implement and flexible enough to be integrated to other techniques in a hybrid algorithm. Despite these advantages, the method suffers from extremely slow convergence. Moreover, as any other gradient methods the steepest descent method is a local method and the success of the search severely depends on the initial point.

I.6.3 Newton's method

As mentioned above the steepest descent method suffers from slow convergence. This is a normal consequence of using a linear function as update strategy. One possible way of improving the convergence speed is thus using quadratic schemes. A family of optimization techniques which use the information of second order derivatives for parameter update is called Newton's method. Given that in the minimum point the objective function is stationary,

$$\nabla T(\bar{p}^{<opt>}) = 0 \qquad \textit{(I-70)}$$

or in other words,

$$T(\bar{p} + \Delta\bar{p}) = T(\bar{p})$$

while $\bar{p}^{<opt>}$ is the point at which optimum solution occurs. Now considering three terms in right hand side of (I-62), would yield,

$$\nabla T(\bar{p}) + H(T(\bar{p})).\Delta\bar{p} \cong 0 \qquad \textit{(I-71)}$$

The step to be taken to reach the minimum (maximum) point is

$$\Delta\bar{p} \cong -\left[H(T(\bar{p}))\right]^{-1}.\nabla T(\bar{p}) \qquad \textit{(I-72)}$$

thus the update equation would have the following form,

$$\bar{p}^{<k+1>} = \bar{p}^{<k>} + \Delta\bar{p} = \bar{p}^{<k>} - w^{<k>}\left[H(T(\bar{p}))\right]^{-1}.\nabla T(\bar{p}) \qquad \textit{(I-73)}$$

Again $w^{<k>}$ is a positive scalar which defines the step size. An example of Newton's method is illustrated in Fig. I- 20. Despite the advantages of Newton's method over steepest descent, The Newton's method is prone to diverge because of a poor initial point. This risk diminishes when the objective function is convex, i.e. the matrix $H(T(\bar{p}))$ is symmetric positive definite.

Newton's method is extensively used for inverse scattering applications, such as image reconstruction, and tomography [83]-[87].

When using Newton's method, the risk of diverging from the optimum increases as the initial point gets far from the final answer. Usually, a combination of steepest descent or other stable methods in first steps followed by Newton's method at the proximity of the response gives the optimum result [88].

The update equation (I-73) required computing and inversion of the Hessian matrix which is computationally expensive. There are a handful of techniques to compute the second order derivatives, both analytically and numerically. When using full-wave EM solvers, the derivatives should be calculated numerically (i.e. by finite differencing), which is very cumbersome. Hessian matrix, on the other hand, carries the risk of being ill-conditioned, which in turn increases the risk of failure in optimization. Different variations have been suggested in order to improve this aspect of Newton's method. Some of these techniques have been addressed here.

Newton methods include several classes, including *discrete* Newton, *quasi* Newton (QN) (also termed *variable metric*), and *truncated* Newton (TN). Historically, the $O(n^2)$ memory requirements and $O(n^3)$ computation associated with solving a linear system directly have restricted Newton methods only: (1) to small problems, (2) to problems with special sparsity patterns, or (3) near a solution, after a gradient method has been applied. Fortunately, advances in computing technology and software are making the Newton approach feasible for a wide range of problems. Particularly, with advances in automatic differentiation as in [89], [90] the appeal of these methods should increase further. Extensive treatments of Newton methods can be found in the literature ([91], [92] for example) and only general concepts will be outlined here.

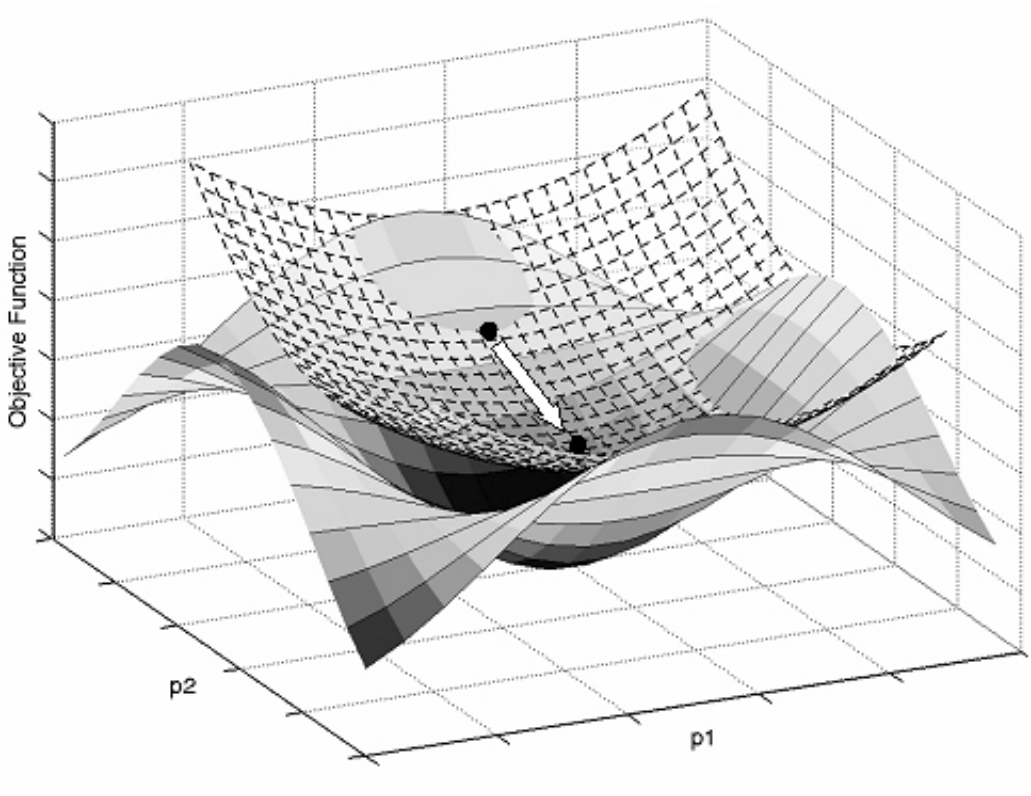

Fig. I- 20. Newton's Method in two dimensional parameter space

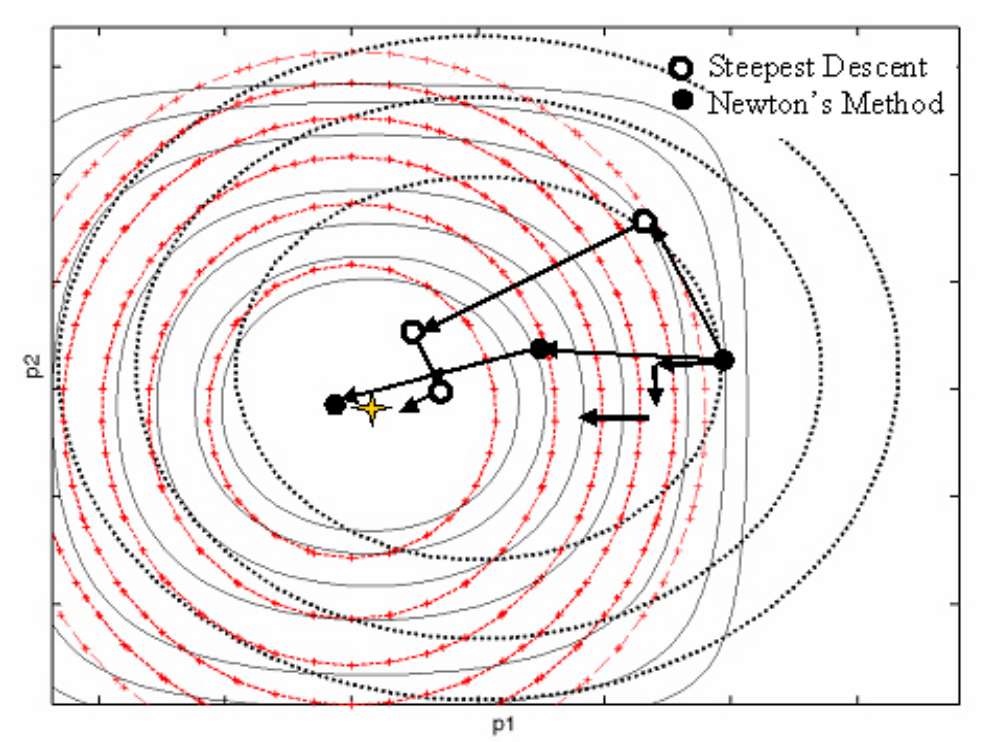

Fig. I- 21. Comparison between steepest descent and Newton's method.

I.6.4 Quasi Newton methods

A major problem with all the "Newton type" methods is that inversion of the Hessian matrix is very time consuming. The central idea underlying quasi-Newton methods is to use an approximation of the inverse Hessian. Quasi Newton methods are simply those groups of methods which approximate the Hessian matrix in order to avoid the inversion of the Hessian matrix. *Quasi-Newton* or *variable metric* methods can be used when the Hessian matrix is difficult or time-consuming to evaluate. Instead of obtaining an estimate of the Hessian matrix at a single point, these methods gradually build up an approximate Hessian matrix by using gradient information from some or all of the previous iterates.

The quasi-Newton methods that build up an approximation of the inverse Hessian are often regarded as the most sophisticated for solving unconstrained problems. The update equation for Newton's and Steepest Descent methods can be written in a general form,

$$\overline{p}^{<k+1>} = \overline{p}^{<k>} + \Delta\overline{p} = \overline{p}^{<k>} - w^{<k>}.S^{<k>}.\nabla T(\overline{p}) \qquad \textit{(I-74)}$$

For steepest descent method S^k is the identity matrix $S^k = I$ while for Newton's method the matrix S^k is the inverse Hessian matrix $S^k = \left[H(T(\overline{p}))\right]^{-1}$. Actually there could be defined several different methods in between Steepest Descent and Newton's, for example,

$$S^k = \left[H(T(\overline{p}^{<0>}))\right]^{-1} \qquad \textit{(I-75)}$$

This means for all the updates, only the inverse of the Hessian at the first iteration is used. Obviously this scheme is not as precise as "pure" Newton's method but however has the advantage of avoiding multiple inversions of the Hessian matrix.

In quasi-Newton methods, instead of the true Hessian, an initial matrix $H^{<0>}$ is chosen (usually $H^{<0>}(T(\overline{p})) = I$ where I is identity matrix) which is subsequently updated by an update formula,

$$H^{<k+1>} = H^{<k>} + H_u^{<k>} \qquad \textit{(I-76)}$$

whereas $H_u^{<k>}$ is the update matrix. This update can also be done with the inverse of the Hessian matrix,

$$\left(H^{-1}\right)^{<k+1>} = \left(H^{-1}\right)^{<k>} + \left(H_u^{-1}\right)^{<k>} \qquad \textit{(I-77)}$$

For an easier follow up, B is introduced as an intermediate function, $B^{<k>} = \left(H^{-1}\right)^{<k>}, B_u^{<k>} = \left(H_u^{-1}\right)^{<k>}$ And (I-77) will have the form,

$$B^{<k+1>} = B^{<k>} + B_u^{<k>} \qquad \textit{(I-78)}$$

The Hessian matrix can be considered as the derivative of the gradient matrix,

$$H(T(\overline{p}^{<k>})).\Delta p^{<k>} = \nabla T(\overline{p}^{<k+1>}) - \nabla T(\overline{p}^{<k>}) \qquad \textit{(I-79)}$$

where $\Delta p^{<k>}$ is calculated through forward-differencing $\Delta p^{<k>} = p^{<k+1>} - p^{<k>}$. If the Hessian is constant, then the following condition would hold as well,

$$B^{<k+1>}.\left[\nabla T(\overline{p}^{<i+1>}) - \nabla T(\overline{p}^{<i>})\right] = \Delta \overline{p}^{<i>}, \qquad i = 1,...,k \qquad \textit{(I-80)}$$

This is called the quasi-Newton condition. Now, substituting (I-78)into (I-80) would yield,

$$\left(B^{<k>} + B_u^{<k>}\right).\left[\nabla T(\overline{p}^{<i+1>}) - \nabla T(\overline{p}^{<i>})\right] = \Delta \overline{p}^{<i>}, \qquad i = 1,...,k \qquad \textit{(I-81)}$$

Again for simplification, we introduce a new variable, $\overline{q}^{<i>}$ as $\nabla T(\overline{p}^{<i+1>}) - \nabla T(\overline{p}^{<i>}) = \overline{q}^{<i>}$.Then (I-81) will take the brief form of,

$$\left(B^{<k>} + B_u^{<k>}\right).\overline{q}^{<i>} = \Delta \overline{p}^{<i>}, \qquad i = 1,...,k \qquad \textit{(I-82)}$$

The equation (I-82) identifies the update steps, or $\Delta \overline{p}^{<i>}$ but there is still an unknown element in the formula: $B_u^{<k>}$ or the update inverse Hessian is not known yet!

Actually a unique solution for Hessian update does not exist, a general form can be written as,

$$B_u^{<k>} = \alpha^{<k>}\mathbf{u}^{<k>}.\left(\mathbf{u}^{<k>}\right)^T + \beta^{<k>}\mathbf{v}^{<k>}.\left(\mathbf{v}^{<k>}\right)^T \qquad \textit{(I-83)}$$

where $\alpha^{<k>}$ and $\beta^{<k>}$ are scalars and the vectors $\mathbf{u}^{<k>}$ and $\mathbf{v}^{<k>}$ should be computed so that they can fit in (I-82). As mentioned before (I-83) is a general form and the second term in the right hand side can be omitted. The choice of β determines the rank of the update. Quasi-Newton methods that take $\beta = 0$ are using rank one updates while the Quasi-Newton methods that take $\beta \neq 0$ are using rank two updates. Note that $\beta \neq 0$ provides more flexibility. There are many update schemes suggested so far, among them all, we present two of them which are more frequently addressed[93],[94],

- Davidson -Fletcher-Powell (DFP) formula
- Broyden-Fletcher-Goldfarb-Shanno (BFGS) formula.

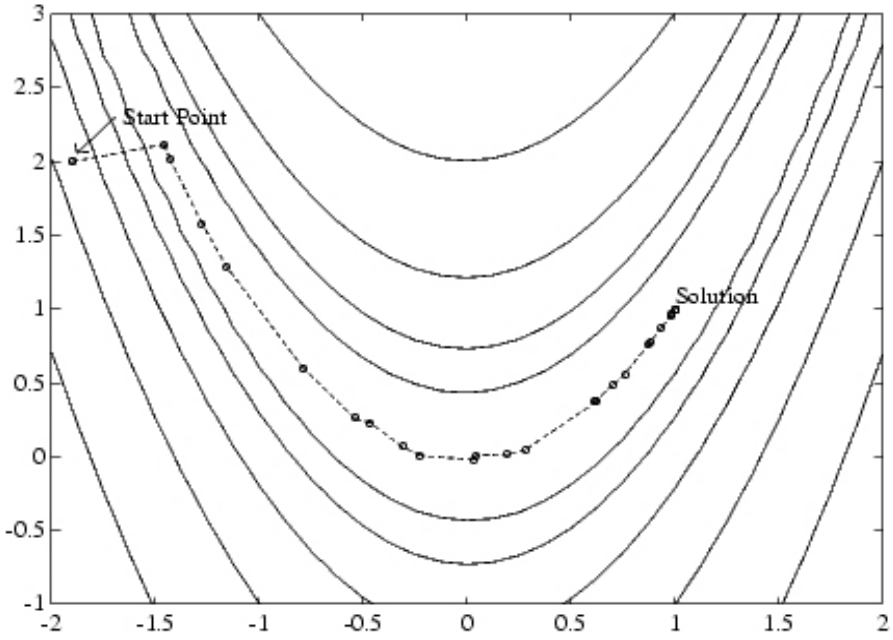

Fig. I- 22. The quasi-Newton method is illustrated by the solution path

I.6.4.1 Davidson-Fletcher-Powell formula

Earliest (and one of the most clever) schemes for constructing the inverse Hessian was originally proposed by Davidson (1959) and later developed by Fletcher and Powell (1963).

It has the interesting property that, for a quadratic objective, it simultaneously generates the directions of the conjugate gradient method while constructing the inverse Hessian.

The method is also referred to as the variable metric method (originally suggested by Davidson). Substituting the update term in the equation (I-83) into (I-82) would give,

$$\left(B^{<k>}+\alpha^{<k>}\mathbf{u}^{<k>}.\left(\mathbf{u}^{<k>}\right)^T+\beta^{<k>}\mathbf{v}^{<k>}.\left(\mathbf{v}^{<k>}\right)^T\right).\overline{q}^{<i>}=\Delta\overline{p}^{<i>},\qquad i=1,...,k \tag{I-84}$$

Now setting

$$\mathbf{u}^{<k>}=\Delta\overline{p}^{<k>} \tag{I-85}$$

$$\mathbf{v}^{<k>}=B^{<k>}\overline{q}^{<k>}$$

$$\alpha^{<k>}\mathbf{u}^T\overline{q}^{<k>}=1$$

$$\beta^{<k>}\mathbf{v}^T\overline{q}^{<k>}=-1$$

will determine the $\alpha^{<i>}$ and $\beta^{<i>}$. The resulting update formula will be,

$$B^{<k+1>}=B^{<k>}+\frac{\Delta\overline{p}^{<k>}\left(\Delta\overline{p}^{<k>}\right)^T}{\left(\Delta\overline{p}^{<k>}\right)^T\overline{q}^{<k>}}-\frac{B^{<k>}\overline{q}^{<k>}\left(\overline{q}^{<k>}\right)^T B^{<k>}}{\left(\overline{q}^{<k>}\right)^T B^{<k>}\overline{q}^{<k>}} \tag{I-86}$$

I.6.4.2 Broyden–Fletcher–Goldfarb–Shanno formula

Any update formula for $B^{<k>}$ can be transformed into a corresponding complimentary formula for $H^{<k>}$ by interchanging the roles of $B^{<k>}$ and $H^{<k>}$ and of $\overline{p}$ and $\overline{q}$. The reverse is also true.

Broyden–Fletcher–Goldfarb–Shanno formula update of $H^{<k>}$ is obtained by taking the complimentary formula of the Davidson-Fletcher-Powel formula,

$$H^{<k+1>}=H^{<k>}+\frac{\overline{q}^{<k>}\left(\overline{q}^{<k>}\right)^T}{\left(\overline{q}^{<k>}\right)^T\Delta\overline{p}^{<k>}}-\frac{H^{<k>}\Delta\overline{p}^{<k>}\left(\Delta\overline{p}^{<k>}\right)^T H^{<k>}}{\left(\Delta\overline{p}^{<k>}\right)^T H^{<k>}\Delta\overline{p}^{<k>}} \tag{I-87}$$

Taking the inverse, the Broyden–Fletcher–Goldfarb–Shanno update formula for $B^{<k+1>}$, would result,

$$\mathrm{B}^{<k+1>} = \mathrm{B}^{<k>} + \left(\frac{1+\left(\overline{q}^{<k>}\right)^T \mathrm{B}^{<k>}\overline{q}^{<k>}}{\left(\overline{q}^{<k>}\right)^T \Delta\overline{p}^{<k>}} \right) \cdot \frac{\Delta\overline{p}^{<k>}\left(\Delta\overline{p}^{<k>}\right)^T}{\left(\Delta\overline{p}^{<k>}\right)^T \overline{q}^{<k>}} - \frac{\Delta\overline{p}^{<k>}\left(\overline{q}^{<k>}\right)^T \mathrm{B}^{<k>} + \mathrm{B}^{<k>}\overline{q}^{<k>}\left(\Delta\overline{p}^{<k>}\right)^T}{\left(\overline{q}^{<k>}\right)^T \Delta\overline{p}^{<k>}} \qquad \textit{(I-88)}$$

It can be noticed that Broyden–Fletcher–Goldfarb–Shanno formula is more complicated than Davidson-Fletcher-Powell (DFP), but it is straightforward to apply. Both DFP and BFGS updates have symmetric rank two corrections that are constructed from the vectors $\Delta\overline{p}^{<k>}$ and $\mathrm{B}^{<k>}\overline{q}^{<k>}$. Weighted combinations of these formulae will therefore also have the same properties. The availability of quasi-Newton methods renders steepest-descent methods obsolete. Both types of algorithms require only first derivatives, and both require a line search. The quasi-Newton algorithms require slightly more operations to calculate iteration and somewhat more storage, but in almost all cases, these additional costs are outweighed by the advantage of superior convergence. At first glance, quasi-Newton methods may seem unsuitable for large problems because the approximate Hessian matrices and inverse Hessian matrices are generally dense. But the method pays off because of a saving the time required for calculating Hessian matrix.

I.6.5 Conjugate gradient method

The problem with the steepest descent method is that the method performs many small steps in going down a long, narrow valley, even if the valley is a perfect quadratic form. The optimistic hope is that, for example, in two dimensions, the first step would take to the valley floor, the second step directly down the long axis; but the new gradient at the minimum point of any line minimization is perpendicular to the direction just traversed. Therefore, with the steepest descent method, the consecutive updates *must* make a right angle turn, which does *not*, in general, provide the shortest path to the minimum. (See Fig. I- 24).

The conjugate gradient method (also known as Powell's method) is based on the idea that the convergence to the solution could be accelerated if we minimize $T(\overline{p})$ over the hyperplane that contains all previous search directions, instead of minimizing

$T(\overline{p})$ over just the line that points down gradient. To determine $\overline{p}^{<k+1>}$ we minimize $T(\overline{p})$ over

$$\overline{p}^{<k+1>} = \overline{p}^{<0>} + \alpha_0 \overline{s}_0 + \alpha_1 \overline{s}_1 + \alpha_2 \overline{s}_2 + .. + \alpha_k \overline{s}_k \qquad \textit{(I-89)}$$

where $\mathbf{s}_k = \Delta\overline{p}^{<k>} = \overline{p}^{<k>} - \overline{p}^{<k-1>}$ represent previous search directions. The scalar products α_k are of fundamental importance for such an update and will be discussed in detail later. An added advantage to this approach is that, if we can select the $\overline{s}_k$'s to be linearly independent, then the dimension of the hyperplane $\overline{p}^{<k+1>} = \overline{p}^{<0>} + \alpha_0 \overline{s}_0 + \alpha_1 \overline{s}_1 + \alpha_2 \overline{s}_2 + .. + \alpha_k \overline{s}_k$ will grow one dimension with each iteration of the conjugate gradient method. This would imply that (assuming infinite precision arithmetic) the in the worst case the optimization will end up in *N* iterations. Ideally the conjugate gradient method is applied when the objective function can be convertible to a quadratic form in terms of the parameter vector

$$T(\overline{p}) = \frac{1}{2}\overline{p}^T A \overline{p} - \overline{p}^T \overline{b} \qquad \textit{(I-90)}$$

where A is a symmetric positive definite matrix and

$\overline{b}$ is an N-dimensional column vector.

Subsequently, these relations will hold true:

$\nabla T(\overline{p}) = A\overline{p} - \overline{b}$ and $H(\overline{p}) = A$

we also define $\overline{r}$ such that $\overline{r}(\overline{p}) = A\overline{p} - \overline{b}$.

Definition- For a given symmetric positive definite matrix *A* we say that two vectors $\overline{r}$ and $\overline{s}$ are *A-conjugate* if

$$\overline{s}^T A \overline{r} = 0 \qquad \textit{(I-91)}$$

Since *A* is symmetric and positive definite, the left-hand side defines an inner product

$$\langle \overline{s}, \overline{r} \rangle_A = \overline{s}^T A \overline{r} \qquad \textit{(I-92)}$$

So, two vectors are conjugate if they are orthogonal with respect to this inner product.

Fig. I- 23 illustrates the conjugate directions in two dimensional Cartesian coordinates. If $\{\hat{u}_1,...,\hat{u}_M\}$ is any set of non-zero conjugate directions in $\mathbb{R}^N$, then $\hat{u}_1,...,\hat{u}_M$ are linearly independent. Also $\hat{u}_1,...,\hat{u}_M$ span $\mathbb{R}^N$ if and only if *M=N*.

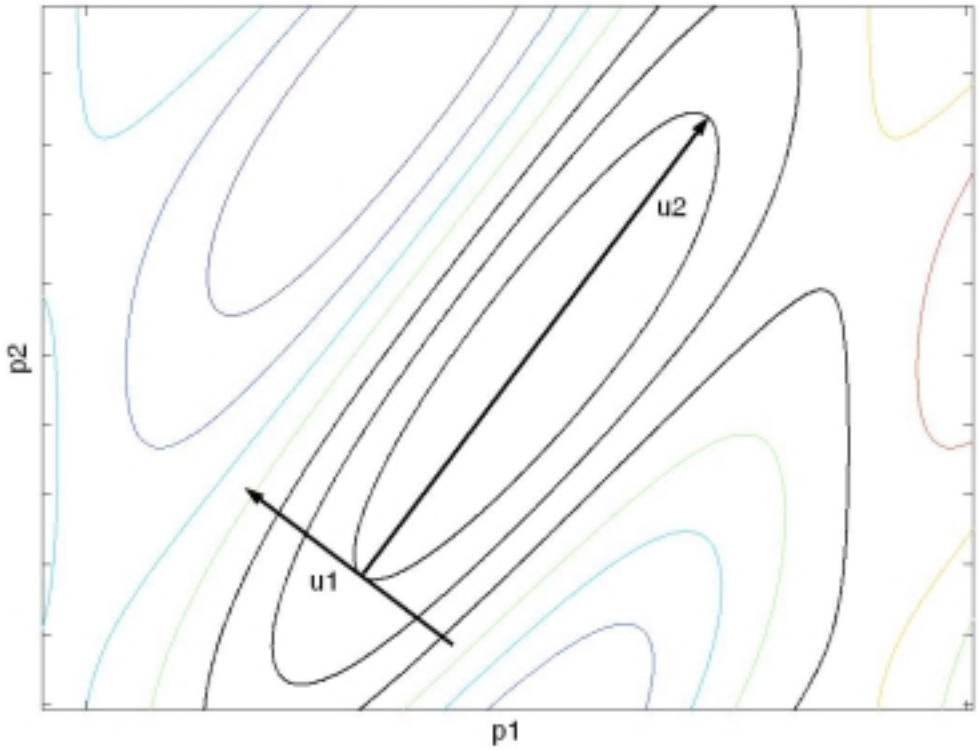

Fig. I- 23. Conjugate directions

Theorem 1.

If A is positive definite symmetric, and if $A\bar{p} = \bar{b}$ and $\{\hat{u}_1,...,\hat{u}_M\}$ is a set of non-zero conjugate directions, then

$$\hat{u}_{M+1} = \bar{p} - \sum_{i=1}^{M} \frac{\hat{u}_i^T \bar{b}}{\hat{u}_i^T A \hat{u}_i} \hat{u}_i \qquad (I\text{-}93)$$

is conjugate to each of $\hat{u}_1,...,\hat{u}_M$.

Theorem 2.

If *A* is positive definite symmetric,

$$T(\bar{p}) = \frac{1}{2} \bar{p}^T A \bar{p} - \bar{p}^T \bar{b} \qquad (I\text{-}94)$$

for some $\bar{b} \in \mathbb{R}^N$ and $\{\hat{u}_1,...,\hat{u}_M\}$ is a set of non-zero conjugate directions, then the minimum of $T(\bar{p})$ in the space spanned by $\{\hat{u}_1,...,\hat{u}_M\}$ occurs at the point $\sum_{i=1}^{M} \beta_i \hat{u}_i$ where

$$\beta_i = \frac{\hat{u}_i^T B\bar{b}}{\hat{u}_i^T A\hat{u}_i} \tag{I-95}$$

Theorem 3.

With the notation of *Theorem 2.*, a fixed j satisfying $1 \le j \le M$ and fixed $\alpha_1, \alpha_2, ..., \alpha_{j-1}, \alpha_{j+1}, ...\alpha_M$ the minimum of,

$$\Psi(\alpha_j) = T\left(\sum_{i=1}^{M} \alpha_i \hat{u}_i\right) \tag{I-96}$$

occurs at $\alpha_j = \beta_j$.

The above theorem simply means that the minimum of a quadratic function can be found by M one dimensional minimizations along nonzero conjugate directions $\hat{u}_1,...,\hat{u}_M$ and the order in which one-dimensional minimizations are done is irrelevant. In order to use this result, we need to be able to create quadratic form. Apart from practical application which is being discussed here, this conclusion is important because it shows that computing partial derivatives is not essential for a quadratic problem.

Let $\bar{p}^{<0>}$ be an initial point in the parameter space. For the first search direction the conventional steepest descent approach is taken,

$$\bar{p}^{<1>} = \bar{p}^{<0>} + \alpha_0 \bar{s}^{<0>} \tag{I-97}$$

whereas

$$\bar{s}^{<0>} = \nabla T(\bar{p}^{<0>}) = A\bar{p}^{<0>} - \bar{b} = \bar{r}^{<0>} \tag{I-98}$$

From the discussion of the method of steepest descent, $\alpha_0 = -\frac{\bar{s}^{<0>T}\bar{s}^{<0>}}{\bar{s}^{<0>T}A\bar{s}^{<0>}}$. Also it worth's to mention that in the steepest descent method the two consecutive update vectors were orthogonal,

$$\overline{s}^{<k+1>T}\overline{s}^{<k>} = 0 \qquad \textit{(I-99)}$$

This means if we follow the same trend in here,

$$\overline{s}^{<1>T}\overline{s}^{<0>} = 0 \qquad \textit{(I-100)}$$

Rather than try to establish the above orthogonality relationships with a calculation, use the following calculus argument. By definition, $\overline{s}^{<1>}$ is the gradient of T at $\overline{p}^{<1>}$, where $\overline{p}^{<1>}$ is the conjugate gradient estimate to follow the initial guess $\overline{p}^{<0>}$.

The conjugate gradient method calls for defining successive approximates by

$$\overline{p}^{<k+1>} = \overline{p}^{<k>} + \alpha_k \overline{s}^{<k>} \qquad \textit{(I-101)}$$

$$\overline{s}^{<k>} = \overline{r}^{<k-1>} + \beta_{k-1}\overline{s}^{<k-1>} \qquad \textit{(I-102)}$$

where $\overline{s}$ and $\overline{r}$ are *A*-conjugates,

$$\overline{r}_k^T A\overline{s}_k = 0 \qquad \textit{(I-103)}$$

The calculation of α_k and β_k are to be discussed shortly. The things to keep in mind when choosing α_k and β_k are :

1. We want the span of the search directions to fill the space we are searching as the number of iterations increases;
2. Searching down *A*-gradients was basically a good idea. But, to guarantee linearly independent successive search directions, we generally need to choose conjugate gradient search directions to be perturbations of steepest descent search directions.

It was already mentioned that the first update is taken through steepest descent method and thus the vectors $\overline{p}^{<0>}, \overline{s}_0$ and $\overline{p}^{<1>}$ are known.

To take the next step using the conjugate gradient method, we must determine values for α_k and β_k so that we can calculate $\overline{p}^{<2>}$ and $\overline{s}_1$. Then we will see a pattern emerge.

In taking this next step in the conjugate gradient method we are seeking to minimize $T(\overline{p})$ over the plane

$$\overline{p}^{<0>} + span(\overline{s}_0, \overline{s}_1) \qquad \textit{(I-104)}$$

This means that the residual $\overline{r}_k$ will have to be orthogonal to both $\overline{s}_0$ and $\overline{s}_1$.

From the requirement that $\overline{s}_0 \overline{r}_1 = 0$, it follows that the search direction $\overline{s}_1$ must be *A*-conjugate to the search direction $\overline{s}_0$. We can now set β_0 as follows,

$$\mathbf{s}_1 = \overline{r}_1 + \beta_0 \overline{s}_0 \qquad \textit{(I-105)}$$

implies

$$A\overline{s}_1 = A\overline{r}_1 + \beta_0 A\overline{s}_0 \qquad \textit{(I-106)}$$

Now considering the fact that $\overline{s}_0$ and $\overline{s}_1$ are conjugate, *or* $\mathbf{s}_0 A \mathbf{s}_1 = 0$, hence,

$$\overline{s}_0 A\overline{s}_1 = \overline{s}_0 A\overline{r}_1 + \beta_0 \overline{s}_0 A\overline{s}_0 = 0 \qquad \textit{(I-107)}$$

This will lead to the calculation of β_0 as,

$$\beta_0 = -\frac{\overline{s}_0 A\overline{r}_1}{\overline{s}_0 A\overline{s}_0} = -\frac{\overline{r}_1 A\overline{r}_1}{\overline{s}_0 A\overline{s}_0} \qquad \textit{(I-108)}$$

Having decided to proceed from $\overline{p}^{<1>}$ to $\overline{p}^{<2>}$ along the search direction defined by $\overline{s}_1 = \overline{r}_1 + \beta_0 \overline{s}_0$, the same calculus argument used to determine gives

$$\alpha_1 = \frac{\overline{r_1 s_1}}{\overline{s}_1 A\overline{s}_1} \qquad \textit{(I-109)}$$

so a step of the conjugate gradient method is complete.

The reader is referred to [61]-[63] for further explanations of the method. Also the application of Powell's method is reported in [62]-[67].

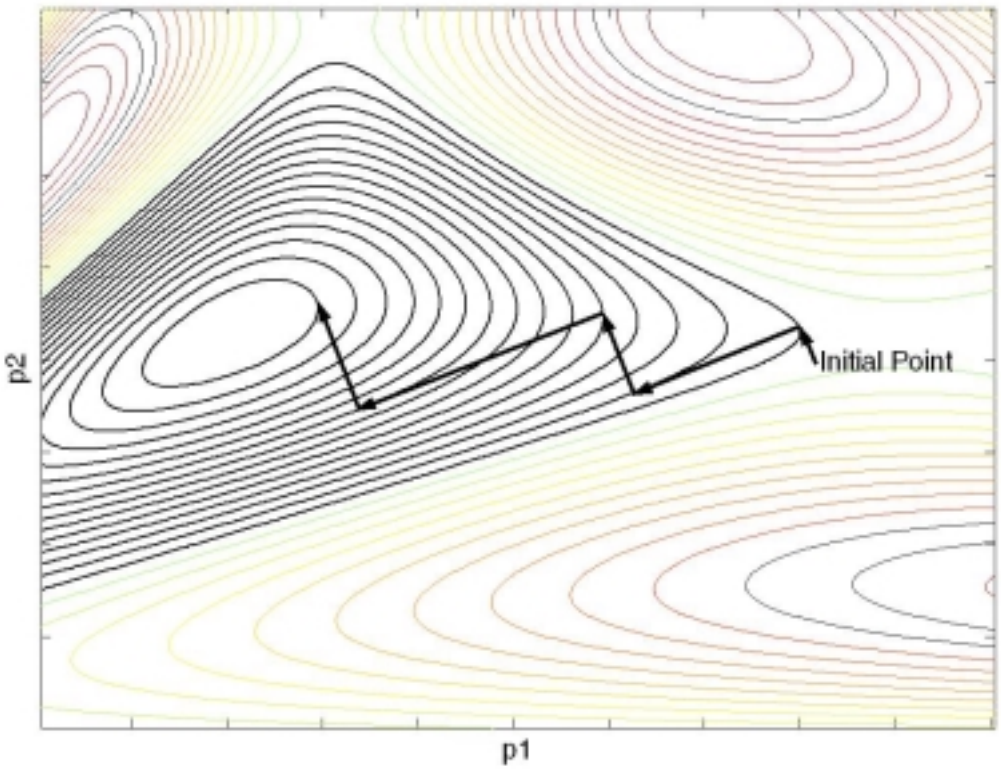

Fig. I- 24. In steepest descent method all the paths are normal to each other

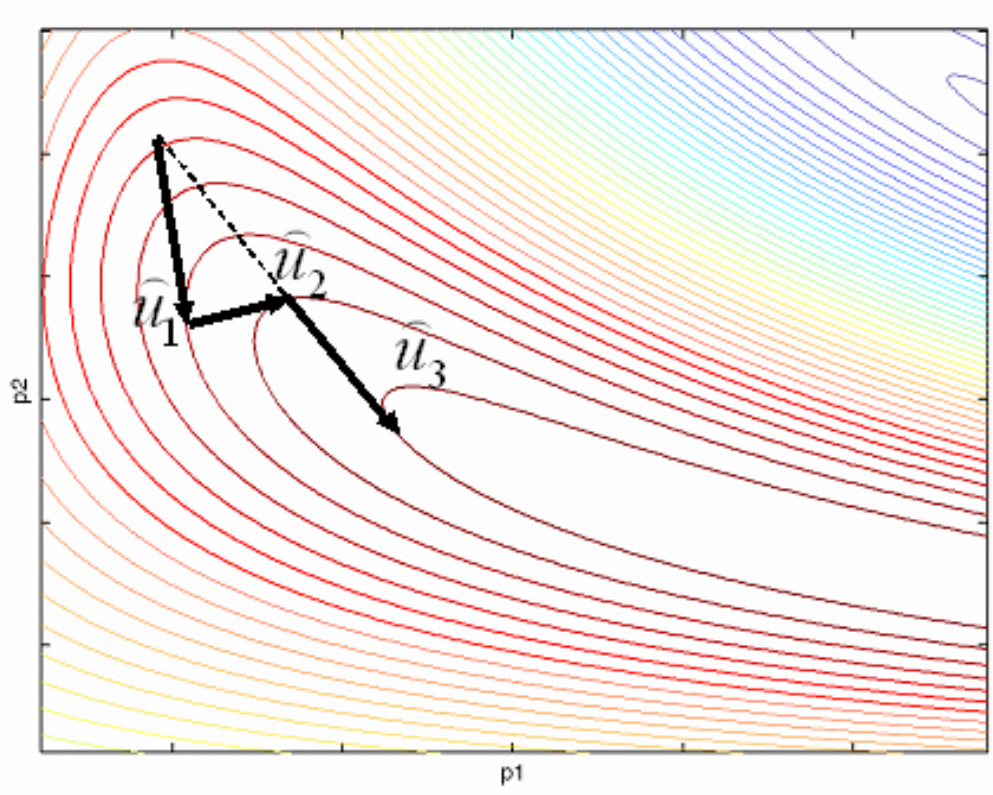

Fig. I- 25. Conjugate gradient convergence.

I.7 Numerical analysis of microwave devices

I.7.1 Introduction

An EM solver typically accepts a geometric description of the microwave device along with material properties for metal and dielectrics, and develops highly accurate electrical response models in the form of S-, Y-, Z-parameters or an extracted model in SPICE format. Today's high frequency EM simulators can provide results that are very accurate-often S-parameters with bounded error.

A numerical technique is the only stand-alone and most critical part of a design loop. The bulk of the time needed for a device design is typically spent for electromagnetic analysis. Due to such significance, numerical analysis of microwave devices and antennas has become one of the main stream research areas in electromagnetics. Different commercial field solvers are available in the market, each using one or more numerical technique or their hybrids. There different factors in considering a numerical techniques, namely:

- nature of the problem,
- computational time,
- accuracy,
- stability.

Of course, these factors are not absolute and each technique might feature of or two depending on the conditions. Despite the amount of ongoing research, the numerical methods in electromagnetics are an established domain. Most of the techniques are now available in the textbooks and being taught in courses. However the numerical techniques in electromegnetics are not the main focus of this dissertation and will not be discussed in detail. For a detailed explanation of these methods the reader is encouraged to refer to the available literature like [95]-[100] along with other publications that will be addressed in this section. In this section a brief categorization of methods will be addressed. Only methods which are more utilized in during the present work will be covered more in more elaboration.

I.7.2 Classification of electromagnetic problems [95]

Classifying EM problems helps to answer the question of what method is best for solving a given problem. Continuum problems are categorized differently depending on the particular item of interest, which could be one of these,

(1) the solution region of the problem,

(2) the nature of the equation describing the problem

(3) the associated boundary conditions.

I.7.2.1 Classification of solution regions

In terms of the solution region or problem domain, the problem could be an interior problem, also variably called an inner, closed, or bounded problem, or an exterior problem, also variably called an outer, open, or unbounded problem.

Consider the solution region R with boundary S, as shown in Fig. I- 26. If part or all of $\partial\Omega$ is at infinity, Ω is exterior/open, otherwise Ω is interior/closed. For example, wave propagation in a waveguide is an interior problem, whereas while wave propagation in free space, scattering of EM waves by raindrops and radiation from a dipole antenna are exterior problems.

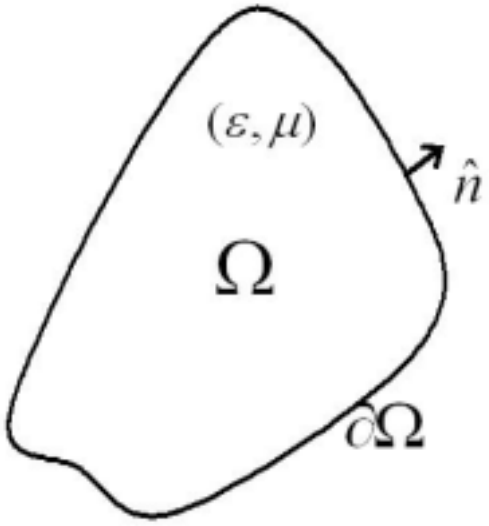

Fig. I- 26. Description of solution regions

A problem can also be classified in terms of the electrical, constitutive properties (σ,ε,μ) of the solution region. The solution region could be linear (or nonlinear), homogeneous (or inhomogeneous), and isotropic (or anisotropic). We shall be concerned, for the most part, with linear, homogeneous, isotropic media in this text.

Classification of differential equations

EM problems are classified in terms of the equations describing them. The equations could be differential or integral or both. Most EM problems can be stated in terms of an operator equation

$$L\Phi = g \qquad \textit{(I-110)}$$

where L is an operator (differential, integral, or integro-differential), g is the known excitation or source, and Φ is the unknown function to be determined.

Generally speaking, electromagnetic problems involve linear, second-order differential equations. The generic form of a second-order partial differential equation (PDE) in 2 dimensional space is given by

$$a\frac{\partial^2\Phi}{\partial x^2}+b\frac{\partial^2\Phi}{\partial x\partial y}+c\frac{\partial^2\Phi}{\partial y^2}+d\frac{\partial\Phi}{\partial x}+e\frac{\partial\Phi}{\partial y}+f\Phi=g \qquad \textit{(I-111)}$$

The coefficients, *a, b* and *c* in general are functions of *x* and *y*; they may also depend on Φ itself, in which case the PDE is said to be *nonlinear*. A PDE in which *g(x, y)* in equation (I-111) equals zero is termed *homogeneous;* it is *inhomogeneous* if it does not.

Notice that (I-111) has the same form as Eq. (I-110) where L is now a differential operator given by,

$$L=a\frac{\partial^2}{\partial x^2}+b\frac{\partial^2}{\partial x\partial y}+c\frac{\partial^2}{\partial y^2}+d\frac{\partial}{\partial x}+e\frac{\partial}{\partial y}+f \qquad \textit{(I-112)}$$

A PDE in general can have both boundary values and initial values. PDEs whose boundary conditions are specified are called *steady-state equations.* If only initial values are specified, they are called *transient equations*.

Any linear second-order PDE can be classified as elliptic, hyperbolic, or parabolic depending on the coefficients *a, b, c, d* and *e*. Assuming $\Delta = b^2 - 4ac$, equation (I-111) is,

elliptic	if	$\Delta < 0$	*(I-113)*
parabolic	if	$\Delta = 0$	
hyperbolic	if	$\Delta > 0$	

Elliptic PDEs are associated with steady-state phenomena, i.e., boundary-value problems. Typical examples of this type of PDE include Helmholtz equation for electric field in two dimensional Cartesian coordinates in free space,

$$\frac{\partial^2 \mathbf{E}}{\partial x^2} + \frac{\partial^2 \mathbf{E}}{\partial y^2} + k_0^2 \mathbf{E} = 0 \qquad \textit{(I-114)}$$

where $\mathbf{E}$ is the electric field vector and k_0 is the propagation constant in free space, $a = c = 1$ and $b = 0$.

An elliptic PDE usually models an interior problem, and hence the solution region is usually closed or bounded.

Hyperbolic PDEs arise in propagation problems. The solution region is usually open so that a solution advances outward indefinitely from initial conditions while always satisfying specified boundary conditions. A typical example of hyperbolic PDE is the wave equation in one dimension,

$$\frac{\partial^2 \Phi}{\partial x^2} = \frac{1}{u^2} \frac{\partial^2 \Phi}{\partial t^2} \qquad \textit{(I-115)}$$

where $a = u^2$, $b = 0$, $c = -1$.

Parabolic PDEs are generally associated with problems in which the quantity of interest varies slowly in comparison with the random motions which produce the variations. The most common parabolic PDE is the diffusion (or heat) equation in one dimension,

$$\frac{\partial^2 \Phi}{\partial x^2} = k \frac{\partial \Phi}{\partial t} \qquad \textit{(I-116)}$$

where $a = 1$, $b = 0 = c$.

Like hyperbolic PDE, the solution region for parabolic PDE is usually open. The initial and boundary conditions typically associated with parabolic equations resemble those for hyperbolic problems except that only one initial condition at $t = 0$ is necessary since (5) is only first order in time. Also, parabolic and hyperbolic equations are solved using similar techniques, whereas elliptic equations are usually more difficult and require different techniques.

The discussion above has been summarized in the table 1.

Type of PDE	**Sign of Δ**	**Application**	**Solution region**
Elliptic	Negative	Poissons equation $\nabla^2\mathbf{E} = \frac{\partial^2\mathbf{E}}{\partial x^2} + \frac{\partial^2\mathbf{E}}{\partial y^2} + \frac{\partial^2\mathbf{E}}{\partial z^2} = \boldsymbol{\rho}(x, y, z)$ Helmholtz for $\mathbf{E}$ equation in free space $\frac{\partial^2\mathbf{E}}{\partial x^2} + \frac{\partial^2\mathbf{E}}{\partial y^2} + \frac{\partial^2\mathbf{E}}{\partial z^2} + k_0^2\mathbf{E} = 0$	Closed/Bounded
Hyperbolic	Positive	Wave equation $\frac{\partial^2\Phi}{\partial x^2} = \frac{1}{u^2}\frac{\partial^2\Phi}{\partial t^2}$	Open
Parabolic	Zero	Diffusion $\frac{\partial^2\Phi}{\partial x^2} = k\frac{\partial\Phi}{\partial t}$	Open

Table 1. Classification of PDE

I.7.2.2 Classification of boundary conditions

In addition to satisfying the equation (1) certain condition should be imposed on the borders.

1- Dirichlet boundary condition

$$\Phi(\mathbf{r}) = 0 \qquad \textit{(I-117)}$$

2- Neumann boundary condition

$$\frac{\partial\Phi(\mathbf{r})}{\partial\vec{\mathbf{n}}} = 0 \qquad \textit{(I-118)}$$

3- Mixed boundary condition:

$$\frac{\partial\Phi(\mathbf{r})}{\partial\vec{\mathbf{n}}} + h(\mathbf{r})\Phi(\mathbf{r}) = 0 \qquad \textit{(I-119)}$$

where $h(\mathbf{r})$ is a known function and $\frac{\partial \Phi(\mathbf{r})}{\partial \vec{\mathbf{n}}}$ is the directional derivative of $\Phi(\mathbf{r})$ along the outward normal to the boundary.

Classification of Numerical Techniques

Numerical techniques can be categorized based on different view points, such as solution domain (time- vs. frequency-domain) and the type of equations (integral vs. differential equations). The general categories of the numerical techniques, based on the solution approach are as follows,

Differential equation methods

- Finite Difference Frequency Domain method (FD)
- Finite Difference Time Domain method (FDTD)
- Transmission Line Matrix (TLM)
- Finite Element method (FEM)

Integral equation methods

- Method of Moments (MOM)
- Generalized Multipole Technique
- Boundary Element Method

Mode Matching (MM)

Numerical methods based on asymptotic approximations

- Ray tracing (geometrical optics)
- Angular Spectrum

A few numbers of so called techniques have been of use within the framework of this dissertation. Some of these techniques such as Finite Element method, Method of Lines and Finite-Difference Time Domain method have been developed in IRCOM Laboratory, while some others such as the Method of Moments are obtained through commercial software.

In the following sections, some of the methods which are used within this dissertation will be explained briefly.

I.7.3 Finite element method (FEM)

Until recently the Finite Element method has been the dominant and the most frequency utilized technique in microwave domain. The systematic generality of the method makes it possible to construct general-purpose computer programs for solving a wide range of problems. Consequently, programs developed for a particular discipline have been applied successfully to solve problems in a different field with little or no modification. The finite element analysis of any problem involves basically four steps [101], [102]:

- discretizing the solution region into a finite number of *sub regions* or *elements*,
- deriving governing equations for a typical element,
- assembling of all elements in the solution region, and
- solving the system of equations obtained.

There are different variations of the finite element method. Here, we briefly present the FEM developed in IRCOM Laboratory [103]. This method has been utilized in some of the 3D examples in the following chapters. The finite elements method developed at IRCOM can analyze three dimensional microwave devices of arbitrary shapes and material distribution. Mixed boundaries are also implementable with the developed software, *i.e.* electric magnetic walls, high impedance surfaces, and absorbing conditions (PML) making the solution of open problems possible.

The structure to be analyzed into 2- or 3-dimensions can be made up of inhomogeneous, anisotropic, lossy media. This method can be applied to the calculation of the coupling between elements, and to the characterization of devices complex, passive microwaves or passive-credits by the introduction of local accesses. A variety of applications of the present software can be found in [104]-[110].

The approximation of the finite elements consists in discretizing the field to be studied in under fields. The geometric standards of reference used for the grid of the structure can be into 1 dimension (segments), 2-D (triangles or quadrangles), in 3-D (tetrahedrons, pentahedrons or hexahedrons).

Before the resolution of the problem, these elements can be deformed to take into account the curved elements of the studied structure. Moreover, geometrical symmetries of the structure can be taken into account, thus reducing volume to be netted. Applying the finite element method, Maxwell’s equations are solved element

by element in order to determine the electric field or the magnetic field. Applying an electric formulation, the electric field is the solution of:

$$\iiint_V (\mu_i^{-1} \vec{r}ot\vec{E}).\vec{r}ot\vec{\phi}\ dV - k_0^2 \iiint_V (\varepsilon_i \vec{E}).\vec{\phi}\ dV \qquad \text{(I-120)}$$
$$= -j\omega\mu_0 \sum_{k=1}^{n} \iint_{Sp_k} \vec{J}_k.\vec{\phi}\ dSp_k - j\omega\mu_0 \sum_{p=1}^{m} \int_{l_p} \vec{I}_p.\vec{\phi}\ dl_p$$

with: $k_0^2 = \omega^2 \varepsilon_0 \mu_{0,}$

V: volume of the structure,

$\vec{E}$: electric field,

$\vec{\phi}$: test function,

n: number of modes in distributed accesses,

Sp_k: surface of the distributed access,

$\vec{J}_k$: current surface distribution,

m: number of localized access,

l_p: contour of the localized access,

$\vec{I}_p$: line distribution of the current

Two possible classes of solutions are available through the present software, namely *forced* and *free* oscillations modes.

In *free* oscillation mode, the terms related to the excitations are cancelled by shorting the ports. The outcome of the equations will be resonant characteristics of the structure such as cut-off frequency of different modes and quality factor. In *forced* oscillation mode, the excitations within a given frequency band are imposed and a modal decomposition on the ports outcomes the propagation and evanescent modes frequencies along with field distributions.

I.7.4 Finite-difference time domain (FDTD) [112]

Finite-difference time domain technique, was originally developed by Kane S. Yee in 1966, but did not attract any attention till ten years later, when Taflove discovered the potentials of the technique [114], [115]. Despite discovering its viability, the FDTD method did not become popular until late 90's. The reason was the FDTD method was computationally expensive method and alternative techniques were still ahead of

FDTD regarding the computational resources. With the advent of fast commercial PC's then FDTD started to become widely used since mid-1990's.

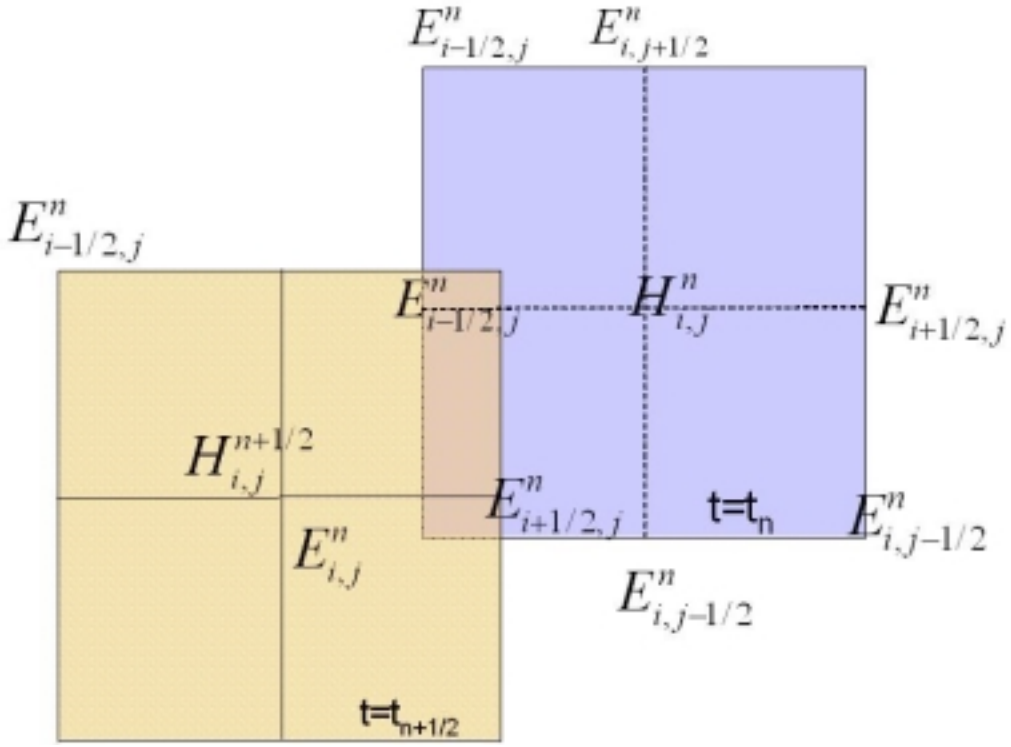

Fig. I- 27. FDTD cell-1

There are different variations of FDTD method; herein the original scheme proposed by Yee will be presented in brief. Despite its simplicity and straightforwardness, Yee's algorithm is still a valid and viable technique for electromagnetic scattering problems. The utilization of FDTD for microwave planar devices was first reported in [117].

In an isotropic medium, Maxwell's curl equations can be written as

$$\nabla \times \vec{E} = -\mu \frac{\partial \vec{H}}{\partial t} \qquad \textit{(I-121)}$$

$$\nabla \times \vec{H} = \sigma \vec{E} + \varepsilon \frac{\partial \vec{E}}{\partial t} \qquad \textit{(I-122)}$$

Decomposing (I-121) and (I-122) into their components will lead to a system of six scalar equations. Following Yee's notation, we define a grid point in the solution region as

$$\mu\frac{\partial H_x}{\partial t}=\frac{\partial E_y}{\partial z}-\frac{\partial E_z}{\partial y} \qquad \text{(I-123)}$$
$$\mu\frac{\partial H_y}{\partial t}=\frac{\partial E_z}{\partial x}-\frac{\partial E_x}{\partial z}$$
$$\mu\frac{\partial H_z}{\partial t}=\frac{\partial E_x}{\partial y}-\frac{\partial E_y}{\partial x}$$

$$\varepsilon\frac{\partial E_x}{\partial t}=\frac{\partial H_z}{\partial y}-\frac{\partial H_y}{\partial z}-\sigma E_x \qquad \text{(I-124)}$$
$$\varepsilon\frac{\partial E_y}{\partial t}=\frac{\partial H_x}{\partial z}-\frac{\partial H_z}{\partial x}-\sigma E_y$$
$$\varepsilon\frac{\partial E_y}{\partial t}=\frac{\partial H_x}{\partial z}-\frac{\partial H_z}{\partial x}-\sigma E_y$$

and any function of space and time as

$$F^n(i,j,k)=F(i\delta,j\delta,k\delta,n\Delta t) \qquad \text{(I-125)}$$

where $\delta=\Delta x=\Delta y=\Delta z$ is the space increment in Cartesian coordinate, and Δt is the time increment, while *i, j, k,* and *n* are integers. Using central finite difference approximation for space and time derivatives that are second-order accurate,

$$\frac{\partial f}{\partial x}\rightarrow\frac{f(x+\Delta x/2,t)-f(x-\Delta x/2,t)}{\Delta x} \qquad \text{(I-126)}$$

$$\frac{\partial f}{\partial t}\rightarrow\frac{f(x,t+\Delta t/2)-f(x,t-\Delta t/2)}{\Delta t} \qquad \text{(I-127)}$$

In applying (I-126)and (I-125) to all the space and time derivatives in Eq. (I-127), Yee positions the components of **E** and **H** about a unit cell of the lattice as shown in Fig. I-27. To incorporate , the components of **E** and **H** are evaluated at alternate halftime steps. For example equation ($\mu\frac{\partial H_x}{\partial t}=\frac{\partial E_y}{\partial z}-\frac{\partial E_z}{\partial y}$) will be expanded as,

$$\mu\frac{H_x(x_i,y_i,z_i,t_{n+1/2})-H_x(x_i,y_i,z_i,t_{n-1/2})}{\Delta t}= \qquad \text{(I-128)}$$
$$\frac{E_y(x_i,y_{i,}z_{i+1/2},t_n)-E_y(x_i,y_{i,}z_{i-1/2},t_n)}{\Delta z}-\frac{E_z(x_i,y_{i+1/2,}z_i,t_n)-E_z(x_i,y_{i-1/2,}z_i,t_n)}{\Delta y}$$

Then the update equation will have the form,

$$H_{x\,i,j,k}^{n+1/2} = H_{x\,i,j,k}^{n-1/2} + \frac{\Delta t}{\mu \Delta z}\left(E_{y\,i,j,k+1}^{n} - E_{y\,i,j,k}^{n}\right) - \frac{\Delta t}{\mu \Delta y}\left(E_{z\,i,j+1,k}^{n} - E_{z\,i,j,k}^{n}\right) \qquad \textit{(I-129)}$$

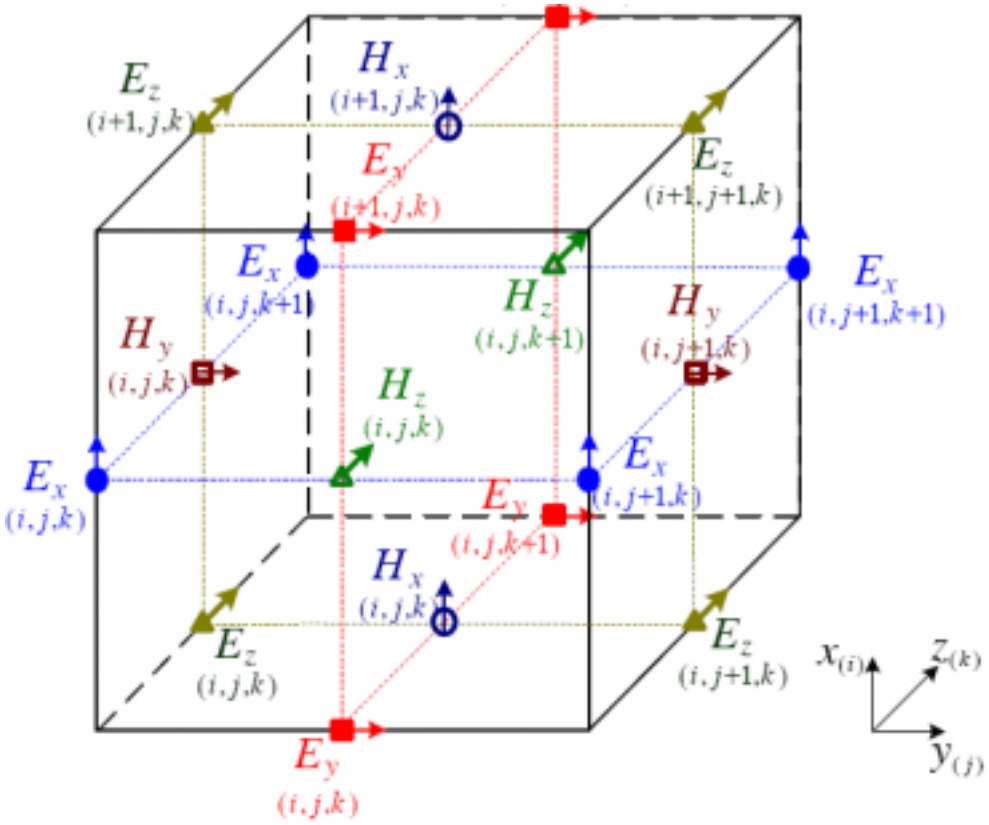

Fig. I- 28. Yee's cell

The second and third equations can be expanded in the same manner. Similarly the equation (I-124),

$$\varepsilon \frac{\partial E_x}{\partial t} = \frac{\partial H_z}{\partial y} - \frac{\partial H_y}{\partial z} - \sigma E_x \qquad \textit{(I-130)}$$

will result,

$$E_{x\,i,j,k}^{n+1} = \left(\frac{1-\sigma\Delta t/2\varepsilon}{1+\sigma\Delta t/2\varepsilon}\right)E_{x\,i,j,k}^{n} + \frac{1}{1+\sigma\Delta t/2\varepsilon}\cdot\left[\frac{\Delta t}{\varepsilon\Delta y}(H_{z\,i,j,k}^{n+1/2} - H_{z\,i,j-1,k}^{n+1/2}) - \frac{\Delta t}{\varepsilon\Delta z}(H_{y\,i,j,k}^{n+1/2} - H_{y\,i,j,k-1}^{n+1/2})\right] \qquad \textit{(I-131)}$$

It should be noted from (I-129)and (I-131) that the components of $\vec{E}$ and $\vec{H}$ are interlaced within the unit cell and are evaluated at alternate half-time steps. All the field components are present in a quarter of a unit cell (known as Yee's cell) as shown in Fig. I- 28.

After individual cells are formed, the entire computational domain is formed by stacking up theses rectangular (cubic) cells into the rectangular volume. One important issue which should be addressed here is the treatment of anisotropic material distribution. In such a case, after discretization, a dielectric constant is assigned to each cell as in Fig. I- 29. Then the dielectric constants of different cells will be averaged,

$$\varepsilon_{eq} = \frac{1}{4}(\varepsilon 1 + \varepsilon 2 + \varepsilon 3 + \varepsilon 4) \qquad \textit{(I-132)}$$

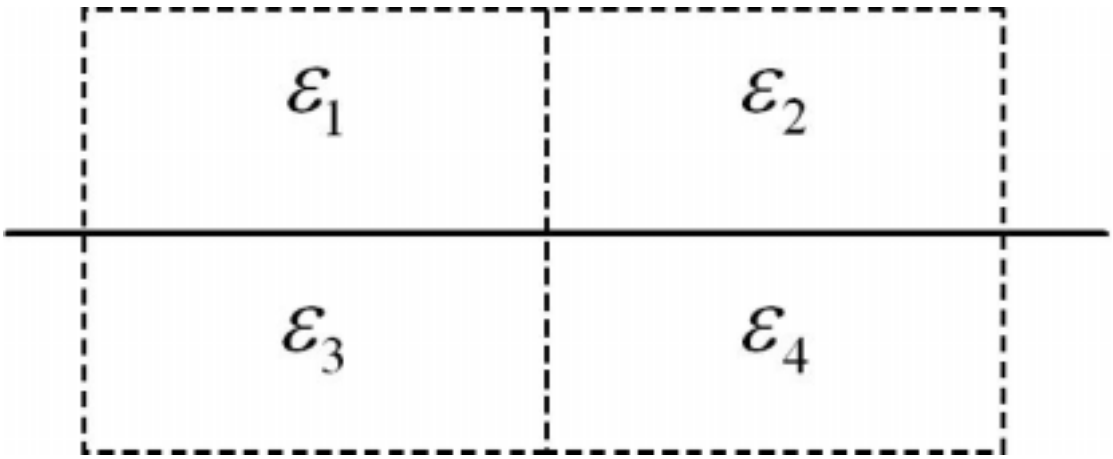

Fig. I- 29. Dielectric borders

Accuracy and stability

To obtain sufficiently accurate results, the spatial increment δ must be small compared to the wavelength (usually $\leq \lambda/10$) or minimum dimension of the scatterer. This amounts to having 10 or more cells per wavelength. To ensure the stability of the finite difference scheme, the time increment must comply with the stability criterion as follows,

$$(c\Delta t)^2 \leq \left(\frac{1}{\Delta x^2} + \frac{1}{\Delta y^2} + \frac{1}{\Delta z^2} \right)^{-1} \qquad \textit{(I-133)}$$

where *c* is the wave phase velocity.

The typical algorithm implementation for FDTD method is as presented below:

- Set-up the geometry,
- Set nominal value of all the filed to zero
- Repeat the following procedure until the response is zero:
    - Impose the Gaussian excitation
    - Calculate $H^{n+1/2}$
    - Calculate $E^{n+1/2}$
    - Set tangential E to zero on conductors
    - Save field values
    - $n \rightarrow n+1$

The FDTD method is still a subject of ongoing research. There are a handful of topics which are not discussed here as a matter of brevity. These topics include:

- FDTD in curvilinear coordinates
- Equivalent circuit parameter extraction
- Different types of Absorbing boundary conditions
- Multi-grid FDTD algorithms

I.7.5 The method of moments

The method owes its name to the process of taking moments by multiplying with appropriate weighting functions and integrating. The method of moments (MoM) was first introduced to the western society by R. F. Harrington in early1960's. But actually the method has originated by two Russian scientists [119]and [120].

In the method of moments, prior to the discretization, Maxwell's electromagnetic equations are transformed into integral equations. These follow from the definition of suitable electric and magnetic Green's functions in the multilayered substrate. This formulation expresses the electric and magnetic field as a combination of a vector and a scalar potential. The unknowns are the electric and magnetic surface currents flowing in segments.

I.8 Conclusion

Different stages of the computer-aided design (CAD) of microwave devices is discussed in this chapter. The design procedure consists in a design loop that updates dimensions of a structure in order to minimize a cost function based on the electromagnetic analysis of the device performance (with different metrics such as S-parameters, impedance, etc). Different elements of such a design loop are discussed in detail. Many significant attempts to improve the speed and the accuracy of microwave CAD have been reported. In the previous work the emphasis has been mostly to improve the efficiency of individual elements of a design loop, more notably,

- The speed and accuracy of EM solvers has been a matter of academic and industrial research,
- The update techniques have been improved continuously.

Since the above mentioned techniques have been conducted within the framework of the conventional optimization procedure their overall effect had some extents. There are two inherent problems of a classical technique which have not been addressed in the literature:

- All the methods reported in the literature, require multiple EM analysis of the structure. Even though using more intelligent update techniques reduces the number of simulations per design, but time overhead of EM analysis is still an obstacle which keeps the design time in the order of hours.
- Both convergence and the duration of these methods highly depend on the choice of initial point in parameter space.

The following chapters addresses some solutions for the two above mentioned issues. One possible solution to avoid multiple simulations is to create a parameterized model of the device. Such a model can be derived with a single EM analysis of the device. Consequent calculations of the objective function can be calculated using this parameterized model which takes several times less than performing a full analysis. In Chapter II derivation of a geometrically parameterized model is presented. The optimization procedure should be adopted to be used with this parameterized model. One of the required modifications to deploy the parameterized model is mesh parameterization. Mesh deformation and parameterization is normally studied in the context of computer graphics and also structural analysis (mechanical engineering).

The issue of mesh parameterization in EM analysis is also investigated in chapter II. This will lead to fully incorporating the parameterized model into an optimization procedure.

Genetic algorithm (GA) has long been in practice because of their being relatively independent of initial point. This property is of specific interest when there is no or a little knowledge about the initial structure. The main drawback with GA is that the method requires many evaluations of the objective function at each iteration. Thus the method lacks speed. Particle swarm optimization (PSO) is a novel evolutionary method that starts with a randomly generated initial population similar to GA, but the evolution is faster. This method is described in chapter III followed by its application to device design.

The common aspect of the described chapters is the attempt to grant more autonomy and robustness to the conventional optimization algorithms.

I.9 References

[1] J. W. Bandler, "Optimization methods for computer aided design," *IEEE Transaction on Microwave Theory and Techniques*, vol. MTT-17, No. 8, pp. 533-552, August 1969.

[2] G.C. Temes and D.A. Calahan (1967), "Computer-aided network optimization the state of-the-art,". *Proc. IEEE*, vol. 55, pp. 1832-1863.

[3] J. M.Johnson and Y.Rahmat-Samii, "Genetic algorithms in electromagnetics," *Proc. IEEE Antennas Propagat. Soc. Int. Symp.* Baltimore, MD, pp. 1480-1483, July 1996.

[4] J. W.Bandler, R. M.Biernacki, S. H.Chen, P. A.Grobelny, and R. H.Hemmers, "Space mapping technique for electromagnetic optimization," *IEEE Trans. Microwave Theory Tech.*, vol. 42, pp. 2536-2544, Dec. 1994.

[5] J. E. Rayas-Sánchez, *Neural space mapping methods for modeling and design of microwave circuits*, Ph.D. dissertation Hamilton, ON, Canada: Dept. Elect. Comput. Eng., McMaster Univ., 2001

[6] J. Robinson and Y. Rahmat-Samii, "Particle swarm optimization in electromagnetics," IEEE *Transactions on Antennas and Propagation*, vol. 52, No. 2, pp. 397 – 407, Feb. 2004

[7] J. W. Bandler, "Optimization methods for computer aided design," *IEEE Transaction on Microwave Theory and Techniques*, vol. MTT-17, No. 8, pp. 533-552, August 1969.

[8] J. W. Bandler, R. M. Biernacki, S. H. Chen, L. W. Hendrick, and D. Omeragic, "Electromagnetic optimization of 3-D structures," *IEEE Transaction on Microwave Theory and Techniques*, vol. MTT-45, No. 5, pp. 770-779, May 1997.

[9] S. Ratnajeevan and H. Hoole, "An integrated system for the synthesis of coated waveguides from specified attenuation," *IEEE Transaction on Microwave Theory and Techniques*, vol. MTT-40, No. 7, pp. 1564-1571, July 1992.

[10] D. Budimir and G. Goussetis, "Design of asymmetrical RF and microwave bandpass filters by computer optimization," *IEEE Transaction on Microwave Theory and Techniques*, vol. MTT- 51, No. 4, pp. 1174-1178, April 2002.

[11] P. Harscher, S. Amari and R. Vahldieck, "A fast finite-element-based field optimizer using analytically calculated gradients," *IEEE Transaction on Microwave Theory and Techniques*, vol. MTT-50, No. 2, pp. 433-439, February 2002.

[12] P. Kozakowski and M. Mrozowski, "Automated CAD of coupled resonator filters," *IEEE Microwave and Wireless Components Letter*, vol. MWCL-12, No. 12, pp. 470-472, December 2002.

[13] D. De Zutter, J. Sercu, T. Dhaene, J. De Geest, F. J. Demuynck, S. Hammadi, C. P. Huang, "Recent trends in the integration of circuit optimization and full-wave electromagnetic analysis," *IEEE Transaction on Microwave Theory and Techniques*, vol. MTT-52, No. 1, pp. 245-256, January 2004.

[14] D. Nair and J. P. Webb, "Optimization of microwave devices using 3-D finite elements and the design sensitivity of the frequency response," *Transaction on Magnetics*, vol. MAG-39, No. 3, pp.1325-1328, may 2003.

[15] J. P. Webb, "Design sensitivity of frequency response in 3-D finite-element analysis of microwave devices," *IEEE Transaction on Magnetics*, vol. MAG-38, No. 2, pp. 1109-1112, March 2002.

[16] N. K. Georgieva, S. Glavic, M. H. Bakr and J. W. Bandler, "Feasible adjoint sensitivity technique for EM design optimization," *IEEE Transaction on Microwave Theory and Techniques*, vol. MTT-50, No. 12, pp. 2751-2758, December 2002.

[17] N. K. Georgieva, J. W. Bandler, and M. H. Bakr "Adjoint techniques for sensitivity analysis in high-frequency structure CAD," *IEEE Transaction on Microwave Theory and Techniques*, vol. MTT-52 , No.1, pp. 403-419 , January 2004.

[18] S. Bila, D. Baillargeat, M. Aubourg, S verdeyme, F. Seyfert, L. Baratchart, C. Boichon, F. Thevenon, J. Puech, C. Zanchi, L. Lapierre and J. Sombrin, "Finite-element modeling fror design optimization of microwave filters," *IEEE Transaction on magnetics*, vol. MAG-40 , No.2, pp. 1472-1475, March 2004.

[19] A. Garcia-Lamperez, S. Llorente-Romano, M. Salazar-Palma and T. K. Sarkar, "Efficient electromagnetic optimization of microwave filters and multiplexers using rational models," *IEEE Transaction on Microwave Theory and Techniques*, vol. MTT-52 , No.2, pp. 508-512, February 2004.

[20] W. A. Atia, A. A. Zaki and A. E. Atia, "Synthesis of general topology multiple coupled resonator filters by optimization," *Proceedings of 1998 IEEE MTT-S International Microwave Symposium*, vol. 2, pp. 821–824, June 1998.

[21] R. Tascone, P. Savi, D. Trinchero and R. Orta, "Scattering matrix approach for the design of microwave filters," *IEEE Transaction on Microwave Theory and Techniques*, vol. MTT-48 , No. 3, pp. 423-430, March 2000.

[22] P. Kozakowski and M. Mrozowski, "gradient-based optimization of filters using FDTD software," *IEEE Microwave and Wireless Components Letters*, vol. MWCL-10, No. 10, pp. 389-391, October 2002.

[23] J. W. Bandler, W. Biernacki, S. H. Chen, D. G. Swanson, and S Ye, "Microstrip filter design using direct EM field simulation," *IEEE Transaction on Microwave Theory and Techniques*, vol. MTT-42 , No. 7, pp. 1353-1359, July 1994.

[24] V. Rizzoli, A. Costanzo, D. Masotti, A. Lipparini and F. Mastri, "Computer-aided optimization of nonlinear microwave circuits with the aid of electromagnetic simulation," *IEEE Transaction on Microwave Theory and Techniques*, vol. MTT-52 , No. 1, pp. 362-377, January 2002.

[25] H. Lee and T. Itoh, "A systematic optimum design of waveguide-to-microstrip transition," *IEEE Transaction on Microwave Theory and Techniques*, vol. MTT- 45 , No. 5, pp. 803-809, May 1997.

[26] M. Gavrilovic and J. P. Webb, "accuracy control in the optimization of microwave devices by finite-element methods," *IEEE Transaction on Microwave Theory and Techniques*, vol. MTT-50, No. 8, pp. 1901-1911, August 2002.

[27] A. Garcia-Lamperez, M. Salazar-Palma, M. J. Padilla-Cruz and I. H. Carpintero, "synthesis of cross-coupled lossy resonator filter with multiple input/output couplings by gradient optimization," *Proceedings of 2003 IEEE MTT-S International Microwave Symposium*, pp. 52–55, June 2003.

[28] S. Bila, D. Baillargeat, S. Verdeyme and P. Guillon, "Automated electromagnetic optimization method for microwave devices," IEEE Microwave and Guided Wave Letters, vol. 7, No. 8, pp. 242 – 244, August 1997.

[29] E. A. Soleiman, M. H. Bakr and N. K. Nikolova, "Accelerated gradient-based optimization of planar circuits," *IEEE Transaction on Antennas and Propagation*, vol. AP-53 , No. 2, pp.880-883, February 2005.

[30] S. Bila, D. Baillargeat, M. Aubourg, S. Verdeyme, P. Guillon, F. Seyfert, J. Grimm, L. Baratchart, C. Zanchi, J. Sombrin, "Direct electromagnetic optimization of microwave filters" *IEEE Microwave Magazine,* vol. 2, Issue 1, pp. 46 – 51, March 2001.

[31] J. E. Rayes-Sanchez, F. Lara-Rojo, and E. Martinez-Guerrero, "A linear inverse space-mapping (LISM) algorithm to design linear and nonlinear RF and microwave circuits," *IEEE Transaction on Microwave Theory and Techniques*, vol. MTT-53, No. 3, pp. 960-968, March 2005.

[32] R. Levy and S. Cohn, "A history of microwave filter research, design and development," *IEEE Transaction on Microwave Theory and Techniques*, vol. MTT-32, No. 9, pp. 1055-1067, September 1984.

[33] S. Bila, D. Baillargeat, M. Aubourg, S. Verdeyme, P. Guillon, C. Zanchi, J. Sombrin, J. Grimm and L. Batchart, "Direct Electromagnetic optimization method for microwave filter design," *Electronics Letters*, vol. 35, No. 5, pp. 400-401, 4th Mrach 1999.

[34] M. Aubourg, J. Villotte, F. Godon and Y. Garault, "Finite element analysis of lossy waveguides- application to microstrip lines on semiconductor substrates," *IEEE Transaction on Microwave Theory and Techniques*, vol. MTT-31, No. 4, pp. 326-331, April 1983.

[35] Y. Yang, A. Bondeson and T. Rylander, " Application of gradient method to shape optimization in 3D," *Proceedings of Computational Electromagnetics EMB04*, Chalmers University of Technology, Göteborg, Sweden, October 2004.

[36] H. Schmidel, " Optimization of arbitrary frequency response of microwave bandstop filter," *Proceedings of 1999 IEEE-Russia Conference: MIA-ME'99*, pp. 11.7-11.12, June 1999.

[37] M. Zhang and T. Weiland, "Automated optimization of waveguide-microstrip transition using an EM optimization driver," *IEEE Transaction on Microwave Theory and Techniques*, vol. MTT-45, No. 5, pp. 861-864, May 1997.

[38] S. W. Director, "Survery of circuit-oriented optimization techniques," *IEEE Transaction on Circuit Theory*, vol. CT-18, No. 1, pp. 3-10, January 1971.

[39] J. W. Bandler, S. H. Chen, S. Daijavad, K. Madsen, "Efficient optimization with integrated gradient approximation," *IEEE Transaction on Microwave Theory and Techniques*, vol. MTT-36, No. 2, pp. 444-455, February 1988.

[40] F. M. Vanin, D. Schmitt, R. levy, "Dimensional synthesis for wide-band waveguide filters and diplexers," *IEEE Transaction on Microwave Theory and Techniques*, vol. MTT-52, No. 11, pp. 2488-2495, November 2004.

[41] J. W. Bandler and C. Charalambous, " Theory of generalized least *p*th approximation," *IEEE Transaction on Circuit Theory*, vol. CT-19, No. 5, pp. 287-289, May 1972.

[42] G. C. Temes, D. Y. F. Zai, "Least *p*th approximation," *IEEE Transaction on Circuit Theory*, vol. CT-16, No. 5, pp. 235-237, May 1969.

[43] M. R. Aaron, "The use of least squares in system design," *IRE Transactions on Circuit Theory*, vol. CT-3, pp. 224-231, December 1956.

[44] J. W. Bandler and P. A. Macdonald, "Optimization of microwave networks by razor search," *IEEE Transaction on Microwave Theory and Techniques*, vol. MTT-17, No. 8, pp. 552-562, August 1969.

[45] J. W. Bandler, "Computer optimization of Inhomogeneous waveguide transformers," *IEEE Transaction on Microwave Theory and Techniques*, vol. MTT-17, No. 8, pp. 563-571, August 1969.

[46] J. W. Bandler and P. A. Macdonald, "Cascaded noncomensurate transmission lines as optimization problems," *IEEE Transaction on Circuit Theory*, vol. CT-16, pp. 391-394, August 1969.

[47] G. C. Temes and D. A. Calahan, "Computer-aided optimization, the state of the art," *Proceedings of IEEE*, vol. 55, pp. 1832-1863, November 1967.

[48] C. W. Carroll, "The created response surface technique for optimizing nonlinear, restrained systems," *Operations Research*, vol. 9, pp. 169-185, 1961.

[49] A. D. Waren, L. S. Lasdon and D. F. Suchman, " Optimization in engineering design," *Proceedings of IEEE*, vol. 55, pp. 1885-1897, November 1967.

[50] J. Bracken and G. P. Mc Cormick, *Selected Applications of Nonlinear Programming*, New York, Wiley, 1968.

[51] H. W. Kuhn and A. W. Tucker, "Non-Linear programming," *Proceedings of 2nd Math, Statistics and Probability*, Berkeley, California:University of California Press, 1951, pp. 481-493.

[52] J. B. Rosen, "The gradient projection method for nonlinear programming, Part I. Linear Constraints," *Journal of SIAM*, vol. 8, pp.181-217, March 1960.

[53] G. Zoutendijk, "Nonliner programming: a numerical survey," *Journal of SIAM Control*, vol. 4.,pp. 194-210, February 1966.

[54] L. Lasdon and A. D. Waren, "Mathematical programming for optimal design," *Electro-Technology*, vol. 80, pp. 55-70, November 1967.

[55] P. E. Gill, W. Murray and M. H. Wright, *Practical optimization*, Elsevier Academic Press, San Diego, 2004.

[56] Cedrick Saboureau, *Analyses électromagnétiques et méthodologies de conception associées, dédiées à l'optimisation de composants et modules millimétriques*, PhD Dissertation, Université de Limoges, September 2004.

[57] G. Matthaei, L. Young and EMT Joned, *Microwave filters, impedance matching networks and coupling structures*, Artech House, 1980.

[58] C. Saboureau, S. Bila, D. Baillargeat, S. Verdeyme and P. Guillon, "Accurate computer aided design of interdigital filters applying a coupling identification method," *Proceedings of 2002 IEEE MTT-S International Microwave Symposium*, pp. 2089–2092, June 2002.

[59] R. P. Brent, Algorthms for minimization without derivatives, Prentice-Hall Series in Automatic computation, New York, 1973.

[60] M. J. D. Powell, "An efficient method for finding the minimum of a function of several variables without calculating derivatives," *Computer Journal*, vol. 7, pp. 155-162, July 1964.

[61] M. J. Box, " A comparison of several current optimization methods, and the use of transformations in costrained problems," *Computer Journal*, vol. 9, pp. 67-77, May 1966.

[62] R. Fletcher, "Function minimization without evaluating derivatives- a review," *Computer Journal*, vol. 8, pp. 33-41, April 1965.

[63] W. I. Zangwill, "Minimizing a function without calculating derivatives," *Computer Journal*, vol. 10, pp. 293-296, November 1967.

[64] M. Celuch-Marcysiak, W. Gwarek; P. Miazga, M. Sypniewski; A. Wieckowski, **"**Automatic design of high frequency structures using a 3-D FD TD simulator in an optimisation loop," Proccedings of 13th International Conference *Microwaves, Radar and Wireless Communications*. 2000. MIKON-2000. vol. 1, May 2000.

[65] E. Sanchez-Sinencio, T. N. Trick, **"**CADMIC-Computer-Aided Design of Microwave Integrated Circuits;" IEEE *Transactions on Microwave Theory and Techniques*, vol. MTT-22, Issue 3, pp. 309 – 316, March 1974

[66] J. W. Bandler, S. H. Chen, S. Daijavad, K. Madsen, "Efficient optimization with integrated gradient approximations,"; IEEE *Transactions on Microwave Theory and Techniques*, vol. MTT-36, No. 2, pp. 444 – 455, February. 1988.

[67] J. W. Bandler, Q. J. Zhang; J. Song; R. M. Biernacki, "FAST gradient based yield optimization of nonlinear circuits**,"** IEEE *Transactions on Microwave Theory and Techniques*, vol. MTT-38, No. 11, pp. 1701–1710, November 1990.

[68] R. Hooke, and T. A. Jeeves, "Direct search solution of numerical and statistical problems," *Journal of ACM*, vol. 8, pp. 212-229, April 1961.

[69] V. G. Gelnovatch, I. L. Chase, "DEMON-an optimal seeking computer program for the design of microwave circuits," IEEE *Journal of Solid-State Circuits*, vol. 5, No. 6, pp. 303 – 309, December 1970.

[70] Spendley, W., Hext, G. R., Himsworth, F. R. *Sequential application of simplex designs in optimisation and evolutionary operation.* Technometrics 4(1962):4 441-461.

[71] J. A. Nelder, R. Mead, "A simplex method for function minimization," *Computer Journal*, vol. 7, pp. 308-313, 1965.

[72] D. Betteridge, A. P. Wade, A. Howard, "Reflections on the modified simplex – II," *Talanta*, vol. 32, No. 8B, pp. 723-734, 1985.

[73] E. R. Aberg, A. G. Gustavsson, "Design and evaluation of modified simplex methods," *Analytica Chimica Acta*, vol. 144, pp. 39-53, 1985.

[74] K. S. Nikita, N. K. Uzunoglu, N. G. Maratos, "Coupled radiation between concentrically placed waveguide applicators: optimization of the deposited power distribution inside a lossy medium," IEEE *International Microwave Symposium Digest* pp. 311 – 314, May 1995.

[75] M. O. Thieme, E. M. Biebl, "A fast and rigorous synthesis procedure for (monolithic) millimeterwave integrated circuit layout," IEEE *International Microwave Symposium Digest* pp. 1009 – 1012, June 1997.

[76] P. E. Gill, W. Murray and M. H. Wright, *Practical optimization*, Elsevier academic press, New York, 2004.

[77] E. Polak, *Computational methods in optimization*, Academic Press, New York, 1991.

[78] J. W. Bandler, "Optimization methods for computer aided design," *IEEE Transaction on Microwave Theory and Techniques*, vol. MTT-17, No. 8. pp. 533-552, August 1969

[79] K. No-Weon, C. Young-Seek, C. Changyul, J. Hyun-Kyo, "A new 2-D image reconstruction algorithm based on FDTD and design sensitivity analysis," *IEEE Transaction on Microwave Theory and Techniques*, vol. MTT-50, No. 12, pp. 2734 – 2740, December 2002.

[80] E. Luneville, J. M. Krieg, E. Giguet, "An original approach to mode converter optimum design," IEEE *Transaction on Microwave Theory and Techniques*, vol. MTT-46, No. 1, pp. 1-9, Jan. 1998.

[81] S. Jinwoo, C. Changyul, "Computer aided optimal design of H-plane W/G circulato," proceedings of IEEE *Antennas and Propagation Society International Symposium*, pp. 506-509, July 1997.

[82] C. Fung-Yuel, "Computer-aided characterization of TEM transmission lines," IEEE *Transactions on Circuits and Systems*, vol. 27, No 12, pp. 1194-1205, December 1980.

[83] F. Qianqian, P. M. Meaney, K. D. Paulsen, "Microwave image reconstruction of tissue property dispersion characteristics utilizing multiple-frequency information," IEEE *Transaction on Microwave Theory and Techniques*, vol. MTT-52, No. 8, pp. 1866-1875, August 2004.

[84] A. E. Souvorov, A. E. Bulyshev, S. Y. Semenov, R. H. Svenson, A. G. Nazarov, Y. E. Sizov, G. P. Tatsis, "Microwave tomography: a two-dimensional Newton iterative scheme," *IEEE Transaction on Microwave Theory and Techniques*, vol. MTT-46, No. 11, pp. 1654-1659, November 1998.

[85] . E. Souvorov, A. E. Bulyshev, S. Y. Semenov, R. H. Svenson, A. G. Nazarov, Y. E. Sizov, G. P. Tatsis, "A two-dimensional Newton iterative scheme for high contrast full-scale microwave tomography," Proceedings of IEEE *Microwave Symposium Digest*, pp. 1871 – 1872, June 1998.

[86] Q. Anyong, L. Ching, "An improved algorithm for microwave imaging of parallel perfectly conducting cylinders," proceedings of IEEE *Antennas and Propagation Society International Symposium* , pp. 1772-1775, July 2000.

[87] M. Santra, K. U. Limaye, "Estimation of complex permittivity of arbitrary shape and size dielectric samples using cavity measurement technique at

microwave frequencies," *IEEE Transaction on Microwave Theory and Techniques*, vol. MTT-53, No. 2, pp. 718 – 722, February 2005.

[88] W. Press, S. A. Teukolsky, W. T. Vetterling and B. P. Flannery, *Numerical recipes*, Cambridge University Press, New York 1992.

[89] Rall, L.B., *Automatic Differentiation - Techniques and Applications*, Lecture Notes in Computer Science 120, Springer-Verlag, Berlin, New York, 1981.

[90] Griewank, A., On Automatic Differentiation, Mathematical Programming 1988, Kluwer Academic Publishers, Japan, 1988, pp. 83-107.

[91] Luenberger, D.G., Linear and Nonlinear Programming, Second Edition, Addison-Wesley, Reading, Massachusetts, 1984.

[92] Gill, P.E., Murray, W., Saunders, M. A. and Wright, M.H., Computing Forward-Difference Intervals for Numerical Optimization, SIAM J. Sci. Stat. Comput. 4, 310-321, 1983.

[93] Dennis Jr., J.E. and More, J.J., Quasi-Newton Methods, Motivation and Theory, SIAM Review 19, 46-89, 1977.

[94] Gilbert, J.C., and Lemarechal, C., Some Numerical Experiments with Variable-Storage Quasi-Newton Algorithms, Math. Prog. 45, 407-435, 1989.

[95] M. Sadiku, *Numerical Techniques in Electromagnetics*, 2nd Edition, CRC Press, 2001.

[96] Peterson at all, *Computational Methods in Electromagentics*, IEEE Press, 1998.

[97] Daniel G. Swanson Jr., Wolfgang J. R. Hoefer, *Microwave Circuit Modeling Using Electromagnetic Field Simulation*, Artech House, Hardcover, June 2003.

[98] Tatsuo Itoh (Editor), Numerical Techniques for Microwave and Millimeter-Wave Passive Structures, Wiley-Interscience, April, 1989.

[99] by W. H. A. Schilders and E.J.W. Ter Maten, *Numerical Methods in Electromagnetics : Special Volume (Handbook of Numerical Analysis), Elsevier Science*, May 2005.

[100] Levent Sevgi, *Complex Electromagnetic Problems and Numerical Simulation Approaches*, IEEE-Wiley Press Series on Electromagnetic Wave Theory, May 2003.

[101] M. N. O. Sadiku, "A simple introduction to finite element analysis of electromagnetic problems," *IEEE Trans. Educ.*, vol. 32, no. 2, May 1989, pp. 85-93.

[102] P.P. Silvester and R.L. Ferrari, *Finite Elements for Electrical Engineers.* Cambridge: Cambridge University Press, 3rd ed., 1996.

[103] Aubourg, M.; Villoite, J.-P.; Godon, F.; Garault, Y. ,"Finite Element Analysis of Lossy Waveguides-Application to Microstrip Lines on Semiconductor Substrate," *IEEE Transactions on Microwave Theory and Techniques*, Volume 83, Issue 4, Page(s):326 – 331, Apr 1983

[104] Bila, S.; Baillargeat, D.; Aubourg, M.; Verdeyme, S.; Seyfert, F.; Baratchart, L.; Boichon, C.; Thevenon, F.; Puech, J.; Zanchi, C.; Lapierre, L.; Sombrin, J., ''Finite-element modeling for the design optimization of microwave filters'', IEEE *Transactions on Magnetics*, Volume 40, Issue 2, March 2004 Page(s):1472 – 1475

[105] M. Simeoni, R. Sorrentino, S.Verdeyme, "The circular wire-patch resonator-theory, numerical analysis, and filter design application," IEEE *Transaction on Microwave Theory and Techniques*, vol. MTT-51, No. 4, pp. 1187-1193, April 2003.

[106] S. Bila, D. Baillargeat, M. Aubourg, S. Verdeyme, P. –Y Guillon, F. Seyfert, J. Grimm, L. Baratchart, C. Zanchi, J. Sombrin, "Direct electromagnetic optimization of microwave filters," IEEE *Microwave Magazine*, vol. 2, No. 1, pp. 46-51, March 2001

[107] D. Baillargeat, S. Verdeyme, P. –Y Guillon, "Slotted dielectric resonators for rigorous design of a four-poles dual mode filter," *IEEE Microwave and Guided Wave Letters*, vol. MGWL-4, No. 10, pp.332-334, October 1994

[108] J. P. Cousty, M. Aubourg, S. Verdeyme and P. –Y Guillon, "Finite elements for microwave device simulation: application to microwave dielectric resonator filters," ," IEEE *Transaction on Microwave Theory and Techniques*, vol. MTT-40, No. 5, pp. 925-932,May 1992.

[109] S. Verdeyme and P. –Y Guillon, "Scattering matrix of dielectric resonator coupled with two microstrip lines," IEEE *Transaction on Microwave Theory and Techniques*, vol. MTT-39, No. 3, pp. 517-520 March 1991.

[110] E. Larique, S. Mons, D. Baillargeat, S.Verdeyme, M. Aubourg, R. Quere, P. Guillon, C. Zanchi, J. Sombrin, "Linear and nonlinear FET modeling applying an electromagnetic and electrical hybrid software," IEEE *Transaction on Microwave Theory and Techniques*, vol. MTT-47, No. 6, pp. 915-918, June 1999.

[111] S. Bila, D. Baillargeat, M. Aubourg, S. Verdeyme, P. –Y Guillon, "Automated electromagnetic optimization method for microwave devices," *IEEE Microwave and Guided Wave Letters*, vol. MGWL-7, No. 8, pp. 242-244, August 1997

[112] A. Taflove and S. C. Hagness, *Computational Electrodynamics: The Finite-Difference Time-Domain Method, 3rd ed.* Norwood, MA: Artech House, 2005.

[113] K. Yee, "Numerical solution of inital boundary value problems involving maxwell's equations in isotropic media" IEEE *Transactions on Antennas and Propagation,* Volume: 14, Issue: 3 page(s): 302- 307May 1966.

[114] A. Taflove and M. E. Brodwin, "Numerical solution of steady-state electromagnetic scattering problems using the time-dependent Maxwell's equations," *IEEE Trans. Microwave Theory and Techniques*, vol.MTT- 23, pp. 623-630, Aug. 1975.

[115] A. Taflove and M. E. Brodwin, "Computation of the electromagnetic fields and induced temperatures within a model of the microwave-irradiated human eye," *IEEE Trans. Microwave Theory and Techniques*, vol. 23, pp. 888-896, Nov. 1975.

[116] D. M. Sheen, S. M. Ali, M. D. Abouzahra, J. A. Kong, "Application of the three-dimensional finite-difference time-domain method to the analysis of planar microstrip circuits," *IEEE Trans. Microwave Theory and Techniques*, vol. MTT-38, No. 7, pp. 849-857, July 1990.

[117] D. M. Sheen, *Numerical modeling of microstrip circuits and antennas*. PhD Dissertation, MIT 1991.

[118] R.F. Harrington, *Field Computation by Moment Methods.* Malabar, FL: Krieger,1968.

[119] L.V. Kantorovich and V.I. Krylov, *Approximate Methods of Higher Analysis*(translated from Russian by C.D. Benster). New York: John Wiley, 1964.

[120] Y.U. Vorobev, *Method of Moments in Applied Mathematics* (translated from Russian by Seckler). New York: Gordon & Breach, 1965.

CHAPTER II

Optimization using Parameterized EM-Models

II.1. Introduction

The classical approach for design of microwave circuits and devices was explained in Chapter I. It can be concluded:

- The most time consuming part of a design loop is the Electromagnetic analysis.
- Calculating gradients requires multiple computations of the objective function.
- The mesh generated at each step is not usable in the next step. Even a slight perturbation might end to a totally different mesh.

The update strategies should adaptively be changed. In order to obtain the system responses within the frequency range of interest, it is a common practice to solve the system equation directly at many frequencies. Subsequently, the results are interpolated to form a continuous curve. However, with the increasing size of the system, solving this system of equations at many discrete frequency points can be very time consuming. Especially when the system possesses frequency range, it may be necessary to solve hundreds of solutions to obtain the desired resolution in the spectrum.

This chapter presents the efforts towards accelerating the optimization procedure through parameterization results. The core idea behind parameterization is to obtain a mathematical model of the response in a design problem, by only one calculation. To achieve a fully parameterized model, final response (e.g. frequency response) and intermediate functions (e.g. structure meshing) are tried to be expressed in terms of polynomials, so that re-calculation of these functions with perturbed parameter space will require much less resources.

But beyond saving some time in a classical design loop (as shown in Fig. 1 of Chapter I), using a parameterized model enables us to redefine the design procedure in such a way that the parameter updates will be carried through a shorter path.

Fig. II.1 illustrates the modified design flow graph with parameterized model. The parameterization has been done in different stages are, mesh parameterization, frequency parameterization, geometrical parameterization.

In practice some or all of these techniques may apply to a specific problem. The major focus in this chapter has been on frequency domain electromagnetic field solvers but the method can be applied to time domain techniques with slight modifications.

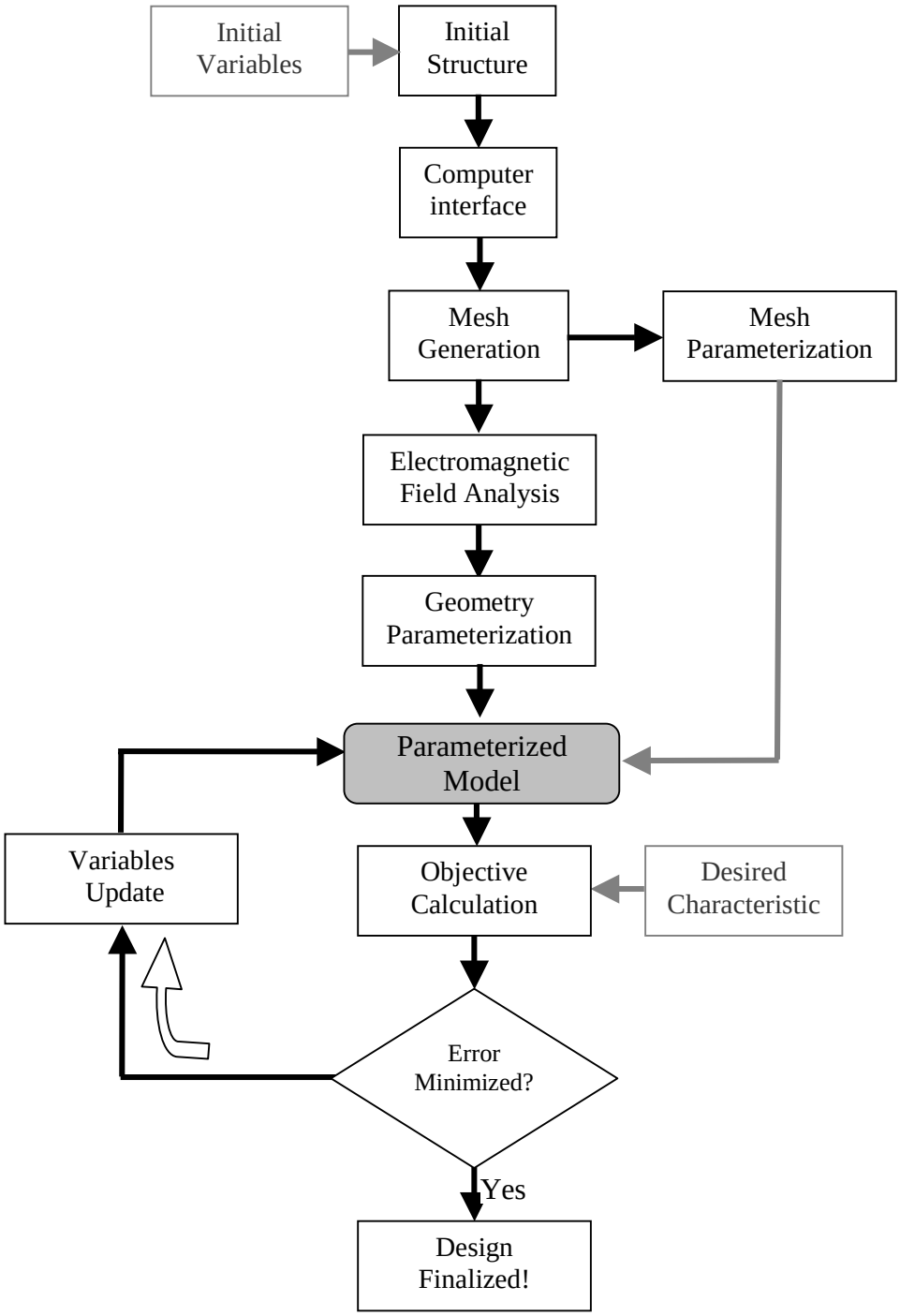

Fig. II.1. The design flowgraph using the parameterized model

II.2. Parameterization

Any design procedure consists of functionals to be optimized (objective function) and design variables (parameters).

In the context of microwave engineering, the objective function is normally a function of electromagnetic fields quantity, impedance, or related parameters such as S-parameters.

Design variables can be geometric variables like dimensions of a physical structure, material properties, or a physical quantity such as frequency or amplitude of input signal of a system or input electromagnetic fields of a two-port microwave network. The numerical procedure in a design problem can be symbolically written as,

$$F(\bar{\phi}, V(\bar{\phi})) = 0 \qquad \text{(II- 1)}$$

where $\bar{\phi}$ is the parameter vector (dimensions, material properties, etc) and $V(\bar{\phi})$ is an arbitrary function representing a physical quantity (i.e. electric field, power, etc).

The goal of parameterization is to construct a continuous function $\tilde{V}(\bar{\phi})$ that approximates the discrete solution of $V(\bar{\phi})$ in the whole parameter space. In practice it is not possible to find an appropriate function which is valid in the whole parameter space. The mathematical functions used for parameterization can only apply in a limited region, thus to span the whole feasible region in an optimization one should parameterize the function $V(\bar{\phi})$ in several points in parameter space.

The mathematical functions used for parameterization vary depending on the behavior of every function with respect to different parameters. For example in order to parameterize the field quantity within a microwave device, the utilized parameterizing function should be a rational function to appropriately fit the poles and zeros.

In the following sections, the parameterization with respect to geometry and frequency are discussed in detail. Consecutively, an optimization technique which deploys this parameterized model is presented. Finally examples of the parameterization will be demonstrated.

II.3. Literature survey

A number of model reduction techniques have been successfully developed for simulating transient responses in circuit analyses [2] finding poles to determine the stability condition in feedback control process [4],and fast frequency-sweep techniques for EM devices modeling [6]. Among them, the asymptotic waveform evaluation (AWE) method? was originally developed for timing analysis of high-speed circuits. Through explicit moment matching, the AWE technique approximates the transient response of a circuit by reducing the problem to a low-order model. The poles of the reduced model are good approximations of the dominant poles of the original system. However, one major problem of the AWE technique is that it does not provide an accurate approximation (even with many moments) when the expansion point is very close to a pole (resonance of transfer function). More stable model reduction approaches (using variants of Krylov subspace methods) are proposed by Gallivan [4]. Furthermore, a Lanczos algorithm with an implicit restart process is proposed in [6], which ensures the reduced model always produces a stable approximation, and a rational Lanczos algorithm is presented in [7] which extracts information from multiple points and, therefore, provides improvements in the rate of convergence. These methods are usually very efficient and numerically stable. However, for Maxwell's equations, particularly with losses presented by lossy dispersive materials, as well as radiation boundary conditions, one has to extend the required Krylov subspaces to general matrix polynomials. In contrast, the explicit AWE can always be applied to realize a Padé approximation. The recently published complex frequency hopping (CFH) technique [7] for EM application is an AWE-based multipoint moment-matching method. It exploited a binary search scheme to match all dominant poles in a systematic manner. This CFH algorithm has been applied to the scalar finite-element formulation of a Helmholtz equation in two dimensions. To the best of our knowledge, it has neither been applied to three-dimensional (3-D) EM problems, nor used with vector finite-element formulations. Moreover, the conventional AWE method chooses the expansion point on the real frequency axis. It is known that the convergence radius of a Taylor expansion is equal to the distance from the expansion point to the nearest singularity (pole). By using only the power series expansion for the transfer function, this typically results in a very small convergence radius. One fact exploited by the AWE method is that the

solution is analytic at the expansion point, and the partial realization, being a Padé approximation, is able to approximate pole behaviors much better than the power series. Nonetheless, when the expansion point is very close to a pole, the calculation of the moments will become increasingly inaccurate. Consequently, the Padé approximation will be polluted due to this inaccuracy of the moment computations, as well as the ill-conditioned matrix that is used to compute the Padé coefficients. To overcome this difficulty, various approaches such as the multipoint Padé approximation, CFH scheme, and rational Lanczos algorithm are proposed in the literature. They avoid extracting information from remote poles by catching multiple poles at multiple points.

II.4. Frequency parameterization

II.4.1. Formulation

The numerical technique ends up solving a matrix equation of the form of the equation (II- 1). To be more specific, a slight change in the notation (II- 1) can be re-written as,

$$A(f,\bar{p}).\mathbf{e}(f,\bar{p}) = \mathbf{B}(f) \qquad \text{(II- 2)}$$

where $A(f,\bar{p})$ is a complex symmetric matrix, $\mathbf{e}(f,\bar{p})$ is a vector whose entries represent the solution of unknown field, and $\mathbf{B}(f)$ is an excitation vector. Equation (II- 1) is typically solved for the unknown vector at a set of discrete frequencies using either a direct method or an iterative matrix solver. As functions of frequency $A(f,\bar{p})$, $\mathbf{B}(f)$ and $\mathbf{e}(f,\bar{p})$ can be assembled through the FEM or any other numerical technique for each specified frequency. For an efficient spectral response evaluation, we need to express $A(f,\bar{p})$ and $\mathbf{B}(f)$ as explicit functions of frequency. One straightforward way is to construct them through a polynomial interpolation, i.e., to expand and as

$$A(\hat{f};\bar{p}) = \sum_{m=0}^{M} a_m(\bar{p}).\hat{f}^m \qquad \text{(II- 3)}$$

$$\mathbf{B}(\hat{f}) = \sum_{q=0}^{Q} \mathbf{b}_q.\hat{f}^q \qquad \text{(II- 4)}$$

where $\hat{f} = (f - f_c)/(f_{\max} - f_{\min})$ is the normalized frequency, and f_c is the central frequency. This normalization maps the frequency band $[f_{\min}, f_{\max}]$ onto interval $[-1,1]$, where $f_{\min}, f_{\max}$ are the lowest and highest frequencies of interest, respectively. The orders of polynomials in (II- 3) and (II- 4) should be determined by the characteristics of the real problem.

If the underlying functions are nearly quadratic, so we choose. To minimize the numerical error and obtain stable interpolation, Chebyshev nodes can be utilized as the sampling points.

II.4.2. Moment matching

Like $A(f,\bar{p})$ and $\mathbf{B}(f)$, solution $\mathbf{e}(f,\bar{p})$ is also a function of frequency and is approximated by

$$\mathbf{e}(f,\bar{p}) = \sum_{m=0}^{M} \mathbf{e}_m(\bar{p})\,\hat{f}^m \qquad \text{(II- 5)}$$

Substituting (II- 3)-(II- 5) into (II- 2) and matching the coefficients with the assumption $M \geq Q$, we end up with the following system of linear equations,

$$\begin{aligned}
&a_0(\bar{p}).\mathbf{e}_0(\bar{p}) = \bar{b}_0 \qquad \text{(II- 6)}\\
&a_0(\bar{p}).\mathbf{e}_1(\bar{p}) + a_1(\bar{p}).\mathbf{e}_0(\bar{p}) = \bar{b}_1\\
&a_0(\bar{p}).\mathbf{e}_2(\bar{p}) + a_2(\bar{p}).\mathbf{e}_1(\bar{p}) + a_2(\bar{p}).\mathbf{e}_0(\bar{p}) = \bar{b}_2\\
&a_0(\bar{p}).\mathbf{e}_Q(\bar{p}) + a_2(\bar{p}).\mathbf{e}_{Q-1}(\bar{p}) + a_2(\bar{p}).\mathbf{e}_{Q-2}(\bar{p}).. = \bar{b}_Q\\
&a_0(\bar{p}).\mathbf{e}_{Q+1}(\bar{p}) + a_2(\bar{p}).\mathbf{e}_Q(\bar{p}) + a_2(\bar{p}).\mathbf{e}_{Q-1}(\bar{p}) + ... = 0\\
&.\\
&.\\
&a_0(\bar{p}).\mathbf{e}_M(\bar{p}) + a_1(\bar{p}).\mathbf{e}_{M-1}(\bar{p}) + a_2(\bar{p}).\mathbf{e}_{M-2}(\bar{p}) = 0
\end{aligned}$$

Subsequently, the power series coefficients of the solution, or the moments, can be obtained recursively by

$$\mathbf{e}_0(\bar{p}) = a_0^{-1}(\bar{p}).\bar{b}_0 \qquad \text{(a)} \qquad \text{(II- 7)}$$

$$\mathbf{e}_1(\bar{p}) = a_0^{-1}(\bar{p}).\left[\bar{b}_1 - a_1(\bar{p}).\mathbf{e}_0(\bar{p})\right] \qquad \text{(b)}$$

In modeling passive microwave components, we are usually most interested in the S-parameters. The actual parameter calculated using a numerical method such as Finite Elements Method is the field quantity. Thus the parameterization should be done over the field quantities,

$$\mathbf{E}(\hat{f},\bar{p}) = \sum_{m=1}^{M} \mathrm{e}_m\,\hat{f}^m \qquad \text{(II- 8)}$$

The number of moments is adaptively determined by the convergence behavior of the expansion, and ultimately depends on the complexity of the system of equation.

II.4.3. Padé approximation

It is known that the power series of (II- 5) or (II- 8) always has, unfortunately, a finite radius of convergence in the presence of poles. The Padé approximation is able to approximate the function beyond the convergent region of its power series.

After obtaining (II- 8), we will force it to agree with a Padé approximate of the electric fields. The idea of Padé approximation is to replace the polynomial with a rational polynomial, which is good at catching poles. The process is letting

$$\mathbf{e}(\hat{f},\overline{p}) = \sum_{m=1}^{M} \mathbf{e}_m(\overline{p})\,\hat{f}^{\,m} = \frac{\sum_{r=0}^{R} \mathbf{e}_r(\overline{p})\,\hat{f}^{\,r}}{1+\sum_{t=1}^{T} \mathbf{s}_t(\overline{p})\,\hat{f}^{\,t}} \qquad \text{(II- 9)}$$

where $T + R = M$. A different combination of T and R will produce the Padé table. This Padé approximation is a partial realization of the original system. The details of computing the Padé coefficients can be found in [5].

II.4.4. Calculating Padé approximants

There are two methods to calculate the coefficients of the Padé approximant of electric fields which will be discussed in this section. The procedure is explained for electric fields, but it can be similarly used for any other parameters in frequency domain.

Consider the Taylor series of the electric fields,

$$\mathbf{e}(f,\overline{p})\big|_{f=f_0} = \sum_{m=1}^{M} \mathbf{e}_m(\overline{p})\big|_{f=f_0}\,(f-f_0)^m \qquad \text{(II- 10)}$$

Provided that $S_{ij}(f,\overline{p})$ is analytic at $f = f_0$. The coefficients can be written as,

$$\mathbf{e}_m(\overline{p})\big|_{f=f_0} = \frac{\dfrac{\partial^m}{\partial f^m} A^{-1}(f,\overline{p})\Big|_{f=f_0}}{m!}.\overline{B}(f) \qquad \text{(II- 11)}$$

The first coefficient can be easily found as,

$$\mathbf{e}_0(\overline{p})\big|_{f=f_0} = A^{-1}(f_0,\overline{p}).\overline{B}(f_0) \qquad \text{(II- 12)}$$

It can be shown that the rest of coefficients are calculated recursively as,

$$\mathbf{e}_{m+1}(f=f_0,\overline{p}) = -A^{-1}(f_0,\overline{p}).\sum_{\kappa=1}^{m+1}\frac{\dfrac{\partial^{\kappa}}{\partial f^{\kappa}}A(f,\overline{p})\Big|_{f=f_0}.\mathbf{e}_m(f=f_0,\overline{p})}{\kappa!} \qquad \text{(II- 13)}$$

Now back to equation (II- 9), there are two methods to find the coefficients of the Padé approximation provided the Taylor coefficients are available. The first method uses a set of linear equations to obtain coefficients directly. The second method calculates the Padé approximation recursively.

II.4.5. Computing Padé approximants using point matching technique

Equation (II- 9) can be expanded as,

$$\sum_{m=1}^{M}\mathbf{e}_m(\overline{p})\,\hat{f}^{\,m} = \mathbf{e}_0(\overline{p})+\mathbf{e}_1(\overline{p})\,\hat{f}^{\,1}+\mathbf{e}_2(\overline{p})\,\hat{f}^{\,2}+\ldots+\mathbf{e}_M(\overline{p})\,\hat{f}^{\,P} \qquad \text{(II- 14)}$$

$$= \frac{a_0(\overline{p})+a_1(\overline{p})\,\hat{f}+a_2(\overline{p})\,\hat{f}^{\,2}+\ldots+a_M(\overline{p})\,\hat{f}^{\,M}}{1+b_1(\overline{p})\,\hat{f}+b_2(\overline{p})\,\hat{f}^{\,2}+\ldots+b_N(\overline{p})\,\hat{f}^{\,N}}$$

Multiplying the denominator polynomial with right hand side in (II- 14) and equating the coefficients of the identical powers of ***f*** gives,

$$\mathbf{e}_0(\overline{p}) = a_0(\overline{p}) \qquad \text{(II- 15)}$$

$$\mathbf{e}_1(\overline{p})+.\mathbf{e}_0(\overline{p}).\overline{b_1}(\overline{p}) = a_1(\overline{p})$$

$$\mathbf{e}_2(\overline{p})+\mathbf{e}_1(\overline{p})\overline{b_1}(\overline{p})+\mathbf{e}_0(\overline{p})\overline{b_2}(\overline{p}) = a_2(\overline{p}).$$

.

.

$$\mathbf{e}_M(\overline{p})+\mathbf{e}_{M-1}(\overline{p}).b_1(\overline{p})+\ldots+\mathbf{e}_0(\overline{p}).b_M(\overline{p}) = a_M(\overline{p})$$

$$\mathbf{e}_{M+1}(\overline{p})+\mathbf{e}_M(\overline{p}).b_1(\overline{p})+\ldots+\mathbf{e}_0(\overline{p}).b_{M+1}(\overline{p}) = 0$$

$$\mathbf{e}_{P+N}(\overline{p})+\mathbf{e}_{P+N-1}(\overline{p}).b_1(\overline{p})+\ldots+\mathbf{e}_0(\overline{p}).b_{P+N}(\overline{p}) = 0$$

Solving these equations would give the coefficients *a* and *b* of the Padé approximant. To Solve these equations one has to start with the last *P+N-M* equations (which are homogenous) and then solve the rest of *M* equations. Note that M, N and P are number of summation terms in (II- 14).

II.4.6. Recursive calculation of Padé approximants

Alternatively, the coefficients of the rational function can be found by means of a recursive computation scheme starting from a polynomial which interpolates the given data set.

This method corresponds to the computation of a cross-diagonal sequence in Padé table [18].

II.4.7. Selection of frequency points

Selection of frequency points is very important both for computational efficiency and accuracy. One possible approach in this regard is to use the ideal characteristic to find the critical points and calculate these points for matching the coefficients. These critical points can be for instance the poles and zeros of ideal characteristics. In order to calculate the approximation with a minimum number of points sufficient enough to approximate the frequency characteristic. The procedure starts with one point expansion at two ends of frequency range of interest, namely $f_{\min}$, $f_{\max}$. The poles are calculated distinctly at these points, if there exists a common pole, and then the calculation will be terminated. Otherwise a different point is chosen in the half way between the two poles computed in the last two stages and the above mentioned criteria will be examined until the poles calculated between every two frequency points are the same. This "binary" search helps to minimize the number of frequency points to be calculated in order to obtain an accurate Padé approximant.

II.4.8. Cauchy method

Cauchy method is an alternative way of approximating a function (that has poles) with a rational function. Although the resulting rational form is very similar to Padé, the derivation method is very different. Here Cauchy method is brought as a matter of completeness.

The field quantities can be described in the following form,

$$\mathbf{e}(\hat{f},\bar{p}) = \sum_{m=1}^{M} \mathbf{e}_m(\bar{p})\,\hat{f}^m = \frac{\sum_{r=0}^{R} a_r(\bar{p})\,\hat{f}^r}{1+\sum_{t=1}^{T} b_t(\bar{p})\,\hat{f}^t} \qquad \text{(II- 16)}$$

It is essential that the function is calculated in $T+R+1$ points. This way up, a set of linear equations are formed (similar to Padé approximation).

An alternative algorithm is suggested by Stoer and Burlisch [19]. This method performs the interpolation on tabulated data in a recursive procedure and thus does not require matrix inversion which was essential when finding coefficients through linear set of equations. Fig. II.2 illustrates the Stoer and Burlisch method for recursive computation of Cauchy approximants.

Let $\mathbb{S}_k = \mathbf{e}(f_k, \overline{p})$ be the value at f_k of the unique rational function of degree zero (i.e., a constant) passing through the point $\left(f_k, \mathbf{e}(f_k, \overline{p})\right)$. Now let $\mathbb{S}_{kl}$ be the rational polynomial of degree one passing through both $\left(f_k, \mathbf{e}(f_k, \overline{p})\right)$ and $\left(f_l, \mathbf{e}(f_l, \overline{p})\right)$. Similarly, for higher order polynomials up to $\mathbb{S}_{123\ldots(k-1)k}$, which is the value of the unique interpolating polynomial through all *k* points, i.e., the desired answer. The various $\mathbb{S}$'s form a tableau with ancestors on the left leading to a single descendant at the extreme right. An example is shown in Fig. II.2.

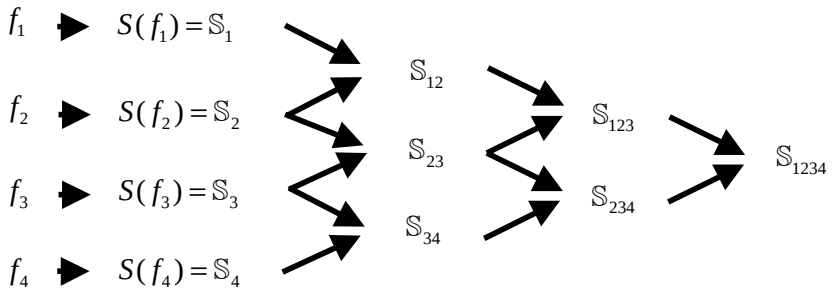

Fig. II.2. Recursive Cauchy method

The Burlisch–Stoer algorithm is a recurrent way of filling in the numbers in the tableau one column at a time. It is based on the relationship between a child and its parents [21] by

$$\mathbb{S}_{k(k+1)\ldots(k+q)} = \mathbb{S}_{(k+1)\ldots(k+q)} + \frac{\mathbb{S}_{(k+1)\ldots(k+q)} - \mathbb{S}_{k\ldots(k+q-1)}}{\dfrac{f - f_k}{f - f_{k+q}} \cdot \left(1 - \dfrac{\mathbb{S}_{(k+1)\ldots(k+q)} - \mathbb{S}_{k\ldots(k+q-1)}}{\mathbb{S}_{(k+1)\ldots(k+q)} - \mathbb{S}_{(k+1)\ldots(k+q-1)}}\right)} \qquad \text{(II- 17)}$$

It produces the so-called diagonal rational function, with the degree of the numerator and denominator equal (if is odd) or with the degree of the denominator larger by one (if is even).

II.4.9. Multidimensional Cauchy method

The rational-function interpolation can be extended to the interpolation of multidimensional functions. Two new approaches are shown here: a multidimensional recursive Cauchy method and a multidimensional rational-function expansion.

The recursive method solves the multidimensional interpolation using a recursive algorithm. The algorithm itself performs a 1-D Cauchy interpolation as described before. Let the set $\mathfrak{G}$ be put together by the pairs of κ sampling points f_1 to f_κ and their function values $\left(f_1, \mathbf{e}(f_1, \bar{p})\right)$ to $\left(f_\kappa, \mathbf{e}(f_\kappa, \bar{p})\right)$. Thus, $\mathfrak{G}$ can be written as

$$\mathfrak{G} = \left\{\left(f_1, \mathbf{e}(f_1, \bar{p})\right), \left(f_2, \mathbf{e}(f_2, \bar{p})\right), ..., \left(f_\kappa, \mathbf{e}(f_\kappa, \bar{p})\right)\right\} \tag{II- 18}$$

The algorithm can be defined as a function G, which yields the interpolated response Λ for using the samples

$$G\left(f, \mathfrak{G}\right) = \left[\left(f, \left\{\left(f_1, \mathbf{e}(f_1, \bar{p})\right), \left(f_2, \mathbf{e}(f_2, \bar{p})\right), ..., \left(f_\kappa, \mathbf{e}(f_\kappa, \bar{p})\right)\right\}\right) \rightarrow \Lambda\right] \tag{II- 19}$$

Using these definitions, the algorithm can now be extended to multidimensional interpolation. For this purpose, the set of sample points must be extended from the 1-D sample point set to a multidimensional sample-point array.

II.4.10. Application to microwave device design

As mentioned before, using frequency parameterization through Padé approximations, will considerably accelerate the design cost. Lately, a frequency parameterization package which works as an add-on module to EMXD electromagnetic field solver package is developed by CADOE company. EMXD is a software package originally developed by IRCOM laboratory which uses Finite Elements Method (FEM) as its computational core. The developed FEM-based frequency parameterization technique is applied to the design of several devices such as the one reported in [83]. The project was conducted in the framework of a scientific collaboration between IRCOM, CADOE and CNES (French Space Agency- Centre National d'Etudes Spatiales).

II.5. Geometry parameterization

In the previous sections of this chapter parameterization of microwave device characteristic using a rational approximant was explained. Through a frequency parameterization, one can get the device frequency characteristics in a shorter time and this way the design lead time is shortened. But the nature of the obtained results has nothing more than if one had to pursue a classical optimization. Thus the optimization process using a frequency parameterized model does not have any fundamental difference with the classical optimization procedure.

This section presents geometrical parameterization of microwave devices. In order to reduce the optimization time, sole frequency parameterization does not drastically help. The objective function is usually a function of frequency and an N-dimensional geometrical parameter vector and parameterizing the objective function with respect to N-dimensional parameter vector will accelerate the optimization process more efficiently than sole parameterization with respect to frequency. Among the few works reported in this context, the work done by Gati *et al* is more prominent and at the same time relevant to the present study [20].

The geometrically parameterized model outcomes curves which represent the phase and amplitude of electromagnetic fields versus a given range of geometry variations at a given frequency. Normally a parameterized model is valid within a domain inside the whole parameter space. Once a parameterized model is generated, it can be used in different iterations until the updated parameter exits the parameterization validity domain. Through such a practice multiple computations can be avoided. The difference between the form of the outcomes of a geometrically parameterized model and a classical numerical model leads to need for a fundamental difference in optimization procedure.

Mathematically, parameterizing a device characteristic with respect to geometrical parameters has a radical difference with frequency parameterization. Here, we do not expect to have poles and zeros when depicting the variations of field quantities with respect to geometrical variation. Thus, the resulting function will be a smooth function and a function different from a rational function, as was used for frequency parameterization.

II.5.1. Mathematical formulation

Consider the response as,

$$\mathbf{e} = \mathbf{e}(f, \overline{p}) \tag{II- 20}$$

Whereas $\mathbf{e}$ is the response (Electric Field in our application), resulting from simulations, f is the real frequency and $\overline{p}_{N\times 1} = \left[p_1\ p_2\ p_3 ... p_N\right]^T$ is an N-dimensional parameter vector. $\mathbf{e}$ can be derived through a linear or nonlinear equation,

$$\tilde{\mathbf{A}}(f, \overline{p}).\mathbf{e}(f, \overline{p}) = \mathbf{B}(f, \overline{p}) \tag{II- 21}$$

Usually the objective function in frequency domain is expressed in terms of S-parameters, so eventually any field quantity should be converted to S-parameters as the intermediate parameter between the objective function and the field quantities,

$$S_{ij} = S_{ij}\left(\mathbf{e}(f, \overline{p})\right) = S_{ij}(f, \overline{p}), \qquad i, j = 1, 2, .., J \tag{II- 22}$$

whereas J is the number of device ports.

A step-by-step procedure will be followed to explain the derivation of a fully parameterized model. At the very first step the parameterization with respect to a single parameter at a fixed frequency will be developed. Such a technique can then be extended to a parameter vector if arbitrary dimension. Finally, the obtained model will be parameterized with respect to frequency.

Assuming that only one parameter p_v varies at any time in a given frequency, the parameter vector can be mentioned as,

$$\overline{p}_{N\times 1} = \left[p_1\ p_2 .. p_v ... p_N\right]^T \tag{II- 23}$$

Then electric field is a function of frequency and dimensions of the structure,

$$\mathbf{e} = \mathbf{e}(f; p_v), \qquad i, j = 1, 2, .., J \tag{II- 24}$$

while the only varying parameter is p_v. For a variation Δp_v of the parameter p_v the solution of the equation

$$\tilde{A}(f, p_v + \Delta p_v).\mathbf{e}(f, p_v + \Delta p_v) = \mathbf{B}(f, p_v + \Delta p_v) \tag{II- 25}$$

can be determined using the Taylor Series,

$$\mathbf{e}(f,\overline{p}_{fix};p_v+\Delta p_v)=\mathbf{e}(f;p_v)+\frac{\partial \mathbf{e}(f;p_v)}{\partial p_v}.\Delta p_v+\frac{1}{2!}\frac{\partial^2 \mathbf{e}(f;p_v)}{\partial p_v^2}.(\Delta p_v)^2+ \\ .....+\frac{1}{(M-1)!}\frac{\partial^{M-1}\mathbf{e}(f;p_v)}{\partial p_v^{M-1}}.(\Delta p_v)^{M-1}+R_M \qquad \text{(II- 26)}$$

where R_M is the remainder of the series and tends to zero when M tends to infinity for any convergent series.

The equation (II- 26) can lead to a parameterized model with respect to the parameter p_v. In fact, with one calculation of the S and its derivatives in any point in the parameter space, the values of $\mathbf{e}$ around that point can be calculated using this parameterized model.

II.5.2. Domain of validity

The parametric expression is (II- 26) can not be used in the whole parameter span. The domain of validity can be defined as,

$$D=\left\{p \,\middle|\, p_{v\min}\le p\le p_{v\max}, \lim_{M\to\infty}\left(R_M(p)\right)=0\right\} \qquad \text{(II- 27)}$$

where,

$$R_M(p)=\frac{1}{M!}\frac{\partial^M \mathbf{e}(f;p)}{\partial p^M}.(\Delta p)^M \qquad \text{(II- 28)}$$

II.5.3. Calculation of the higher order derivatives

At a first glance deriving the parameterized model seems to be as complicated as doing multiple computations through different iterations of optimization procedure. This is not true because of the fact that the derivatives of the function S can be computed iteratively.

The first derivatives of (II- 25) can be taken as,

$$A(f,\overline{p}).\mathbf{e}^{(1)}(f,\overline{p})+A^{(1)}(f,\overline{p}).\mathbf{e}(f,\overline{p})=\mathbf{B}^{(1)}(f,\overline{p}) \qquad \text{(a)} \qquad \text{(II- 29)}$$

or

$$A(f,\overline{p}).\mathbf{e}^{(1)}(f,\overline{p})=\mathbf{B}^{(1)}(f,\overline{p})-A^{(1)}(f,\overline{p}).\mathbf{e}(f,\overline{p}) \qquad \text{(b)}$$

Here the superscripts in the parentheses show the order of the derivatives. Taking the second derivative of (II- 29) would thus yield,

$$A(f,\overline{p}).\mathbf{e}^{(2)}(f,\overline{p})+A^{(1)}(f,\overline{p}).\mathbf{e}^{(1)}(f,\overline{p})= \\ \mathbf{B}^{(2)}(f,\overline{p})-A^{(1)}(f,\overline{p}).\mathbf{e}(f,\overline{p})-A^{(1)}(f,\overline{p}).\mathbf{e}^{(1)}(f,\overline{p}) \qquad \text{(a)} \qquad \text{(II- 30)}$$

$$A(f,\bar{p}).\mathbf{e}^{(2)}(f,\bar{p}) = \mathbf{B}^{(2)}(f,\bar{p}) - A^{(1)}(f,\bar{p}).\mathbf{e}(f,\bar{p}) - 2A^{(1)}(f,\bar{p}).\mathbf{e}^{(1)}(f,\bar{p}) \quad \text{(b)}$$

And for the *M*th derivative we would have,

$$A(f,\bar{p}).\mathbf{e}^{(m)}(f,\bar{p}) = \mathbf{B}^{(m)}(f,\bar{p}) - \sum_{j=1}^{m} C_j^m A^{(j)}(f,\bar{p}).\mathbf{e}^{(m-j)}(f,\bar{p}) \quad \text{(II- 31)}$$

Equation (II- 31) can now be used to calculate *m*'th derivative through successive iterations.

Several techniques have been reported for automatic computation of the derivatives. The reader is encouraged to view to [22]-[37].

II.5.4. Parameterization with respect to two or more geometrical parameters

The parameterization concept can be extended for two or more geometric parameters. To this end the field quantity should be expressed using a multi-dimensional Taylor Series. As an example, to parameterize the function $\mathbf{e}$ with respect to two parameters p_v and p_u,

$$\tilde{\bar{p}}_{N\times 1} = [p_1 \ldots p_v \ldots p_u \ldots p_N] \quad \text{(II- 32)}$$

With the unchanged parameter vector defined as,

$$\bar{p}_{fix_{(N-1)\times 1}} = \left[p_1 \ldots p_{v-1} p_{v+1} \ldots p_{u-1} p_{u-+} . p_N\right]^T_{(N-1)\times 1} \quad \text{(II- 33)}$$

And thus the argument of $\mathbf{e}$ is redefined,

$$\mathbf{e} = \mathbf{e}(f; p_v, p_u), \qquad i, j = 1, 2, .., J \quad \text{(II- 34)}$$

Now $\mathbf{e}$ can be expanded with the two dimensional Taylor series,

$$\mathbf{e}(f; p_v + \Delta p_v, p_u + \Delta p_u) = \mathbf{e}(f; p_v, p_u) + \frac{\partial \mathbf{e}(f; p_v, p_u)}{\partial p_v}.\Delta p_v + \frac{\partial \mathbf{e}(f; p_v, p_u)}{\partial p_u}.\Delta p_u + \frac{1}{2!}\left[\frac{\partial^2 \mathbf{e}(f; p_v, p_u)}{\partial p_v^2}.(\Delta p_v)^2 + 2\frac{\partial^2 \mathbf{e}(f; p_v, p_u)}{\partial p_v \partial p_u}.\Delta p_v \Delta p_u + \frac{\partial^2 \mathbf{e}(f; p_v, p_u)}{\partial p_u^2}.(\Delta p_u)^2\right] + \ldots \quad \text{II-35)}$$

or in short form,

$$\mathbf{e}(f; p_v + \Delta p_v, p_u + \Delta p_u) = \mathbf{e}(f; p_v, p_u) + \sum_{m=1}^{M-1} \sum_{j=1}^{m} \frac{1}{m!} \frac{\partial^m \mathbf{e}(f; p_v, p_u)}{\partial p_v^i \partial p_u^{m-i}} . \Delta p_v^i \Delta p_u^{m-i} + R_M \quad \text{(II- 36)}$$

This formulation can be extended to all N dimensions of the parameter space. In practice the cross term errors appear as an obstacle for arbitrarily increasing parameterization dimensionality.

The technique is applied to Finite Elements Method by CADOE. To this end, the FEM technique developed by IRCOM laboratory is used as the field solver. The project was sponsored by CNES (Centre National d'Etudes Spatiales).

II.6. Mesh parameterization

Every time the structure dimensions are updated, the conventional optimization loop requires regenerating meshes. The meshes are generated through pseudo random methods. Any given structure can be discretized into a mesh grid in infinite different combinations through any given method. This affects the efficiency of optimization in different ways, namely it causes discontinuous gradients and after all it is a time-consuming procedure. Fig. II.3 shows the flowchart of the gradient computation through finite differencing.

The gradients of the objective function with respect to geometric parameters are normally obtained through finite differencing of the value of objective function for slightly perturbed geometry and its initial geometry. A totally brand new mesh should be generated for a slightly perturbed geometry. This "new" mesh is different both in number of nodes and their relation. On the other hand, the accuracy of any numerical method relies on the quality of the discretization. However, the quality of generated meshes varies each time, resulting some changes in the result accuracy. This altered accuracy is not considerable, of course, but can mask the changes due to slight perturbation. In other words gradients obtained through finite differencing of regenerated meshes are inaccurate.

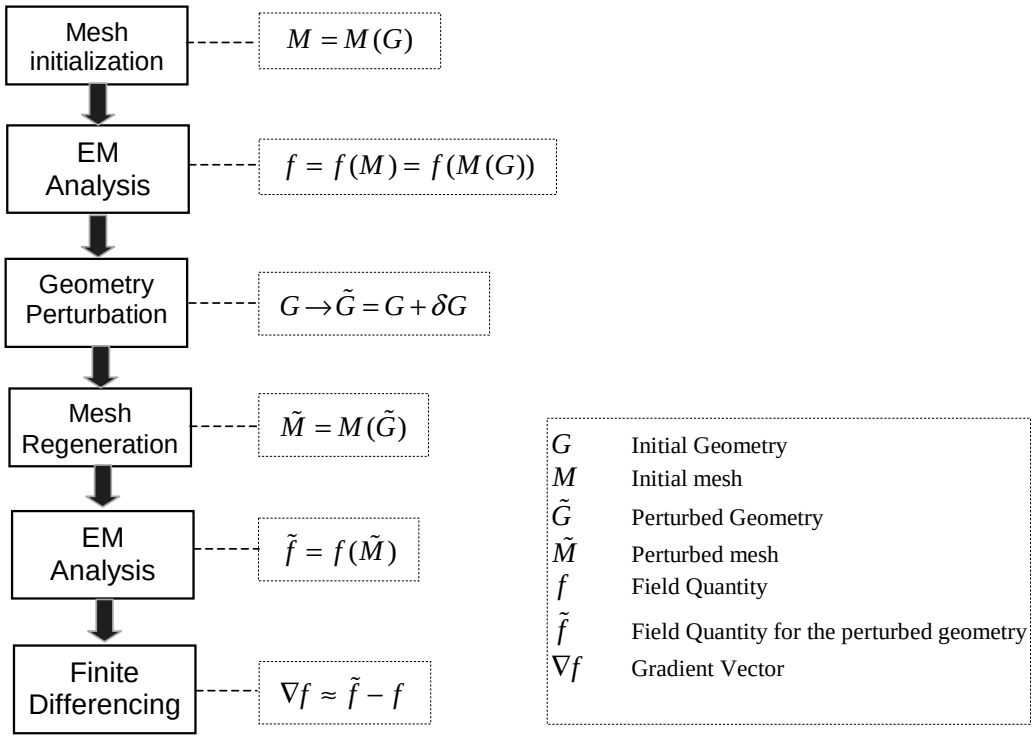

Fig. II.3. Calculating gradient through finite differencing

An appropriate solution would be to express mesh nodes as a function of structure geometry. Such a function should be smooth so that first and second order derivatives exist.

Once a mesh is generated, automatically or manually, the location of nodes can be parameterized with respect to geometry borders. Then the same mesh can be deformed to accommodate any perturbed geometry.

Another advantage of mesh parameterization is the time efficiency. The time consumed for mesh generation is usually a considerable portion of calculation through Finite-Elements methods or any numerical technique. By parameterizing meshes the mesh generation time reduced to the time required for evaluation of an algebraic expression.

Some promising works have been done and reported in the fluid mechanics discipline. But no effort has been reported in electromagnetic domain to extent of authors' knowledge. The following section explains some conventional methods used for mesh deformation.

II.6.1. Mesh deformation techniques [38]

Most of the already developed methods for mesh deformation are based on real world physical approaches such a network of springs, linear solid elastic body and so on. Actually there exists simpler techniques but these trivial techniques are just applicable to structured grid, while generating structures meshes for complex geometric domains is rather a tedious task.

Here the methods are described for two-dimensional case, where they can be easily extended to the three-dimensional case without loss of generality.

Referring to Fig. II.4 let's name the original geometry in two dimensions *D*, and the deformed geometry *D'*. Our aim would be to find the proper displacement vector which maps the mesh on *D* to a valid mesh on *D'*. Let also the point $a(x,y)$ on *D* be mapped to the point $a'(x',y')$ on *D'*. As a result we will have the point deformation updates via the equation,

$$\begin{pmatrix} x' \\ y' \end{pmatrix} = \begin{pmatrix} x \\ y \end{pmatrix} + \begin{pmatrix} u \\ v \end{pmatrix} \qquad \text{(II- 37)}$$

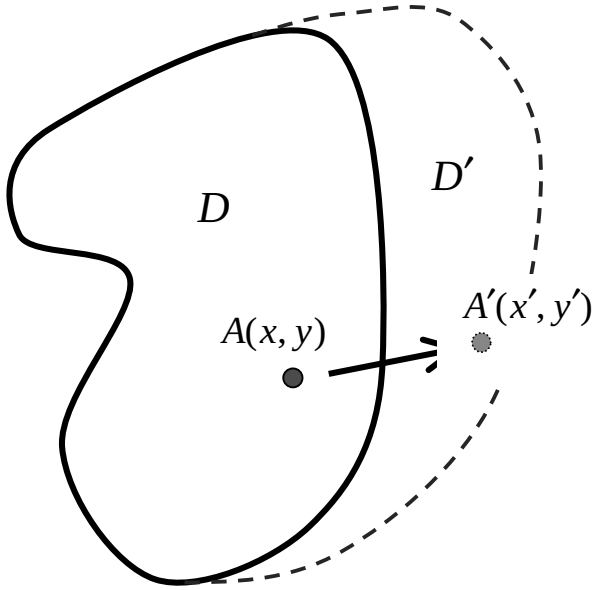

Fig. II.4. The typical geometry used for mesh deformation

II.6.1.1 Spring analogy approach

In this approach the mesh is modeled as a network of springs. When a cell edge is displaced, a force is induced in the spring assigned to this edge. The strain energy contained in the spring system is given by a sum over the set of edges,

$$H = \sum_{k \in E} k_{pq} \left[\left(u_p - u_q \right)^2 + \left(v_p - v_q \right)^2 \right] \quad p, q \in D(k) \tag{II- 38}$$

where k_{pq} is the spring stiffness and $k_{pq} = l_{pq}^{-m}$. l_{pq} is assumed to be the length of the edge connecting node *i* and *j* and *m* is set to be one for small and simple networks [41]. For large deformation m should be set to larger values to avoid nodes being crossed cell edges. In (II- 38) *E* is the set of edges and $D(k)$ is the set of points defining the edge *k*. Obtaining the gradient of energy function is extremely crucial for an efficient solution,

$$\frac{\partial H}{\partial w_i} = \sum_{j \in N(i)} k_{ij} (w_i - w_j) \qquad \forall i \in V \tag{II- 39}$$

where *V* is the set containing all the vertices and *N(i)* is the set of immediate neighbors of the vertex *i*. For minimization of *H* a preconditioned conjugate gradient technique, provided by MATLAB™ optimization toolbox was utilized.

As mentioned earlier, the main disadvantage of this method appears when the border deformations or displacements are of greater value than the actual size of the original geometry. In other words as it really happens to the real-world case of a spring grid,

when a border is too radically stretched, it could cause a relocation of other borders whom are supposed to hold their original position after all transformations. To treat this problem, as mentioned in [42] one can increase the spring stiffness to solidify the grid to prohibit far grids movements. However this issue should be taken into account for a class of problems when on dimension of the structure is drastically larger than the other, *e.g.* when meshing the substrate thickness of a planar structure with relatively big plate areas and very thin substrate.

The very important feature of the approach is its comprehensibility through a clear physical interpretation, which in turn, leads to simpler and error-free numerical manipulation. A sample of the mesh modified through spring analogy is shown in Fig. II.5. The rigidity factor *m* is set to unity in this example.

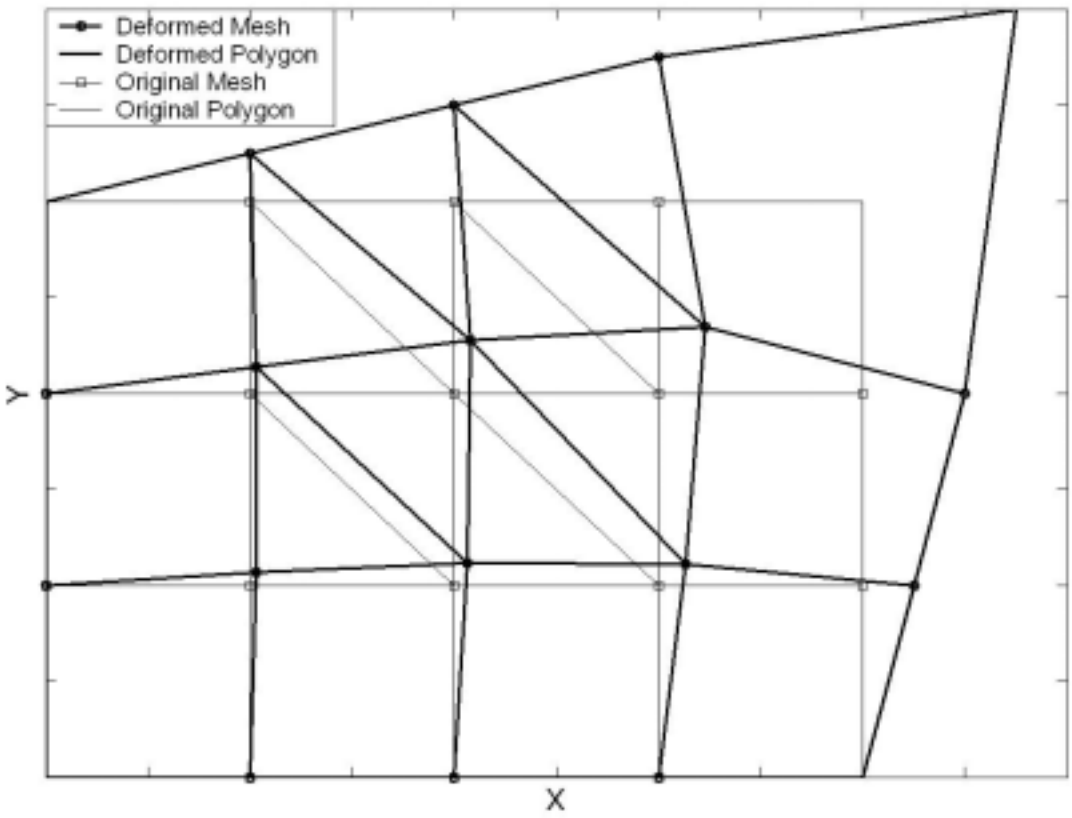

Fig. II.5. An example of a mesh deformed through spring analogy, original (grey) and deformed (black) meshes

II.6.1.2 Harmonic equations

Harmonic equations are a classical approach used to deform an already generated mesh with deformed borders. A non-coupled system of Laplacian equations,

$$\nabla^2 u = 0 \qquad \text{(a)} \qquad \text{(II- 40)}$$

$$\nabla^2 v = 0 \qquad \text{(b)}$$

can be considered as the governing equation for deformation of a grid. The idea comes from a conventional technique of using partial differential equations (PDE's) for generating a grid inside a structure [43].Since the Laplacian is a linear operator, the original and renewed meshes and their difference, the vector *(u,v)* should comply with this equation. Regardless of the technique used to generate the primary grid, one can expect that this idea will accommodate the mesh deformation. The main disadvantage of the Laplace equation or its variants is the lack of any coupling between different components of the displacement. If the borders move in a direction parallel to only one direction, say *x*, the coordinate of mesh points in *y* direction remain unchanged [44].

Another variation of this method is reported in [45]. The pair of biharmonic equations has been used to finely model mesh deformations in a two dimensional space. The method is capable of applying two different conditions at each geometry border which gives a relative degree of liberty.

II.6.1.3 Solid body elasticity model

The solid body elasticity method for mesh deformation was first introduced in [46] about two decades ago, and has been extensively used in aerodynamics. The technique models the grid as the particles of a linear elasticity solid body. In the absence of any prescribed forces on the body the motion of the grid points comply with the strain energy functional,

$$F = \sum_i A_i^{n-1} \int_{A_i} f \, dx \, dy \qquad \text{(II- 41)}$$

where

$$f = \frac{\partial^2 u}{\partial x^2} + \left(\frac{\partial u}{\partial y} + \frac{\partial v}{\partial x}\right)^2 + \frac{\partial^2 v}{\partial y^2} \qquad \text{(II- 42)}$$

II.6.2. Deformation measure

Defining a measure for quantifying the overall relocation of vertices or the accumulative effect of changes in angles of the mesh could be a proper measure to learn about the grid deformations. A very successful measure, introduced by Baker [44] is used here to quantify the grid deformation. Specifically speaking in two dimensions, with triangular elements an edge matrix T_n can be defined as,

$$T_n = (-1)^n (\overline{w}_{n+1} - \overline{w}_n, \overline{w}_{n+2} - \overline{w}_n) \quad \text{(II- 43)}$$

where $\overline{w}_n = (x_n, y_n)^T$ are the associate positions of vertices associated with very triangle. A simple mathematical manipulation would show that T is a two times the area of a triangle formed by $\overline{w}_n, \overline{w}_{n+1}, \overline{w}_{n+2}$. Accordingly, the edge matrix, associated to the deformed mesh is defined in a similar manner, let this matrix be named T_n'. The deformation matrix, B_n is defined in such a way that it links the original and deformed matices,

$$T_n' = B_n.T_n \quad \text{(II- 44)}$$

As proven in [44] the matrix B_n does not depend on the choice of the vertices and could be calculated without any ambiguity. B_n can be decomposed as $B = P.U$ where P is a positive definite matrix and U is an identity matrix. The elements of P correspond to the modes of distortion. An eigenvalue bigger than unity corresponds to stretching along with the eigenvector and similarly eigenvalues less than unity represent compression. The eigenvalues of the matrix P are singular values of the matrix B and can be easily found by using Matlab software. For the case of pure rotation minimum and maximum singular values of B are both equal to unity and for the case of uniform linear scaling by a factor of k both eigenvalues will be equal to the scaling factor.

The difference between edge angles can provide another basis or quantifying the grid deformation,

$$M = \sum_i (\Delta\beta_i)^2 \quad \text{(II- 45)}$$

Here $\Delta\beta_i$ represents the difference between the angles of the deformed and initial grids both corresponding to the i'th node.

II.6.3. Mesh parameterization

II.6.3.1 Mesh parameterization barycentric coordinates

All of the methods introduced so far have been relying on a sort of analogy to physical problems. This approach, although very easy to implement, but has shortcomings which have been addressed when explaining methods. Thus the search has been directed towards finding a pure mathematic scheme which can accommodate the need for a parameterization technique.

Barycentric coordinates, known for centuries, have been used by the computer engineers at early ages for interpolation purposes, ray tracing, and surface smoothing. Because of their linear accuracy, barycentric coordinates can also be found in Finite-Elements literature [47].

II.6.3.2 Barycentric coordinates

Barycentric coordinates are triplets of numbers (w_1, w_2, w_3) corresponding to masses placed at the vertices of a reference triangle $\triangle \mathbf{g}_1\mathbf{g}_2\mathbf{g}_3$ (see Fig. II.6). These masses then determine a point *P*, which is the geometric centroid of the three masses, and is identified with coordinates (w_1, w_2, w_3). The vertices of the triangle are given by (1,0,0), (0,1,0), and (0,0,1). Barycentric coordinates were discovered by Möbius in 1827.

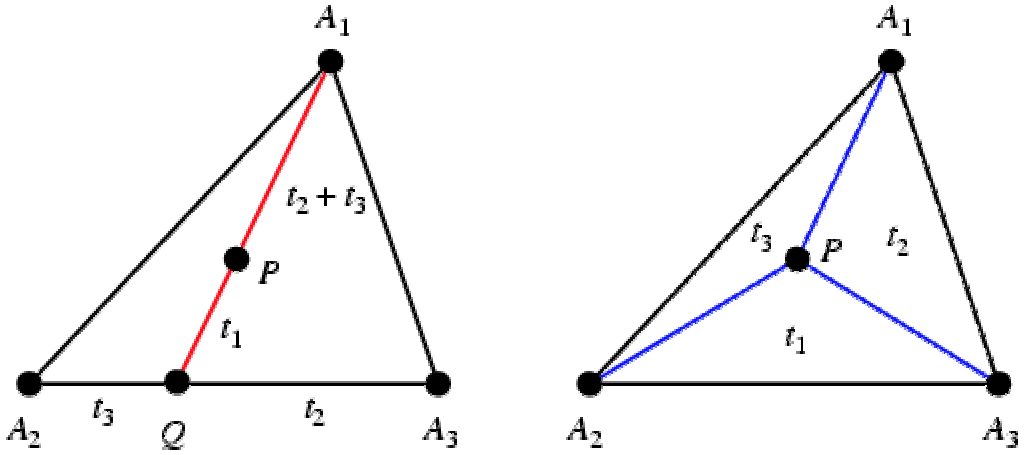

Fig. II.6. Barycentric coordinates - Classical definition

To find the barycentric coordinates for an arbitrary point $\mathbf{a}$, find w_2 and w_3 from the point *Q* at the intersection of the line $\mathbf{g}_1\mathbf{a}$ with the side $\mathbf{g}_2\mathbf{g}_3$, and then determine w_1 as the mass at $\mathbf{g}_1$ that will balance a mass $w_2 + w_3$ at *Q*, thus making *P* the centroid

(Fig. II.6). Furthermore, the areas of the triangles $\triangle \mathbf{g}_1\mathbf{g}_2\mathbf{a}$, $\triangle \mathbf{g}_1\mathbf{g}_3\mathbf{a}$, and $\triangle \mathbf{g}_2\mathbf{g}_3\mathbf{a}$ are proportional to the barycentric coordinates w_3, w_2, and w_1 of $\mathbf{a}$.

Barycentric coordinates are homogeneous, so

$$(w_1, w_2, w_3) = (\mu w_1, \mu w_2, \mu w_3) \tag{II- 46}$$

for $\mu \neq 0$.

Barycentric coordinates which are normalized so that they become the actual areas of the sub-triangles are called homogeneous barycentric coordinates, and barycentric coordinates normalized as

$$w_1 + w_2 + w_3 = 1 \tag{II- 47}$$

so that the coordinates give the areas of the subtriangles *normalized by the area of the original triangle* are called *areal* coordinates.

In barycentric coordinates, a line has a linear homogeneous equation. In particular, the line joining points (r_1, r_2, r_3) and (s_1, s_2, s_3) has equation

$$\begin{vmatrix} r_1 & r_2 & r_3 \\ s_1 & s_2 & s_3 \\ w_1 & w_2 & w_3 \end{vmatrix} = 0 \tag{II- 48}$$

If the vertices $\mathbf{a}_i$ of a triangle $\triangle \mathbf{a}_1\mathbf{a}_2\mathbf{a}_3$ have barycentric coordinates (x_i, y_i, z_i), then the area of the triangle is

$$\triangle \mathbf{a}_1\mathbf{a}_2\mathbf{a}_3 = \begin{vmatrix} x_1 & y_1 & z_1 \\ x_2 & y_2 & z_2 \\ x_3 & y_3 & z_3 \end{vmatrix} \triangle \mathbf{g}_1\mathbf{g}_2\mathbf{g}_3 \tag{II- 49).}$$

II.6.4. Mesh deformation using generalized barycentric coordinates

II.6.4.1 Generalized barycentric coordinates

Barycentric coordinates has the potential of being used for mesh parameterization. It basically provides a function that expresses any point inside a triangle so that if the vertices of the triangle are displaced, that internal point will move accordingly.

The only problem with using the barycentric coordinates is that these coordinates are used only to parameterize a triangle and can not accommodate complicated geometries of actual structures. Obviously the geometries of microwave devices are, more complicated than to be represented by simple triangles. The original form of the barycentric coordinate which was explained earlier can not be extended to polygons.

II.6.4.2 Notations

Due to wide variety of applications of grid parameterization techniques different notations have been used for mesh generation, deformation and relevant topics. It necessitates us to define a concise notation before we proceed developing formulation.

Referring to Fig. II.7, let $\mathbf{g}_1, \mathbf{g}_2, ..., \mathbf{g}_i, .. \mathbf{g}_N$ be N vertices of the polygon Γ (with $N \geq 3$) in two dimensional Cartesian coordinates, where

$$\mathbf{g}_i = \begin{bmatrix} \mathbf{g}_{xi} \\ \mathbf{g}_{yi} \end{bmatrix} \tag{II- 50}$$

As a matter of convenience we have picked x-y plane as our reference plane. Also let the vector,

$$\mathbf{g} = \left[\mathbf{g}_1 \, \mathbf{g}_2 \, ... \mathbf{g}_{i-1} \, \mathbf{g}_i \, \mathbf{g}_{i+1} \, ... \mathbf{g}_N \right]^T \tag{II- 51}$$

represents the vertices of the polygon. The edges are numbered as,

$$\mathbf{e}_i = \mathbf{g}_{i+1} - \mathbf{g}_i \tag{II- 52}$$

and obviously $\mathbf{e}_N = \mathbf{g}_1 - \mathbf{g}_N$.

Now let $\mathbf{a}_1, \mathbf{a}_2, ..., \mathbf{a}_j, .. \mathbf{a}_M$ be a set of arbitrary points inside the polygon Γ. The internal points are also referred to in a vector format,

$$\mathbf{a} = \left[\mathbf{a_1} \, \mathbf{a_2} \, ... \mathbf{a_{j-1}} \, \mathbf{a_j} \, \mathbf{a_{j+1}} \, ... \mathbf{a_M} \right]^{\mathbf{T}} \tag{II- 53}$$

Each of these internal points forms a triangle with a couple of vertices. The triangle formed between three points $\mathbf{a}_j$, $\mathbf{g}_i$ and $\mathbf{g}_{i+1}$ is named τ_{ij}:

$$\triangle \tau_{ij} = \triangle \mathbf{g}_i \mathbf{g}_{i+1} \mathbf{a}_j \tag{II- 54}$$

This is a general trend for naming the internal triangles, for example the points $\mathbf{a}_3$, $\mathbf{g}_N$ and $\mathbf{g}_1$ is named τ_{N3}. The internal angles formed inside triangles are named as follows,

$$\angle\alpha_{ij} = \angle\mathbf{g}_i\mathbf{a}_j\mathbf{g}_{i+1} \quad \text{(a)} \qquad \text{(II- 55)}$$

$$\angle\gamma_{ij} = \angle\mathbf{a}_j\mathbf{g}_i\mathbf{g}_{i+1} \quad \text{(b)}$$

$$\angle\theta_{ij} = \angle\mathbf{g}_i\mathbf{g}_{i+1}\mathbf{a}_j \quad \text{(c)}$$

The original concept of barycentric coordinates was explained earlier. The aim of this section is to extend the barycentric coordinate concept to a polygon.

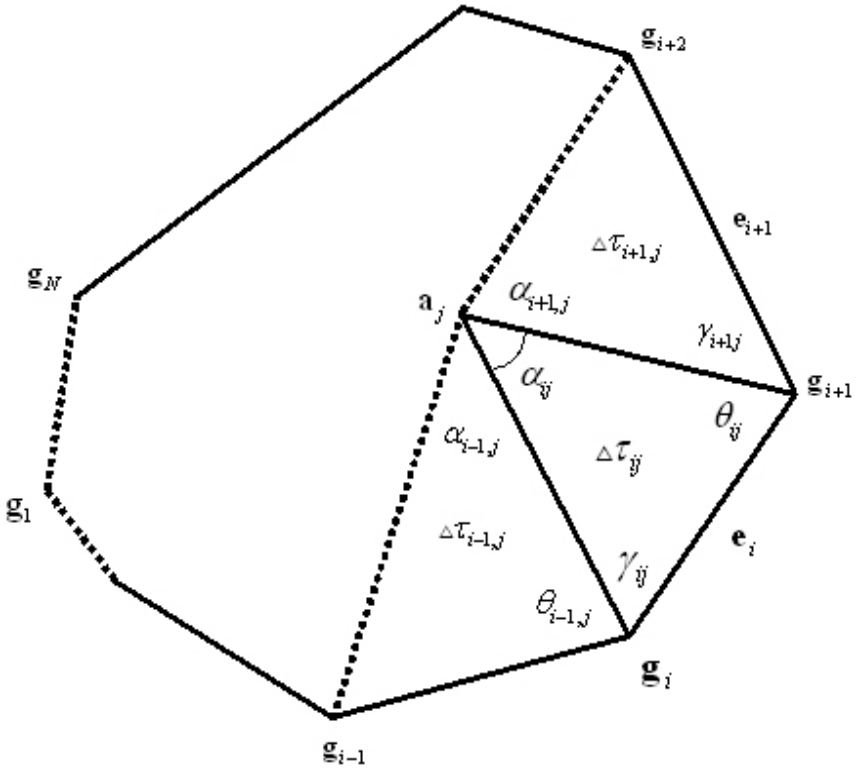

Fig. II.7. Description of the geometry used for generalized barycentric coordinate and relevant notations.

To this end, the properties of generalized barycentric coordinates of $\mathbf{a} = \left[\mathbf{a_1}\,\mathbf{a_2}\,\mathbf{...a_{j\text{-}1}}\,\mathbf{a_j}\,\mathbf{a_{j+1}}\,\mathbf{...a_M}\right]^{\mathbf{T}}$ with respect to $\mathbf{g} = \left[\mathbf{g}_1\,\mathbf{g}_2\,...\mathbf{g}_{i-1}\,\mathbf{g}_i\,\mathbf{g}_{i+1}\,...\mathbf{g}_N\right]^T$ is any set of real coefficients $w_{ij} = \left[w_{1j}...w_{Nj}\right]_{1\times N}^T$ .in such a way that:

1- The interior points can be expressed as an affine combination of vertices as,

$$\mathbf{a}_j = \sum_{i=1}^{N} w_{ij}\mathbf{g}_i \qquad \text{(II- 56)}$$

whereas

$$\sum_{i=1}^{N} w_{ij} = 1, \qquad j = 1,...,M. \tag{II- 57}$$

The equation (II- 56) can also be written as,

$$\sum_{i=1}^{N} w_{ij}(\mathbf{g}_i - \mathbf{a}_j) = 0 \tag{II- 58}$$

2- The combination much be convex, or,

$$w_{ij} \geq 0, \qquad i = 1,...,N,\ j = 1,...M. \tag{II- 59}$$

3- The elements of $w_{ij} = \left[w_{1j} ... w_{Nj} \right]_{1\times N}^{T}$ should be infinitely differentiable with respect to $\mathbf{a}_j$ and $\mathbf{g}_i$. This ensures smoothness in the variation of the coefficients j when we move any vertex.

II.6.4.3 Literature survey

Several researchers have attempted to generalize barycentric coordinates to arbitrary n-gons. Due to the relevance of this extension in CAD, many authors have proposed or used a generalization for *regular n-sided polygons* [55], [54], [56]. Their expressions nicely extend the well-known formula to find barycentric coordinates in a triangle, Unfortunately, none of the proposed affine combinations leads to the desired properties for irregular polygons. However, Loop and DeRose [55] note in their conclusion that barycentric coordinates defined over arbitrary convex polygons would open many extensions to their work.

Pinkall and Polthier [57][57], and later Eck *et al* [51], presented a conformal parameterization for a triangulated surface by solving a system of linear equations relating the positions of each point p to the positions of its first ring of neighbors

$$\sum_{i=1}^{N} \left[\tan^{-1}(\gamma_{i-1,j}) + \tan^{-1}(\theta_{i,j}) \right](\mathbf{g}_i - \mathbf{a}_j) = 0 \tag{II- 60}$$

where the angles are defined in Fig. II.7. As Desbrun *et al.* showed in [50], this formula expresses the gradient of area of the 1-ring with respect to **p**, therefore smoothness is immediately satisfied. The only problem is that the weights can be negative which means that the combinations can not be convex. This alters the second property (convexity).

Floater [52], [53] also attempted to solve the problem of creating a parameterization for a surface by solving linear equations. However, in 1975, Wachpress proposed a construction of rational basis functions over polygons that leads to the appropriate properties.

II.6.4.4 Computation of generalized barycentric coordinates

The same concept as in original barycentric coordinates can be used to derive the extended version which is applicable to any convex irregular polygon.

Following the same procedure as original barycentric coordinates, in order to find the coefficient w_{ij}, the weights of the polynomial can be defined as the area of the two triangles which share the line segment between the vertex $\mathbf{g}_i$ and internal point $\mathbf{a}_j$,

$$\tilde{w}_{ij} = \frac{A(\triangle \mathbf{g}_{i-1}\mathbf{g}_i\mathbf{g}_{i+1})}{A(\tau_{i-1}).A(\tau_i)} \tag{II- 61}$$

Here $\tilde{w}_{ij}$ is the non-normalized weight. This can be later normalized as,

$$w_{ij} = \frac{\tilde{w}_{ij}}{\sum_{i=1}^{N} \tilde{w}_{ij}} \tag{II- 62}$$

In equation (II- 61) *A* represents the area of the triangle. The denominator in (II- 61) provides a measure of proximity, in other words, the closer the internal point $\mathbf{a}_i$ is to the vertex $\mathbf{g}_i$, the smaller becomes the denominator. On the other hand, the nominator is a measure of proximity of the vertex $\mathbf{g}_i$ to its adjacent vertices $\mathbf{g}_{i-1}$ and $\mathbf{g}_{i+1}$, as well as the angle $\angle g_i$. The closer the point $\mathbf{a}_j$ gets to the vertex $\mathbf{g}_i$, the larger becomes $\tilde{w}_{ij}$. Once the point $\mathbf{a}_j$ falls inside $\triangle \mathbf{g}_{i-1}\mathbf{g}_i\mathbf{g}_{i+1}$, the $\tilde{w}_{ij}$ becomes greater than unity. Equation (II- 61) can now be extended as,

$$\begin{aligned} \tilde{w}_{ij} &= \frac{\sin(\angle g_i)\|\mathbf{e}_{i-1}\|\|\mathbf{e}_i\|}{\sin(\theta_{i-1}).\|\mathbf{e}_{i-1}\|.\|\mathbf{g}_i - \mathbf{a}_j\|^2\|\mathbf{e}_i\|.\sin(\gamma_i)} \\ &= \frac{\sin(\angle g_i)}{\|\mathbf{g}_i - \mathbf{a}_j\|^2 \sin(\theta_{i-1})\sin(\gamma_i)} \end{aligned} \tag{II- 63}$$

Therefore, using trigonometric identities

$$\sin(\angle g_i) = \sin(\theta_{i-1} + \gamma_i) = \sin(\theta_{i-1})\cos(\gamma_i) + \cos(\theta_{i-1})\sin(\gamma_i) \tag{II- 64}$$

would yield,

$$\tilde{w}_{ij} = \frac{\tan^{-1}(\theta_{i-1}) + \tan^{-1}(\gamma_i)}{\left\|\mathbf{g}_i - \mathbf{a}_j\right\|^2} \quad \text{(II- 65)}$$

Using (II- 65), the required information are only the vertex $\mathbf{g}_i$ and angles $\angle\theta_{i-1}$ and γ_i. In a mesh parameterization practice, such a feature is quite significant: It gives the flexibility of parameterizing a node locally, with respect to one, or few vertices, without a need for going through the whole structure. However, for star-shaped polygons the coordinate in (II- 65) can be inconsistent, and, in fact, will be so precisely when $\angle g_i > \pi$.

II.6.5. Mean value coordinates

The equation (II- 65) solely depends on the angles seen from vertex. An alternative formulation, often called mean value coordinates uses the harmonic mapping concepts to derive the weights as follows,

$$\tilde{w}_{ij} = \frac{\tan(\alpha_{i-1,j}/2) + \tan(\alpha_{i,j}/2)}{\left\|\mathbf{g}_i - \mathbf{a}_j\right\|} \quad \text{(II- 66)}$$

The main feature of the equation is that it only depends on the angles seen from the interior point $\mathbf{a}_j$. These weights can be derived from an application of the mean value theorem for harmonic functions, which suggests calling them mean value coordinates. Not only are these coordinates positive, but we can bound them away from zero. The lower and upper bounds of the coefficient $\tilde{w}_{ij}$ can be found as,

$$2\frac{\tan(\min\{\alpha_{i-1},\alpha_i\}/2)}{\max\left\{\left\|\mathbf{g}_i - \mathbf{a}_j\right\|\right\}} \le \tilde{w}_{ij} \le 2\frac{\tan(\max\{\alpha_{i-1},\alpha_i\}/2)}{\min\left\{\left\|\mathbf{g}_i - \mathbf{a}_j\right\|\right\}} \quad \text{(II- 67)}$$

II.6.6. Three dimensional generalized barycentric coordinates

Mean value coordinates were introduced as a way of expressing a point in the kernel of an arbitrary polygon as a convex combination of the vertices. These coordinates can be successfully used to compute good parameterizations for surfaces represented as triangular meshes. Since these coordinates already have several concrete applications, it seems worthwhile generalizing these coordinates to three dimensions. The notation used for the two dimensional case is extended to three dimensions. The N vertices of polyhedron Γ are named $\mathbf{g}_1, \mathbf{g}_2, ..., \mathbf{g}_i, ..\mathbf{g}_N$ (with $N \ge 4$) in three dimensional Cartesian coordinates, where

$$\mathbf{g}_i = \begin{bmatrix} \mathbf{g}_{xi} \\ \mathbf{g}_{yi} \\ \mathbf{g}_{zi} \end{bmatrix} \tag{II- 68}$$

A vertex $\mathbf{g}_i$ is *simple* if $\mathbf{g}_i$ is the intersection of *h* half-spaces, i.e. κ exactly contains *h* indices. A polygone Γ is simple if every vertex of Γ is simple. Note that convex polygons are always simple while only a subset of convex polyhedra are simple. For example, tetrahedrons, cubes and triangular prisms are simple while square pyramids and octahedrons are not. A complete definition of geometrical terms is presented in Appendix C.

Referring to Fig. II.7, assume that κ is the set of all the facets (lines) in three (two) dimensions that contains $\mathbf{g}_i$.

The $\mathbf{g}_i$ is *simple* if it is the intersection of *h* half-spaces, i.e. κ exactly contains *h* indices. $\mathbf{\Lambda}_k$'s are the normal vectors to the facets (edges) *k*. The matrix containing all the normal vectors of the facets which form the polyhedron. Also let $[\Lambda_\kappa]_{h\times h}$ correspond to the sub-matrix of Λ whose rows are the vectors $\mathbf{\Lambda}_k$ where $k \in \kappa$. For a given point $\mathbf{a}_j$ strictly inside the polyhedron, as suggested in [70], one can write,

$$\tilde{w}_{ij}(\kappa) = \frac{\left|Det(\Lambda_\kappa)\right|}{\prod_{l=1}^{h} d_l(\mathbf{a}_j)} \tag{II- 69}$$

where $d_l(\mathbf{a}_j)$ is the distance between internal point $\mathbf{a}_j$ and every facet (edge). In particular, the determinant in the numerator corresponds to the volume (area) of the parallelepiped spanned by the outward normal vectors $\mathbf{\Lambda}_k$ associated with the facets incident on $\mathbf{g}_i$. The discussion will be continued with a couple of examples on finding the barycentric coordinates with the mentioned method.

II.6.7. Algorithms implementation

Following the same nomenclature as addressed above, the barycentric and mean value coefficients can be derived through computing intermediate variables.

It will be tried to explain the algorithm in brief. The polygon sides are defined in vector form as,

$$\bar{g} = [\mathbf{g}_2 - \mathbf{g}_1 \quad \mathbf{g}_3 - \mathbf{g}_2 \ldots\ldots \quad \mathbf{g}_N - \mathbf{g}_{N-1} \quad \mathbf{g}_1 - \mathbf{g}_N] \tag{II- 70}$$

and also the matrix F as,

$$F = \begin{bmatrix} \mathbf{g}_1 - \mathbf{a}_1 & \mathbf{g}_1 - \mathbf{a}_2 & . & . & \mathbf{g}_1 - \mathbf{a}_M \\ \mathbf{g}_2 - \mathbf{a}_1 & . & & & \mathbf{g}_2 - \mathbf{a}_M \\ . & . & & & . \\ . & . & & & . \\ \mathbf{g}_N - \mathbf{a}_1 & . & . & . & \mathbf{g}_N - \mathbf{a}_M \end{bmatrix} \quad \text{(II- 71)}$$

Let matrix α be defined as,

$$\alpha_{ij} = \frac{\left\langle F_{i,j}, F_{i+1,j} \right\rangle}{\left| F_{i,j} \right| \left| F_{i+1,j} \right|} \quad \text{(II- 72)}$$

So the elements of α reflect the angles between rays connecting an interior point and two consecutive vertices.

The angles γ_{ij} and θ_{ij} are computed with a similar approach,

$$\gamma_{ij} = \frac{\left\langle F_{i,j}, \mathbf{g}_{i+1} - \mathbf{g}_i \right\rangle}{\left| F_{i,j} \right| \left| \mathbf{g}_{i+1} - \mathbf{g}_i \right|} \quad \text{(II- 73)}$$

and

$$\theta_{ij} = \pi - \gamma_{ij} - \alpha_{ij} \quad \text{(II- 74)}$$

Now to compute the Barycentric and mean value coordinates will be straightforward using (II- 65) and (II- 66), respectively.

Consequently, having the coordinates of the (already generated) mesh nodes and polygon vertex, a matrix describing the mesh edges is formed as follows,

$$L = \left[\begin{array}{cccc|cccc} \overbrace{}^{mesh\ nodes} & & & & \overbrace{}^{polygon\ vetrex} & & & \\ edge\,1\left\{\begin{matrix}0 & 1 & . & .\end{matrix}\right. & & & & \begin{matrix}0 & . & . & .\end{matrix} & & & \\ \begin{matrix}0 & 0 & 0 & .\end{matrix} & & & & \begin{matrix}0 & 1 & 0 & 0\end{matrix} & & & \\ edge\,2\left\{\right. & & & & & & & \\ & & & & & & & \\ . & & & & & \cdot & & \\ . & & & & & & & \\ edge\,m\left\{\right. & & & & & & & \\ & & & & & & & \\ & & & & & & & \end{array}\right] \quad \text{(II- 75)}$$

Where L is a matrix that specifies the mesh edges. Every couple of consecutive rows show two ends of an edge. Thus the coordinates of the endpoints of the edges can be derived as,

$$K = L.[\mathbf{a}:\mathbf{g}] \qquad \text{(II- 76)}$$

The matrix L is the only components which is constant during the procedure. While deforming a polygon and its internal mesh points, all the coordinates will change, but the nodes and vertex forming mesh edges will remain unchanged. Thus after deformation, by multiplying the deformed coordinates to L would yield the new grid.

II.6.8. Mesh deformation examples

II.6.8.1 Scaling

The implemented algorithm for mesh deformation has been tried on few meshes. As the first example, consider a rectangle as shown in Fig. II.8. A very plain mesh is demonstrated as a matter of simplicity of the demonstration.

The rectangle $\mathbf{g}$ with the vertices at the point (0,0), (2,0), (2,1) and (0,1) is represented in matrix form as,

$$\mathbf{g} = \begin{bmatrix} 0 & 0 \\ 2 & 0 \\ 2 & 1 \\ 0 & 1 \end{bmatrix}$$

The rectangle is segmented with a simple mesh with three nodes represented by $\mathbf{a}$,

$$\mathbf{a} = \begin{bmatrix} 1.7000 & 0.2000 \\ 1.0000 & 0.6000 \\ 0.5000 & 0.4000 \end{bmatrix}$$

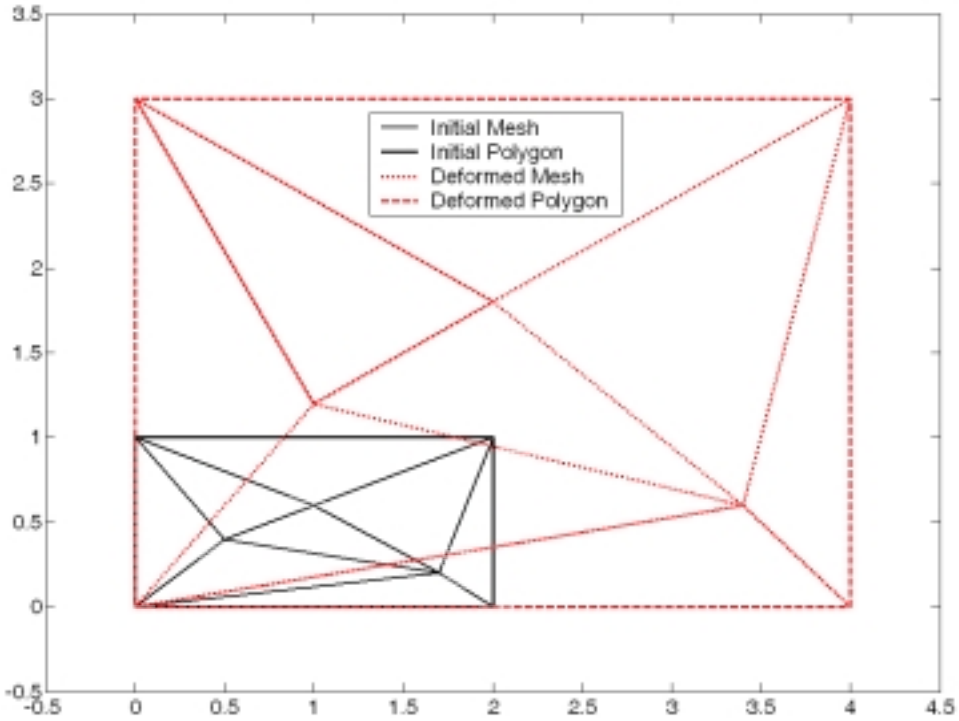

Fig. II.8. Example demonstration of the implementation of mean value coordinate.

Now the rectangle is scaled in it both dimensions to yield,

$$\mathbf{g}' = \begin{bmatrix} 0 & 0 \\ 4 & 0 \\ 4 & 3 \\ 0 & 3 \end{bmatrix}$$

The goal is to find the coordinates of the new mesh nodes named $\mathbf{a}'$.

Using the same notations as in the section II. 6.4. the internal angles will be as follows,

$$\boldsymbol{\alpha} = \begin{bmatrix} 139.6001 & 118.0725 & 126.4088 \\ 103.1340 & 52.7652 & 36.7328 \\ 85.3549 & 136.3972 & 108.0042 \\ 31.9110 & 52.7652 & 88.8542 \end{bmatrix},$$

$$\boldsymbol{\gamma} = \begin{bmatrix} 6.7098 & 30.9638 & 38.6598 \\ 56.3099 & 59.0362 & 75.0686 \\ 69.4440 & 21.8014 & 21.8014 \\ 64.7989 & 68.1986 & 39.8056 \end{bmatrix},$$

and

$$\boldsymbol{\theta} = \begin{bmatrix} 33.6901 & 30.9638 & 14.9314 \\ 20.5560 & 68.1986 & 68.1986 \\ 25.2011 & 21.8014 & 50.1944 \\ 83.2902 & 59.0362 & 51.3402 \end{bmatrix}.$$

angles are all in degrees.

The normalized Mean value coordinates are computed as,

$$w = \begin{bmatrix} 0.1098 & 0.6902 & 0.1598 & 0.0402 \\ 0.2000 & 0.2000 & 0.3000 & 0.3000 \\ 0.4538 & 0.1462 & 0.1038 & 0.2962 \end{bmatrix}.$$

Now using the matrix w, the deformed mesh nodes can be computed,

$$\mathbf{a}' = \begin{bmatrix} 3.4000 & 0.6000 \\ 2.0000 & 1.8000 \\ 1.0000 & 1.2000 \end{bmatrix}$$

$\mathbf{a}'$ is the coordinates of the mesh nodes belonging to the scaled geometry.

II.6.8.2 Moving vertices inward and outward

As a second mesh parameterization example consider the original geometry Γ_1 and deformed geometries (Γ_2, Γ_3) are shown in Fig. II.9 for this example the mesh morphing for inward and outward movements of the vertices are to be examined. Intentionally the geometry is not convex.

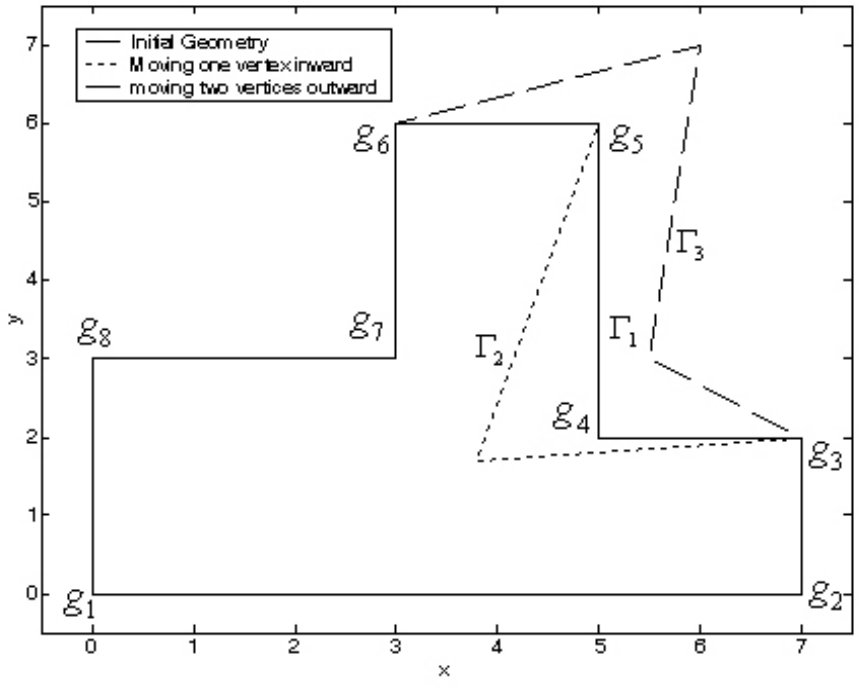

Fig. II.9. Example: the original and deformed geometries.

The polygon Γ_1 is represented in matrix form as,

$$\mathbf{g}_1 = \begin{bmatrix} 0 & 0 \\ 4.0000 & 0 \\ 5.5000 & 0 \\ 7.0000 & 0 \\ 7.0000 & 2.0000 \\ 5.0000 & 2.0000 \\ 5.0000 & 6.0000 \\ 3.0000 & 6.0000 \\ 3.0000 & 3.0000 \\ 0 & 3.0000 \end{bmatrix}$$

The rectangle is segmented with a simple mesh with three nodes represented by $\mathbf{a}_1$,

$$\mathbf{a}_1 = \begin{bmatrix} 2.0000 & 1.0000 \\ 4.0000 & 0.5000 \\ 6.0000 & 1.0000 \\ 4.5000 & 5.0000 \end{bmatrix}$$

The mesh is parameterized through mean value coordinates as

The polygon Γ_1 is deformed by moving one vertex (g_4) inward as shown here,

$$\mathbf{g}_2 = \begin{bmatrix} 0 & 0 \\ 4.0000 & 0 \\ 5.5000 & 0 \\ 7.0000 & 0 \\ 7.0000 & 2.0000 \\ 3.8000 & 1.7000 \\ 5.0000 & 6.0000 \\ 3.0000 & 6.0000 \\ 3.0000 & 3.0000 \\ 0 & 3.0000 \end{bmatrix}$$

matrix $\mathbf{a}_2$ now is calculated as,

$$\mathbf{a}_2 = \begin{bmatrix} 2.0024 & 1.1329 \\ 3.9373 & 0.4843 \\ 5.6759 & 1.1462 \\ 4.2470 & 4.7111 \end{bmatrix}$$

Fig. II.10 shows the deformed geometry Γ_2 with one inward moved vertex g_4. The whole grid, even those points which are affected by deformation. When moving the points towards the interior of polygon, there is always a risk for having some nodes of

the deformed geometry moved out of the geometry borders. One approach to avoid such a scenario is to split a polygon to a number of convex shapes.

Now the original polygon Γ_1 is deformed by moving two vertices (g_4 and g_5) outward,

$$\mathbf{g}_3 = \begin{bmatrix} 0 & 0 \\ 4.0000 & 0 \\ 5.5000 & 0 \\ 7.0000 & 0 \\ 7.0000 & 2.0000 \\ 5.5000 & 3.0000 \\ 6.0000 & 7.0000 \\ 3.0000 & 6.0000 \\ 3.0000 & 3.0000 \\ 0 & 3.0000 \end{bmatrix}$$

the new deformed mesh is calculated as follows,

$$\mathbf{a}_3 = \begin{bmatrix} 2.0962 & 1.2110 \\ 4.0400 & 0.5661 \\ 6.0014 & 1.3994 \\ 5.0658 & 5.4632 \end{bmatrix}$$

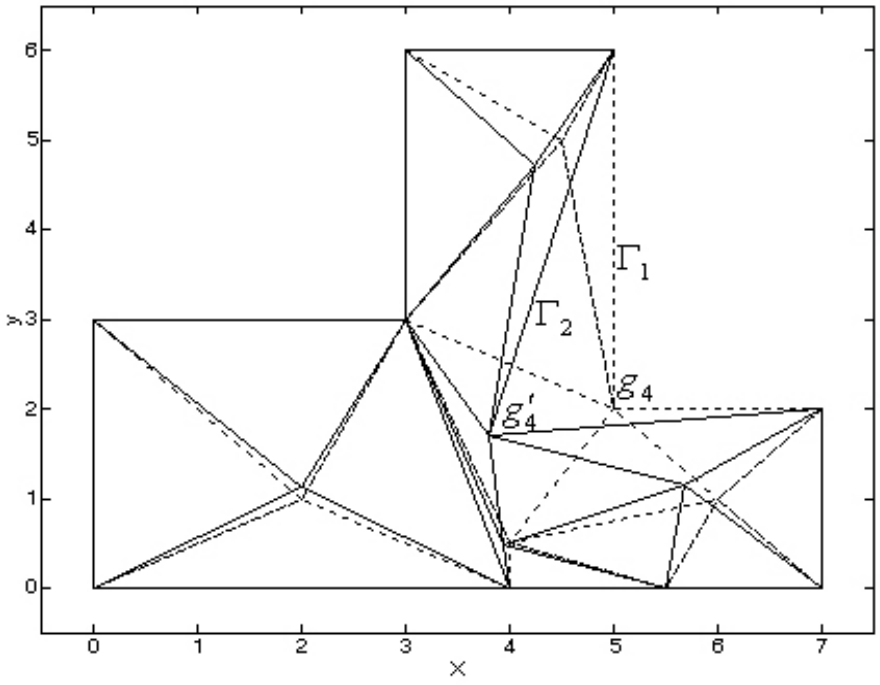

Fig. II.10. Moving one vertex inward (the original and deformed geometries)

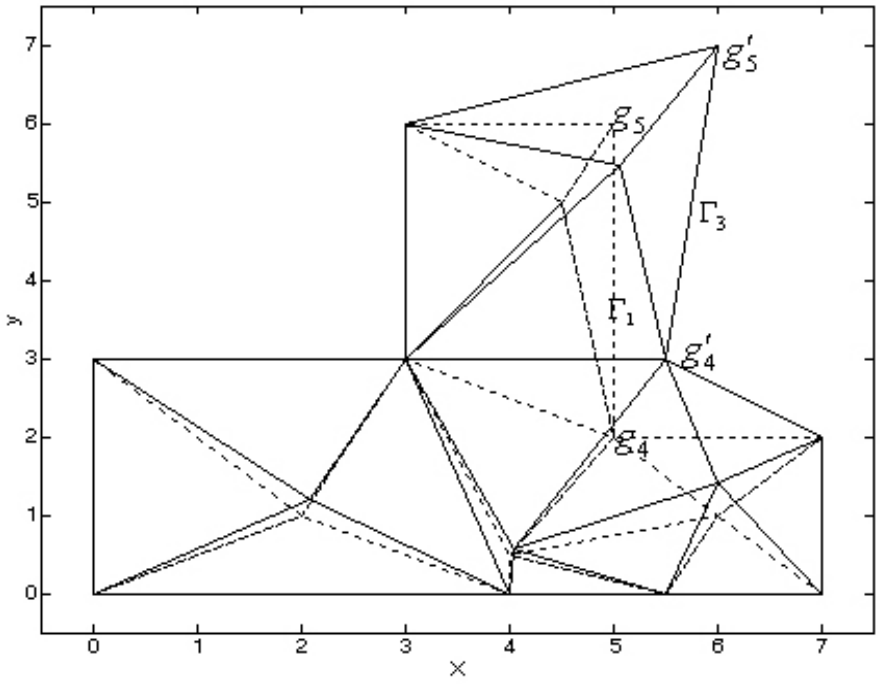

Fig. II.11. Moving two vertices outward (the original and deformed geometries)

II.7. Design example – Optimization of a dual-mode cavity filter

So far the different aspect of optimization of microwave structures have been studied extensively. Despite the fact that the proposed techniques are well established in mathematics, there are many detail which are specifically important in a microwave engineering point of view. To further clarify this, the efforts to use the already discussed method for optimizing a relatively complicated microwave device is presented in detail.

II.7.1. Description of the structure

Despite their being in use for many decades, microwave filters that manipulate the Chebyshev filtering functions are of great interest. Their being highly selective, gives an acceptable compromise between lowest signal degradation and highest noise/interference rejection. In the applications where filters are used for channeling, very high close-to-band rejections are required to prevent interference to or from closely neighboring channels; at the same time, the incompatible requirements of in-band group-delay and amplitude flatness and symmetry are demanded to minimize signal degradation.

A 5th order filter is designed that provides a band-pass pseudo elliptic transfer function, with 23dB return loss and 2 symmetrical transmission zeros at ± 1.435. The objective is a flat 37.5MHz pass-band centered at 12.35GHz. The structure is described in Fig. II.12. The filter works on its TE_{113} dual-mode: 2 polarizations are coupled in the two first cavities and only one polarization is coupled in the last one. The ideal scattering parameters are presented in Fig. II.13.

II.7.1.1 The design parameters

The twelve design variables as shown in Fig. II.12 are:

- 5 tuning screws, each to tune one resonant frequency,
- 2 coupling screws for the adjustment of coupling within dual mode cavities,
- 3 coupling irises, for coupling between adjacent cavities,
- 2 excitation irises, for input/output coupling.

These parameters form a sophisticated parameter space which could assure having embraced the desired filtering response.

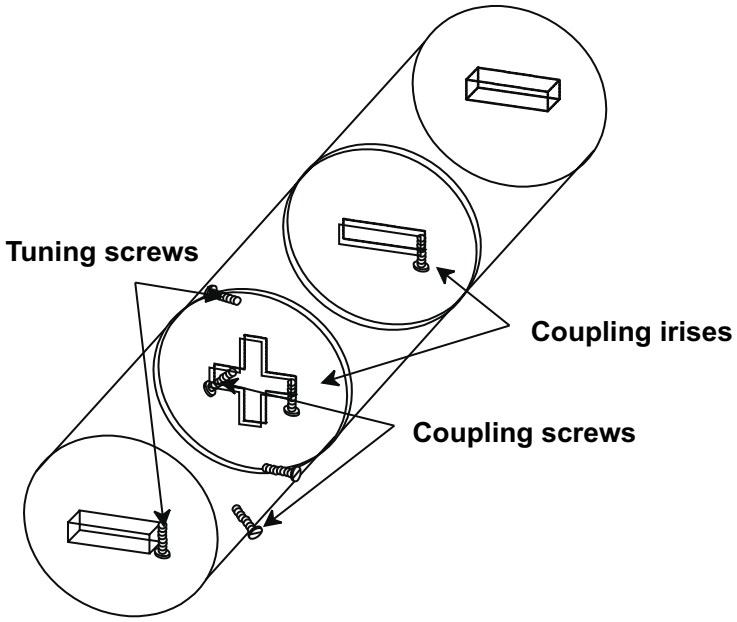

Fig. II.12. The 5-pole cavity filter and relevant notations.

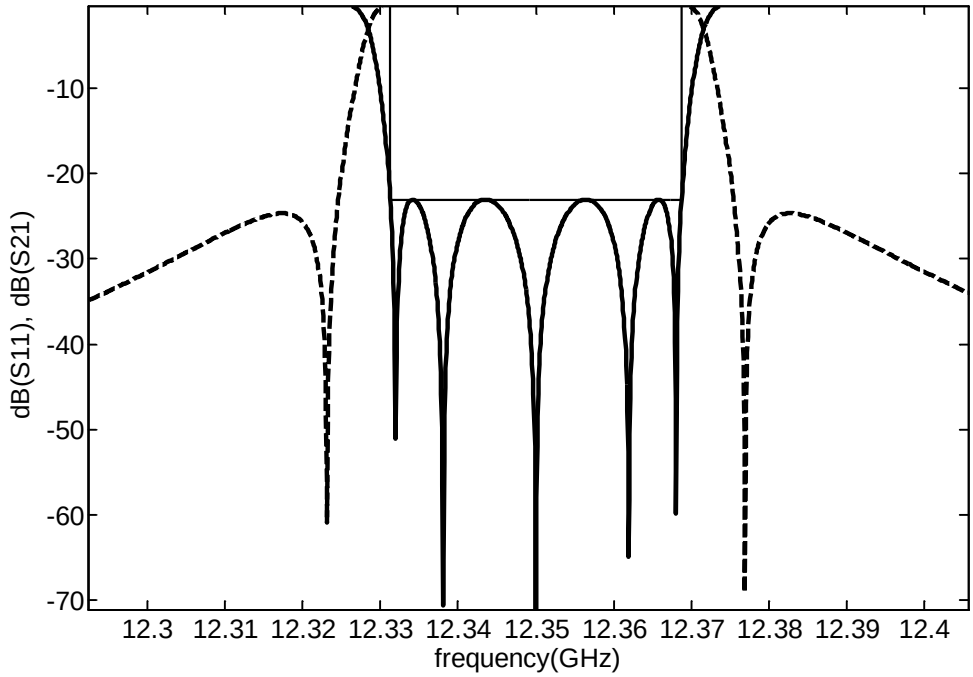

Fig. II.13. The ideal transfer function

The initial dimensions are computed using an electromagnetic synthesis **[83]**. Each distributed element is analyzed individually. The dimensions of the cavities may be computed applying analytical formulas. The input/output iris dimensions are then determined by analyzing a cavity coupled to the standard waveguide through a

rectangular iris. Then, the coupling iris dimensions are determined by analyzing two cavities coupled through a rectangular iris. The initial dimensions of the structure are shown in Tables I and II

Dimension	Value (mm)
Height of cavity 1	42.2
Height of cavity 2	42.6
Height of cavity 3	42.2
Diameter of cavities	27
Width of I/O irises	2
Width of coupling irises	1
Thickness of irises	1.02

Table I. Fix dimensions

Parameter	Value (mm)
Length of input iris	9.25
Length of iris 1-2	7.25
Length of iris 2-5	5.4
Length of iris 3-4	7.1
Length of output iris	9.25
Length of screw 1-1	2.15
Length of screw 2-2	2.15
Length of screw 3-3	2.15
Length of screw 4-4	2.60
Length of screw 5-5	1.50
Length of screw 2-3	0.75
Length of screw 4-5	1.25

Table II. Initial design parameters

II.7.1.2 Geometrical parameterization

The structure was parameterized with respect to all the twelve geometrical parameters mentioned. The details of the parameterization procedure developed by CADOE are discussed before in II.5.

The resulting polynomial is used to calculate the electric field within the structure. The parameterized model is expressed only in terms of one parameter at a single frequency. Parameterizing both with respect to frequency **[82]** and geometry or parameterizing with respect to more than one geometrical parameter at a time would result in approximate cross terms that aggrandize the error values accumulatively. As

a consequence, the electric field, the scattering parameters and all related functions are defined as functions of only one parameter pm, $m \in [2, \ldots, M]$, at a single frequency *fs*.

The parameterization has been done in 19 frequency points. The choice of appropriate frequency points is very critical. With an intelligent choice of frequency point one can skip calculating the objective function in for too many times which makes the optimization more cost efficient.

Table III shows the exact frequency points chosen for this optimization practice.

No	Frequency (GHz)	No	Frequency (GHz)
1	**12.3170**	11	**12.3560**
2	**12.3230**	12	**12.3610**
3	**12.3240**	13	**12.3660**
4	**12.3280**	14	**12.3680**
5	**12.3300**	15	**12.3680**
6	**12.3321**	16	**12.3710**
7	**12.3340**	17	**12.3750**
8	**12.3381**	18	**12.3760**
9	**12.3430**	19	**12.3820**
10	**12.3500**		

Table III. The frequencies in which the electric fields are parameterized with respect to geometrical parameters

II.7.2. Interpolating discrete frequency characteristic

The geometrical parameterization ends up with a set of results in the form of

$$\tilde{S}_n = S(\tilde{f}, \tilde{\tilde{p}}_n) \qquad \text{(II- 77)}$$

where $\tilde{f}$ is the vector including all the frequency points where the field is parameterized versus frequency $\tilde{f} = \{f_1, f_2, ..., f_{Nf}\}$

$\tilde{\tilde{p}}_n$ is the parameter vector with the *n*'th element p_n being varied in a range $\tilde{\tilde{p}}_n = [p_1 \ p_2 \ldots [p_{n,1} \ldots p_{n,M}] \ldots p_N]$ while other parameters are constant.

Fig. II.14 shows this parameterized vector versus the frequency. As can be seen at each frequency point, the values of S-parameters are given while one parameter is varying.

The calculated S-parameter in discrete frequency point is not appropriate for calculating errors. The error calculated by connecting these points is too imprecise to be a basis for integrating errors. This is further clarified in Fig. II.14. Please note that in order to calculate gradients, we will need to track the variations of S-parameter due to fine variations. To this end, we will need to interpolate the S-parameter versus frequency to be able to express it as a continuous function. Such an interpolating function should be able to precisely comply with specific features of a frequency characteristic such as poles and zeros.

Different interpolating functions have been used to interpolate the discrete characteristic. The results are presented in this section.

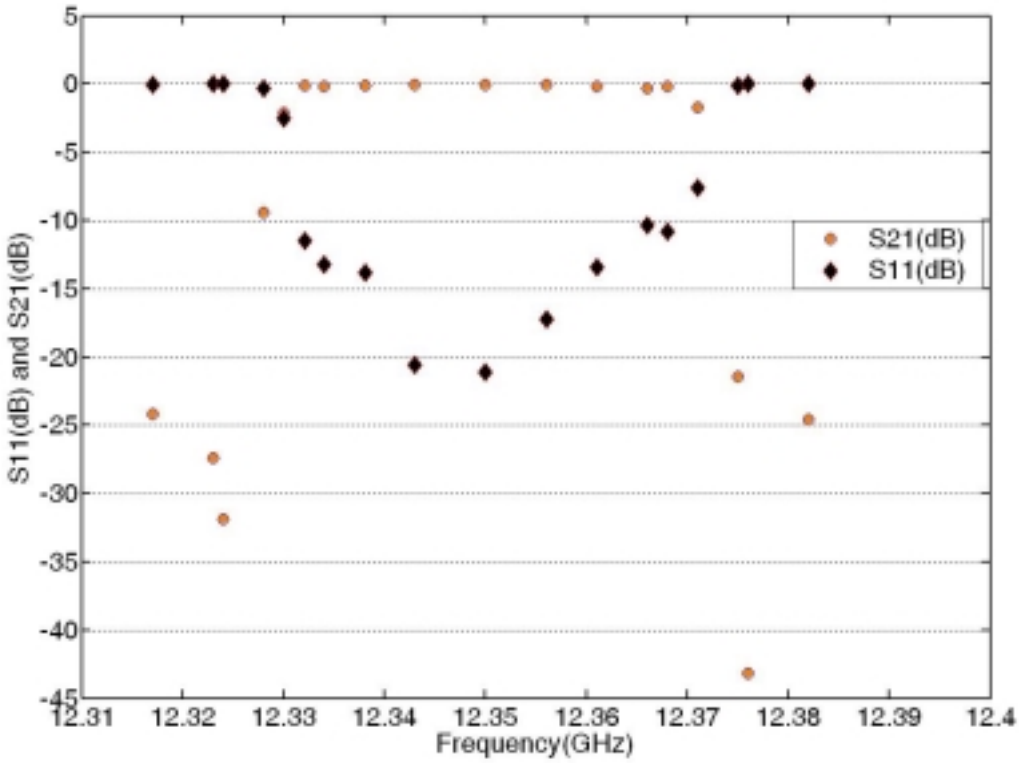

Fig. II.14. The explanation of $\tilde{S}_n = S(\tilde{f}, \tilde{\bar{p}}_n)$.Connecting the discrete frequency points to obtain a continuous characteristic of S-parameters does not give precise results

II.7.2.1 Curve fitting by least squares method

The method of least squares assumes that the best-fit curve of a given type is the curve that has the minimal sum of the deviations squared (*least square error*) from a given set of data.

The fitting curve $S(f,\tilde{\tilde{p}}_m)$ has the deviation (error) d from each frequency point, i.e.,

$d_1 = S(f_1,\tilde{\tilde{p}}_n) - \tilde{S}(f_1,\tilde{\tilde{p}}_n)$, $d_2 = S(f_2,\tilde{\tilde{p}}_n) - \tilde{S}(f_2,\tilde{\tilde{p}}_n)$, ... $d_{Nf} = S(f_{Nf},\tilde{\tilde{p}}_n) - \tilde{S}(f_{Nf},\tilde{\tilde{p}}_n)$.

According to the method of least squares, the best fitting curve has the property that:

$$d_1^2 + d_2^2 + d_3^2 + ... + d_{Nf}^2 = \sum_{i=1}^{Nf} d_i^2 = \sum_{i=1}^{Nf} \left[S(f_1,\tilde{\tilde{p}}_n) - \tilde{S}(f_1,\tilde{\tilde{p}}_n) \right]^2 \quad \text{(II- 78)}$$

is minimum.

To fit a polynomial of degree *M* such as,

$$S(f_1,\tilde{\tilde{p}}_n) = a_0 + a_1 f + ... + a_M f^M \quad \text{(II- 79)}$$

to the data points that we have calculated through parameterization, we would have to substitute the equation (II- 79) into (II- 78) such that,

$$\Pi = \sum_{i=1}^{Nf} \left[(a_0 + a_1 f_i + ... + a_M f_i^M) - \tilde{S}(f_i,\tilde{\tilde{p}}_n) \right]^2 \quad \text{(II- 80)}$$

is minimal.

To obtain the least square error, the unknown coefficients a_0 to a_M must yield zero first derivatives

$$\frac{\partial \Pi}{\partial a_m} = 2\sum_{i=1}^{Nf} f_i^m \left[(a_0 + a_1 f_i + ... + a_M f_i^M) - \tilde{S}(f_i,\tilde{\tilde{p}}_n) \right] = 0 \quad \text{(II- 81)}$$

The unknown coefficients will thus be calculated through the linear system of equations.

The results of fitting the curve through least squares is presented in Fig. II.15. Different degrees of polynomial have been tried ranging from 4 to 19 (the maximum possible through least squares method). Noting that the time for calculating coefficients increases almost linearly with the polynomial degree. In practice it was seen that increasing the degree of polynomial more than 8 was not affecting the results.

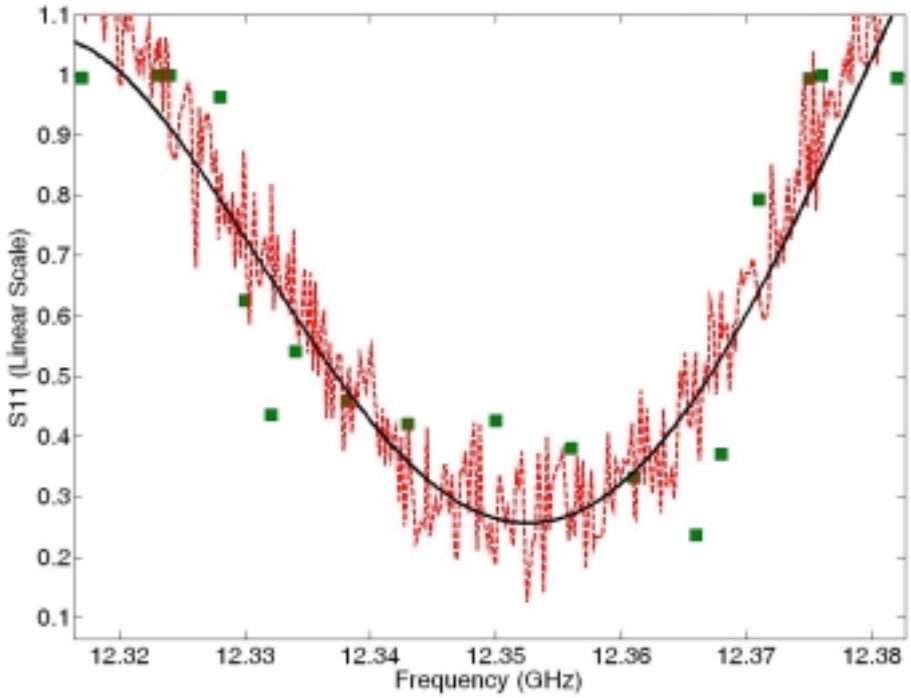

Fig. II.15. The interpolated results through the least squares method

II.7.2.2 Interpolation using Padé approximants

As mentioned earlier, rational functions are usually used to comply the filtering characteristics. The derivation of Padé approximant has been discussed in detail when explaining frequency parameterization. Here, a slightly different scheme has been utilized to fit *Nf* points of parameterized S-parameters with respect to frequency. Assuming that the resultant interpolation function has the form,

$$S = S(f, \tilde{\bar{p}}_n) = \frac{a_0 + a_1 f + ... + a_P f^P}{1 + b_1 f + ... + b_Q f^Q} \tag{II- 82}$$

The equation (II- 82) can be re-written as,

$$S_i = S(f_i, \tilde{\bar{p}}_n) = a_0 + a_1 f_i + ... + a_P f_i^P - b_1 f_i - b_2 f_i^2 ... - b_Q f_i^Q \tag{II- 83}$$

The resulting equation can be represented as in matrix form as,

$$\bar{S} = [X].\bar{A} \tag{II- 84}$$

where

$$\bar{S} = \left[S(f_1, \bar{p})\ S(f_2, \bar{p}) .... S(f_{Nf}, \bar{p}) \right]^T$$

$$\bar{A} = \left[a_0\ a_1 .. a_p .. a_P \mid b_0\ b_1 ... b_q ... b_Q \right]^T$$

$$X=\begin{bmatrix} 1 & f_1 & f_1^2 & \dots & f_1^P & -S(f_1,\bar{p}).f_1 & -S(f_1,\bar{p}).f_1^2 & .. & . & -S(f_1,\bar{p}).f_1^Q \\ 1 & f_2 & f_2^2 & \dots & f_2^P & -S(f_2,\bar{p}).f_2 & -S(f_2,\bar{p}).f_2^2 & .. & . & -S(f_2,\bar{p}).f_2^Q \\ . & . & . & \dots & . & . & . & .. & . & . \\ . & . & . & \dots & . & . & . & .. & . & . \\ . & . & . & \dots & . & . & . & .. & . & . \\ 1 & f_{Nf} & f_{Nf}^2 & \dots & f_{Nf}^P & -S(f_{Nf},\bar{p}).f_{Nf} & -S(f_{Nf},\bar{p}).f_{Nf}^2 & .. & . & -S(f_{Nf},\bar{p}).f_{Nf}^Q \end{bmatrix}$$

If $Nf = P+Q$ the solution of (II- 84)is simply calculated by inversion of X.

$$\bar{A} = [X]^{-1}.\bar{S} \quad \text{if } Nf = P+Q \tag{II- 85}$$

$$\bar{A} = \left[[X]^T.[X]\right]^{-1}[X]^T.\bar{S} \quad \text{if } Nf > P+Q$$

For the case $Nf < P+Q$, the system of equations will be under-determined and solution will not be precise. The algorithm is implemented with MATLAB. The interpolated function is shown in Fig. II.16.

To have a more precise result it is essential that complex values of S at sampling points be utilized for interpolation. This significantly ameliorates accuracy.

Although the Padé approximant showed a better accuracy than the least squares, but anyways it is still nowhere near an acceptable range to follow up the small perturbation.

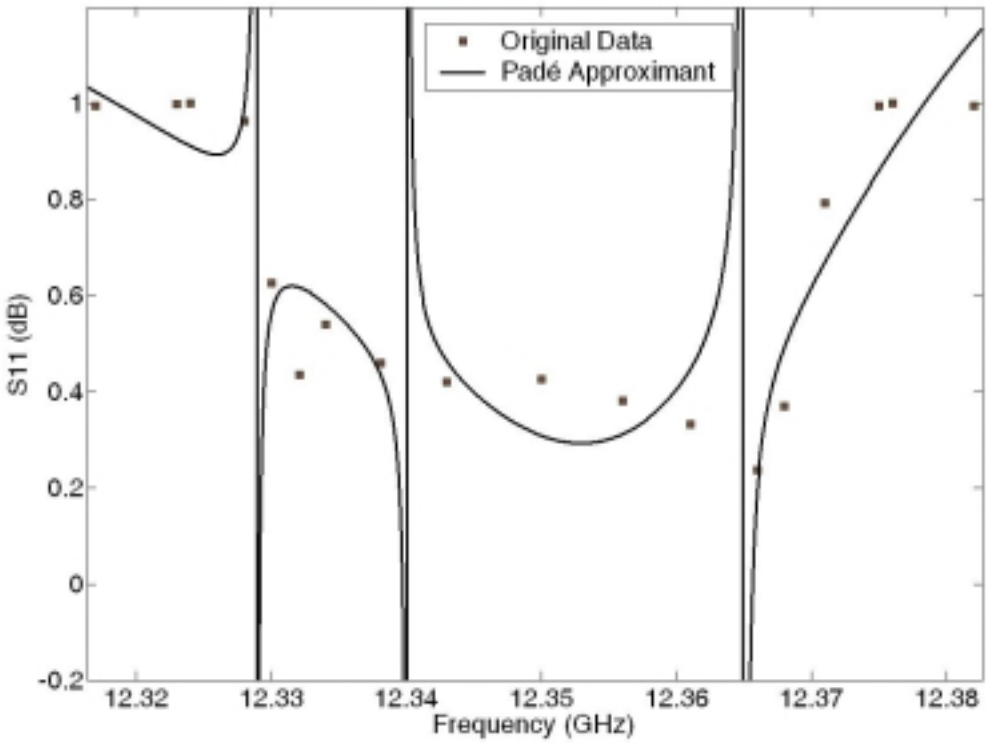

Fig. II.16. The S-parameter interpolated using Padé approximants

II.7.2.3 Interpolation by splines

The goal of cubic spline interpolation is to get an interpolation formula that is smooth in the first derivative, and continuous in the second derivative, both within an interval and at its boundaries. Using spline interpolation, a set on *Nf* piecewise polynomials can be computed. There is a polynomial for each interval, each with its own coefficients,

$$S_i = S(f_i, \tilde{\tilde{p}}_n) = a_i(f - f_i)^2 + b_i a_i(f - f_i)^3 + c_i(f - f_i) + d_i, \;\; f_i \le f \le f_{i+1} \qquad \text{(II- 86)}$$

Since there are *Nf* -1 intervals and four coefficients for each we require a total of *4(Nf-1)* parameters to define the spline. In other words *4(Nf-1)* independent conditions are needed to compute all the coefficients. It is already known that *2(Nf-1)* of these conditions come from matching the beginning and the end of each interval,

$$S_i = \tilde{S}(f_i, \tilde{\tilde{p}}_n), \;\; S_{i+1} = \tilde{S}(f_{i+1}, \tilde{\tilde{p}}_n) \qquad \text{(II- 87)}$$

There are still *2(Nf-1)* more conditions needed. Since we would like to make the interpolation as smooth as possible, we require that the first and second derivatives also be continuous,

$$\left.\frac{dS_i}{df}\right|_{f=f_i} \quad \left.\frac{dS_{i+1}}{df}\right|_{f=f_i} \qquad \text{(II- 88)}$$

and

$$\left.\frac{d^2S_i}{df^2}\right|_{f=f_i} = \left.\frac{d^2S_{i+1}}{df^2}\right|_{f=f_i}$$

The boundary conditions mentioned above will furnish *4Nf-2* condition. The remaining two conditions should be provided through setting the second derivatives zero at the start and the end of the whole domain,

$$\frac{d^2S_1(f_1, \tilde{\tilde{p}}_n)}{df^2} = 0 \qquad \text{(II- 89)}$$

$$\frac{d^2S_{Nf}(f_{Nf}, \tilde{\tilde{p}}_n)}{df^2} = 0$$

These terminating conditions are called natural in the literature.

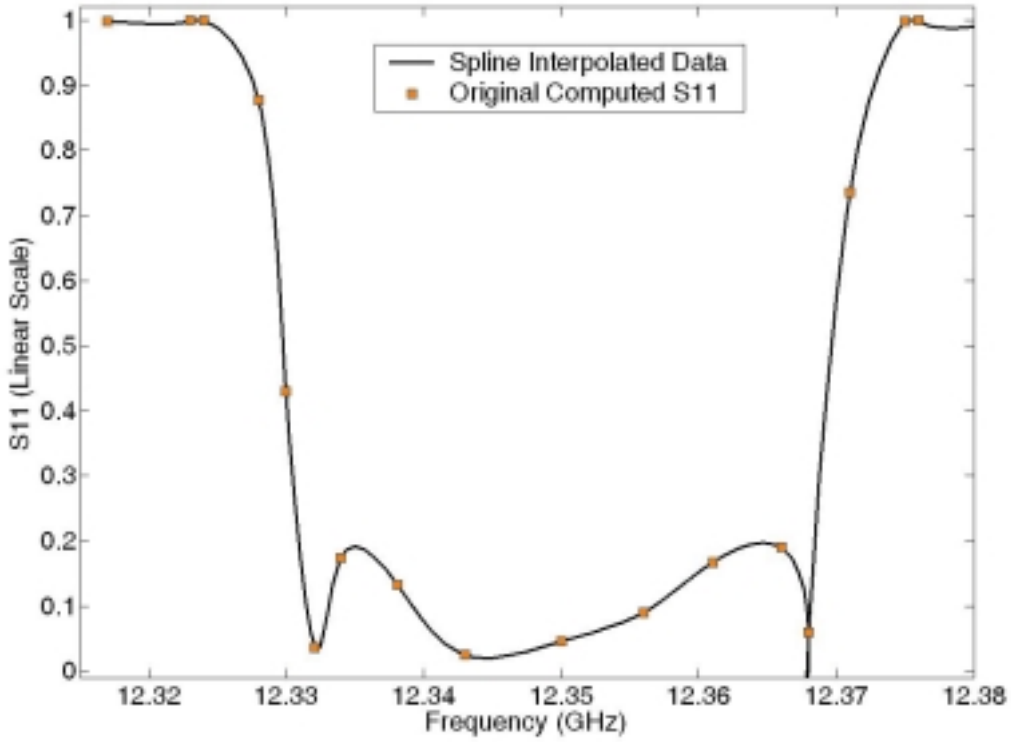

Fig. II.17. The discrete frequency characteristic is interpolated through splines

Now solving this set of linear equations will give a smooth curve as can bee seen, for example, in Fig. II.17. The curve is satisfactorily and follows the probable characteristic of a filtering characteristic.

II.7.3. Data structure

The parameterization with respect to geometrical parameters is always done based on a parametric model in a single frequency. This means that the outcome of parameterization is in the form of

$$S(f_1,\tilde{\tilde{p}}_n)=\left\{S(f_1,\left[p_1\ p_2\ p_{3..}\ p_n=p_{n,1}\dots p_N\right]),S(f_1,\left[p_1\ p_2\ p_{3..}\ p_n=p_{n,2}\dots p_N\right]),\dots,S(f_1,\left[p_1\ p_2\ p_{3..}\ p_n=p_{n,Np}\dots p_N\right])\right\} \quad \text{(II- 90)}$$

$$S(f_2,\tilde{\tilde{p}}_n)=\left\{S(f_2,\left[p_1\ p_2\ p_{3..}\ p_n=p_{n,1}\dots p_N\right]),S(f_2,\left[p_1\ p_2\ p_{3..}\ p_n=p_{n,2}\dots p_N\right]),\dots,S(f_2,\left[p_1\ p_2\ p_{3..}\ p_n=p_{n,Np}\dots p_N\right])\right\}$$

.

.

$$S(f_{Nf},\tilde{\tilde{p}}_n)=\left\{S(f_{Nf},\left[p_1\ p_2\ p_{3..}\ p_n=p_{n,1}\dots p_N\right]),S(f_{Nf},\left[p_1\ p_2\ p_{3..}\ p_n=p_{n,2}\dots p_N\right]),\dots,S(f_{Nf},\left[p_1\ p_2\ p_{3..}\ p_n=p_{n,Np}\dots p_N\right])\right\}$$

The calculated data now should be re-grouped in such a way that similar parameter sets of different frequencies form a new vector in the form of,

$$S(\tilde{f}, \bar{p}_{1,1}) = \left\{S(\left[f_1, f_2, ..., f_{Nf} \right], \left[p_1 = p_{1,1} \;\; p_2 \; p_{3..} \; p_n ... p_N \right])\right\} \quad \text{(II- 91)}$$

$$S(\tilde{f}, \bar{p}_{1,2}) = \left\{S(\left[f_1, f_2, ..., f_{Nf} \right], \left[p_1 = p_{1,1} \;\; p_2 \; p_{3..} \; p_n ... p_N \right])\right\}$$

.

$$S(\tilde{f}, \bar{p}_{1,Np}) = \left\{S(\left[f_1, f_2, ..., f_{Nf} \right], \left[p_1 = p_{1,1} \;\; p_2 \; p_{3..} \; p_n ... p_N \right])\right\}$$

.

.

$$S(\tilde{f}, \bar{p}_{N,1}) = \left\{S(\left[f_1, f_2, ..., f_{Nf} \right], \left[p_1 \;\; p_2 \; p_{3..} \; p_n ... p_N = p_{N,1} \right])\right\}$$

.

.

$$S(\tilde{f}, \bar{p}_{N,1}) = \left\{S(\left[f_1, f_2, ..., f_{Nf} \right], \left[p_1 \;\; p_2 \; p_{3..} \; p_n ... p_N = p_{N,Np} \right])\right\}$$

The above data manipulation is depicted in Fig. II.18.

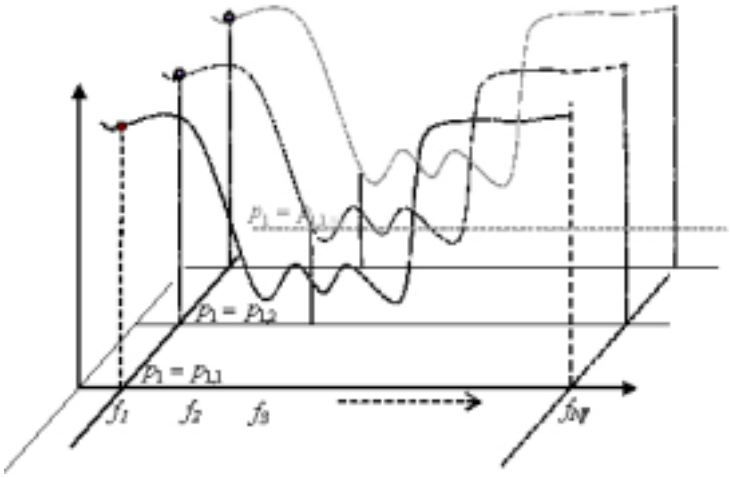

Fig. II.18. The S-parameters are computed for every frequency.

The interpolation which was explained in the previous section has been conducted over one set of discrete frequency points, which means that the same procedure is needed to be performed over different parameter values of each parameter. The data structure for different parameter variations is shown in Fig. II.19.

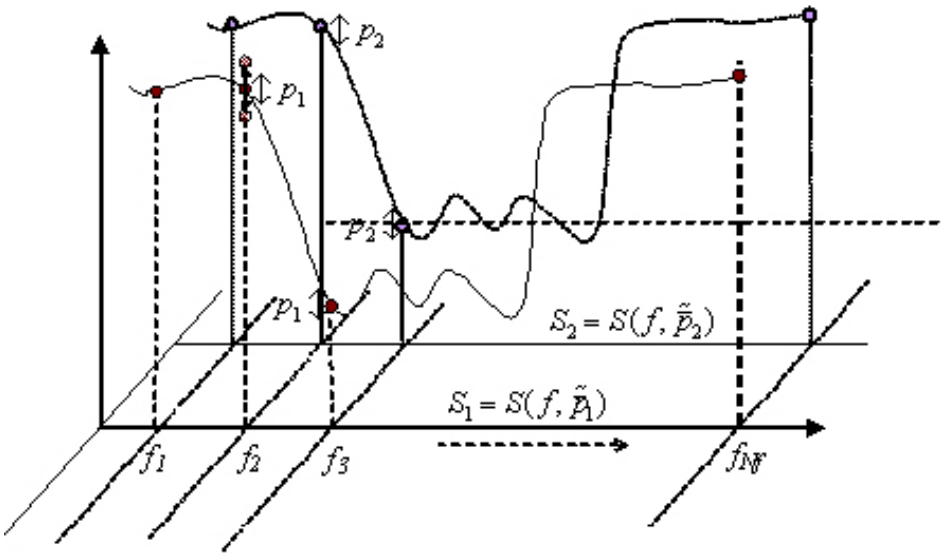

Fig. II.19. The parameterized model should be computed for variations of every parameter

II.7.4. Objective function

The objective function is defined using frequency characteristics of the S-parameters. As mentioned before, the parameterized model operates at a single frequency. Calculating the objective function in a complete frequency band would be cumbersome. Instead, the $T_{s,m}(f,\bar{p})$ function is defined as,

$$\begin{aligned} T_{s,m}(f,\bar{p}) &= T_m(f_s,\bar{p}) \\ &= T(f_s,p_m) \\ &= T(S_{ij}(f_s,p_m),S_{ij}^{<ID>}(f_s)) \end{aligned} \qquad \text{(II- 92)}$$

fs's are critical frequencies where the objective function has to be computed accurately.

The frequencies could be poles and zeros of the ideal transmission and reflection functions, obtained by a mathematical filter approximation such as Chebyshev, Butterworth, etc. The choice of the functions $S_{11}^{<ID>}$ and $S_{12}^{<ID>}$ should comply in general with the desired specifications. In other words one does not necessarily need to approximate the specifications with a predefined mathematical function.

The resulting sampled frequency space is then interpolated to obtain a fine model in such a way that,

$$T_m(\bar{p}) = \int_{f_{\min}}^{f_{\max}} T(f,p_m).df \qquad \text{(II- 93)}$$

Herein the cubic spline functions have been used for interpolating the sampled S-parameters. The goal of cubic spline interpolation is to get an interpolation formula that is smooth in the first derivative, and continuous in the second derivative, both within an interval and at its boundaries. The only drawback with splines is their being piecewise approximations; i.e. there is a second order polynomial defined between every two points. However, such a constraint would not affect the viability of splines for the purpose of this work. A couple of other alternatives are polynomial interpolation and rational functions. For the present case, a Legendre function was to be insufficient, because it is incapable of chasing the zeros of the filtering function. Padé approximations have also been examined. Although interpolating with Padé approximant somehow met the accuracy for the present application, there appear some spikes which eventually reduce the sensitivity of the error function to geometry perturbations. Incorporating the phase value of S-parameters helps to diminish the spikes to some extent.

As a by-product, the gradients of S-parameters could be obtained through the parameterized model by a Finite Difference scheme. Using a chain derivatives rule, in turn, the sensitivities of the objective function are attainable through a set of M simulations.

The ideal pseudo-elliptic filtering characteristic was shown in Fig. II.13 The primary objective function is formed by summation of the differences between the ideal function and the actual one at each step,

$$T(\bar{p}) = \sum_{s=1}^{S} \left| S_{11}(f_s, \bar{p}) - S_{11}^{<ID>}(f_s, \bar{p}) \right| + \sum_{s=1}^{S} \left| S_{12}(f_s, \bar{p}) - S_{12}^{<ID>}(f_s, \bar{p}) \right| \quad \text{(II- 94)}$$

As recommended in **[84]** minimizing this objective function is converging very rapidly when zeros of the initial response *Sij* correspond to the ideal response. When there is a little discrepancy between $S_{ij}^{<ID>}$ and S_{ij} due to sharp descents, the gradients obtained will be inaccurate. This leads to the definition of a generalized objective function which is independent of the ideal transfer function poles and zeros, i.e. a combination of rectangular functions which represents the ideal reflection and transmission specifications. The modified global objective function is represented as follows,

$$T(\bar{p}) = \alpha \int_{f_{\min}}^{f_{\max}} T_{11}(f, \bar{p}).df + \beta \int_{f_{\min}}^{f_{\max}} T_{21}(f, \bar{p}).df \tag{II- 95}$$

where the function Tij and its sub-functions are defined as,

$$T_{ij}(f, \bar{p}) = Q(f).W\left(r_{ij}(f).D_{ij}(f, \bar{p})\right) \tag{II- 96}$$

with $$W(x) = \begin{cases} \eta \exp(x) & x > 0, 0 < \eta \le 1 \\ 0 & x \le 0 \end{cases}$$

$$r_{ij}(f) = \begin{cases} 1 & \text{if } i = j \text{ in the passband} \\ & \text{or } i \ne j \text{ in the stopband} \\ -1 & \text{if } i \ne j \text{ in the passband} \\ & \text{or } i = j \text{ in the stopband} \end{cases}$$

$$D_{ij}(f, \bar{p}) = S_{ij}(f, \bar{p}) - S_{ij}^{<ID>}(f)$$

$$Q(f) = \begin{cases} 1 & \textit{Within transition bands} \\ 0 & \textit{Elsewhere} \end{cases}$$

$$S_{11}^{<ID>}(f) = \begin{cases} S_{11}^{inband} & |f - f_c| \le BW/2 \\ S_{11}^{outband} & |f - f_c| \ge BW/2 \end{cases}$$

The $S_{11}^{<ID>}(f)$ is a rectangular region in which the final result should fit. Such an ideal response is utilizable as long as the initial response has a considerable overlap with this rectangular region. What happens in a real design practice is somehow different. Normally the detuning is quite considerable in such a way that the ideal and actual pass-bands have no or a very small overlap. This would make gradients approximated through finite differencing meaningless. As a possible way, the proposed ideal response is slightly modified so that the gradient can be obtained when ideal and actual functions have no overlap; i.e. when the filter is strongly detuned. As one possible way, the proposed ideal response is slightly modified so that gradient can be obtained when ideal and actual functions have no overlap; i.e. when the antenna is strongly detuned. The modified ideal function can be expressed as,

$$S_{11}^{<MOD>}(f) = \begin{cases} |R|.\left(1 - \exp\left(\dfrac{f - f_c - BW/2}{\zeta}\right)\right) & f \ge f_c - BW/2 \\ S_{11}^{inband} & |f - f_c| \le BW/2 \\ |R|.\left(1 - \exp\left(\dfrac{f - f_c + BW/2}{\zeta}\right)\right) & f \le f_c - BW/2 \end{cases} \tag{II- 97}$$

with $R = S_{11}^{inband} - S_{11}^{outband}$.

The modified ideal response is shown in Fig. II.20. Using this ideal response, the gradients are less precise or better to say less sensitive to variations of the dimensions. This is because when integrating the error between the actual and ideal S_{11} the area under the ideal response is relatively larger and the error produced in this way is less sensitive to variations of the dimensions. On the other hand, using a bigger ζ would guarantee catching a more exaggerated detuning; *i.e.* when the initial working band is very far from the desired characteristic.

It is important to remember here that the parameters Sij are computed only at critical frequencies *fs* and the interpolated using splines. The errors are then calculated for the interpolated S-parameters. α and β are weights, applied to errors. All these sub-functions are depicted in Fig. II.21.

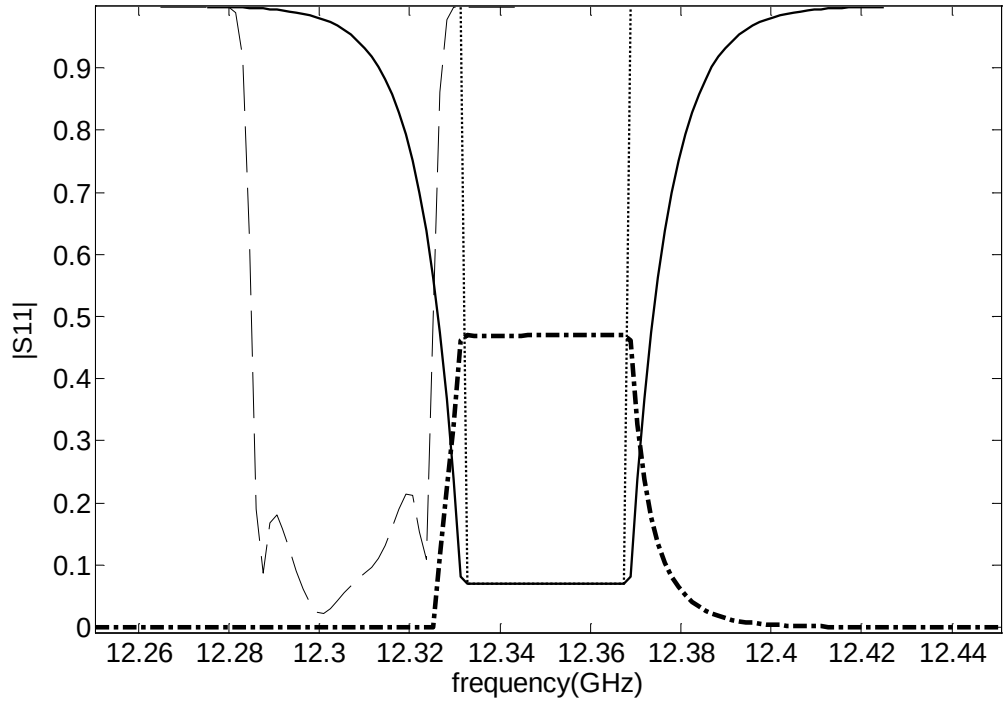

Fig. II.20. The modified ideal response and calculated weighted error, $T_{ij}(f, \bar{p})$.

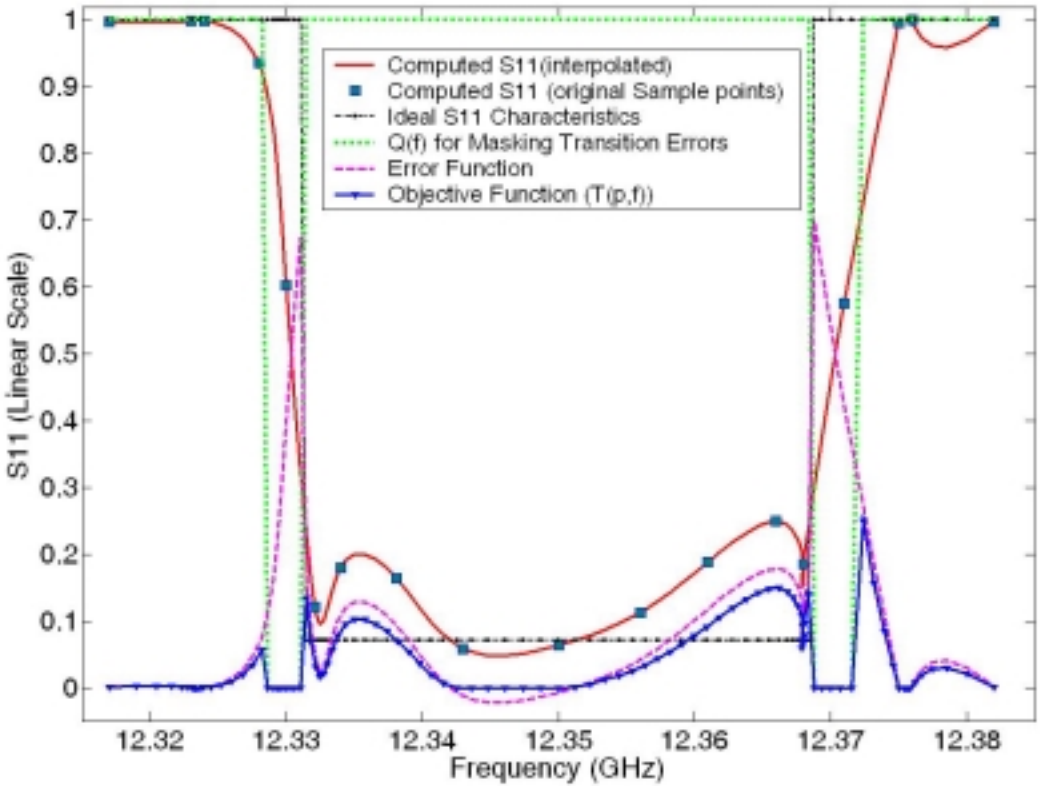

Fig. II.21. Different sub-functions of the $T_{ij}(f, \overline{p})$

II.7.5. Gradient approximation

These derivatives are calculated through finite differencing of the slightly perturbed parameterized objective function. A 2-D scheme of the finite differencing is shown in Fig. II.22.

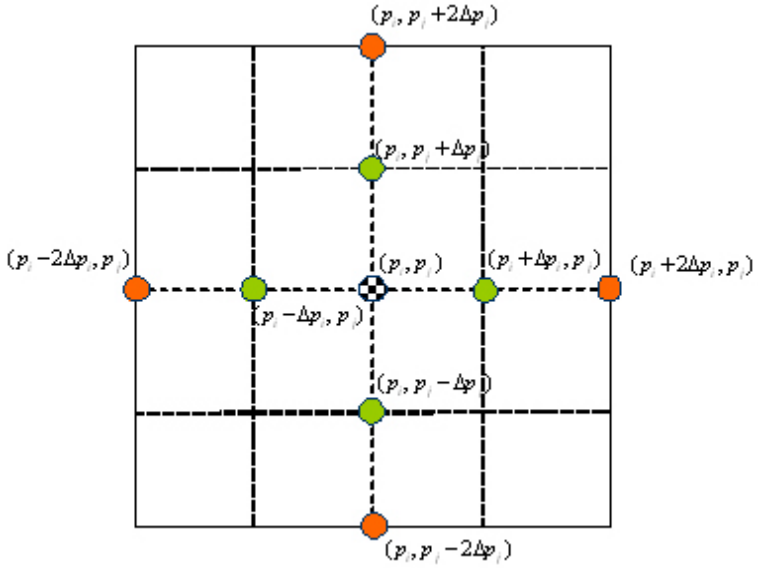

Fig. II.22. Calculating gradients by finite differencing

The central differenced approximation of the first and second derivatives of the function $T(p_1, p_2)$ can be calculated as follows,

$$\frac{\partial T(p_i, p_j)}{\partial p_i} = \frac{T(p_i + \Delta p_i) - T(p_i - \Delta p_i)}{2\Delta p_i} \qquad \text{(II- 98)}$$

$$\frac{\partial^2 T(p_i, p_j)}{\partial^2 p_i} = \frac{T(p_i + 2\Delta p_i, p_j) + T(p_i - 2\Delta p_i, p_j) - 2T(p_i - 2\Delta p_i, p_j)}{(2\Delta p_i)^2}$$

Thus for an N-dimensional parameter space, 2N computation of the (parameterized) objective function is required to calculate the first derivative. This makes the computation very ponderous with parameter spaces of high dimensionality. A stochastic method can be used for an accelerated gradient approximation **[85]**, **[86]**. To this end, the vector $\Delta_k \subset \mathbb{R}^N$ is defined as a vector of N mutually independent mean-zero random variables. It could be proven that in addition to specification of Δ_k series, $E\left|\Delta_k^{-1}\right| \prec L (L \in \mathbb{R})$ which implicitly precludes normal or uniform distribution of Δ_k. Now let define $y_{(.)}^{<k>}$ as,

$$y_{(+)}^{<k>} = T^{<k>}(\bar{p}^{<k>} + c_k \Delta_k) \qquad \text{(a)} \qquad \text{(II- 99)}$$

$$y_{(-)}^{<k>} = T^{<k>}(\bar{p}^{<k>} - c_k \Delta_k) \qquad \text{(b)}$$

whereas c_k is a positive scalar. Now, the gradient vector at iteration k could be defined as,

$$\nabla \tilde{T}^{<k>} = \left[\frac{y_{(+)}^{<k>} - y_{(-)}^{<k>}}{2c_k \Delta_{k1}} \quad . \quad . \quad , \quad \frac{y_{(+)}^{<k>} - y_{(-)}^{<k>}}{2c_k \Delta_{kN}} \right]^T \qquad \text{(II-100)}$$

where $\nabla \tilde{T}^{<k>}$ indicates the gradient vector obtained through simultaneous perturbations. The gradient approximation presented in (II-100) has the obvious advantage over the classical gradient that instead of *2N* computation of cost function, it just needs two calculations of cost function per iteration. To obtain a better accuracy, the gradient approximation in (II-100) is repeated *M* times where *M*<<*N* and then a more accurate gradient can be derived as,

$$\nabla T^{<k>} = 1/M \sum_{i=1}^{M} \nabla_i T^{<k>} \qquad \text{(II-101)}$$

while each of $\nabla_i T^{<k>}$ are obtained according to (II- 99) with a new randomly generated $\nabla T^{<k>}$ vector.

Once the coefficients are obtained, the polynomial is formed around each point $\bar{p}^{<k>}$ in the parameter space. There are different available algorithms for choosing the initial point $\bar{p}^{<0>}$. As proposed in **[72]**, the first few steps could be taken with an evolutionary (pseudo-random) method. A robust method could be using the parameterized model to have a coarse evaluation of the objective function over the entire or a major part of the parameter space. This parameterized model calculated in nominal point for the unperturbed geometry is not sufficiently precise to be the basis for optimization but it could approximately locate the global minimum.

II.7.5.1 The optimization algorithm

The gradient-based search is a well established strategy. Having calculated the variations of the S-parameters with respect to each parameter the first and second order derivatives are available. Here, a modified scheme is utilized which converges quadratically with an improved stability.

An iterative scheme which converges quadratically is utilized to find the optimum parameter set,

$$\bar{p}^{<k+1>} = \arg\min\left\{T(p^{<k>})\right\} \tag{II-102}$$

$\bar{p}^{<k>}$ is the base parameter vector at *k*th iteration. The optimum at each iteration is pursued around the base vector. The function $T(p^{<k>})$ is a quadratic function, as follows,

$$T^{<k>}(\bar{p}) = \sum_{r=1}^{M}\sum_{s=1}^{M} a_{rs}^{<k>}\, p_r^{<k>} p_s^{<k>} + \sum_{t=1}^{M} c_t^{<k>} p_t^{<k>} + d^{<k>} \tag{II-103}$$

The coefficients $a_{rs}^{<k>}$ and $c_t^{<k>}$ are derived using the derivatives of the objective function,

$$a_{rs}^{<k>} = \frac{1}{1+\delta_{rs}} \frac{\partial^2 T^{<k>}(\bar{p})}{\partial p_r^{<k>} \partial p_s^{<k>}} \tag{II-104}$$

(a)

$$c_t^{<k>} = \frac{\partial T^{<k>}(\bar{p})}{\partial p_t^{<k>}} - \sum_{u=1}^{M} (1+\delta_{ut}) a_{ut}^{<k>} . p_u^{<k>} \qquad \text{(b)}$$

and δ_{ij} is the Kronecker Delta function.

Let the vector of parameters at iteration k be $\bar{p}^k$, the error function could be expressed as a polynomial, as shown in (II-103). Then, the vector of parameter values at step *k+1* are chosen in such a way to minimize $T^{<k+1>}(\bar{p})$. The quadratic polynomial is calculated using first, second and cross derivatives of the objective function.

II.7.5.2 Discussion

Due to its quadratic behavior, the proposed search algorithm is definitely faster than steepest descent, but on the other hand the risks for divergence are considerable. Let the equation (II- 81) be represented in linear matrix format,

$$T^{<k>}(\bar{p}) = \bar{p}^{<k>T} . A^{<k>} . \bar{p}^{<k>} + C^{<k>T} . \bar{p}^{<k>} + d^{<k>} \qquad \text{(II-105)}$$

The matrix *A* is the Hessian. If the bowl represented by the quadratic form is convex, we can simply hop to its minimum:

$$\bar{p}_{opt}^{<k>} = -A_k^{-1} . C^{<k>} \qquad \text{(II-106)}$$

Since matrix *A* is a symmetric matrix, the only challenging point for its convexity is its being positive definite. Here we have used a scheme, originally inspired by Levenberg and Marquardt as a solution to nonlinear equations and optimization problems **[88]**.

Let us assume that matrix *A* is weakly indefinite in such a way that all its eigenvalues represented here as λ_i , *i=[1,...,M]* are positive and real except for one of them which possesses a small negative value.

Now let matrix $\tilde{A}$, be defined as,

$$\tilde{A}^k = \varepsilon_k I + A^k \qquad \text{(II-107)}$$

whereas ε_k is a small positive scalar and I is the identity matrix.

Now the sufficient condition for $\tilde{A}$ to be positive definite is that all its eigenvalues are positive and real. Given that the only non-positive eigenvalue is small enough not to dominate the positivity of the summation of eigenvalues, we can conclude

$$\sum_{i=1}^{N} \lambda_i^{New} = \sum_{i=1}^{N} \lambda_i^{Old} + N\varepsilon > 0 \tag{II-108}$$

The only remaining restriction would be to find the smallest value of ε_k in such a way that the product of the eigenvalues (det(A)) is positive. This leads to an inequality,

$$\prod_{i=1}^{N} \lambda_i^{New} = det\left(A(\varepsilon)\right) = h(\varepsilon) > 0 \tag{II-109}$$

where *h* is a nonlinear function. A linear approximation of (II-105) would yield:

$$\varepsilon \geq \frac{det(A)}{\sum_{i=1}^{N} \prod_{k=1, k\neq i}^{N} \lambda_k} \tag{II-110}$$

This algorithm applies for a broader class of problems with less level of certainty. For instance when there are more than one non-positive small eigenvalues subject to a positive sum of eigenvalues for the general case, equation (II-106) does not hold true.

II.7.5.3 Results

The results of optimization are presented in Fig. II.23. The optimization converged in four iterations. The final design parameters are given in Table IV. The chosen device is a classical case, which has been the subject of several studies, and can serve as an appropriate basis for comparison. The optimum dimensions and characteristics are compared with theoretical and experimental results in **[83]**, as depicted in Fig. II.24.

Parameter	Value (mm)
Length of input iris	9.2350
Length of iris 1-2	7.290
Length of iris 2-5	5.5500
Length of iris 3-4	7.2200
Length of output iris	9.2350
Length of screw 1-1	2.1525
Length of screw 2-2	2.1700
Length of screw 3-3	2.1950
Length of screw 4-4	2.5825
Length of screw 5-5	1.5165
Length of screw 2-3	0.7800
Length of screw 4-5	1.2500

Table IV. Final design parameters

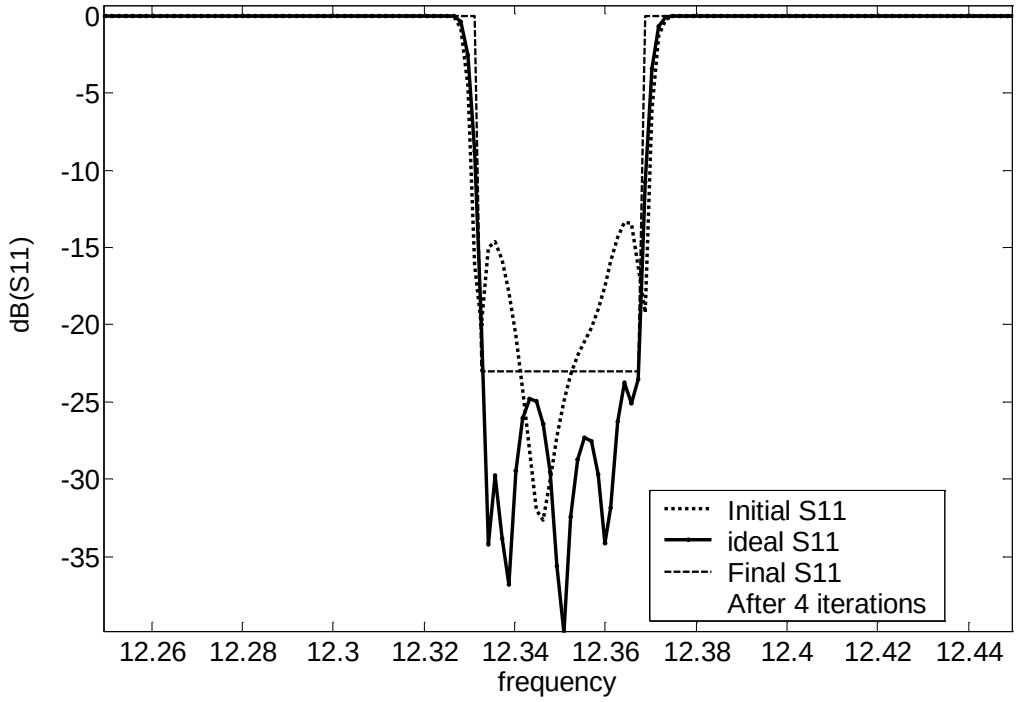

Fig. II.23. The different iterations

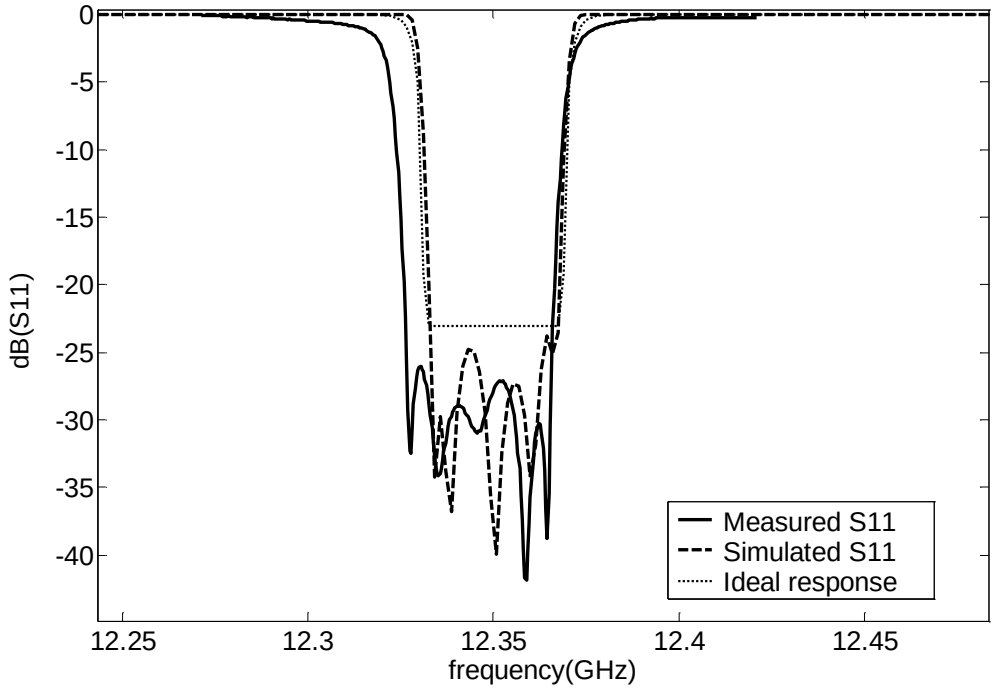

Fig. II.24. Comparison with the experimental results.

II.8. Conclusion

The parameterization of the electromagnetic behavior of microwave devices has been presented in this chapter. Within the context of optimization, three different parameters have been of premier interest, namely, frequency, geometry and mesh parameterization. Frequency parameterization has been discussed in a fair detail although it was not the main scope of this dissertation. Although using a frequency parameterized model can accelerate the optimization procedure, but in fact such a parameterized model does not affect the optimization procedure as a whole. In other words the parameterized model (with respect to frequency) can easily replace the classical EM model within an optimization cycle.

The main scope of the chapter has been to discuss geometrical parameterization of microwave devices. Due to the nature of the variations of the device performance to the changes in dimensions, a Taylor series featuring higher order derivatives has been used to parameterize the EM response of the structure. Unlike the frequency parameterization, the optimization procedure that uses geometrically parameterized model is fundamentally different from the classical optimization scheme. Using the geometrically parameterized model could create a shortcut in the cycle so that several numerical analysis of the device is avoided.

Finally mesh parameterization of the microwave devices is discussed in the chapter. Different possible techniques for describing a point in a grid in terms of the borders of the structure are discussed. Generalized Barycentric coordinates and mean value coordinates have been found to be the most viable approaches. The classical approach for such a purpose is to depict an analogy between the grid and mechanical systems such as a network of springs or solid body elasticity. For obvious reasons using derivatives of Barycentric coordinates is advantageous over mechanical analogy. Few algorithms have been implemented and the results are presented in this chapter.

The chapter ends with a detailed example. A 5-pole cylindrical cavity filter was chosen as a design example. The structure is optimized using a geometrically parameterized model. A mesh parameterization was also conducted in intermediate stages to give a fully integrated CAD model. The results of the optimization through geometrical parameterization seem to be quite satisfactory given that the optimization could converge to the satisfactory results in only four iterations for a 12 dimensional parameter space.

There are certain aspects of the work in this chapter which need to be ameliorated. The current geometrical parameterization can only consider one parameter at a time in a single frequency point. Parameterizing with respect to two or more variables with the current formulation ends up with an indecent accuracy. Furthermore the frequency and geometry parameterizations are done in separate steps. Having said that one is obliged to conduct the geometrical parameterization in discrete frequency point and then interpolate them. This, however can be avoided if a fully parameterized model (both with respect to geometry and frequency) is developed.

II.9. References

[1] L. T. Pillage and R. A. Rohrer, "Asymptotic waveform evaluation for timing analysis," *IEEE Trans. Computer-Aided Design*, vol. 9, pp. 352–366, Apr. 1990.

[2] Frédéric Thevenon, Application de la méthode des dérives d'ordre élevé dans la résolution de problèmes linéaires et non- linéaires, PhD Dissertation, INSA, November 2000.

[3] S. Kumashiro, R. A. Rohrer, and A. J. Strojwas, "Asymptotic waveform evaluation for transient analysis of 3-D interconnect structures," *IEEE Trans. Computer-Aided Design*, vol. 12, pp. 988–996, July 1993.

[4] K. Gallian, E. Grimme, and P. Van Dooren, "Asymptotic waveform evaluation via a Lanczos method," *Appl. Math. Lett.*, vol. 7, pp. 75–80, 1994.

[5] X. Yuan and Z. J. Cendes, "A fast method for computing the spectral response of electromagnetic circuits," presented at the APS/URSI Meeting, Ann Arbor, MI, 1993.

[6] E. J. Grimme, D.C. Sorensen, and P. Van Dooren, "Model reduction of state-space systems via an implicitly restarted," *Numer. Algorithms*, vol.12, pp. 1–32, Apr. 1996.

[7] K. Gallian, E. Grimme, and P. Van Dooren, "A rational Lanczos algorithm for model reduction," *Numer. Algorithms*, vol. 12, pp. 33–64, Apr. 1996.

[8] E. Chiprout and M. S. Nakhla, "Analysis of interconnect networks using complex frequency hopping (CFH)," *IEEE Trans. Computer-Aided Design*, vol. 14, pp. 186–200, Feb. 1995.

[9] P. Feldmann and R. W.Freund, "Efficient linear circuit analysis by Padé approximation via the Lanczos process," *IEEE Trans. Computer-Aided Design*, vol. 14, pp. 639-649, May 1995.

[10] M. Celik and A. C. Cangellaris, "Simulation of dispersive multiconductor transmision lines by Padé aproximation via the Lanczos process," *IEEE Trans. Microwave Theory Tech.*, vol. 44, pp. 2525-2535, Dec. 1996.

[11] R. W. Freund and P. Feldmann, "Reduced-order modeling of large linear passive multi-terminal circuits using matrix-Padé approximation," *Proc. Design Automat. Test Europe Conf.*, 1998, pp. 530-537.

[12] X. Zhang and J. Lee, "Application of the AWE method with the 3-D TVFEM to model spectral responses of passive microwave components," *IEEE Trans. Microwave Theory Tech.*, vol. 46, pp. 1735-1741, Nov. 1998.

[13] Z. Tingdong, S. L. Dvorak, J. L. Prince, "Characterization of electromagnetic systems using Pade/spl acute/ approximation with expansion at infinity," *IEEE Transactions on Advanced Packaging*, vol. 26, No. 4, pp.347- 352, November 2003

[14] L. Kulas, M. Mrozowski, "Macromodels in the frequency domain analysis of microwave resonators," IEEE *Microwave and Wireless Components Letters*, vol. 14, issue. 3pp. 94- 96, , March 2004

[15] J.Ureel, N.Fache, D.De Zutter, and P.Lagasse, "Adaptive frequency sampling algorithm of scattering parameters obtained by electromagnetic simulation," *IEEE AP-S Symp. Dig.*, pp. 1162-1167, 1994.

[16] S.Sakata, "Partial realization of 2-D discrete linear system and 2-D Pade´ approximation and reduction of 2-D rational transfer functions," *Proc. IEEE*, vol. 78, pp. 604-613, Apr. 1990.

[17] K.Kottopalli, T.Sarkar, Y.Hua, E.Miller, and G. J.Burke, "Accurate computation of wide-band response of electromagnetic systems utilizing narrow-band information," *IEEE Trans. Microwave Theory Tech.*, vol. 39, pp. 682-687, Apr. 1991.

[18] Padé approximation and its applications, Bad Honnef, 1983 : proceedings of a conference held at Bad Honnef, Germany, March 7-10, 1983 / edited by H. Werner and H.J. Bünger.

[19] J. Stoer and R. Bulirsch, *Introduction to Numerical Analysis.* Berlin, Germany: Springer-Verlag, 1980, sec. 2.2.

[20] A. Gati, M. F. Wong, V. Fouad Hanna,"New technique using poles and modes derivatives for frequency and geometry parameterization of microwave structure," *Proceedings of International Microwave Symposium* IMS2001, pp.1019-1022, June 2001.

[21] W. H. Press, B. P. Flannery, S. A. Teukolsky and T. Vetterling, *Numerical Recipes, The Art of Scientific Computing*, Cambridge, UK, Cambridge University Press, 1989.

[22] BERZ, M. Differential algebraic description of beam dynamics to very high orders. Particle Accelerators 24, 2 (1989), 109-124.

[23] CHRmT~A~SON, B. Automatic hessians by reverse accumulation. IMA g Numer. Anal. To appear.

[24] GERTH, J. A., AND ORTH, D.L. Indexing and merging in APL APL88--APL Quote Quad. 18, 2 (Dec. 1987), 156-161.

[25] GRIEWANK, A. On automatic differentiation. In Mathematical Programming: Recent Developments and Applications, M. Iri, and K. Tanabe, Eds. Kluwer, Amsterdam, 1989, 83-108.

[26] IRI, M. Simultaneous computation of functions, partial derivatives and estimates of rounding errors--Complexity and practicality. Japan J. Appl. Math. 1, 2 (1984), 223-252.

[27] R H F Jackson , G P McCormick, The polyadic structure of factorable function tensors with applications to high-order minimization techniques, Journal of Optimization Theory and Applications, v.51 n.1, p.63-94, Oct. 1986

[28] H Kagiwada, Numerical derivatives and nonlinear analysis, Plenum Press, New York, NY, 1986

[29] KALABA, R., TESFATSION, L., AND WAN~, J.-L. A finite algorithm for the exact evaluation of higher order partial derivatives of functions of many variables. J. Math. Anal. Appl. 92, 2 (1983), 552-563.

[30] Gershon Kedem, Automatic Differentiation of Computer Programs, ACM Transactions on Mathematical Software (TOMS), v.6 n.2, p.150-165, June 1980

[31] MOORE, R.E. Methods and Applications of Interval Analysis. SIAM Studies in Applied Mathematics 2, SIAM, Philadelphia, Pa., 1979, 24-31.

[32] RALL, L.B. The arithmetic of differentiation. Math. Mag. 59, 5 (Dec. 1986), 275-282.

[33] RALL, L. B. Automatic Differentiation: Techniques and Applications. Lecture Notes in Computer Science 120, Springer-Verlag, New York, 1981.

[34] L B. Rall, Differentiation in PASCAL-SC: type GRADIENT, ACM Transactions on Mathematical Software (TOMS), v.10 n.2, p.161-184, June 1984

[35] R. E. Wengert, A simple automatic derivative evaluation program, Communications of the ACM, v.7 n.8, p.463-464, Aug. 1964

[36] Anthony S. Wexler, An algorithm for exact evaluation of multivariate functions and their derivatives to any order, Computational Statistics & Data Analysis, v.6 n.1, p.1-6, Jan. 1988

[37] Anthony S. Wexler, Automatic evaluation of derivatives, Applied Mathematics and Computation, v.24 n.1, p.19-46, Oct. 1987

[38] A. Mahanfar, S. Bila, M. Aubourg and S. verdeyme, "Mesh deformation techniques for optimization of microwave devices," *IEEE conference on Antennas and Propagation*, Columbus, June 2002.

[39] Pascal Jean Frey and Paul Louis George: Mesh Generation. Hermes Science Publishing, Oxford, Paris

[40] Paul-Louis George: Automatic mesh generation: Applications to Finite Element Methods. John Wiley, 1991.

[41] J. T. Batania. Unsteady euler algorithm with unstructured dynamic mesh for complex aircraft aeroelastic analysis," proceedings of AIAA-89-1189, Monteray, July 1989.

[42] F. J. Blom, "Considerations on the spring analogy," International Journal of Numerical methods in Fluids, vol. 32, pp. 647-668, 2000.

[43] P. L. George, Äutomatic mesh generation,"Ch. 7, John Wiley , Paris, 1991.

[44] T. Baker, "Mesh movement and metamorphosis," proceedings of 10th international meshing roundtable, Newport Beach, CA, 2001.

[45] B. Helenbrook, "mesh deformation using the biharmonic operator,"Int. journal for Numerical methods in Engineering, 2001.

[46] D. Lynch and K. O'Neil, "Elastic grid deformation for moving boundary problems in two space dimensions," in *Finite Elements in Water resources*, University of Mississippi Press, 1980.

[47] E. Wachpress, *A rational finite-element basis*, manuscript, 1975

[48] M. Meyer, H. Lee, A. Barr, M. Desburn, "Generalized Barycentric coordinates on irregular polygons,"_*Journal of Graphics Tools 2002, Volume 7, Issue 1, pages 13-22*.

[49] Mathieu Desbrun, Mark Meyer, and Pierre Alliez. Intrinsic Parameterizations of Surface Meshes. In *Eurographics '02 Proceedings*, 2002.

[50] Mathieu Desbrun, Mark Meyer, Peter Schroder, and Alan Barr. Implicit Fairing of Arbitrary Meshes using Laplacian and Curvature Flow. In *ACM SIGGRAPH'99 Proceedings*, pages 317–324, 1999.

[51] Matthias Eck, Tony DeRose, Tom Duchamp, Hugues Hoppe, Michael Lounsbery, and Werner Stuetzle. Interactive Multiresolution Surface Viewing. In *ACM Siggraph'95 Conference*, pages 91–98, August 1995.

[52] Michael S. Floater. Parametrization and smooth approximation of surface triangulations. *Computer Aided Geometry Desing*,14(3):231–250, 1997.

[53] Michael S. Floater. Parametric Tilings and Scattered Data Approximation. *International Journal of Shape Modeling*, 4:165–182, 1998.

[54] S. Kuriyama. Surface Generation from an Irregular Network of Parametric Curves. *Modeling in Computer Graphics, IFIP Serieson Computer Graphics*, pages 256–274, 1993.

[55] Charles Loop and Tony DeRose. A multisided generalization of B'ezier surfaces. *ACM Transactions on Graphics*, 8:204–234, 1989.

[56] S. Lodha. Filling N-sided Holes. *Modeling in Computer Graphics, IFIP Series on Computer Graphics*, pages 319–345, 1993.

[57] Ulrich Pinkall and Konrad Polthier. Computing Discrete Minimal Surfaces and Their Conjugates. *Experimental Mathematics*, 2:15–36, 1993.

[58] Pascal Volino and Nadia Magnenat-Thalmann. The SPHERIGON: A Simple Polygon Patch for Smoothing Quickly your Polygonal Meshes. In *Computer Animation '98 Proceedings*, 1998.

[59] Joe Warren. Barycentric Coordinates for Convex Polytopes. *Advances in Computational Mathematics*, 6:97–108, 1996.

[60] M. Eck, T. DeRose, T. Duchamp, H. Hoppe, M. Lounsbery, and W. Stuetzle, Multires- solution analysis of arbitrary meshes, Computer Graphics Proceedings, SIGGRAPH 95 (1995), 173-182.

[61] M. S. Floater, Parametrization and smooth approximation of surface triangulations, Comp. Aided Geom. Design 14 (1997), 231-250.

[62] M. S. Floater, Parametric tilings and scattered data approximation, Intern. J. Shape Modeling 4 (1998), 165-182.

[63] M. S. Floater and C. Gotsman, How to morph tilings injectively, J. Comp. Appl. Math. 101 (1999), 117-129.

[64] C. Gotsman and V. Surazhsky, Guaranteed intersection-free polygon morphing, Com- puters and Graphics 25-1 (2001), 67-75.

[65] A. Iserles, A rst course in numerical analysis of differential equations, Cambridge University Press, 1996.

[66] C. Loop and T. DeRose, A multisided generalization of Bezier surfaces, ACM Trans. Graph. 8 (1989), 204-234.

[67] M. Meyer, H. Lee, A. Barr, and M. Desbrun, Generalizing Barycentric coordinates to irregular n-gons, preprint, Caltech, 2001.

[68] FLOATER M., KOS G., REIMERS M.: Mean value coordinates in 3d. *To appear in CAGD* (2005).

[69] J. Warren, Barycentric coordinates for convex polytopes, Adv. Comp. Math.

[70] Warren J., Schaefer S., Hirani A. and Desbrun M., "Barycentric coordinates for convex sets" To appear(2005).

[71] J.W.Bandler, "Optimization Methods for Computer-Aided Design," IEEE Trans on Microwav Theory Tech., Vol. MTT-17, pp. 533 - 552, Aug 1969.

[72] J.W.Bandler, Q.S.Cheng, S.A.Dakroury, A.S.Mohamed, M.H.Bakr, K.Madsen, J.Sondergaard, "Space Mapping: the State of the Art," IEEE Trans. Microwave Theory Tech., Vol. MTT-52, pp. 337 - 361, Jan. 2004.

[73] J.M.Johnson, Y.Rahmat-Samii, "Genetic Algorithms in Engineering Electromagnetics", IEEE Antennas Propagat. Mag., Vol. AP-39, pp. 7 – 21, Aug 1997.

[74] J.W.Bandler, R.M.Biernacki, C.Shao-Hua, L.W.Hendrick, D.Omeragic, "Electromagnetic Optimization of 3-D Structures", IEEE Trans. Microwave Theory Tech., Vol. MTT-45, pp. 770 – 779, May 1997.

[75] J.W.Bandler, S.H.Chen, S.Daijavad, K.Madsen, "Efficient optimization with integrated gradient approximations," IEEE Trans. Microwave Theory Tech., Vol. MTT-36, pp. 444-454, Feb. 1988.

[76] P.Harscher, S.Amari, R.Vahldieck, "A fast finite-element-based field optimizer using analytically calculated gradients," IEEE Trans. Microwave Theory Tech., Vol. MTT-50, pp. 433 – 439, Feb. 2002

[77] R.Safian, N.K.Nikolova, M.H.Bakr, J.W.Bandler, "Feasible Adjoint Sensitivity Technique for EM Design Exploiting Broyden's Update," in Proc. of International Microwave Symp., pp. 299 – 302, June 2003.

[78] N. K. Nikolova, J. W. Bandler, M.H. Bakr, "Adjoint Techniques for Sensitivity Analysis in High-frequency Structure CAD," IEEE Trans. Microwave Theory Tech., Vol. MTT-52, pp. 403 – 419, Jan. 2004.

[79] Description Of the structure_Example1

[80] R. J. Cameron, "General coupling matrix synthesis methods for Chebyshev filtering functions," IEEE Trans. Microwave Theory Tech., vol. 47, pp. 433-442, Apr. 1999.

[81] E.Atia and A. E.Williams, “Narrow-bandpass waveguide filters,” IEEE Trans. Microwave Theory Tech., vol. MTT-20, pp. 258-265, Apr. 1972.

[82] A.Mahanfar, S.Bila, M.Aubourg, S.Verdeyme, “Mesh Deformation Techniques for Geometrical Optimization of Microwave Devices,” in Proc. IEEE Antennas Propagat. Int. Symp., pp. 56 – 59, June 2003

[83] B.Thon, D.Bariant, S.Bila, D.Baillargeat, M.Aubourg, S.Verdeyme, P.Guillon, F.Thevenon, M.Rochette, J.Puech, L.Lapierre, J.Sombrin, “Coupled Pade approximation-finite element method applied to microwave device design,” in Proc. IEEE Int. Microwave Symp., pp. 1889 – 1892, June 2002.

[84] S.Bila; D.Baillargeat, M.Aubourg, S.Verdeyme, F.Seyfert, L.Baratchart, C.Boichon, F.Thevenon, J.Puech, C.Zanchi, L.Lapierre, J.Sombrin, ”Finite-element modeling for the design optimization of microwave filters,” IEEE Trans. on Magnetics, Vol. 40, pp. 1472 – 1475, Mar 2004.

[85] W.A.Atia, K.A.Zaki, A.E.Atia, “Synthesis of general topology multiple coupled resonator filters by optimization,” in Proc of Int. Microwave Symp., Vol. 2, pp. 821 – 824, June 1998.

[86] D. C.Chin, “Comparative study of stochastic approximation algorithms for system optimization based on gradient approximations,” IEEE Trans. Syst., Man, and Cybern., vol. 27, pp. 244-249, 1997.

[87] J. C.Spall, “Multivariate stochastic approximation using a simultaneous perturbation gradient approximation,” IEEE Trans. Automat. Contr., vol. 37, pp. 332-341, Mar. 1992.

[88] D.G.Luenburger, 1984, Linear and Nonlinear Programming: Addison-Wesley Publishing Company, Reading, Mass.

[89] De Boor, C. 1978, *A Practical Guide to Splines* (New York: Springer-Verlag).

CHAPTER III

Evolutionary Algorithms for EM-based Optimization

III.1. Introduction

Improving optimization techniques yet has another aspect other than efficiency. In addition to the speed of the optimization technique, autonomy is an important issue which should not be neglected. As far as the modification of a given component is concerned, a key point is the development of microwave CAD environments where the component is modified automatically by the microwave tool itself with an improvement of the component performances without any contribution by the designer. The methods studied so far have been local methods. The search algorithms, no matter how fast and accurate, were bound around the closest (local) minimum point. Thus the appropriate choice of the initial point has a significant role in the success of these methods. If, for any reason the automated algorithm is trapped in a local minimum, then the operator should restart the procedure with a different initial point.

In fact optimization techniques can be classified into two groups, gradient and stochastic methods. Gradient methods have been discussed so far. Evolutionary algorithms are a subset of stochastic methods which mimic the search process of natural evolution. This class of optimization algorithms relies on the collective learning process within a population of individuals, each of which represents a search point in the space of potential solutions to the given problem. Because of an implicit parallelism in the search behavior they avoid the common pitfalls of local minimization algorithms, but hold the promise of finding novel solutions perhaps not thought to exist.

Perhaps the best known evolutionary method so far is the genetic algorithm (GA) [1]-[4]. This algorithm has been utilized in a wide variety of applications in electromagnetic domain. The design of microwave passive devices using genetic algorithm is presented in [5]-[9]. In [6] the potentials of an evolutionary algorithm to create unknown planar topologies has been discovered. [5] and [8] report the use of genetic algorithm for the design of waveguide filters. There are various applications such as equivalent circuit parameter extraction (see for example, [10] and [13]), microwave absorber design [15], and material characterization [12]. Perhaps the majority of the work on use of genetic algorithms in electromagnetic domain has been reported in antenna design. References [15]-[21] represent some of the previous work

done in antenna design. Despite the mentioned advantage of the genetic algorithms, the major problem with genetic algorithm and evolutionary methods in general, is their high computational cost. Even for a simple design problem, an evolutionary design has to go through many iterations which make them impractical for most of applications. In fact evolutionary algorithms look for optima in the points that was not expected. But obviously such a mindless search can not be cost-free. The price paid for lack of intelligence is the exponential increase in time for optimum search. Here comes a compromise in mind: to add a sort of intelligence to these methods. This can be achieved through combining evolutionary methods with gradient methods. Such a "hybrid" technique will use the evolutionary technique to localize the global optimum point, then the gradient method can chase the optimum point more efficiently. Such a technique looks straightforward. The only issue will then be how and when to integrate these two methods, *i.e.* to find a method to distinguish the time, when the optimum point has been localized is not very trivial.

Particle Swarm Optimization (PSO) is relatively a new approach which is aiming the global optimum search in a more intelligent manner. The method is similar to GA in that both are stochastic in principle, and both use an analogy to real life behaviors. The major distinction of PSO is that in PSO the randomly initiated population of parameter vectors learn about each other "successes". Such a feature can drastically accelerate the stochastic algorithm.

In this chapter evolutionary optimization of microwave components is presented. Genetic algorithm is already a well established technique in device optimization. Thus the core of the chapter deals with the Particle Swarm Optimization (PSO). But to understand well the advantages of PSO, a general preview of GA is essential. This issue is addressed in the next section, followed by an example application. Section 3 explains the principles of PSO method. In Section 4 an example design is explained using PSO. The three proceeding sections more profoundly explore the features and potentials of PSO. Finally the chapter ends by few design examples using PSO technique.

III.2. Genetic algorithm for the optimization of microwave devices

Genetic-algorithm optimizers are a group of search methods which function on the basis of natural selection and evolution. The global nature of the search mechanism allows its being utilized in complicated problems when there is no, or a little knowledge about initial structure. Some important terminology and concepts of GA optimizers are presented in a sidebar. This section presents the basic elements of a genetic-algorithm optimizer.

III.2.1. Terminology

As mentioned earlier the genetic algorithms work on the basis of the concept of natural evolution through generations. Thus it is imperative to use the original terminology where the concept has been borrowed from. This also helps developing the algorithm in a more heuristic manner.

Population – A set of parameter vectors. Any population is a subset of parameter space.

Generation –Successively created populations; the population created at each iteration.

Fitness – The value of the objective function belonging to each individual (parameter vector).

Parent – A parameter vector (an individual) belonging to the current generation (iteration) which is chosen (through a criteria) to contribute in generation of the next generation.

Child – Parameter vector (an individual) belonging to the next generation.

Chromosome – Coded form of the features carried in a parameter vector, these feature are partially transferred from a parent to its child through an evolution.

III.2.2. Description of the algorithm

The block diagram of genetic algorithm optimization procedure is depicted in Fig.1. Many different variations of this simple algorithm have been suggested but the core idea remains the same.

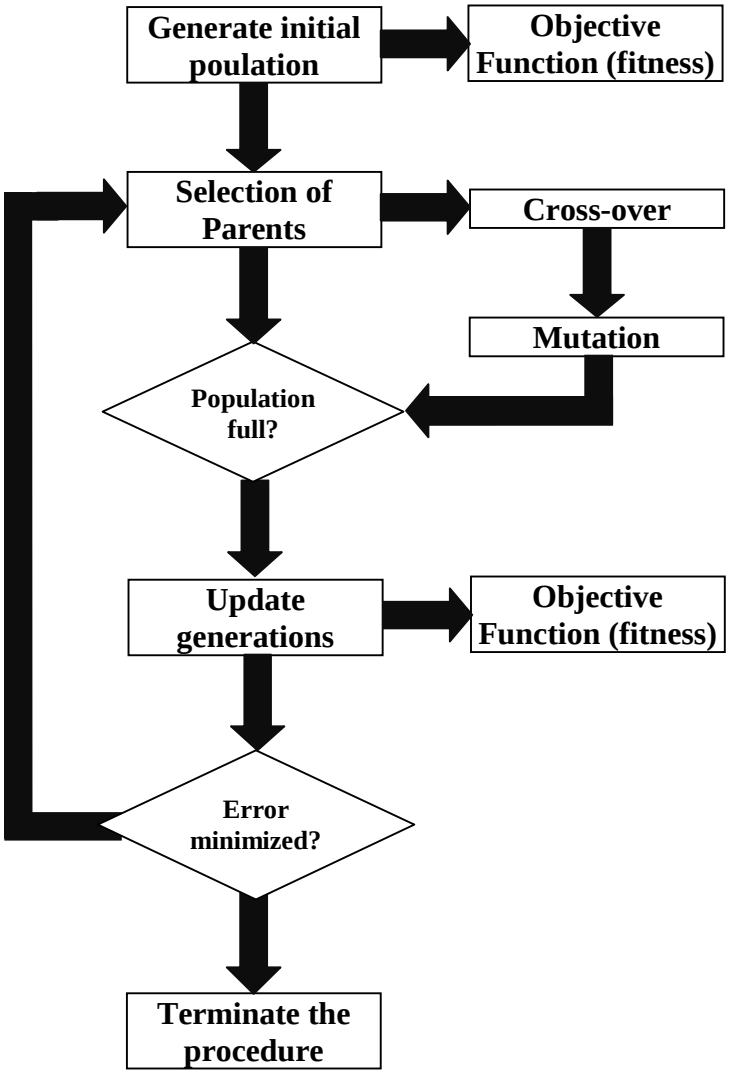

Fig. III.1. The block diagram of basic Genetic Algorithm

In general, a GA iteratively runs the procedure shown bellow until the ending criteria is met,

1. Generate the initial population. This population is a subset of the parameter space. In principle such population can be generated arbitrarily, although incorporating some intelligence in generating this population would help the speed.
2. Define genes based on the features that contribute significantly the objective function.
3. Create a string of the genes to form a chromosome.
4. Evaluate fitness values (objective function) to each parameter vector in the population.

5. Perform reproduction through the fitness-weighted selection of individuals from the population.
6. Conduct reproduction operators (crossover, mutation, and recombination) to produce the next generation.

In the simple, typical genetic algorithm shown in Fig. 1, initialization consists of filling an initial population with a predetermined number randomly created, parameter strings (chromosomes). Each of these chromosomes represents an individual prototype solution or, simply, an *individual.* The set of individuals is called the current generation. Each individual in the set is assigned a fitness value by evaluating the fitness function for each individual.

In reproduction, a pair of individuals is selected from the population to act as parents. The parents produce a pair of children. Note that in order to keep the population of each generation, the every couple of parents should produce two children. These children are then placed in the new generation. The selection, crossover, and mutation operations are repeated until enough children have been generated to fill the new generation. In some GA available in literature, the algorithm is slightly varied. Selection is used to fill the new generation, and then crossover and mutation are applied to the individuals in the new generation, through random pairings. In either case, the new generation replaces the old generation. In the simple genetic algorithm presented here, the new generation is the same size as, and completely replaces, the current generation. This is known as a *generational* GA. Furthermore, the new generation can be of a different size than its predecessor.

Another variation of genetic algorithm, often called *steady-state* genetic algorithms, incorporates some overlap between the new generation and the old generation. In the generation-replacement phase, the new generation replaces the current generation, and fitness values are evaluated for and assigned to each of the new individuals. The termination criterion is then evaluated and, if it has not been met, the reproduction process is repeated.

III.2.3. Regeneration mechanisms

Having defined the general infrastructure of the genetic algorithm, now, we will try to set some details. The two main mechanisms of any GA are

1- The way a population is formed,

2- The mechanism of producing a child by a couple of parents (genetic operators).

In this section these two mechanisms are discussed in detail, knowing that there are several other variations which are not covered in here, mostly because it has not been the main focus of the present work.

III.2.3.1. Forming a population

As mentioned earlier, a population is a set of individuals, or parameter vectors, which is used to form a generation. There are different mechanisms under an individual (parameter vector) is chosen among a population to be considered as a parent. Different mechanisms are used to judge about an individual's being eligible to be included inside a population. But all these criteria are based on the fitness value. However, selection cannot be based solely on choosing the best individual, because the best individual may not be very close to the optimal solution. Instead, some chance that relatively unfit individuals are selected must be preserved, to ensure that genes carried by these unfit individuals are not "lost" prematurely from the population. In general, selection involves a mechanism relating an individual's fitness to the average fitness of the population. A number of selection strategies have been developed and utilized for GA optimization. These strategies are generally classified as either stochastic or deterministic. Usually, selection results in the choice of parents for participation in the reproduction process. The three main strategies to form a population are decimation, proportionate selection and tournament selection. Several of the more important and most widely used of these selection strategies are discussed below

III.2.3.1.1. Decimation

The simplest of the deterministic strategies is population decimation. In population decimation, individuals are ranked according to their fitness values. An arbitrary minimum fitness is chosen as a cutoff point, and any individual with a lower fitness than the minimum is removed from the population. The remaining individuals are then used to generate the new generation through random pairing. The pairing and application of GA operators are repeated until the new generation is filled.

The advantage of population-decimation selection lies in its simplicity. All that is required is to determine which individuals are fit enough to remain in the population,

and to then provide a means for randomly pairing the individuals that survive the decimation process. The disadvantage of population decimation is that once an individual has been removed from the population, any unique characteristic of the population possessed by that individual is lost.

This loss of diversity is a natural consequence of all successful evolutionary strategies. However, in population decimation, the loss can, and often does, occur long before the beneficial effects of a unique characteristic are recognized by the evolutionary process. The normal action of the genetic algorithm is to combine good individuals with certain characteristics to produce better. Unfortunately, good traits may not be directly associated with the best fitness in the early stages of evolution toward an optimal solution. Fig. 2. shows a simple scheme of decimation.

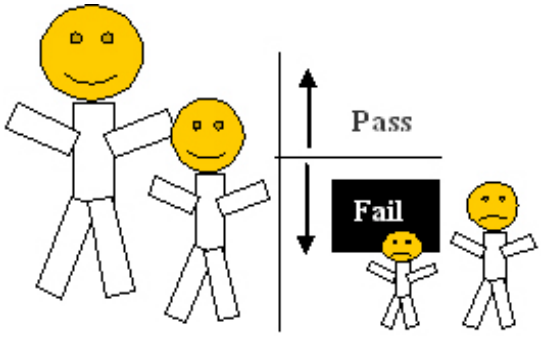

Fig. III.2. Decimation

III.2.3.1.2. Proportionate selection

Individuals can be selected based on a probability of selection as bellow

$$\rho = \frac{T(\overline{p}_i^{<k>})}{\sum_{i=1}^{N_p} T(\overline{p}_i^{<k>})} \qquad \text{(III- 1)}$$

where $T(\overline{p}_i^{<k>})$ is the fitness of the *i*th parent at *k*th generation. The probability of selecting an individual from the population is purely a function of the relative fitness of the individual. Individuals with high fitness will participate in the creation of the next generation more often than less-fit individuals. This has the same effect as the removal of the least fit in population decimation, in that characteristics associated with higher fitness are represented more in subsequent generations. The distinction between population decimation and proportionate selection is that in proportionate selection, there is still a finite probability that highly unfit individuals will participate in at least some of the matings, thereby preserving their genetic information. Proportionate selection is further illustrated in Fig. 3.

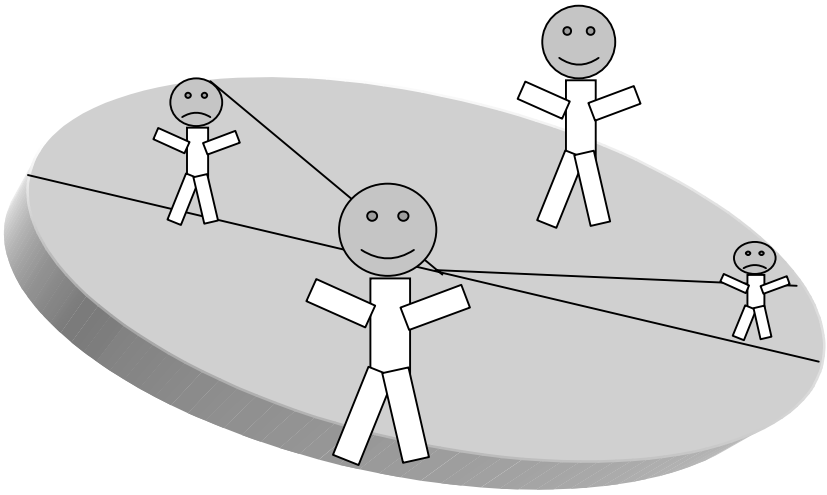

Fig. III.3. Proportionate Selection

III.2.3.1.3. Tournament selection

A second popular strategy (and perhaps among the most effective for many applications) is tournament selection. Tournament selection is depicted in Fig. 4. In tournament selection, a subset of the population of N_p individuals is chosen at random from the population. The individuals of this sub-population compete on the basis of their fitness. The individual in the sub-population with the highest fitness wins the tournament, and becomes the selected individual. All of the sub-population members are then placed back into the general population, and the process is repeated. The most commonly used form of tournament selection is binary tournament selection, ($N_p = 2$).

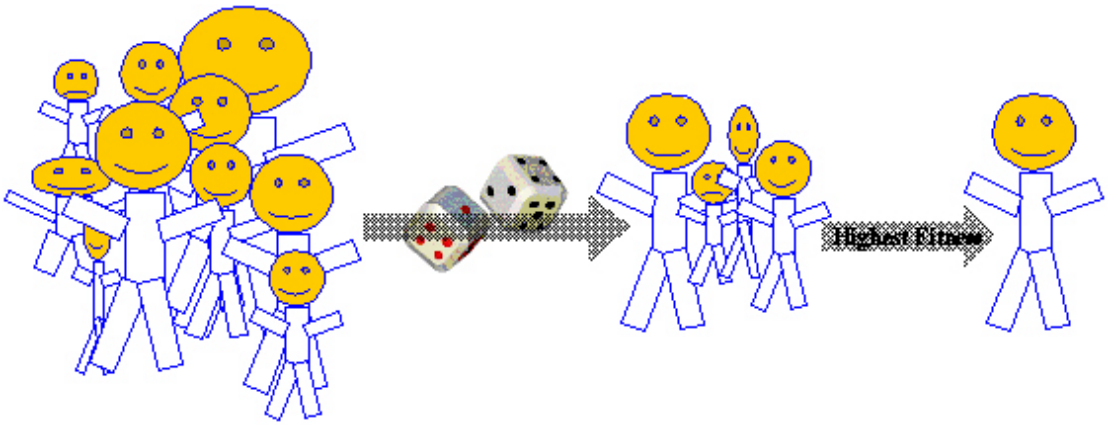

Fig. III.4. Tournament selection

III.2.3.2. Genetic operators

The way the features of the parents from one generation are transferred to the successors is also very significant in the genetic conception.

Once a pair of individuals has been selected as parents, a pair of children is created by recombining and mutating, the chromosomes of the parents, utilizing the basic genetic-algorithm operators, crossover and mutation.

A probability is assigned to each of these operators. The assigned probability is then compared to $\rho^{<k>}$ a normalized random number at *k*th iteration. If the random number is bigger than the assigned operator probability, the operator will be effective, and otherwise ignored.

III.2.3.2.1. Mutation

In genetic algorithms, mutation is a genetic operator used to maintain genetic diversity from one generation of a population of chromosomes to the next. It is analogous to biological mutation.

The classic example of a mutation operator involves a probability that an arbitrary bit in a genetic sequence will be changed from its original state. A common method of implementing the mutation operator involves generating a random variable for each bit in a sequence. This random variable tells whether or not a particular bit will be modified.

The purpose of mutation in genetic algorithms is to allow the algorithm to avoid local minima by preventing the population of chromosomes from becoming too similar to each other, thus slowing or even stopping evolution. This reasoning also explains the fact that most GA systems avoid only taking the fittest of the population in generating the next but rather a random (or semi-random) selection with a weighting toward those that are more fit.

In mutation, if $\rho^{<k>} > \rho_{mutation}$, an element in the string making up the chromosome is randomly selected and changed. In the case of binary coding, this amounts to selecting a bit from the chromosome string and inverting it. In other words, a "1" becomes a "0" and a "0" becomes a "1." If higher order alphabets are used, slightly more complicated forms of mutation are required.

Generally, it has been shown that mutation should occur with a low probability, usually on the order of $\rho_{mutation} = 0.01 - 0.1$. Fig. 5. shows a randomly selected

element in a chromosome (shaded element) being changed to a new form (0 → 1 and 1 → 0 in the binary case).

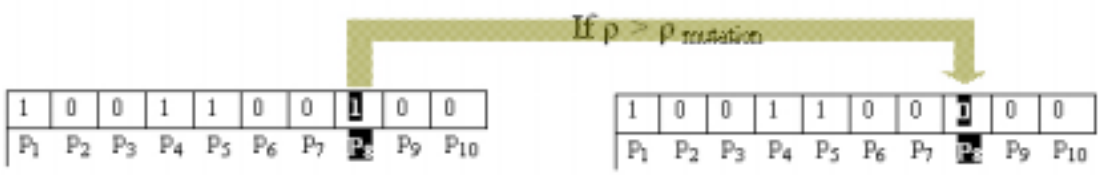

Fig. III.5. Mutation

III.2.3.2.2. Crossover

The crossover operator accepts the parents and generates two children. Many variations of crossover have been developed. The simplest of these is single-point crossover. In single-point crossover, shown in Fig. 6, if $\rho^{<k>} > \rho_{crossover}$ a random location in the parent's chromosomes is selected. The portion of the chromosome preceding the selected point is copied from parent number 1 to child number 1, and from parent number 2 to child number 2. The portion of the chromosome of parent number 1 following the randomly selected point is placed in the corresponding positions in child number 2, and vice versa for the remaining portion of parent number 2's chromosome. If $\rho^{<k>} < \rho_{crossover}$, the entire chromosome of parent number 1 is copied into child number 1, and similarly for parent number 2 and child number 2.

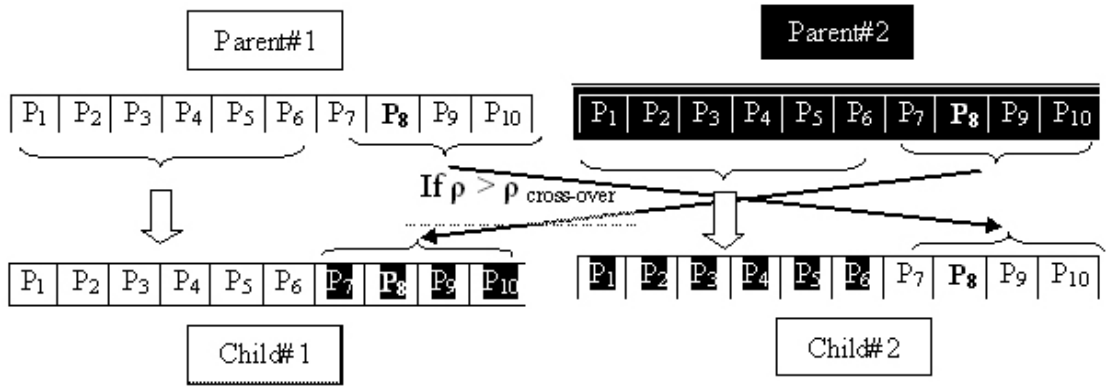

Fig. III.6. Cross-Over

The effect of crossover is to rearrange the genes, with the objective of producing better combinations of genes, thereby resulting in more fit individuals. It has been shown [6] that the recombination process is the more important of the two GA operators. Typically, it has been found that probability $\rho_{crossover}$ values of 0.6-0.8 are optimal.

III.2.4. Fitness functions

The fitness function, or object function, is used to assign a fitness value to each of the individuals in the GA population. The fitness function is the only connection between the physical problem being optimized and the genetic algorithm. The only constraints on the form and content of the fitness function, imposed by the simple GA, are that:

1 the fitness value returned by the fitness function is in some manner proportional to the *goodness* of a given trial solution, and
2 the fitness be a positive value. In some implementations of the GA optimizer, the constraint that the fitness value be a positive value is not even required.

Genetic algorithms are maximizers by nature. To find a minimum, a slight modification to the usual functional form is required. It can be either taking the inverse of the fitness function or the subtracting it from a number

III.2.5. Example- Optimization of a coupled line filter

Coupled line filters have always been appropriate gauges for optimization techniques. It is partially due to their flexibility in design parameters as well as their versatile frequency characteristics. They are also easy to manipulate and thus appropriate for model validation.

III.2.5.1. Description of the structure

The structure used is a coupled line filter, as shown in the Fig. 7. The structure consists of five line segments connecting the two ports. All the lines have aimed to have the same length. The substrate is chosen as Rogers RO4350 [22] material with 20 mil thickness (0.787 mm). The dielectric constant of the substrate is 3.38 with the loss tangent of 0.004.

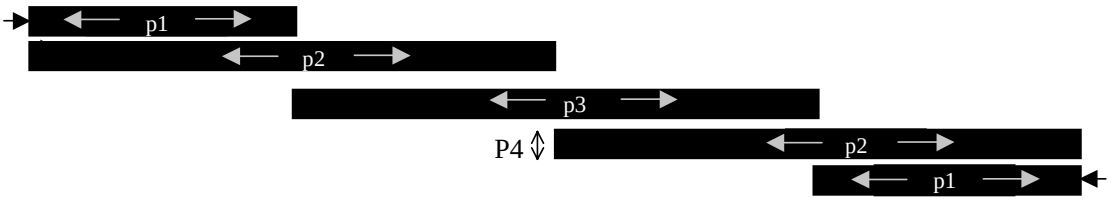

Fig. III.7. The coupled line filter

III.2.5.2. The design goal

The goal is to design an ultra-wideband mask filter with a 3-dB pass-band from 3.1 GHz to 10.6 GHz. Such a mask is utilized to assure that the transmitted signal would comply with FCC regulations. The desired in-band insertion loss was less than 1 dB and an out-band rejection of 25 dB has been targeted.

III.2.5.3. The design variables

The parameters chosen for this optimization practice are the length of the segments and the width of the lines. The parameters are shown in Fig. 7. The initial parameter set, was generated randomly. This parameter set is presented in Table III.1. Also the initial response resulted from this initial set of design variable is presented in Fig. III.8.

Parameter	Value(mm)
p	7.10
p	15.00
p	18.02
p	0.23

Table III.1. The initial parameter set for the Example 1.

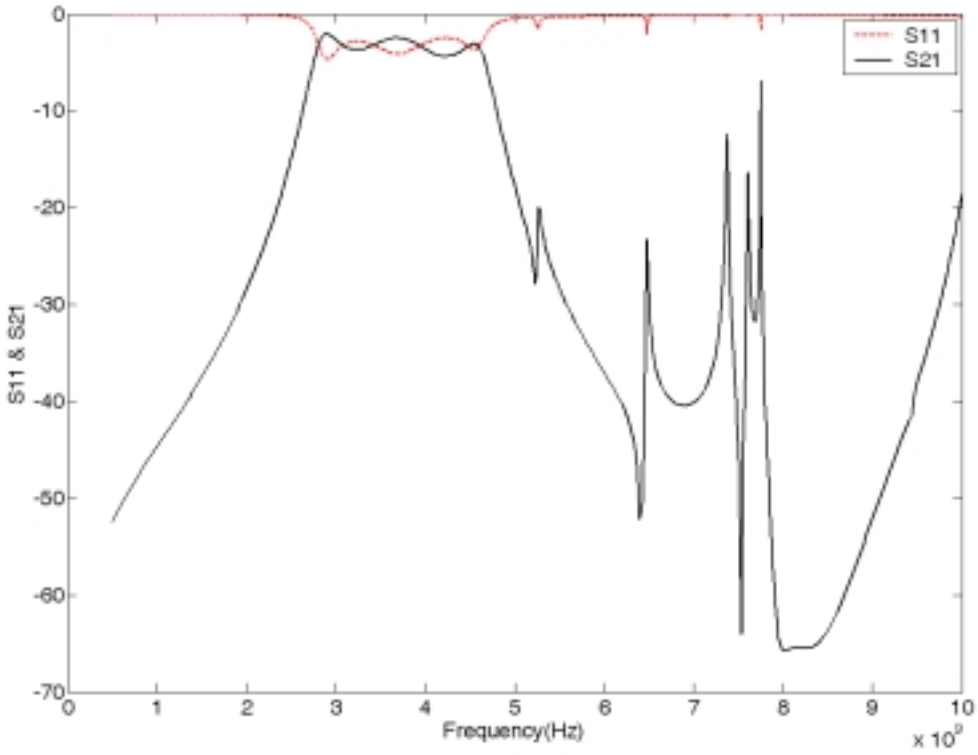

Fig. III.8. The initial coupled line filter response

III.2.5.4. The methodology

The original genetic algorithm was used to optimize the structure. The initial parameter set has been chosen randomly. In order to minimize the computation cost, two symmetry planes along with x-and y-axes have been considered, dividing the number of parameter into a quarter.

III.2.5.5. Implementation

The Momentum™ package has been used as the electromagnetic field solver. Momentum uses the Method of Moments to compute S-parameters.
The optimization algorithm, was developed using AEL, the language used by Advanced Design System™ for customized coding.

III.2.5.6. Results

The structure was optimized through a GA cycle. About 83 iterations were needed for optimizing. One important aspect was the drawbacks during the optimization, which is natural consequence of the random nature of the algorithm. The finalized values of the parameters is presented in Table III.2. The S-parameters of the structure are shown in Fig. III.9.

Parameter	Value(mm)
p	8.249
p	16.453
p	16.408
p	0.16

Table III.2. The finalized parameters

As mentioned earlier, the GA suffers from poor convergence, although the algorithm is relatively stable, given the initial population is large enough. The convergence is shown in Fig. III.10.

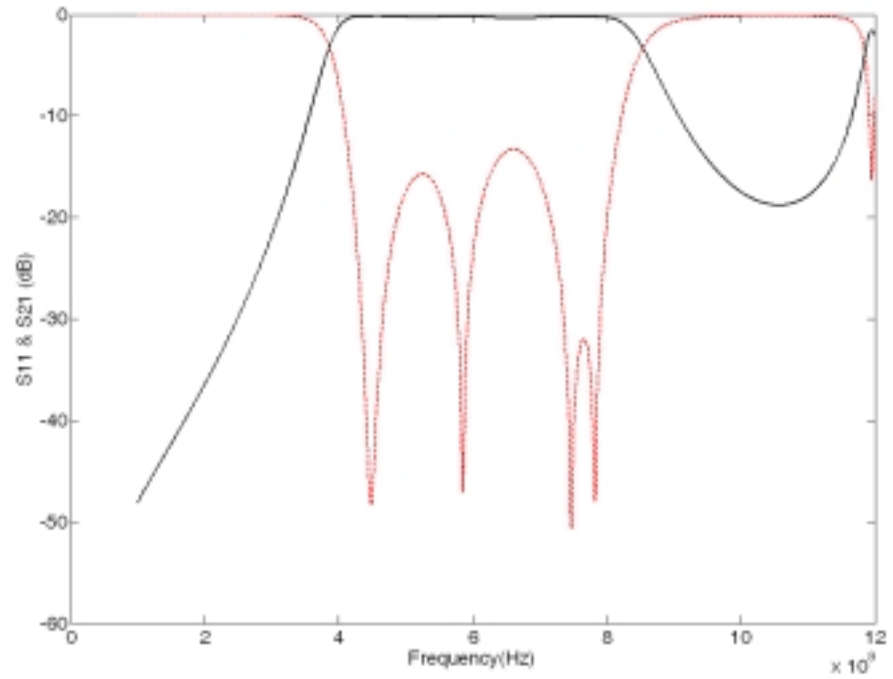

Fig. III.9. The response of the optimized filter

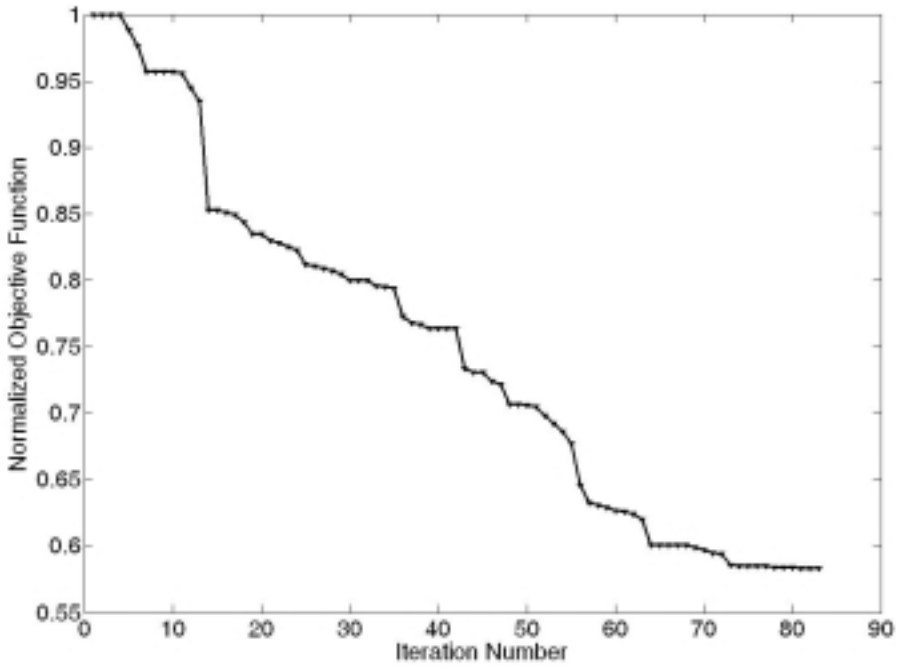

Fig. III.10. The error function versus iteration number. The convergence started after about 30 iterations.

III.3. Particle swarm optimization

III.3.1. Introduction

The particle swarm optimization (PSO) is a novel stochastic evolutionary optimization technique based on the movement and intelligence of swarms. Particle swarm optimization has roots in two main component methodologies. Perhaps more obvious are its ties to artificial life in general, and to bird flocking, fish schooling, and swarming theory in particular. It is also related, however, to evolutionary computation, and has ties to genetic algorithms.

III.3.2. Terminology

The terminology of the particle swarm optimization is borrowed from social studies of animal behavior due to the existing analogy.

III.3.2.1. Particle

In the PSO terminology, a parameter vector is called particle. All the particles in the swarm act individually under the same governing principle: accelerate toward the best personal and best overall location while constantly checking the value of its current location.

III.3.2.2. Position

The position of the parameter vector in the parameter space is particle position.

III.3.2.3. Fitness

As in all evolutionary computation techniques there must be some function or method to evaluate the goodness of a position. The fitness function must take the position in the solution space and return a single number representing the value of that position. In the analogy above the fitness function would simply be the density of flowers: the higher the density, the better the location. In general this could be antenna gain, weight, peak cross-polarization, or some kind of weighted sum of all these factors. The fitness function provides the interface between the physical problem and the optimization algorithm.

III.3.2.4. Personal best

The location with the highest fitness value individually discovered by a particle is known as the personal best. Each particle has its own *personal best* determined by the path that it has taken.

III.3.2.5. Global best

The location of highest fitness value encountered by all the particles up to a certain moment in time (iteration) is known as the *global best*. For the entire swarm there is one *global best.* Each particle has some way of knowing the global best discovered by the entire swarm. At each point along the path every particle compares the fitness of its current location to that of *global best*. If any particle reaches is at a location of higher fitness, *global best* is replaced by that particles current position.

III.3.3. Development of the particle swarm optimization algorithm

Understanding the conceptual basis of the PSO, the task then becomes to develop the algorithmic tools needed to implement the optimization. Fig. III.11. shows a general scheme of particle swarm optimization. Despite its novelty, many variations of the concept have been suggested and tried on different problems, some of these variations will be discussed later. The PSO randomly initializes the position and velocity of each particle within the swarm at the beginning of the optimization. The detailed explanation of the method is addressed in [3]. Each position $p_{i,j}^{<k>}$ represents a possible solution to the problem and is specified with,

$$P^{<k>} = \begin{bmatrix} p_{1,1}^{<k>} & \cdots & p_{1,N}^{<k>} \\ . & . & . \\ p_{M,1}^{<k>} & . & p_{M,N}^{<k>} \end{bmatrix} \qquad \text{(III- 2)}$$

where M is the number of particles (the initial population) and N is the number of dimensions of the problem. The bracketed superscript k denotes the iteration number. Every row in matrix P is a possible solution for $\overline{p}^{<k>}$. In other words the rows of the matrix P are each a parameter vector, resulting the matrix P have N columns. Each particle has an associated velocity as well, which is a function of the distance from its current position to the positions which have previously resulted in a good fitness value,

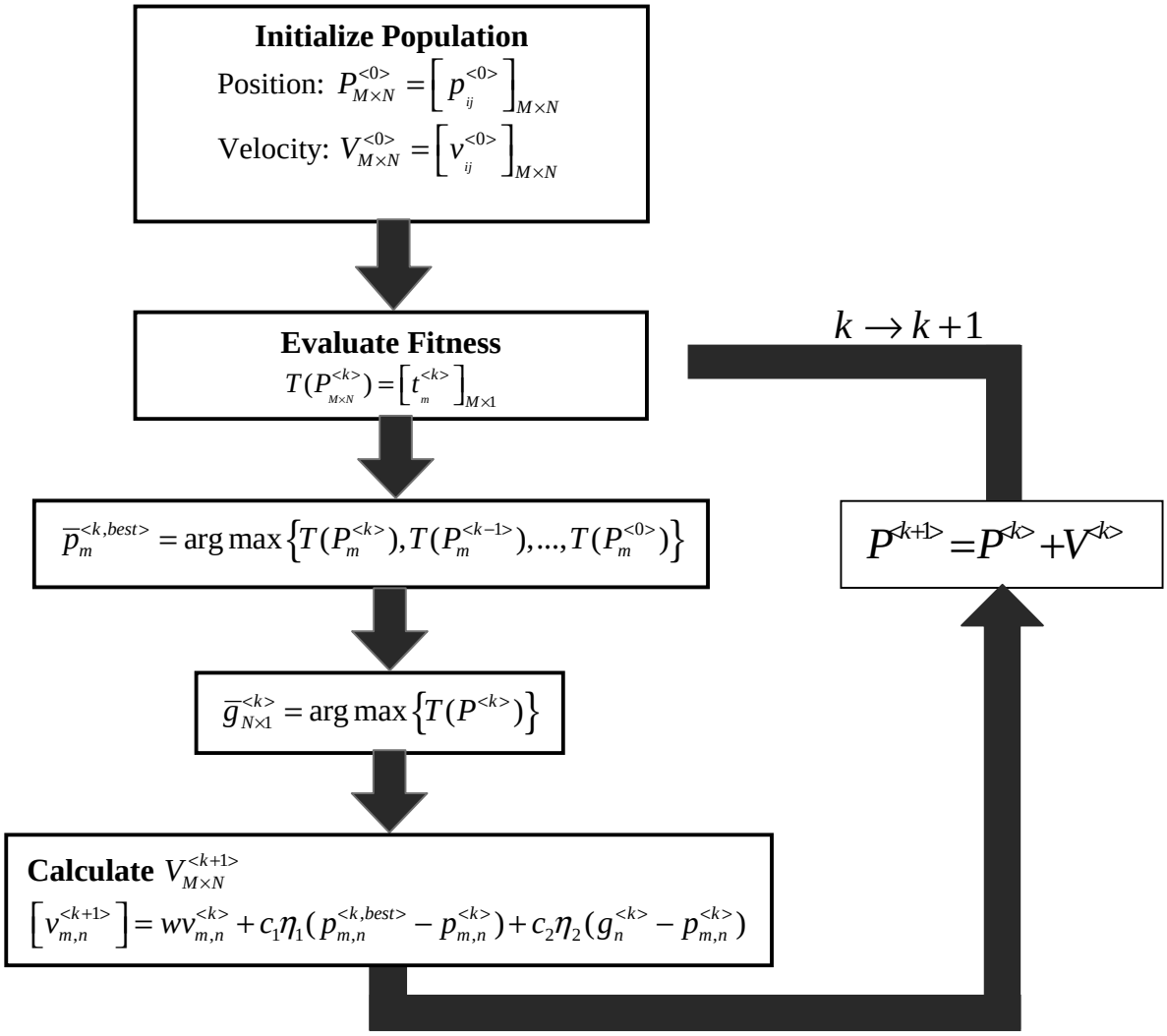

Fig. III.11. The particle swarm optimization algorithm

$$v^{<k>}=\begin{bmatrix} v_{1,1}^{<k>} & \cdots & v_{1,N}^{<k>} \\ . & . & . \\ v_{M,1}^{<k>} & . & v_{M,N}^{<k>} \end{bmatrix} \qquad \text{(III- 3)}$$

The velocity matrix is updated at each iteration. Every particle is also aware of the global and personal best positions. Let the personal and global best positions be named $\left[P_{best}^{<k>}\right]_{M\times N}$ and $\left[\bar{G}_{best}^{k}\right]_{1\times N}$, respectively. Fig. III.12 further clarifies the definitions of the personal and global bests.

Now, for every dimension, the particles move in the direction specified by the velocity matrix according to,

$$P^{k+1}=P^{k}+V^{k} \qquad \text{(III- 4)}$$

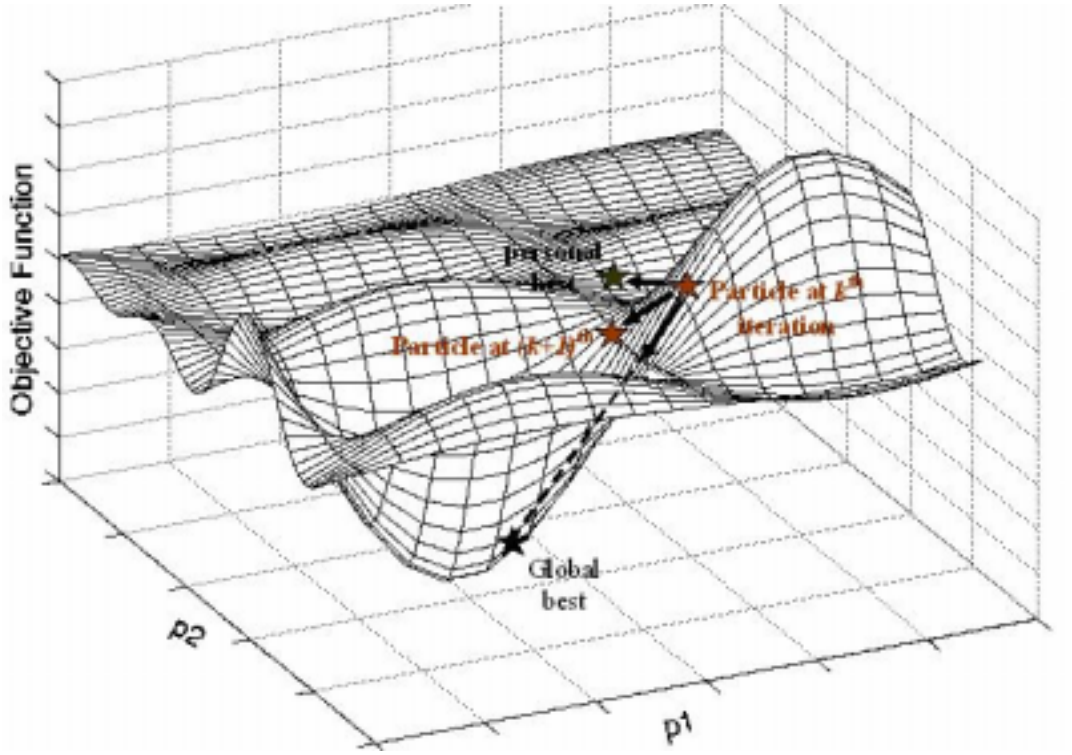

Fig. III.12. (a) Global and personal best

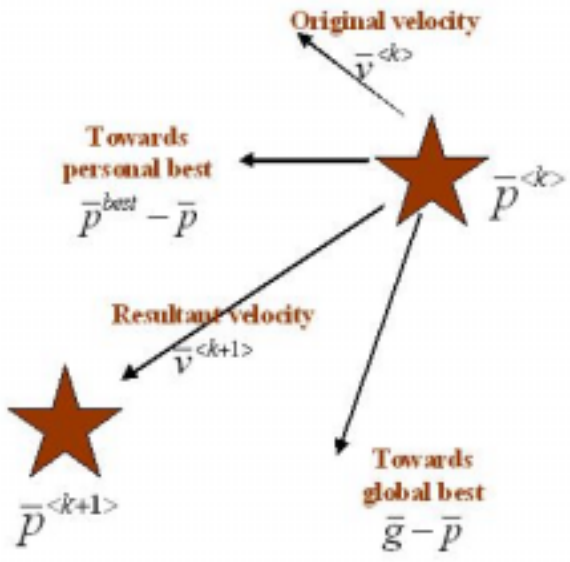

Fig. III.12- (b) A sample path of the particles in the solution space

The update strategy for the velocity vector is to "move" particles towards the global best and their corresponding personal best positions,

$$v_{m,n}^{<k+1>} = wv_{m,n}^{<k>} + c_1\eta_1(p_{m,n}^{<k,best>} - p_{m,n}^{<k>}) + c_2\eta_2(g_n^{<k>} - p_{m,n}^{<k>}) \quad \text{(III- 5)}$$

whereas

$v_{m,n}^{<k>}$ is the velocity of the *n*th element of the *m*th particle in the swarm at *k*th iteration,

$p_{m,n}^{<k>}$ is the *n*th element of the *m*th particle in the swarm at *k*th iteration, $\overline{p}_m^{<k>}$ is the *m*th particle (parameter vector) in the swarm,

$p_{m,n}^{<k,best>}$ represents the elements of the *personal best* of *m*th particle at *k*th iteration,

c_1, c_2 and w are positive scalars which define the weight of every component of the velocity,

w is a positive scalar called *inertia weight*,

η_1 and η_2 are normalized uniform random variables.

c_1 and c_2 specify the relative weight of the global best to the personal best positions. Empirically the value 2.0 is found to be a reasonable value for these coefficients [23].

Through the iterations, corrections have been made to the positions of *personal best*, and *global best* before letting the particles fly around for another second. Repetition of this cycle is continued until the termination criteria are met. There are several methods to determine these termination criteria.

One possible criterion is to define a maximum number of iterations for terminating. At any time if a solution is found that is greater than or equal to the target fitness value, then the PSO is stopped at that point.

III.3.4. Improved particle swarm optimization algorithms

As mentioned previously, the algorithm explained in Fig. 11 has been patched with many variations. Since the introduction of the PSO algorithm, several improvements have been suggested. Some of these improvements have already been incorporated in the original formulation, *e.g.* the original PSO did not have an *inertia weight*; this improvement was introduced by Shi and Eberhart [31]. The addition of the inertia weight results in faster convergence.

In [32] Kennedy has suggested a technique referred to as "social stereotyping". A clustering algorithm is used to group individual particles into "stereotypical groups."

> *"Individuals in the particle swarm population were "stereotyped" by cluster analysis of their previous best positions. The cluster centers then were substituted for the individuals' and neighbors' best previous positions in the algorithm. The experiments, which were inspired by the social-psychological metaphor of social stereotyping, found that performance could be generally improved by substituting individuals', but not neighbors', cluster centers for their previous bests"*

The *cluster center* $\tilde{p}_{m,n}^{<k>}$ is computed for each group and then substituted into (III- 5), yielding three strategies to calculate the new velocity

$$v_{m,n}^{<k+1>} = wv_{m,n}^{<k>} + c_1\eta_1(\tilde{p}_{m,n}^{<k>} - p_{m,n}^{<k>}) + c_2\eta_2(g_n^{<k>} - p_{m,n}^{<k>}) \quad \text{(III- 6)}$$

$$v_{m,n}^{<k+1>} = wv_{m,n}^{<k>} + c_1\eta_1(p_{m,n}^{<k,best>} - p_{m,n}^{<k>}) + c_2\eta_2(\tilde{p}_{m,n}^{<k>} - p_{m,n}^{<k>}) \quad \text{(III- 7)}$$

$$v_{m,n}^{<k+1>} = wv_{m,n}^{<k>} + c_1\eta_1(\tilde{p}_{m,n}^{<k>} - p_{m,n}^{<k>}) \quad \text{(III- 8)}$$

The results presented in [32] indicate that only the method in (III- 6) performs better than the standard PSO. The drawback with this method is the added cost of calculating the clusters and their centers.

III.3.4.1. Cooperative learning

The core concept in genetic algorithm is competition. Every member of the population tries to produce the best solution by combining best properties from other individuals. The stronger individual is rewarded with more opportunities to reproduce. But another aspect in GA is cooperation. Crossover operation as information exchange, the GA can be considered to be a cooperative system. Cooperation involves a collection of agents that interact by communicating information to each other while solving a problem.

The same concept can produce hints for improvements in particle swarm optimization. Instead of having one swarm (of particles) trying to find the optimal *N*–dimensional vector, the vector is split into its components so that swarms (of particles each) are optimizing a one-dimensional vector. The solution vector is split into parts,

each part being optimized by a swarm with particles. This allows for combinations for constructing the composite –component vector. The simplest approach is to select the best particle from each swarm (how to calculate which particle is best will be discussed later).

In the classical PSO, update equation (III- 5) is aimed to change the whole *N*-dimensional vector at every step. This allows for the possibility that some components in the vector have moved closer to the solution, while others actually moved away from the solution. As long as the effect of the improvement is dominant to the effect of the components that have downgraded, the standard PSO will consider the new vector an overall improvement, even though some components of the vector may have moved further from the solution.

III.3.4.2. Cooperative particle swarm optimization algorithm

The original PSO uses a population of *N*–dimensional vectors. These vectors can be partitioned into swarms of 1-D vectors, each swarm representing a dimension of the original problem. Each swarm attempts to optimize a single component of the solution vector, essentially a 1-D optimization problem. One complication to this configuration is the fact that the function to be minimized $T(\overline{p})$ requires an N-dimensional vector as input. If each swarm represents only a single dimension of the search space, it is clearly not possible to directly compute the fitness of the individuals of a single population considered in isolation. A *context vector* is required to provide a suitable context in which the individuals of a population can be evaluated.

The simplest scheme for constructing such a context vector is to take the global best particle from each of the swarms and concatenating them to form such an N-dimensional vector. To calculate the fitness for all particles in swarm, the other components in the context vector are kept unchanged (with their values set to the global best particles from the other swarms).

Fig. III.13 illustrates the cooperative algorithm first introduced by Van den Bergh and Engelbrecht in [29].

Extending the convention introduced in Fig. 11, now refers to the position of particle of swarm, which can therefore be substituted into the *i*th component of the context vector when needed. Each of the swarms now has a global best particle.

This algorithm has the advantage that the error function is evaluated after each component in the vector is updated, resulting in much finer-grained credit assignment.

The current "best" context vector will be denoted. Note that is a strictly non-increasing function, since it is composed of the global best particles of each of the swarms, which themselves are only updated when their fitness improves.

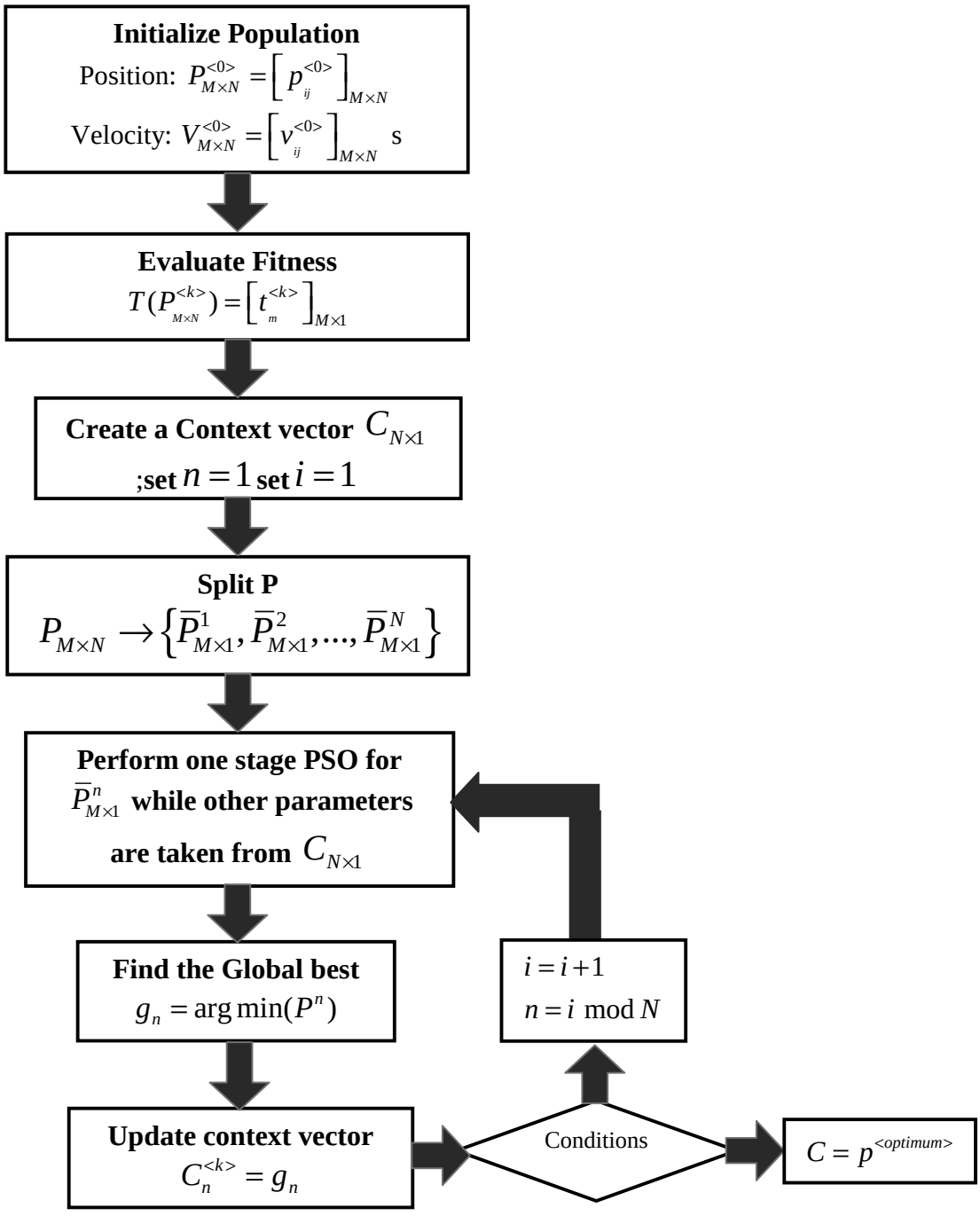

Fig. III.13. Cooperative particle swarm optimization

Each swarm in the group only has information regarding a specific component of the solution vector; the rest of the vector is provided by the other swarms. This promotes cooperation between the different swarms, since they all contribute to, the context

vector. Another interpretation of the cooperative mechanism is possible. Each particle of swarm represents a different context in which the vector is evaluated, so that the fitness of the context vector itself is measured in different contexts. The most successful context, corresponding to the particle yielding the highest fitness, is retained for future use.

One important issue to address in here is that the correlated elements of parameter vector can be grouped and the update algorithm is applied to such a group at one time.

III.3.5. Stability of particle swarm optimization

The present study and also growing number of publications on PSO show that the algorithm is well capable of handling various types of problems. At this stage a more profound look at the mechanism of particle swarm optimization seems to be necessary.

The present analysis begins with a highly simplified deterministic version of the particle swarm in order to provide an understanding about how it searches the problem space [4], then continues on to analyze the full stochastic system. A generalized model is proposed, including methods for controlling the convergence properties of the particle system. Finally, some empirical results are given, showing the performance of various implementations of the algorithm on a suite of test functions.

In the PSO update equation (III- 5) the variables η_1 and η_2 are random positive numbers, drawn from a uniform random distribution.

The random weighting of the control parameters in the algorithm results in an action similar to explosion. An important source of the swarm's search capability is the interactions among particles as they react to one another's findings. Analysis of interparticle effects is beyond the scope of this section, which focuses on the trajectories of single particles.

III.3.5.1. Analogy of particle swarm optimization to gradient methods

We begin the analysis by stripping the algorithm down to a most simple form; we will add things back in later.

In equation (III- 5), with the substitution of variables,

$$\frac{\eta_1 p_{m,n}^{<k,best>} + \eta_2 g_n^{<k>}}{\eta_1 + \eta_2} \rightarrow \hat{\mathbf{p}}_{m,n}^{<k>} \tag{III- 9}$$

and assuming w= c_1 = c_2 =1, The velocity expression can be reduced into two terms without loss of generality. Hence (III- 5) will reduce to,

$$v_{m,n}^{<k+1>} = v_{m,n}^{<k>} + \eta(\hat{\mathbf{p}}_{m,n}^{<k>} - p_{m,n}^{<k>}) \tag{III- 10}$$

where

$$\eta = \eta_1 + \eta_2 \tag{III- 11}$$

Simple algebraic operations would show that (III- 10) and (III- 5) are actually equivalent.

Let assume the one-dimensional parameter space. Also let's assume the *j*th particle is the particle which achieves the global best so far. This way the equation (III- 10) will reduce to,

$$v_m^{<k+1>} = v_m^{<k>} + \eta(p_j^{<k>} - p_m^{<k>}) \tag{III- 12}$$

The equation (III- 12) is now substituted into (III- 4),

$$\overline{p}_m^{<k+1>} = p_m^{<k>} + v_m^{<k>} + \eta(p_j^{<k>} - p_m^{<k>}) \tag{III- 13}$$

The third term in (III- 13) can be compared to the gradient update formulas (*e.g.* steepest descent),

$$\overline{p}^{<k+1>} = \overline{p}^{<k>} - \eta \vec{s}^{<k>} \tag{III- 14}$$

whereas superscripts *k* shows the iteration number, and η is a positive scalar called weighting factor which can be chosen adaptively and $\vec{s}^{<k>}$ is the gradient vector. In one dimension the gradient is the same as derivative of the objective function to the only parameter. Equations (III- 13) and (III- 14) have some analogy in part. Note that the gradient vector, at each point directs to the minimum (or maximum) value of the objective function. The same definition can apply to the term $(p_j^{<k>} - p_m^{<k>})$ in equation (III- 13). This fact implied the "gradient" nature of the PSO update strategy. The same statement can be extended to N-dimensions. Of course there is a little difference between the way the gradient is calculated in here and in a "real" gradient method. In a gradient optimization technique the variations of the objective function

in all directions are tried and the parameter vector is moved toward the direction which minimizes the objective function, while in here the vector $(p_j^{<k>} - p_m^{<k>})$ tends to the gradient if the global best is sufficiently close to the ultimate optimum point. Fig. III.14 depicts such an analogy in a two dimensional parameter space.

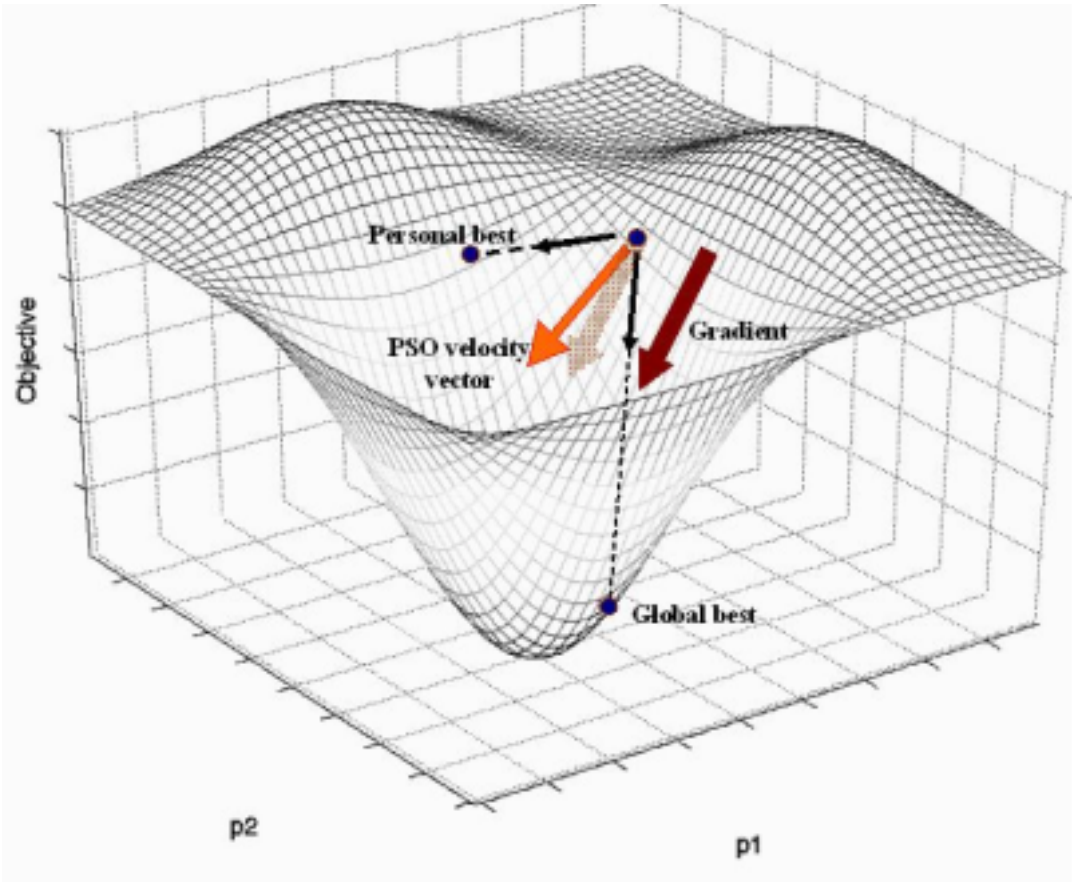

Fig. III.14. Analogy between gradient methods and particle swarm optimization

III.3.5.2. An analytic point of view

The procedure can also be seen in an analytic point of view as suggested in [30]. Continuing the assumption of working only in a one-dimensional parameter space the reduced system can be expressed as in (III- 12),

(III- 14)

$$\overline{v}_m^{<k+1>} = \overline{v}_m^{<k>} + \eta(\hat{\mathbf{p}}_m^{<k>} - p_m^{<k>})$$

and

$$\overline{p}_m^{<k+1>} = \overline{p}_m^{<k>} + \overline{v}_m^{<k+1>} \qquad \text{(III- 15)}$$

Extending (III- 12) in time would yield,

$$\overline{v}_m^{<k+2>} = \overline{v}_m^{<k+1>} + \eta(\hat{\mathbf{p}}_m^{<k+1>} - p_m^{<k+1>}) \quad \text{(III- 16)}$$

and thus,

$$\overline{v}_m^{<k+1>} - \eta\, p_m^{<k+1>} + (1-\eta)\overline{v}_m^{<k+1>} - \overline{v}_m^{<k>}\overline{v}_m^{<k+2>} + (\eta-2)\overline{v}_m^{<k+2>} + \overline{v}_m^{<k>} = 0 \quad \text{(III- 17)}$$

This, in continuous domain implies the ordinary differential equation,

$$\frac{\partial^2 v_m}{\partial t^2} + (c_1 + c_2)\frac{\partial^2 v_m}{\partial t^2} + c_1.c_2 v_m = 0 \quad \text{(III- 18)}$$

where $c_i = \ln(\tilde{c}_i), i = 1, 2.$ and $\tilde{c}_1$ and $\tilde{c}_2$ are the roots of the equation,

$$\tilde{c}^2 + (\eta - 2)\tilde{c} + 1 = 0 \quad \text{(III- 19)}$$

Please note that to obtain the above equation it has been assumed $k \to t$ and $(v^{<k+1>} - v^{<k>}) \to \partial v/\partial t$ and so on. The roots of (III- 19) can be derived as follows,

$$\tilde{c}_{1,2} = 1 - \frac{\eta}{2} \pm \frac{\sqrt{\eta^2 - 4\eta}}{2} \quad \text{(III- 20)}$$

The general solution for (III- 18) is,

$$v_m(t) = a_1\tilde{c}_1(\eta, t) + a_2\tilde{c}_2(\eta, t) \quad \text{(III- 21)}$$

This implicitly infers that the velocity vector is composed of a phase and amplitude. In order to avoid the oscillation or instability of the particles path, the parameter η should be chosen in such a way that $\tilde{c}$ is not purely imaginary.

III.4. Design examples using particle swarm optimization

III.4.1. Design of planar microwave filters using a simple FDTD model and particle swarm optimization

The objective of this contribution is to present a simple and universal design procedure for planar microwave filters. To accelerate the computation phase an equivalent circuit topology is derived from FDTD formulation. The method is fast and robust and well suits with fast paced engineering design environment. As a case study, a microwave band-pass filter is designed.

III.4.1.1. Formulation of the problem

Let us consider the structure shown in Fig. III.15 as the structure to be modeled. The substrate is subdivided into a uniform square grid. The currents involved in a given unit cell are depicted in Fig. III.16. The separation between two planes (the dimension *d*) is considered to be small compared to the smallest operating wavelength. The problem is formulated using the Hertzian vector potentials, and the substrate is assumed to be rectangular. The space in which the wave is transmitted is restricted by two electric walls at z = 0, and z = a. The propagation modes could be both *En* and *Hn*. The Hertz potential vectors are defined as,

$$\vec{\pi}_e^{\,n} = \hat{a}_z P_e^n(x,y)\,\cos(\frac{n\pi}{d}z).e^{j\omega t} \qquad \text{(III- 22)}$$

$$\vec{\pi}_h^{\,m} = \hat{a}_z P_h^m(x,y)\,\sin(\frac{m\pi}{d}z).e^{j\omega t} \qquad \text{(III- 23)}$$

Here, $\vec{\pi}_{e\,or\,h}$ is the electric or magnetic Hertzian vector potential (corresponding to indexes *e* or *h*), $P_{e\ or\ \mathrm{h}}$ is the cross-section eigenfunction, *d* is the separation distance between power and ground planes, and a_z is the unit vector along the z-axis. Following the mathematical relations of Hertzian electric and magnetic vector potentials, the electric and magnetic field components are listed in equation (III- 24).

$$E_z = P_e^n(x,y)\cos(\frac{n\pi}{d}z).\beta_t^2.e^{j\omega t} \qquad \text{(III- 24)}$$

$$E_t = -\frac{n\pi}{d}\nabla P_e^n(x,y).\sin(\frac{n\pi}{d}z).e^{j\omega t}$$

$$H_t = -j\omega\varepsilon\hat{a}_z \times \nabla P_e^n(x,y)\cos(\frac{n\pi}{d}z)\,.e^{j\omega t}$$

$$H_z = 0$$

$$\beta_t^2 = \omega^2\mu\varepsilon - (\frac{n\pi}{d})^2$$

The scalar potential is defined as,

$$V_e = -d.P_e^n(x,y)\beta_t^2 e^{j\omega t} \qquad \text{(III- 25)}$$

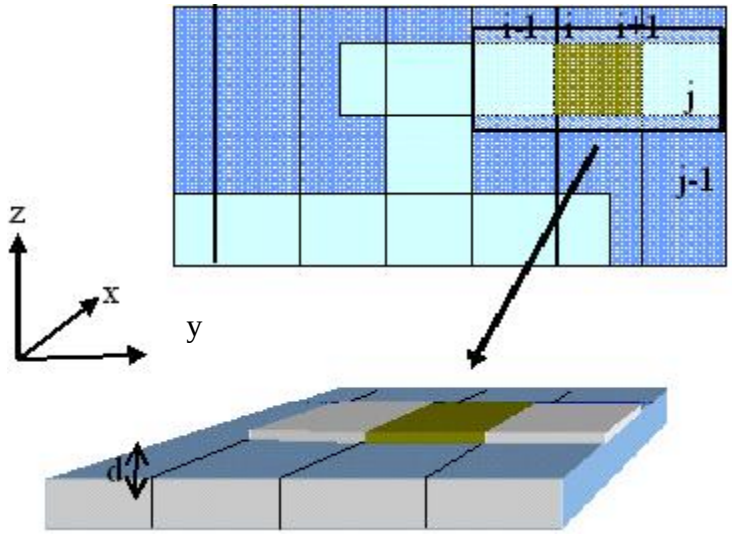

Fig. III.15. Geometry of the structure. The structure is divided into a uniform grid.

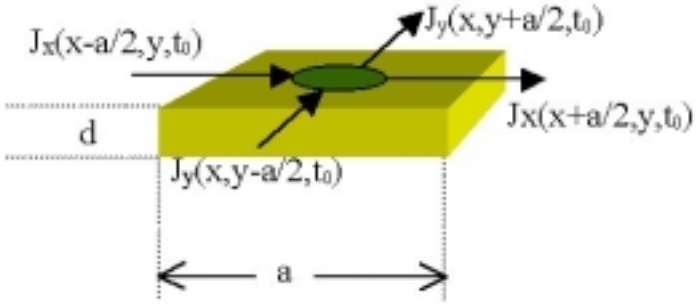

Fig. III.16. Currents passing through a unit grid-cell

Now the relation between the surface current $J_{e\text{ or }h}$ and the potential could be written as,

$$\nabla V_e = -j\frac{\beta_t^2}{\omega\varepsilon}.d.\vec{J}_e \qquad \text{(III- 26)}$$

$$\nabla . \vec{J}_e = -j\frac{\omega\varepsilon}{d}V_e \qquad \text{(III- 27)}$$

The relation between V and $J_{e\ or\ h}$ may be presented in time domain as,

$$\nabla V(x,y,t) = -L_s \frac{\partial \vec{J}(x,y,t)}{\partial t} \quad \text{(III- 28)}$$

$$\nabla . \vec{J}(x,y,t) = -C_s \frac{\partial V(x,y,t)}{\partial t} \quad \text{(III- 29)}$$

Assuming $a << \lambda$ and $\Delta t << 2\pi / \omega$, the planes are subdivided into a square grid, and the differentials are replaced with finite differences:

$$J_x(x_l + \frac{a}{2}, y_k, t_0 + \frac{\Delta t}{2}) = J_x(x_l + \frac{a}{2}, y_k, t_0 - \frac{\Delta t}{2}) - (V(x_l + a, y_k, t_0) - V(x_l, y_k, t_0)) \frac{\Delta t}{L_s a} \quad \text{(III- 30)}$$

$$J_x(x_l, y_k + \frac{a}{2}, t_0 + \frac{\Delta t}{2}) = J_x(x_l, y_k + \frac{a}{2}, t_0 - \frac{\Delta t}{2}) - (V(x_l, y_k + a, t_0) - V(x_l, y_k, t_0)) \frac{\Delta t}{L_s a} \quad \text{(III- 31)}$$

$$V(x_l, y_k, t_0 + \Delta t) = V(x_l, y_k, t_0) - (J_x(x_l + \frac{a}{2}, y_k, t_0 + \frac{\Delta t}{2}) - J_x(x_l - \frac{a}{2}, y_k, t_0 + \frac{\Delta t}{2}) + J_x(x_l, y_k + \frac{a}{2}, t_0 + \frac{\Delta t}{2}) - J_x(x_l, y_k - \frac{a}{2}, t_0 + \frac{\Delta t}{2})) . \frac{\Delta t}{C_s a} \quad \text{(III- 32)}$$

III.4.1.2. Optimization of planar filters

III.4.1.2.1. Design strategy

As illustrated in Fig. III.15 the substrate is discretized into a uniform grid of square patches. Each of these patches could be either metalized on non-metalized. A two dimensional binary-valued vector $\eta(i, j)$ is defined as,

$$\eta^k(i,j) = \begin{cases} 1 & for\ metalized\ \ segment \\ 0 & non-metalized\ segment \end{cases} \quad \text{(III- 33)}$$

where *i* and *j* represent the segment numbers. The superscript *k* shows the number of iterations. The function $C^k(\eta)$ represents overall distribution of metalized and non-metalized patches. Although $C^1(\eta)$ (the initial geometry) could be chosen arbitrarily, but to have a faster convergence, its better to start form an appropriate initial point. The same applies for update strategy throughout the iterations. Existence of a constraint in updates of $C^k(\eta)$ considerably limits the number of possible parameter vectors which is an essential step for reducing the number of computations required at each step. Design parameters $\overline{p}^k(C(\eta))$ are defined to restrict the geometry variations

to specific directions. $\overline{p}$ is a *N* dimensional vector that represents a small parameter vector which could be few critical dimensions of the structure.

III.4.1.2.2. Objective function

The ideal filtering function is defined with the universal objective function for a filter could be defined as,

$$T\left(\overline{p}^k(C(\eta))\right)=\alpha\int_{f_{\min}}^{f_{\max}} T_{11}\left(f,C^k(\eta)\right)df+\beta\int_{f_{\min}}^{f_{\max}} T_{12}\left(f,C^k(\eta)\right)df \quad \text{(III- 34)}$$

$$T_{ij}\left(f,\overline{p}^k(C(\eta))\right)=Q(f).W\left(r_{ij}(f).\left(S_{ij}^{actual}\left(f,C^k(\eta)\right)-S_{ij}^{ideal}(f)\right)\right) \quad \text{(III- 35)}$$

$$W(x)=\begin{cases}\chi\exp(x) & x\succ 0,0\prec\chi\le 1\\ 0 & x\le 0\end{cases} \quad \text{(III- 36)}$$

r equals to 1 (-1) when $i=j$ in the passband (stopband) or or $i\neq j$ in the stopband (passband). The transition bands are removed via function *Q(f)* which is equal to zero in transition and one otherwise. $S_{ij}^{actual}\left(f,C^k(\eta)\right)$is the computed S-parameter, $S_{ij}^{ideal}(f)$ is the desired S-parameter (which is a function of frequency) and $W(x)$ is the weighted error function. The derivation of nonlinearly weighted errors is described in chapter I.

III.4.1.2.3. Particle swarm optimization

The PSO randomly initializes the position and velocity of each particle within the swarm at the beginning of the optimization. The detailed explanation of the method is addressed in [3]. Each position represents a possible solution to the problem and is specified as,

$$P^k=\begin{bmatrix} p_{11}^k & \dots & p_{1N}^k\\ . & . & .\\ p_{M1}^k & . & p_{MN}^k\end{bmatrix} \quad \text{(III- 37)}$$

where M is the number of particles (the initial population) and N is the number of dimensions of the problem. Every row in matrix P is a possible solution for $\overline{p}^k$ .Each particle has an associated velocity, named $\overline{V}_{M\times N}$, which is a function of the distance between the current position and best previously achieved fitness positions. The velocity matrix is updated at each iteration. Every particle is also aware of the global

and personal best positions. Let the personal best positions be named $\left[P_{best}^{k}\right]_{M\times N}$ and the global best position be a vector $G_{best}^{k}=\left[g_{1}^{k}\, g_{2}^{k}\ldots g_{N}^{k}\right]$.

Now, for every dimension, the particles move in the direction specified by the velocity matrix according to,

$$P^{k+1}=P^{k}+V^{k} \tag{III- 38}$$

The update strategy for the velocity vector can be addressed as,

$$v_{mn}^{k+1}=v_{mn}^{k}+c_{1}\zeta_{1}(p_{mn}^{best}-p_{mn}^{k})+c_{2}\zeta_{2}(g_{n}^{k}-p_{mn}^{k}) \tag{III- 39}$$

whereas $0<\zeta_{1,2}<1$ are uniform random variables and c_1 and c_2 specify the relative weight of the global best to the personal best positions (here $c_1=c_2=2$ *see* [27]).

III.4.2. Design of a double folded stub filter

As an example a double folded stub filter which is shown in Fig. III.17 is designed and fabricated. A symmetric 3GHz band pass frequency characteristic centered at 13.5GHz is desired. The $\left|S_{21}^{ideal}\right|$ should be less than -30dB for stop band and more than -3dB in sidebands. A transition band of 3GHz is considered where the errors are masked. Substrate is 5 mils thick with dielectric constant of 9.8. The three parameters are shown in Fig. III.17 as well.

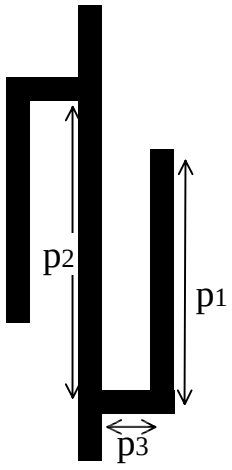

Fig. III.17. The DFS filter , the design variables are as follows mil, p1=6.4 mil, p2=84.8 and p3=86.4 mil.

The square cell sizes are equal to 0.1mil*0.1mil. The search was done for a range of 1.5 mills around the initial geometry.. The results are compared with numerical

analysis obtained by Momentum [35] and with measurement results in Fig. III.18. However the results show a slight discrepancy in magnitude compared to measurement while the frequencies are accurate to a satisfactory extent.

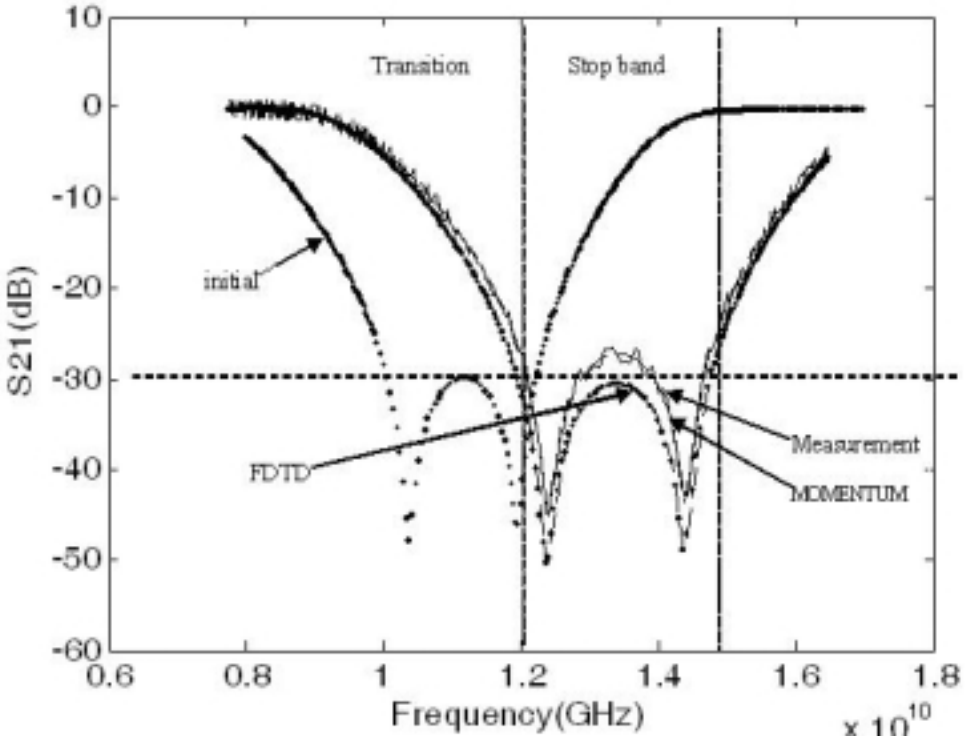

Fig. III.18. The initial and final transmission (S_{21}) characteristic, measured and calculated

III.4.3. Optimization of a planar UWB band-pass filter with a 3GHz-6GHz bandwidth and low insertion loss

The emerging attention to ultrawideband technology has raised requirements for different system components such as filters, antennas, amplifiers, etc. As it is apparent from its name, ultrawideband wireless systems can use relatively a wide band of 3.1GHz-10.6GHz. Using such a wide band for data transmission and reception, on the one hand increases the risk of interference by other sources such as 5.8GHz ISM band, harmonics of 2.45GHz ISM band and other sources of interference. On the other hand FCC regulation absolutely requires the lower cutoff frequency of the emitted fields be limited to 3.1GHz. In order to accommodate the above mentioned requirements, a filter is used both in transmitter side (before the antenna) and in the receive end (after the LNA). Among the other typical requirements for a filter design, a low insertion loss is highly desirable because of low power of the transmitted signal.

III.4.3.1. Description of the structure

For the design of the filter a composite structure composed of a stepped-impedance low-pass and a high-pass planar topologies is selected [36]. The structure is shown in Fig. III.19. As can be seen the structure comprises of three stepped impedance.

The substrate is chosen to be Rogers 4350 with 20 mils (0.508mm) of thickness [22].

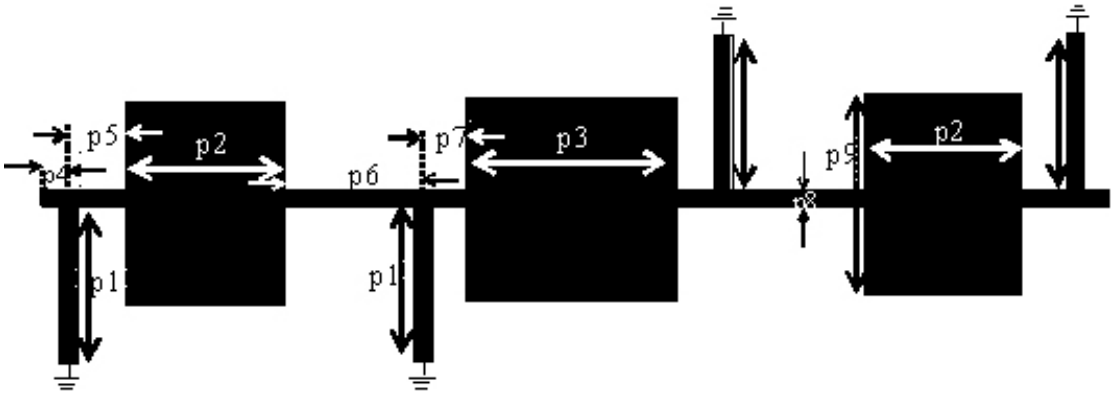

Fig. III.19. The topology of the UWB bandpass filter.

III.4.3.2. The initial dimensions and response

The initial dimensions are presented in Table III.3. The optimum search was conducted in a parameter space within ±30% of the initial parameter set.

Parameter	Value(mils)
*p*1	150
*p*2	120
*p*3	200
*p*4	15
*p*5	40
*p*6	100
*p*7	40
*p*8	12.
*p*9	162.

Table III.3. Initial parameter set for UWB band-pass filter

III.4.3.3. Optimization by PSO/steepest descent

A PSO/SD optimization algorithm was implemented using AEL language (integrated with ADS). The structure was analyzed using Momentum software

A relatively big swarm (with 50 members) was generated as the initial population to assure the global convergence. After 8 iterations, the global optimum was localized

and then the optimization was continued by a smaller population of 20 members. Finally the last stages were done using the steepest descent (SD) method for three consecutive iterations. Fig. III.20 compares convergence diagrams applying PSO and GA. The optimized dimensions are shown in Table III.4.

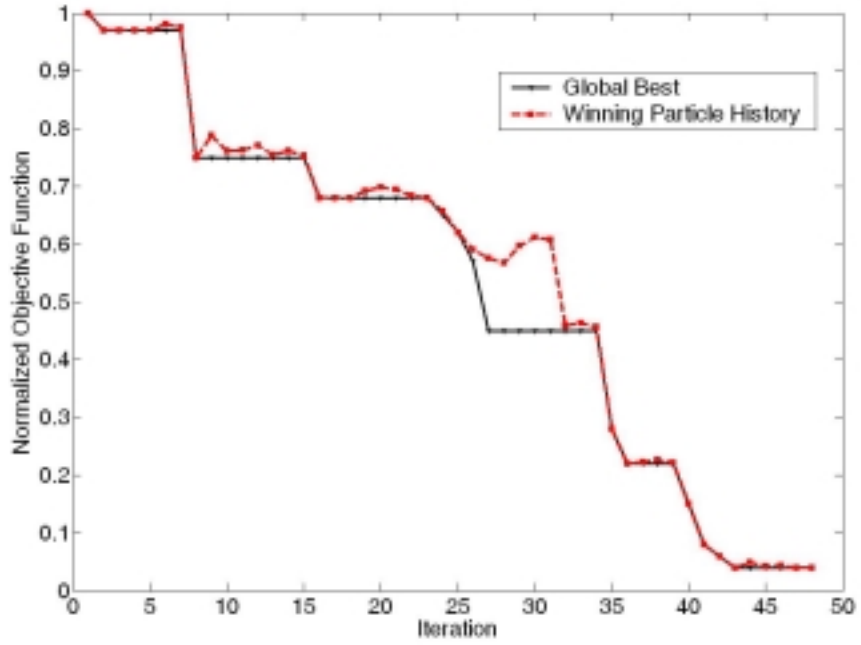

(a)

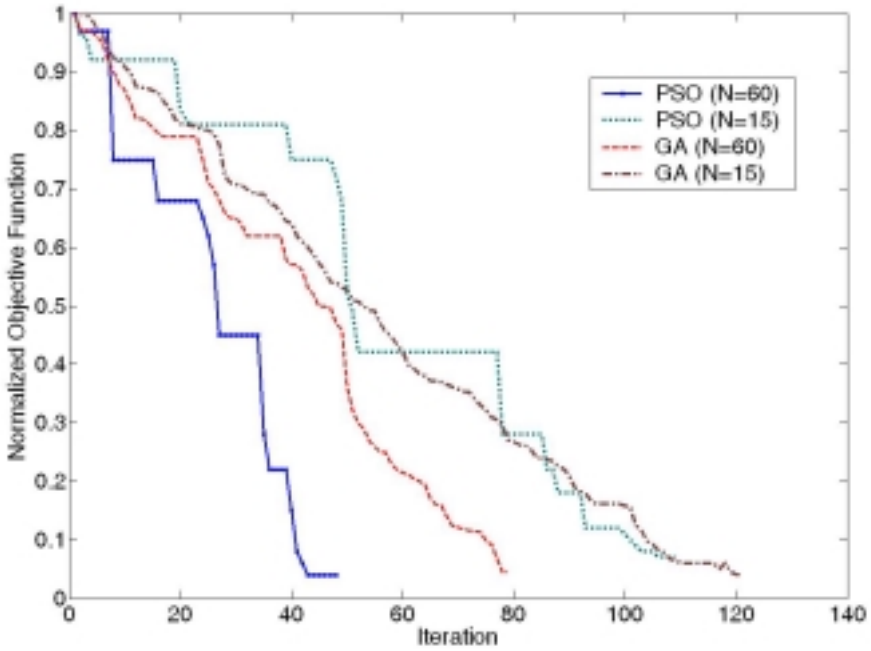

(b)

Fig. III.20. Convergence diagram (a) comparing the global best and the winning particle history (b) comparison with genetic algorithms both for initial populations of 15 and 60.

Parameter	Value(mils)
$p1$	129
$p2$	131.23
$p3$	172.21
$p4$	15.91
$p5$	37.33
$p6$	108.63
$p7$	31.41
$p8$	12.
$p9$	162.

Table III.4. Optimal values for the parameter set for UWB band-pass filter

III.4.3.4. Optimization of the filter characteristic

The simulated and measured frequency characteristics of the filter are presented in Fig. III.21 and Fig. III.22, respectively. As mentioned the filter was fabricated with a 20 mils Rogers 4350 substrate. The picture of the filter is shown in Fig. III.23.

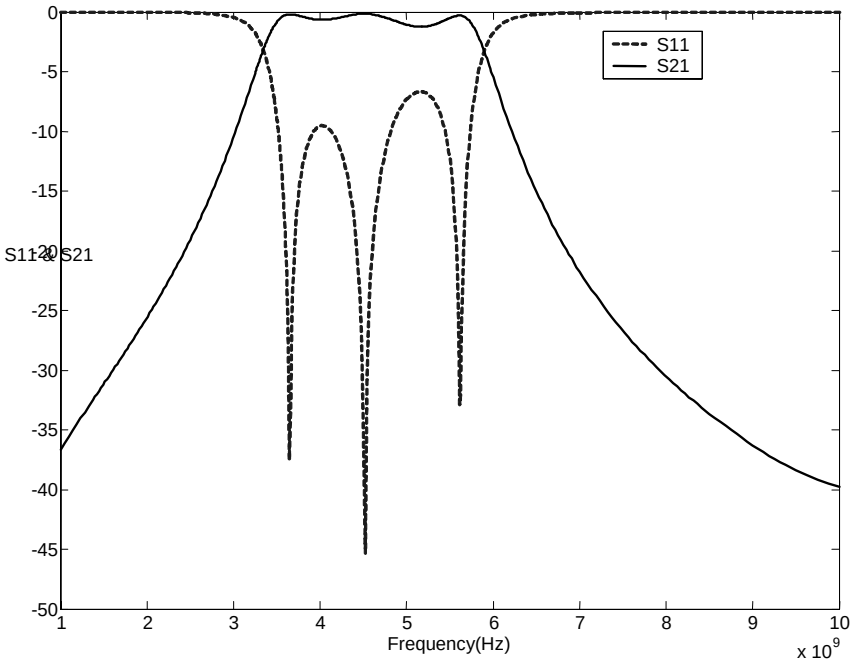

Fig. III.21. The optimized insertion and return loss characteristic of the UWB bandpass filter.

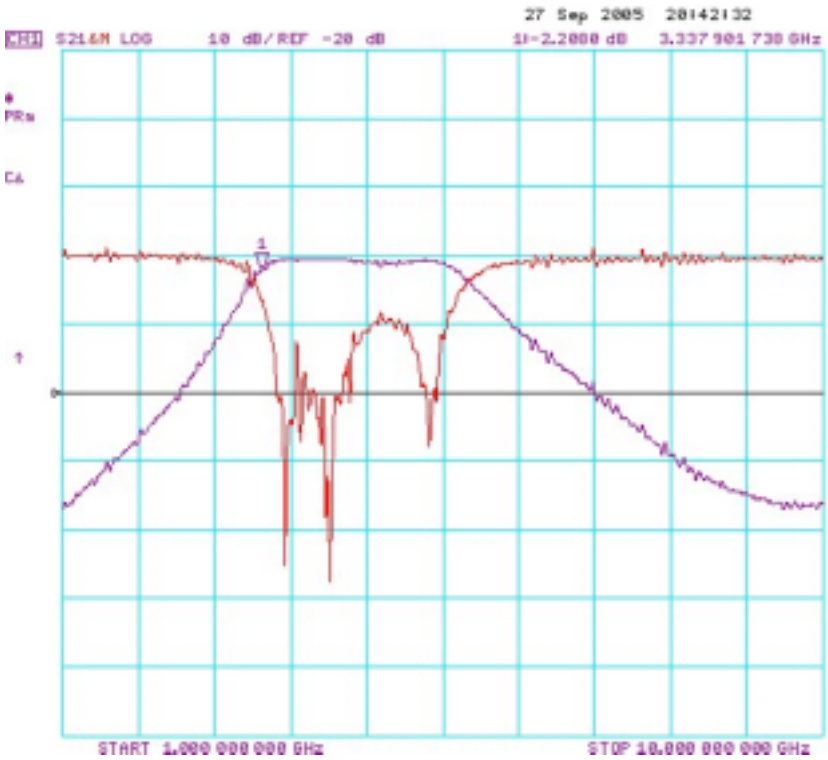

Fig. III.22. The measured response

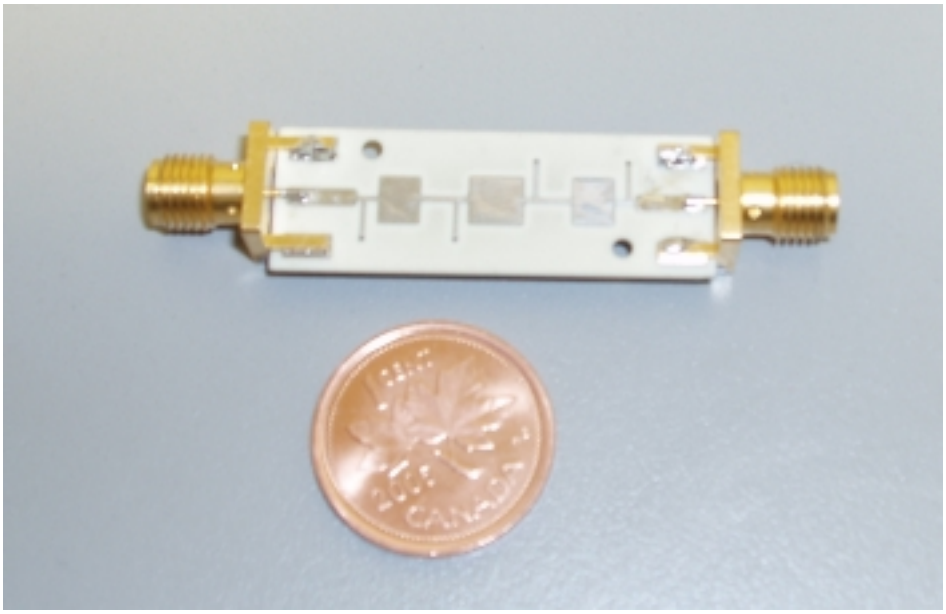

Fig. III.23. The fabricated prototype

III.4.4. Optimization of a planar UWB band-pass filter with a 3GHz-8GHz bandwidth

Another UWB filter with a wider bandwidth is designed and optimized using PSO algorithm. Five band-pass shorted stubs are designed as the initial circuit. In order to simplify the optimization procedure, the width of the line connecting the input and output is fixed. The structure is decided to be symmetric, leaving only three parameters to be optimized. The initial parameter set and the initial response are presented in Table III.5 and Fig. III.24, respectively. The initial parameter space has been limited to ± 50% of the initial parameter set which is relatively a large space for search.

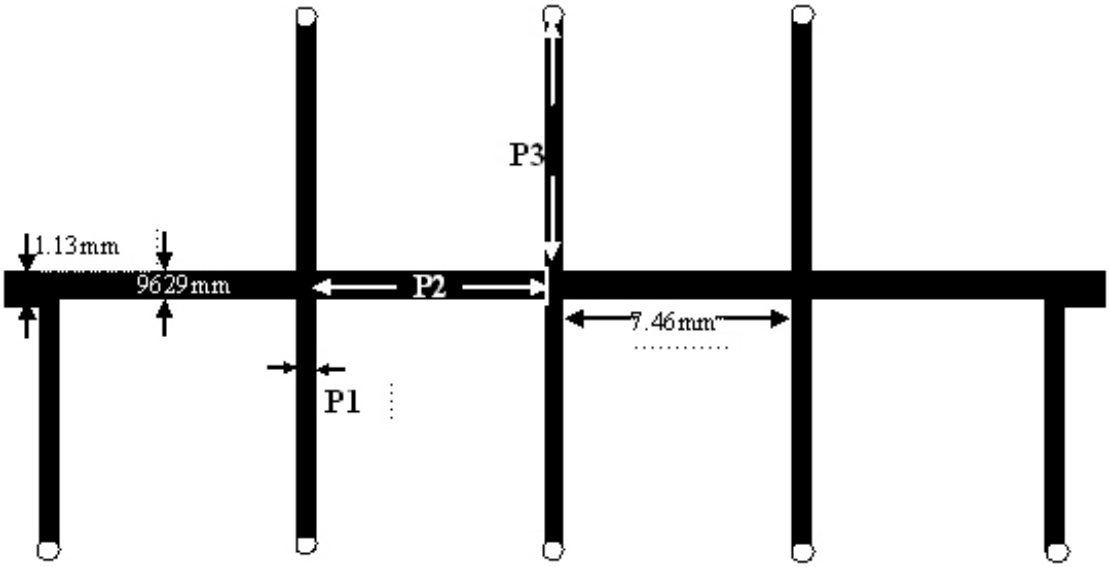

Fig. III.24. Example-Structure to be optimized. The parameters are depicted as well.

Parameter	Value(mm)
p	0.585
p	12.211
p	4.356

Table III.5. Initial parameter set for planar band-pass filter

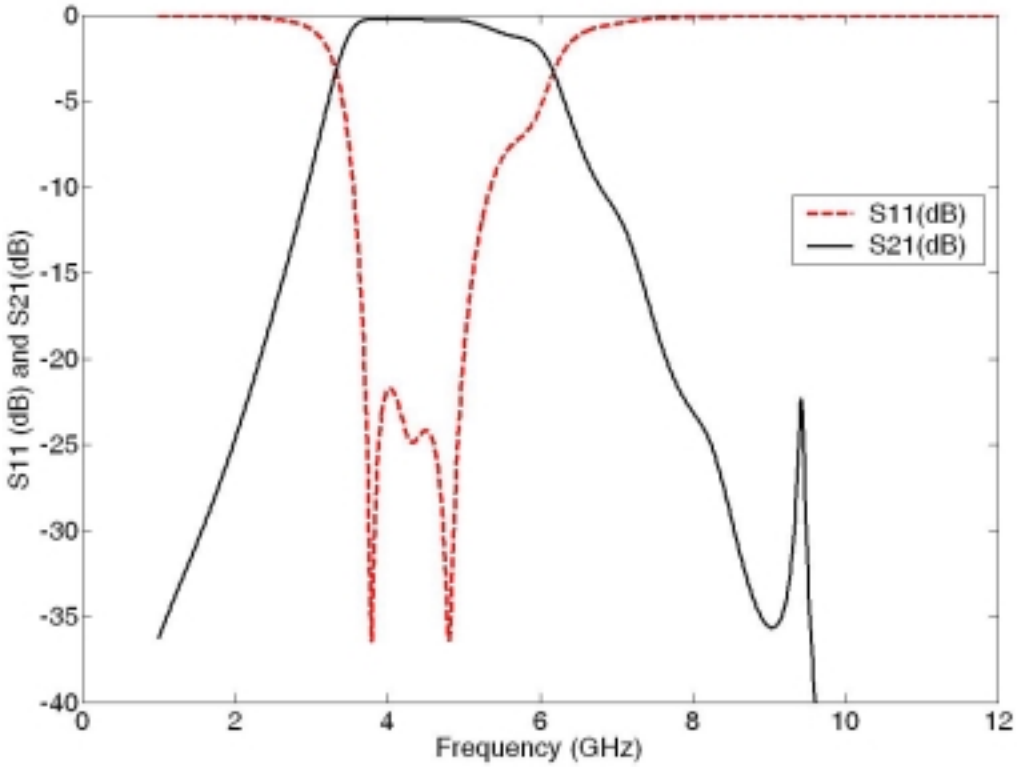

Fig. III.25. The initial response of the UWB mask filter

A cooperative PSO scheme is used in order to find the global optimum in the three dimensional parameter space. At each step, the parameters P3, P1 and P2 were cooperatively updated. The final set of parameters is presented in Table III.6 followed by the final characteristics in Fig. III.26, all calculated by Momentum. The convergence was unexpectedly slow, because of the relatively large band. The convergence versus iteration numbers is presented in Fig. III.27.

Parameter	Value(mm)
p	0.287
p	7.475
p	7.833

Table III.6. The optimized parameters

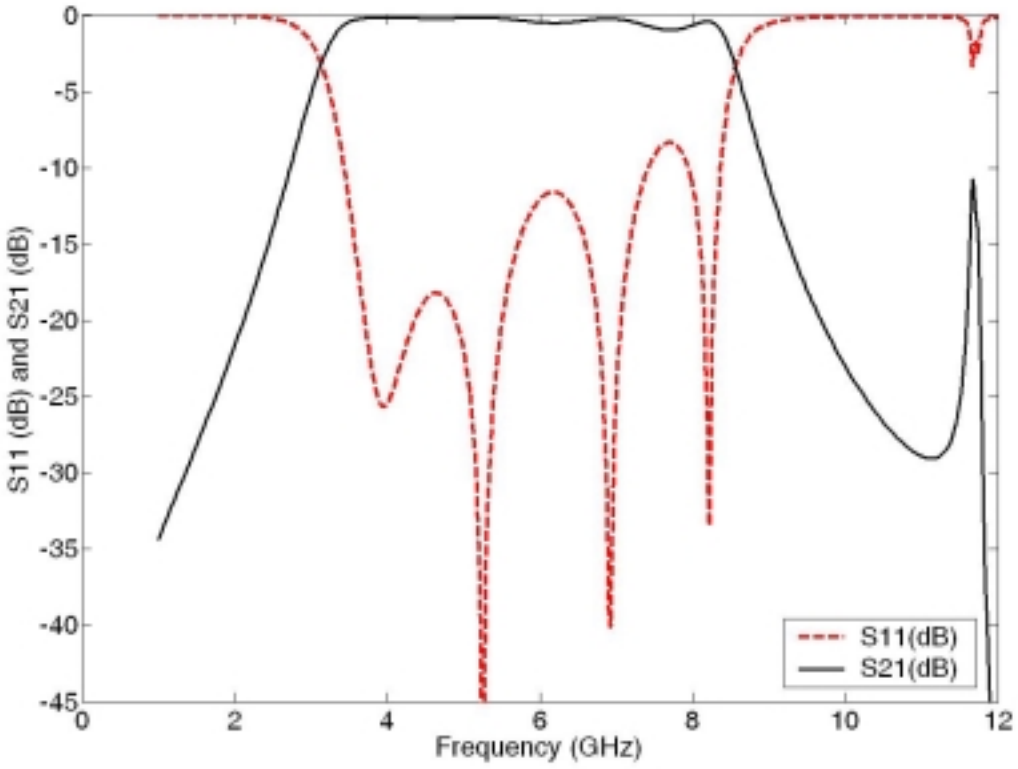

Fig. III.26. The final result of UWB mask filter

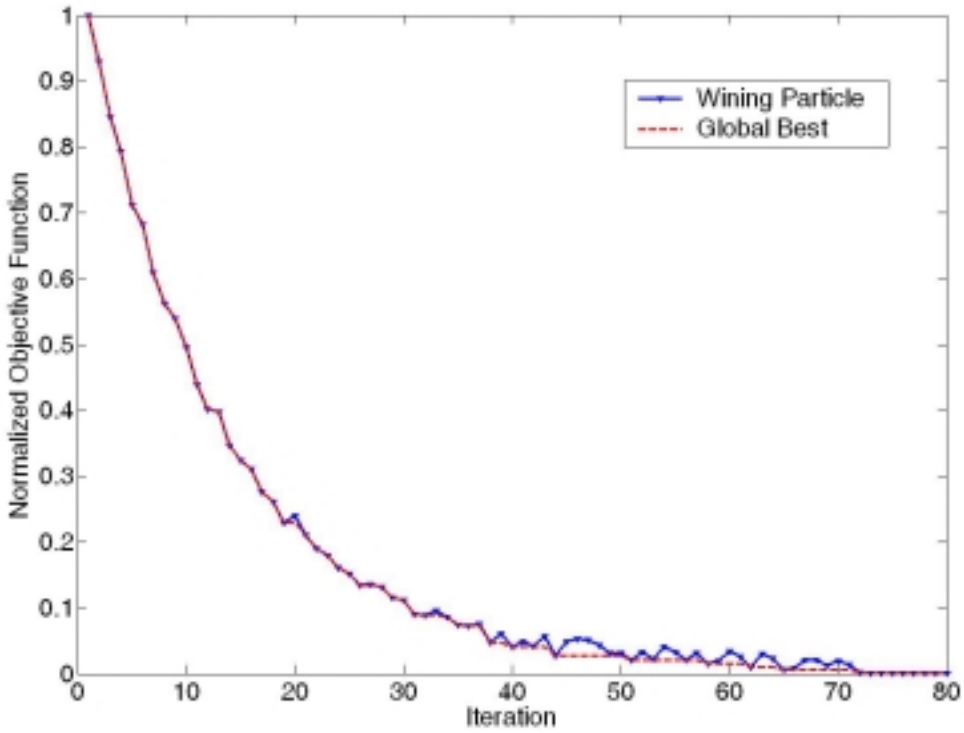

Fig. III.27. The error function belonging to the ultimate winner versus iteration number.

III.4.5. Optimization of a sapphire resonator with distributed Bragg reflectors

Simple metal cavity resonators, where the enclosure wall losses determine the achievable Q, were superceded by dielectric loaded cavities which attained higher Q's by confining more of the field of the resonant mode away from the lossy enclosure walls. Lately, sapphire resonators have helped to achieve higher quality factors. This case is specially interesting as an optimization because the objective function is radically different from typical filter design problems.

III.4.5.1. Description of the structure

The physical shape of the distributed Bragg resonator resonant structure has the form of an interpenetrating set of dielectric plates and cylinders as shown in Fig. III.28. This resonant dielectric structure fits inside of a metal enclosure. The way it is seen from the central cavity region, concentric cylinders in the radial dimensions form a DBR.

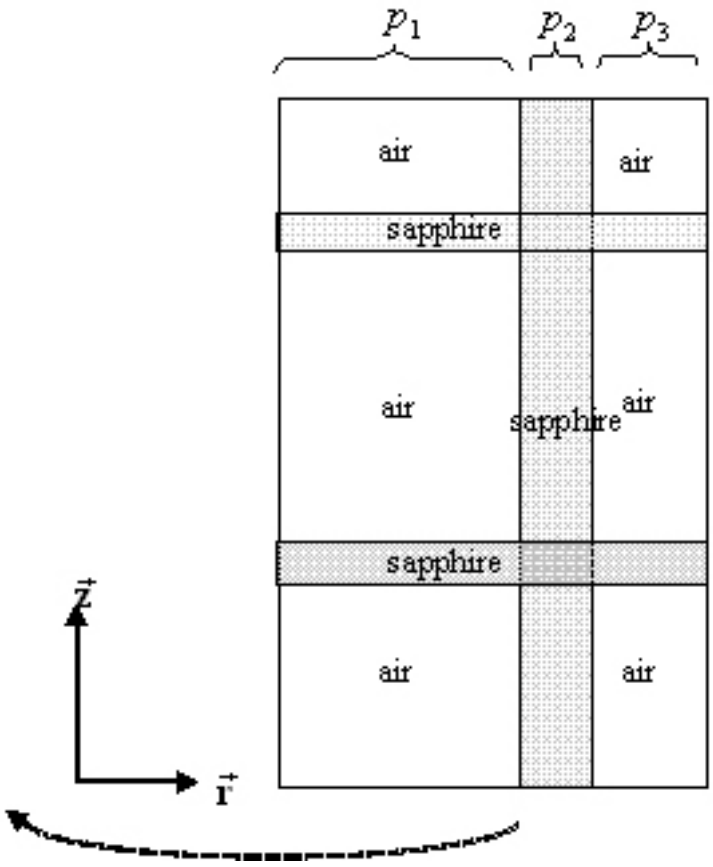

Fig. III.28. The geometry of the distributed sapphire Bragg resonator

III.4.5.2. Method of analysis

The structure is analyzed by the Method of Lines. The details of the analysis are addressed in [37]. This method allows the approximate solution of all the dimensions of a multilayered dielectric cylindrical resonant cavity that constitutes a distributed Bragg refection (DBR) resonator. The analysis can considers an arbitrary number of alternating dielectric and free-space layers of cylindrical geometry enclosed by a metal cylinder.

III.4.5.3. Objective function

The definition of the objective function is very critical in this case. The design goal is to find the dimensions for resonant frequency of TE_{011} mode to be10GHz, while the quality factor is 300,000. The desired resonant mode imposes another constrain for the optimization algorithm. The formation of the electric field must follow a specific pattern, so that the electric field has one major peak along one axis. Thus the objective function is determined as,

$$T(f_c, Q_t, \mathbf{p}) = \alpha \left| f_c - f_c^{ideal} \right| + \beta \left| Q_t - Q_t^{ideal} \right| + \gamma \Phi(\sigma) \qquad \text{(III- 40)}$$

where,

f_c, f_c^{ideal} are the resonant frequency and ideal resonant frequency, respectively

Q_t, Q_t^{ideal} are the computed and ideal quality factor at resonant frequency, respectively

$\mathbf{p} = [p_1, p_2, p_3]$ is the vector of the design variables(dimensions to be optimized)

α, β are weighting coefficients that moderates the different scales of frequency and quality factor,

$$\frac{\alpha}{\beta} = \kappa \frac{Q_t^{ideal}}{f_c^{ideal}}$$

where $0.5 \le \kappa \le 1.5$

σ is the number of the peaks of the electric field along with radial axis

$\Phi(\sigma)$ is the weighted field indicator,

$$\Phi(\sigma) = \begin{cases} 1 & \sigma > 1 \\ 0 & \sigma = 1 \end{cases}$$

γ is the weighting factor for the number of peaks and is normally comparable to the order of magnitude of the frequency(to dominate the objective function)

III.4.5.4. Optimization algorithm

A hybrid optimization technique is used for this design problem. At first step a very big swarm ($N_T = 80$-100 particles) is chosen randomly within the domain of the design parameters. A tournament selection is then chosen to filter out those solutions which have resulted unwanted field distribution, i.e. those with $\Phi(\sigma) = 1$. A swarm of those particles which produce a desired field distribution is formed. This swarm is considered as the initial swarm for the PSO algorithm with the number of particles being N_S . A cooperative PSO scheme is then used for minimizing the objective function. At this stage, the ideal response parameters were:

$$f_c^{ideal} = 10GHz$$

$$Q_c^{ideal} = 300,000$$

$$1.5\text{mm} \le p_1 \le 2.3\text{mm}$$

$$0.18\text{mm} \le p_2 \le 0.28\text{mm}$$

$$0.69\text{mm} \le p_3 \le 0.1\text{mm}$$

$$\alpha = 1,\ \beta = 33\times10^3, \gamma = 10^9$$

After the first tournament, the number of particles who win the first round tournament is a random function, forming the following particle matrix,

$$\mathbf{p}^{<1>} = \begin{bmatrix} p_{11}^{<1>} & . & . & . & p_{1N_S}^{<1>} \\ p_{21}^{<1>} & . & p_{ij}^{<1>} & . & p_{2N_S}^{<1>} \\ p_{31}^{<1>} & . & . & . & p_{3N_S}^{<1>} \end{bmatrix} \quad \text{(III- 41)}$$

This number determines the size of the initial swarm for PSO. Obviously the bigger the size of initial swarm, the higher is the chances of success.

The velocities were initialized as

$$v_{ij}^{<1>} = 0.3\,p_{ij}^{<1>} + 0.2\,p_{ij}^{<1>} \times rand(N_s, 3) \quad \text{(III- 42)}$$

whereas *rand(.)* is a uniform random function.

For the consecutive steps, the velocity vector is chosen as,

$$v_{ij}^{<k+1>} = 0.4v_{ij}^{<k>} + 2\eta_1 (p_{i,best}^{<k>} - p_{ij}^{<k>}) + 2\eta_2 (g_{i,best}^{<k>} - p_{ij}^{<k>}) \quad \text{(III- 43)}$$

where $0 \le \eta_{1and\,2} \le 1$ are generated through a uniform, random function.

Fig. III.29 shows the convergence of the normalized objective function for a sample optimization procedure. The procedure was repeated to a number of times. The final (optimum) dimensions are as follows:

$$p_1 = 1.9699\,\text{mm}$$
$$p_2 = 0.2352\,\text{mm}$$
$$p_3 = 0.8651\,\text{mm}$$

The achieved frequency is

$$f_c^{optimum} \simeq 9.9925\ GHz$$

and the overall quality factor is

$$Q_c^{optimum} = 3.199 \times 10^5$$

The field distribution for the optimized response is presented in Fig. III.30.

Several tests have been conducted to achieve better frequency response, at this stage it would be very tedious with PSO method. A better approach (once the optimum point located) is to use a classical gradient method such as steepest descent or Newton's method.

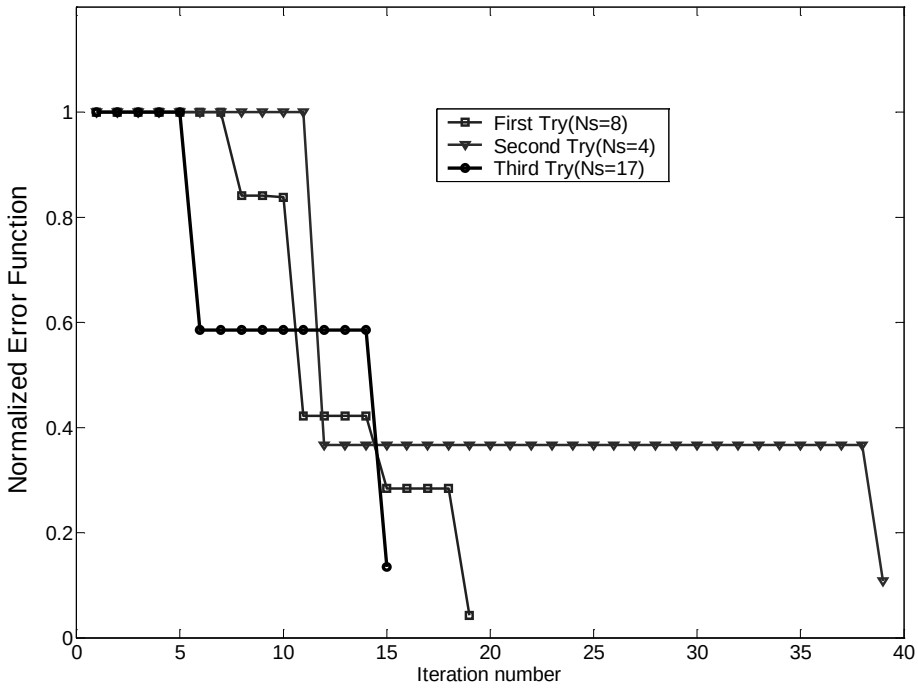

Fig. III.29. The objective function (global best) as a function of the iteration number for different tests and the corresponding size of swarms

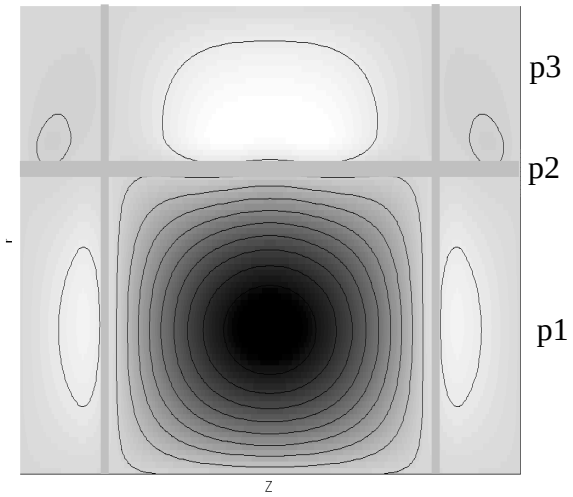

Fig. III.30. The field distribution for the optimized response(N_s =7)

III.5. Conclusion

The potentials of particle swarm optimization for being deployed as a global optimization technique in microwave design is investigated in this chapter. PSO is a novel evolutionary algorithm with a faster convergence. PSO has the advantage of incorporating a pseudo-gradient scheme for updating the parameter vector.

Despite such a fundamental difference with genetic-like algorithms, PSO can still best fits in the category of evolutionary algorithms.

In order to provide an appropriate context for PSO, genetic algorithm is introduced in this chapter, followed by an example. In the second part of the chapter, PSO algorithm is explained. Basically, PSO employs the analogy between parameter vectors in a parameter space with social movement of birds in a flock. In such an analogy, the movement of the parameter vectors towards the global optimum is achieved through comparing the position of each member of the flock with the position of individual and best fitness ever achieved.

Several improvements to the conventional PSO are suggested in this section. It was shown that having every particle know about the personal best position of other particles would improve the speed of the optimization. This “cooperative” learning provides and extra feedback for individuals (parameter vectors) in a swarm to modify their direction in (parameter) space.

Few microwave devices are designed using different variations of PSO. A simple FDTD scheme was employed to design a band-reject filter while the dimension updates were calculated using PSO.

The stability of PSO is also studied in this chapter. Through a simple mathematical manipulation, the gradient nature of PSO is claimed.

Despite many contributions in the last year, PSO is still an immature technique and probably a hybrid of PSO and parameterized model can help to obtain a fast and global design optimization algorithm.

III.6. References

[1] J. M. Johnson and Y. Rahmat-Samii, "An introduction to genetic algorithms," *Electromagnetic Optimization by Genetic Algorithms*, Y. Rahmat-Samii and E. Michielssen, Ed. New York: Wiley, 1999, pp. 1-27.

[2] D. S. Wiele and E. Michielssen, "Genetic algorithm optimization applied to electromagnetics: A review," *IEEE Trans. Antennas Propagat.*, vol. 45, pp. 343-353, Mar. 1997.

[3] J. M. Johnson and Y. Ramat-Samii, "Genetic algorithms in engineering electromagnetics," *IEEE Antennas Propagat. Mag.*, vol. 39, pp. 7-25, 1997.

[4] R. L. Haupt and S. E. Haupt, *Practical Genetic Algorithms.*, New York: Wiley, 1997.

[5] M. Lecouve, P. Jarry, E. Kerheve, N. Boutheiller, and F. Marc, "Genetic algorithm optimization for evanescent mode waveguide filter design," in *IEEE Int. Circuits Systems Symp.*, vol. III, May 2000, pp. 411-414.

[6] C. Delabie, M. Villegas, and O. Picon, "Creation of new shapes for resonant microstrip structures by means of genetic algorithms," *Electron. Lett.*, vol. 33, pp. 1509-1510, Aug. 1997.

[7] D. Pavlidis and H. L. Hartnagel, "The design and performance of three-line microstrip couplers," *IEEE Trans. Microwave Theory Tech.*, vol. MTT-24, pp. 631-640, Oct. 1976.

[8] E. Michielssen, J. M. Sajer, and R. Mittra, "Design of multilayered FSS and waveguide filter using genetic algorithms," in *IEEE AP-S Int. Symp. Dig.*, 1993, pp. 1936-1939.

[9] A. John and R. H. Jansen, "Evolutionary generation of (M)MIC component shapes using 2.5D EM simulation and discrete genetic optimization," in *IEEE MTT-S Int. Microwave Symp. Dig.*, 1996, pp. 745-748.

[10] T. Nishino and T. Itoh, "Evolutionary generation of microwave line-segments circuits by genetic algorithms," *IEEE Trans. Microwave Theory Tech.*, vol. 50, pp. 2048-2055, Sept. 2002.

[11] E. Michielssen, J. M. Sajer, S. Ranjithan, and R. Mittra, "Design of lightweight broad-band microwave absorber using genetic algorithms," *IEEE Trans. Microwave Theory Tech.*, vol. 41, pp. 1024-1031, June 1993

[12] J. Haala, W. Wiesbeck, and T. Zwick, "A genetic algorithm for the evaluation of material parameters of compound multilayered structures," *IEEE Trans. Microwave Theory Tech.*, vol. 50, pp. 1180-1187, Apr. 2002.

[13] P. L. Werner, R. Mittra, and D. H. Werner, "Extraction of equivalent circuits for microstrip components and discontinuities using the genetic algorithm," *IEEE Microwave Guided Wave Lett.*, vol. 8, pp. 333-335, Oct. 1998.

[14] Wang Wen, Lu Yilong, J.S. Fu, Xiong Yong Zhong, "Particle swarm optimization and finite-element based approach for microwave filter design," IEEE *Transactions on Magnetics*, vol. 41, No. 5, pp. 1800 - 1803, May 2005.

[15] A. Boag, E. Michielssen, and R. Mittra, "Design of electrically loaded wire antennas using genetic algorithms," *IEEE Trans. Antennas Propagat.*, vol. 44, pp. 687-695, May 1996.

[16] F. Ares, S. R. Rengarajan, E. Villanueva, E. Skochinski, and E. Moreno, "Application of genetic algorithms and simulated annealing technique in optimizing the aperture distributions of antenna array patterns," *Electron. Lett.*, vol. 32, no. 3, pp. 148-149, 1996.

[17] P. L. Werner, R. Mittra, and D. H. Werner, "Extraction of SPICE-type equivalent circuits of microwave components and discontinuities using the genetic algorithm optimization technique," *IEEE Trans. Adv. Packag.*, vol. 23, Feb. 2000.

[18] C. Chien-Ching and C. Wei-Ting, "Electromagnetic imaging for an imperfectly conducting cylinder by the genetic algorithm," *IEEE Trans. Microwave Theory Tech.*, vol. 48, pp. 1901-1905, Nov. 2000.

[19] J. M. Johnson and Y. Rahmat-Samii, "Genetic algorithms and method of moments (GA/MoM) for the design of integrated antennas," *IEEE Trans. Antennas Propagat.*, vol. 47, pp. 1606-1614, Oct. 1999.

[20] L. Alatan, M. I. Aksun, K. Leblebicioglu, and M. T. Birand, "Use of computationally efficient method of moments in the optimization of printed antennas," *IEEE Trans. Antennas Propagat.*, vol. 47, pp. 725-732, Apr. 1999.

[21] L. Chaung, T. Chang, and W. D. Burnside, "An ultrawide-bandwidth tapered resistive TEM horn antenna," *IEEE Trans. Antennas Propagat.*, vol. 48, pp. 1848-1857, Dec. 2000.

[22] http://www.rogers-corp.com/mwu/translations/french.htm

Particle Swarm Optimization- General

[23] J. Kennedy and R. C. Eberhart, "Particle swarm optimization," *Proc. the 1995 IEEE Int. Conf. Neural Networks (Perth, Australia)*, 1995, vol. IV, pp. 1942-1948.

[24] R. Eberhart and J. Kennedy, "A new optimizer using particle swarm theory," in *Proc. 6th Int. Symp. Micro Machine Human Sci. (MHS'95)*, 1995, pp. 39-43.

[25] G. Ciuprina, D. Ioan, and I. Munteanu, "Use of intelligent-particle swarm optimization in electromagnetics," *IEEE Trans. Magn.*, vol. 38, pp. 1037-1040, Mar. 2002.

[26] B. Brandstätter and U. Baumgartner, "Particle swarm optimization—mass-spring system analogon," *IEEE Trans. Magn.*, pt. 1, vol. 38, pp. 997-1000, Mar. 2002.

[27] J. Robinson, S. Sinton, and Y. Rahmat-Samii, "Particle swarm, genetic algorithm, and their hybrids: optimization of a profiled corrugated horn antenna," in *Proc. IEEE Int. Symp. Antennas Propagation* San Antonio, TX, vol. 1, 2002, pp. 314-317.

[28] S. Sinton, J. Robinson, and Y. Rahmat-Samii, "Standard and micro genetic algorithm optimization of profiled corrugated Horn antennas," *Microwave Opt. Technol. Lett.*, vol. 20, no. 6, pp. 449-453, Dec. 2002.

[29] F. Van den Bergh and A. P. Engelbrecht, "A Cooperative approach to particle swarm optimization," IEEE *Transactions on Evolutionary Computation*, vol. 8, Issue 3, pp. 225 – 239, June 2004.

[30] M. Clerc and J. Kennedy, "The particle swarm—explosion, stability, and convergence in a multidimensional complex space," *IEEE Trans. Evolutionary Computat.*, vol. 6, pp. 58-73, Feb. 2002.

[31] Y. Shi and R. C. Eberhart, "A modified particle swarm optimizer," in *Proc. IEEE Int. Conf.*

Evolutionary Computation, Anchorage, AK, May 1998.

[32] J. Kennedy, "Stereotyping: Improving particle swarm performance with cluster analysis," in *Proc. 2000 Congr. Evolutionary Computing*, 2000, pp. 1507–1512.

[33] G. Matthaei, E.M.T. Jones, L. Young, *Microwave Filters, Impedance-Matching Networks, and Coupling Structures,* Artech House Publishers, February 1980.

[34] Jia-Shen G. Hong, M. J. Lancaster, *Microstrip Filters for RF/Microwave Applications,* Wiley-Interscience, June 22, 2001.

[35] Momentum Software, Agilent Technologies

[36] C. L. Hsu, F. C. Hsu and J. T. Kuo, "Microstrip bandpass filters for ultra-wideband (UWB) wireless communications," proceedings of 2005 International Microwave Symposium IMS2005, Long Beach, June 2005.

[37] O. Piquet, A. Laporte, D. Cros, S. Verdeyme, and M. Tobar, "High-Q sapphire resonator with distributed Bragg reflector," *Electronics Letters*, Vol. 39 No. 25. 11th December 2003

CONCLUSION GENERALE

CONCLUSION GENERALE

Ce travail de thèse est dédié à l'amélioration des méthodes d'optimisation classiquement utilisées pour la conception électromagnétique des circuits et dispositifs micro-ondes.

Ces méthodes utilisent un modèle électromagnétique analysé par une méthode numérique à chaque itération et dirigé par une stratégie de mise à jour des paramètres le plus généralement basée sur un calcul de gradient.

Les améliorations apportées par ce travail ont concerné deux axes :

- L'utilisation de modèles électromagnétiques paramétrés permettant d'accélérer les procédures d'optimisation en court-circuitant les simulations numériques,
- L'utilisation de méthodes évolutionnaires efficaces comme stratégie d'optimisation pour réduire les risques de divergence traditionnellement rencontrés avec les stratégies de type gradient.

Le manuscrit commence par introduire au premier chapitre quelques généralités sur les méthodes d'optimisation électromagnétique appliquées à la conception assistée par ordinateur (CAO) des dispositifs micro-ondes. Divers concepts assez généraux en optimisation sont d'abord abordés.

Ensuite, quelques problèmes spécifiques aux méthodes d'optimisation faisant appel à une simulation numérique sont explorés plus en détail. En particulier, nous montrons à quel point la définition de la fonction objectif est critique pour l'obtention de la solution optimale dans un temps raisonnable.

Plusieurs méthodes d'optimisation classiques de type gradient sont ensuite étudiées en présentant différentes variantes de la plus simple à la plus élaborée.

Enfin, la dernière partie de ce chapitre expose brièvement les techniques d'analyse numériques basées sur les lois de l'électromagnétisme utilisées couramment pour modéliser les dispositifs micro-ondes.

Au cours du deuxième chapitre, nous introduisons tout d'abord les différents aspects de la paramétrisation des modèles électromagnétiques.

Un état de l'art des techniques de paramétrisation du champ électromagnétique en fonction de la fréquence et de la géométrie est tout d'abord présenté dans les deux premières sections.

Pour la paramétrisation géométrique efficace d'un modèle électromagnétique, la déformation de son maillage, c'est à dire de sa discrétisation en éléments simples (2-D ou 3-D), doit être paramétrée en fonction des paramètres géométriques pour éliminer les discontinuités dans le calcul des gradients du champ. Plusieurs techniques de paramétrisation du maillage sont alors présentées et illustrées avec quelques exemples.

La dernière partie du deuxième chapitre présente l'optimisation électromagnétique d'un circuit hyperfréquence en utilisant son modèle électromagnétique paramétré en géométrie. Le cas test est un filtre 5 pôles en cavités cylindriques bimodes dont le modèle électromagnétique est paramétré suivant 12 dimensions géométriques à l'aide d'un logiciel développé par CADOE et couplé au code éléments finis du laboratoire dans le cas d'une action de R&T du CNES.

L'utilisation du modèle paramétré permet alors de s'affranchir de l'analyse électromagnétique globale du circuit à chaque itération. La stratégie de mise à jour des variables est basée sur une technique de type gradient. Après quelques itérations, le comportement en fréquence du modèle, dont les dimensions ont été initialisées relativement efficacement, converge facilement vers l'objectif.

Le troisième chapitre introduit les algorithmes évolutionnaires présentées comme des méthodes d'optimisation plus globales que les méthodes de type gradient.

L'algorithme génétique qui est certainement la technique évolutionnaire la plus connue et la plus appliquée dans le domaine des circuits et dispositifs micro-ondes est tout d'abord présentée et illustrée par un exemple. Le principal désavantage de cette dernière technique est sa lourdeur de mise en œuvre et d'utilisation qui en font une méthode relativement lente.

Une nouvelle technique évolutionnaire, très récemment introduite dans le domaine de l'électromagnétisme est la méthode des « essaims particulaires » (Particle swarm optimization - PSO). Cette technique commence similairement à l'algorithme génétique par la génération d'une population initiale aléatoire mais la nature de type

gradient de l'optimisation permet d'obtenir une convergence beaucoup plus rapide. Les détails de la technique sont tout d'abord donnés puis appliqués à l'optimisation de circuits et dispositifs micro-ondes à travers plusieurs exemples.